Temporal distribution of cold-water corals in the northwest Atlantic through the Late Quaternary: footprint of intermediate water mass circulation

Dissertation zur Erlangung des
Doktorgrades in den Naturwissenschaften

Dr. rer. nat.

im Fachbereich Geowissenschaften
der Universitat Bremen

vorgelegt von

Lélia Maria Lages Nunes de Matos Branco

Bremen, Mai 2017

Temporal distribution of cold-water corals in the northwest Atlantic through the Late Quaternary: footprint of intermediate water mass circulation

Dissertation for obtaining the
Doctoral degree in natural sciences

Dr. rer. nat.

in the Department of Geosciences
University of Bremen

presented by

Lélia Maria Lages Nunes de Matos Branco

Bremen, May 2017

Main Supervisor: Prof. Dr. Dierk Hebbeln
Center for Marine Environmental Sciences (MARUM)
University of Bremen, Germany

Co-supervisor: Prof. Dr. Fatima Abrantes
Portuguese Institute for Sea and Atmosphere, I. P. (IPMA), Portugal

Co-supervisor: Dr. Marina R. Cunha
Center for Environmental and Marine Studies (CESAM)
Department of Biology, University of Aveiro, Portugal

Doctoral colloquium

Date: 13-06-2017

Title:
Climate change-triggered pacing of cold-water coral occurrence in the northwestern Atlantic

Committee:
Prof. Dr. David van Rooij, *Renard Centre for Marine Geology, Univ. Ghent, Belgium*
Prof. Dr. Dierk Hebbeln, *MARUM, Univ. Bremen, Germany*
Prof. Dr. Andre Freiwald, *Senckenberg am Meer and Univ. Bremen, Germany*
PD Dr. Christian Winter, *MARUM, Univ. Bremen, Germany*
Dr. Claudia Wienberg, *MARUM, Univ. Bremen, Germany*
Katharina Wetterauer, *Univ. Bremen, Germany*

"When it is not in our power to follow what is true,

we ought to follow what is most probable."

Rene Descartes

ABSTRACT

Over the last two decades, extensive geological investigations on cold-water coral (CWC) areas of the northeastern Atlantic revealed that the temporal occurrence of framework-forming CWC presents a climate-dependent pattern. The pattern follows the glacial-interglacial changes of the surface ocean conditions and intermediate-depth water masses. Over geological time scales, CWC can form substantial seabed features, called CWC mounds that may serve as archives for assessing their long-term development. Several CWC mound areas have been described in the northwestern Atlantic, where the presence of living reef-like structures advocates for favorable conditions for CWC at present. A limited number of ages of fossil CWC collected from various sites in the northwestern Atlantic further suggests that conditions were also favorable during the last glacial. However, the less of a handful of available ages emphasizes the need for a thorough investigation of the temporal pattern of CWC occurrence in this area.

This study was designed (1) to identify the periods of sustained CWC growth in two coral mound areas of the northwestern Atlantic (the Campeche CWC Province, southern Gulf of Mexico, and the Cape Lookout CWC area, off North Carolina) and (2) to detect the environmental factors influencing their long-term development. The temporal occurrence of CWC was established by using U-series dating, while a multi-proxy approach was followed to reconstruct the present and past environmental conditions (incl. water column analyses; ROV video observation and sampling; foraminifera-based stable isotope analyses, Mg/Ca-thermometry and assemblage analyses; grain size and carbonate content analyses of sediments).

The results suggest that for the last 260,000 years, pronounced coral growth at these two coral mound areas was restricted to interglacial periods, which confirms a climate influence on the CWC temporal occurrence also in these northwestern Atlantic areas. The pattern coincides with the glacial-interglacial changes of the intermediate-depth water masses, where periods favorable for CWC growth are marked by enhanced hydrodynamics that increase the food supply to the CWC. At the Campeche CWC area, such conditions result from the density gradient between the Antarctic Intermediate Water and the overlying Tropical Atlantic Central Water, whereas at the Cape Lookout CWC area, coral growth is steered by the Gulf Stream presence. Although similar occurrence patterns were found in the two studied areas, they differ from the few ages previously reported for the NE Gulf of Mexico and the East Florida Strait CWC mound areas, where CWC occur today but obviously also occurred under glacial conditions. Therefore, it is necessary to conduct further research in order to better constrain the general pattern of CWC occurrence in coral mound areas of the northwestern Atlantic and its possible connection to the intermediate-depth circulation.

ZUSAMMENFASSUNG

Umfangreiche geologische Untersuchungen während der letzten zwei Jahrzehnte in Gebieten des Nordostatlantiks mit Kaltwasserkorallen (KWK) haben gezeigt, dass das zeitliche Auftreten von strukturbildenden KWK einem klima-abhängigen Muster folgt. Dieses Muster wird von den glazial-interglazialen Änderungen in den Oberflächenwasser-Bedingungen und in den Strömung in den Zwischenwassertiefen gesteuert. Über geologische Zeitskalen können KWK ausgeprägte Strukturen am Meeresboden bilden und diese sogenannten KWK-Hügel können als Archive dienen, die langfristige Entwicklung der KWK zu erfassen. Auch für den Nordwestatlantik wurden einige Gebiete mit KWK-Hügeln beschrieben, für die die Anwesenheit von lebenden riff-ähnlichen Strukturen günstige heutige Bedingungen für KWK belegt. Eine begrenzte Anzahl an Altersbestimmungen an fossilen KWK zeigt außerdem, dass zumindest stellenweise die Bedingungen während der letzten Glazialzeit ebenfalls günstig waren. Die wenigen vorhandenen Datierungen zeigen aber auch die Notwendigkeit, das zeitliche Muster des Vorkommens von KWK in diesem Gebiet detailliert zu erforschen.

Die vorliegende Studie wurde entwickelt, 1) um die Zeiträume mit langanhaltendem KWK-Wachstum in zwei Gebieten mit Korallenhügeln im Nordwestatlantik (Campeche KWK Provinz, südlicher Golf von Mexiko, und Kap Lookout KWK-Gebiet vor North Carolina) zu erfassen und, 2) um die Umweltbedingungen, die ihre langfristige Entwicklung bestimm(t)en, zu identifizieren. Die temporäre Verteilung der KWK wurde mit Uran-Thorium-Datierungen ermittelt, während ein Multi-Proxy-Ansatz verfolgt wurde, um die Umweltbedingungen in der Jetztzeit und in der Vergangenheit zu rekonstruieren (inklusive Wassersäulenanalysen; ROV Video-Beobachtungen und Beprobungen; Analysen stabiler Isotopenverteilungen, Mg/Ca-Spurenelementanalysen zur Temperaturrekonstruktion und Faunenanalysen an Foraminiferen; Korngrößen- und Karbonatgehaltsbestimmungen in den Sedimenten).

Die Ergebnisse zeigen, dass sich ausgeprägtes KWK-Wachstum für die beiden Untersuchungsgebiete während der letzten 260.000 Jahre auf die Interglazialperioden beschränkte, was einen Klimaeinfluss auf die temporäre Verteilung der KWK auch für diese Gebiete im Nordwestatlantik bestätigt. Dieses Verbreitungsmuster geht mit glazial-interglazial Änderungen in der Zwischenwasserzirkulation einher, wobei für das KWK-Wachstum günstige Zeiträume durch eine verstärkte Hydrodynamik gekennzeichnet sind, die die Nahrungszufuhr zu den KWK verbessert. Im Campeche KWK-Gebiet resultieren derartige Bedingungen aus dem Dichtegradienten zwischen dem antarktischen Zwischenwasser und dem tropischen Atlantik-Zentralwasser, wohingegen im Kap Lookout-Gebiet das Korallenwachtsum durch die

Anwesenheit des Golfstromes gesteuert wird. Obwohl ähnliche Verteilungsmuster in beiden Arbeitsgebieten gefunden wurden, unterscheiden sie sich in den Altern von KWK-Hügelgebieten im nordöstlichen Golf von Mexiko und in der östlichen Floridastraße, wo neben heute lebenden auch Korallen mit glazialen Altern gefunden wurden. Es ist daher notwendig, weitere Untersuchungen durchzuführen, um die generellen Muster der KWK-Verteilung in den Korallenhügelgebieten des Nordwestatlantiks und die eventuellen Zusammenhänge mit der Zwischenwasserzirkulation besser zu verstehen.

TABLE OF CONTENTS

1 Introduction

1.1 Framework-forming cold-water corals: ecology and distribution

Cold-water corals (CWC) are corals that, unlike their tropical shallow-water counterparts, live mostly below the photic zone (i.e. below 200 m water depth) and lack zooxanthellae (symbiotic, photosynthetic algae) (Roberts et al., 2009). Among them, the scleractinian corals (or stony corals), which possess hard calcium carbonate skeletons, are most important from a geological perspective as their solid skeletal remains may be preserved in the sedimentary record. Furthermore, some colonial scleractinians are framework-forming, i.e. they have the ability of forming reef-like structures that, when preserved in the geologic record, can serve as important sedimentary archives. The most common framework-forming CWC species in the North Atlantic are *Lophelia pertusa* (Linnaeus, 1758) (Fig. 1) and *Madrepora oculata* Linnaeus, 1758 (Wienberg and Titschack, *in press*).

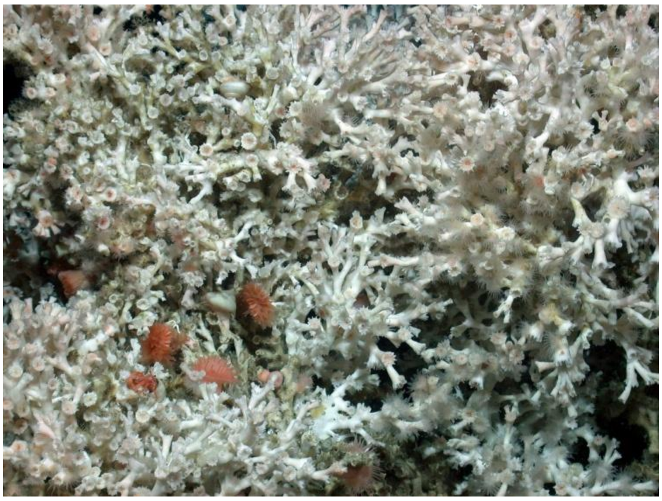

Figure 1. Thickets of living *L. pertusa*, showing some exposed coral polyps, and associated fauna from a CWC mound area off Ireland. Photo credits: MARUM.

Lophelia pertusa is the most common framework-forming CWC species worldwide, being frequently found in the North Atlantic (Fig. 2), but also in the Mediterranean Sea, Gulf of Mexico, Caribbean Sea and at some locations in the Indian and Pacific Oceans (Roberts et al., 2009; Zibrowius, 1980). The species is known to occur at depths ranging between 39 and 2775 m (Roberts et al., 2009), while it has been more frequently found at 200–250 m and between 500 and 900 m (Wienberg and Titschack, *in press*).

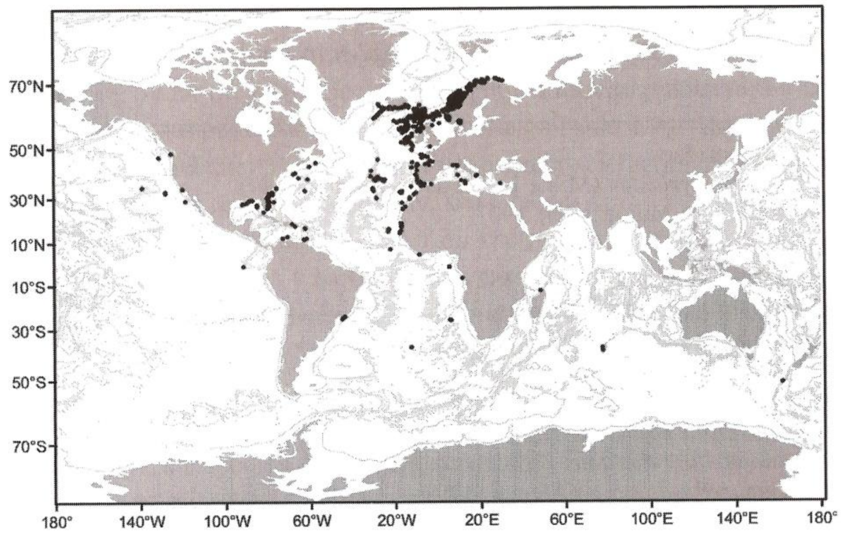

Figure 2. Worldwide distribution of *Lophelia pertusa* (isobaths at 2000 m, 5000 m and 9000 m) (Roberts et al., 2009). The uneven research effort (higher in the NE Atlantic) may have biased the current distribution pattern and further investigations could extend it.

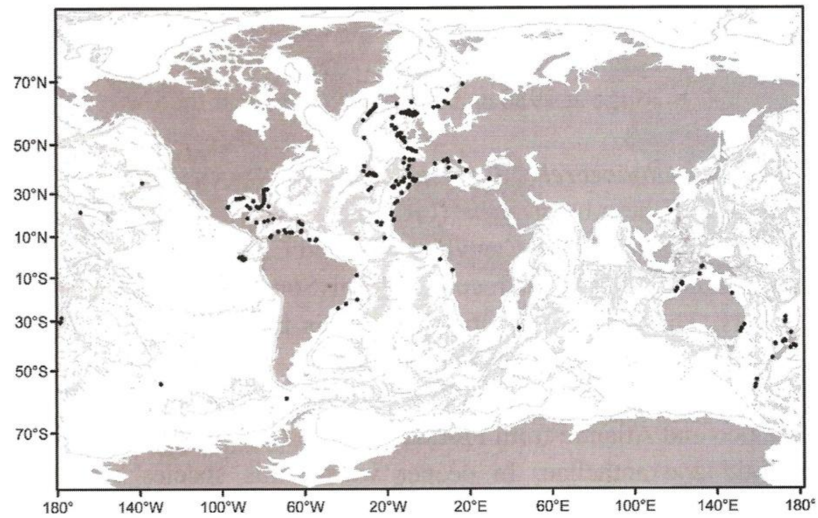

Figure 3. Worldwide distribution of *Madrepora oculata* (isobaths at 2000 m, 5000 m and 9000 m) (Roberts et al., 2009). The uneven research effort (higher in the NE Atlantic) may have biased the current distribution pattern and further investigations could extend it.

Madrepora oculata Linnaeus, 1758, although less abundant than *L. pertusa*, also has a wide distribution (Fig. 3). It is able to dominate the coral community in some areas of the NE Atlantic and the Mediterranean Sea, and may be further found in the NW Atlantic and in some areas of the Indian and Pacific Oceans (Roberts et al., 2009). *Madrepora oculata* occurs between 55 and 1950 m water depth (Roberts et al., 2009), with most of the currently known observations concentrated between 500 and 1000 m (Wienberg and Titschack, *in press*).

Distinct environmental conditions are required by the framework-forming CWC species. Firstly, as sessile organisms, they require a hard substrate that allows coral larvae to settle and a hydrodynamic setting that enhances food delivery. Food availability for such species depends not only on the primary production at the ocean surface but also on food delivering mechanisms that allow the food particles to reach (or accumulate) at the depth of CWC occurrence. Some of the suggested mechanisms include: geostrophic currents, internal waves and tides, or Taylor columns (e.g. White et al., 2005); formation of intermediate and bottom nepheloid layers (Mienis et al., 2007); and processes of downwelling and cascading (e.g. Davies et al., 2009). However, further species-specific environmental boundaries have been reported. The environmental tolerances of *L. pertusa* include temperatures ranging between -1.8 and 14.9 °C, salinity between 31.7 and 38.8, dissolved oxygen concentrations of 2.7 to 7.2 ml l^{-1}, and aragonite saturations between 0.6 and 4 units (mode values around 1.5 and 2 units) (Davies et al., 2010, 2008; Davies and Guinotte, 2011). Water density has also been referred as a possible constraining parameter in *L. pertusa*-dominated reef-like structures, which in the northeastern Atlantic varies between sigma-theta values of 27.35 and 27.65 kg m^{-3} (Dullo et al., 2008), although slightly lower values (27.18–27.29 kg m^{-3}) have been reported for the northeastern Gulf of Mexico (Davies et al., 2010). Overall, a recent database-supported review has shown that living *L. pertusa* occurs more frequently in waters of 6.5 to 8 °C, salinities of 35 to 35.75 and dissolved oxygen concentrations of around 6.25 ml l^{-1} (Wienberg and Titschack, *in press*). While living *M. oculata* has been found more frequently associated to temperatures of 8.5 °C to 10 °C, salinities ranging between 35 and 35.75 and dissolved oxygen values of about 5.25 ml l^{-1} (Wienberg and Titschack, *in press*).

1.2 Cold-water coral mounds: formation and development

Within the framework-forming CWC species of the North Atlantic, three are also known to be responsible for the development of CWC mounds: *L. pertusa*, *M. oculata* and *Oculina varicosa* Le Sueur, 1820 (Wienberg and Titschack, *in press*). Cold-water coral mounds are three-dimensional seabed structures formed by scleractinian coral remnants, which may be associated with the remains of other coral-associated fauna, embedded in fine hemipelagic sediments (e.g. de Haas et al., 2009; Dorschel et al., 2005; Paull et al., 2000). The mounds owe their origin on the occurrence of CWC reef-like structures (Fig. 4) that accumulate through successive periods of thicket development and mound sedimentation (Roberts et al., 2009). This way, mound formation depends on the proliferation of corals and, thus, on environmental conditions favoring CWC growth (see section 1.2), balanced by a sufficient input of sediment to guarantee the infilling of the coral framework and the stabilization of the structure (see Wienberg and Titschack (*in press*) for a review). The baffling capacity of the CWC framework potentiates the entrapment and deposition of both vertically and laterally advected sediment particles, even when strong bottom currents imposes non-depositional or erosional conditions in the adjacent areas (de Haas et al., 2009; Mienis et al., 2014; Thierens et al., 2013; Titschack et al., 2009). Mound growth occurs in distinct phases including: (1) mound initiation or colonization, when corals settle in a hard substrate, colonizing it; (2) development or aggradation, when coral thickets grow forming a framework that is infilled and secured by sediment; (3) retirement or demise, a phase with decreased or absent coral growth, increased framework fragmentation and change of sediment deposition that may lead to mound growth stagnation or mound burial; and (4) re-colonization, new phase of coral colonization on a previously existing mound (Roberts et al., 2006; Wienberg and Titschack, *in press*). Mounds may be classified as 'active' when they exhibit a vivid coral community; and considered 'inactive' during the retirement phase, when living coral cover is not observed and the mound becomes subject to erosion or burial (Huvenne et al., 2005; Wienberg and Titschack, *in press*). During erosional periods, the coral framework and the surrounding sediment may be lost, which will cause a hiatus in the geological mound record (e.g. Dorschel et al., 2005).

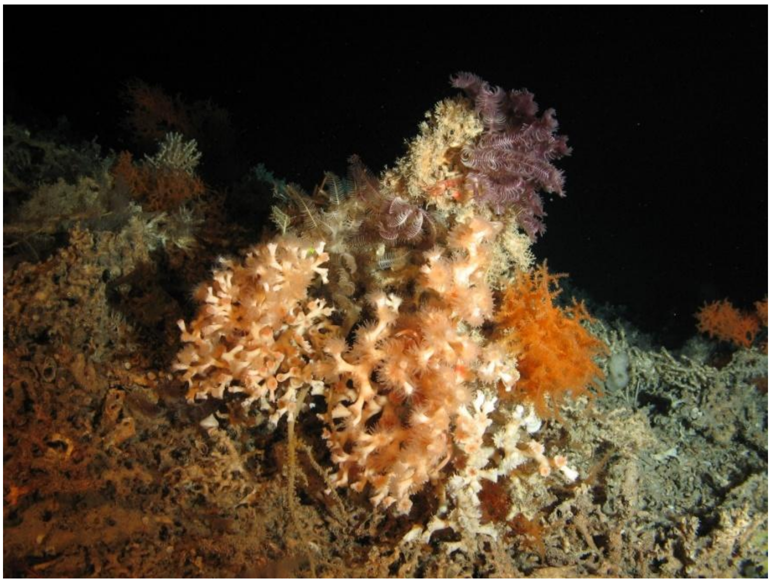

Figure 4. Thicket of living *L. pertusa* growing over dead coral framework, and its associated fauna, on a CWC mound area off Ireland. Photo credits: MARUM.

The generalized definition of coral mounds (named in the past *carbonate* mounds) implies recurring cycles of mound growth separated by long (tens-to-hundreds of thousand years) periods of mound retirement (Roberts et al., 2009). In this work, however, shorter cycle-periods such as the Holocene were also considered, in order to include the mound structures studied off Norway and Scotland (e.g. Douarin et al., 2013; López Correa et al., 2012). Cold-water coral mounds vary in height (from a few meters to hundreds of meters), in diameter or length, as well as in shape (e.g. conical, oval, elongated, ridge-like, or V-like shapes); and they may appear isolated or arranged in clusters or provinces consisting of hundreds to thousands of mounds (Wienberg and Titschack, *in press* and references therein). Coral mounds have been documented in several continental shelf and slope areas of the North Atlantic (Fig. 5).

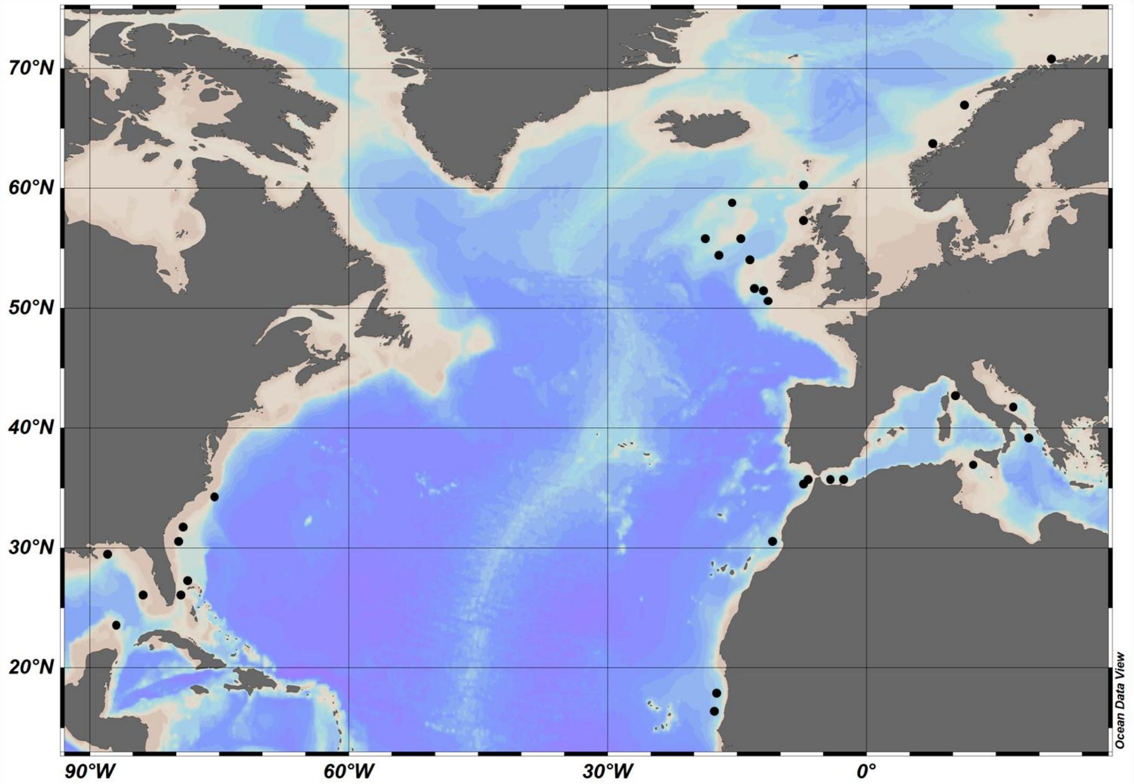

Figure 5. Approximate location of CWC mound areas in the North Atlantic, including the Mediterranean Sea and Gulf of Mexico (Roberts et al., 2009; Wienberg and Titschack, *in press*).

Mound development can result in substantial meter-thick mound sediment accumulation, giving rise to important geological archives that register successive periods of sustained CWC proliferation and decline (Wienberg and Titschack, *in press*). Given the predominantly intermediate-depth distribution of CWC and coral mounds (Roberts et al., 2009; Wienberg and Titschack, *in press*), the study of their temporal distribution (and the environmental conditions affecting it) is one of the tools available to improve our knowledge on the past variability of intermediate water masses. Some studies regarding this relationship have been already developed for the NE Atlantic.

1.3 The northeastern Atlantic cold-water coral mound areas

For the past two decades, several CWC mound areas in the NW Atlantic have been studied, namely off Norway, off Scotland, off Ireland, in the Gulf of Cadiz and off Mauritania (Fig. 6). A review on these areas regarding the regional hydrography and the periods of coral occurrence and coral mound development, as well as their main environmental drivers, is given below.

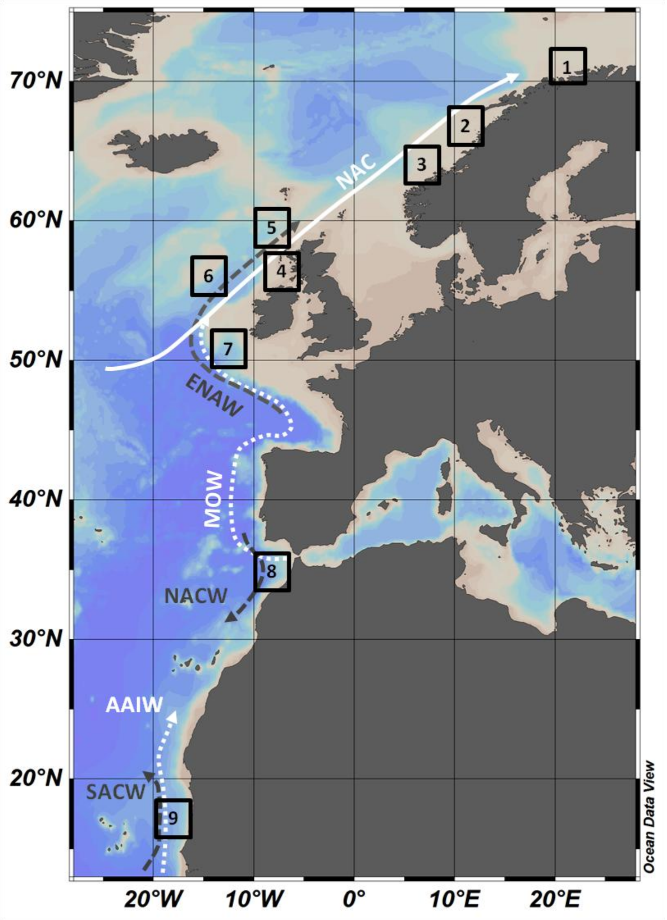

Figure 6. Approximate location of CWC mound areas of the NE Atlantic where CWC dating has been performed: (1) Stjernsund Reef, (2) Røst and Træna Deep Reefs, and (3) Sula Ridge Reef, off Norway; (4) Mingulay Reef Complex and (5) Darwin mounds, off Scotland; (6) Logachev mounds in the SW Rockall Trough and (7) the Magellan, Hovland and Belgica Mound Provinces in the Porcupine Seabight, off Ireland; (8) Gulf of Cadiz; and (9) Banda Mound Province, off Mauritania; and of the main water masses affecting them: North Atlantic Current (NAC), Eastern North Atlantic Water (ENAW), Mediterranean Outflow Water (MOW), North Atlantic Central Water (NACW), Antarctic Intermediate Water (AAIW) and South Atlantic Central Water (SACW).

1.3.1 Water mass distribution

The main water masses affecting the CWC mound areas are different in the northern and southern regions of the NE Atlantic. In the northern NE Atlantic, the main water masses identified at the intermediate depths where coral mounds occur include the deeper part of the North Atlantic Current (NAC; also named North Atlantic Drift Current) off Norway and off Scotland (e.g. Dullo et al., 2008; Inall et al., 2009); the Eastern North Atlantic Water (ENAW) at the Darwin mounds and off Ireland (e.g. New and Smythe-Wright, 2001; Vermeulen, 1997); and the Mediterranean Outflow Water (MOW) at the Porcupine Seabight (e.g. Vermeulen, 1997) (Fig. 6). In the southern NE Atlantic the intermediate water masses identified at coral mound areas off Morocco include the North Atlantic Central Water (NACW) and, occasionally, the MOW (Aït-Ameur and Goyet, 2006; Foubert et al., 2008), whereas off Mauritania the South Atlantic Central Water (SACW) and the Antarctic Intermediate Water (AAIW) (Mittelstaedt, 1991; Stramma and Schott, 1999) were identified (Fig. 6). Changes in the intermediate water mass distribution (and their boundaries) driven by cyclic climatic changes have been linked to the temporal pattern of CWC occurrence in some coral mound areas of the NE Atlantic (such as off Ireland; see section 1.3.2).

1.3.2 Coral mound development in the northeastern Atlantic

The Norwegian shelf gives home to the most exuberant living CWC areas dominated by *L. pertusa*, which also grow on coral mounds of a few meters in height at 220 to 410 m water depth (e.g. Fosså et al., 2005; Freiwald, 2003). The Holocene occurrence of CWC and coral mound growth, with earliest occurrence documented at 10.9 ka (López Correa et al., 2012), is thought to be driven by the presence of the NAC steering the tidal dynamics (Rüggeberg et al., 2011), which enhance the food supply (e.g. Frederiksen et al., 1992). During glacial periods the present-day Norwegian shelf was covered by the Fennoscandian ice sheet and, thus, could not serve as a habitat for CWC (Frank et al., 2011).

Off Scotland, Holocene CWC occurrence and coral mound development is documented for the Mingulay Reef Complex and the Darwin mounds (Fig. 6), two areas with small (<5 m) *L. pertusa* mounds (e.g. Roberts et al., 2005; Victorero et al., 2016). In the Mingulay Reef Complex (72–215 m water depth), CWC occurrence through the last 4.3 kyr is attributed to increased primary productivity and downward particle transport steered by strong tidal currents, caused by the NAC inflow over the shelf, which enhanced the food supply to the CWC (Douarin et al., 2013; Roberts et al., 2009; Roberts et al., 2005). At the Darwin Mounds (at 900–1100 m water depth) coral mound aggradation initiated at 10.3 ka and followed in various intervals since then (Victorero et al., 2016). Periods of reduced (or absent) mound growth are probably due to decreased or extremely enhanced current velocities (caused by the relative strength of the ENAW) resulting in either reduced food availability or coral abrasion (Victorero et al., 2016).

Slightly to the south, the Irish margin is among the best studied areas regarding CWC mound development, where investigations have been performed in the Porcupine Seabight and along the SW Rockall Trough. Coral mounds in the SW Rockall Trough, densely covered by *L. pertusa* and *M. oculata*, occur between 600 and 1100 m depth and may be up to 380m in height (the highest coral mounds discovered so far) (de Haas et al., 2009; Mienis et al., 2009; Van Weering et al., 2003). The CWC, presently located within the ENAW (e.g. Read, 2000), benefit from the continuous food supply of the local nepheloid layer and strong tidal currents (Duineveld et al., 2007; Kenyon et al., 2003; Mienis et al., 2007; White et al., 2005). *Lophelia pertusa* has been present in the area for the past 11.3 kyr (de Haas et al., 2009; Frank et al., 2009, 2005; Mienis et al., 2009), but two older ages, 246 ka and 363 ka, suggest additional earlier periods of coral mound aggradation interspersed by large hiatuses (Mienis et al., 2009). During cold climatic periods, a reduced food supply lowered CWC vitality decreasing coral coverage of the mounds, which were then exposed to erosion (Mienis et al., 2009).

Extensive studies were also performed in three CWC mound provinces within the Porcupine Seabight (Fig. 6): the Magellan mound province, characterized by many buried mounds of up to 90 m high, occurring in water depths of 450 to 700 m (De Mol et al., 2002; Huvenne et al., 2003); the Hovland mound province, consisting of high (up to 200 m) mounds with moderately developed CWC thickets, in water depths of 700 to 900 m (De Mol et al., 2002; Hovland et al., 1994; Huvenne et al., 2005); and the Belgica mound province, composed by mounds of up to 150 m-high that host some of the densest and best developed CWC thickets along the Irish margin, occurring in water depths of 600 to 900 m (De Mol et al., 2002; Foubert et al., 2005; Huvenne et al., 2005). A compilation of the Late Pleistocene (<500 ka) records from the Porcupine Seabight reveals that coral mound development was facilitated during interglacial and interstadial periods (Dorschel et al., 2007; Eisele et al., 2008; Frank et al., 2009; Kano et al., 2007; Raddatz et al., 2014). The Late Pleistocene, marked by an increased amplitude of glacial-interglacial changes, led to more severe local glacial conditions driven by a diminished primary production and a deepening of the pycnocline, between the ENAW and MOW (where food particles accumulate due to the density contrast), which reduced the food supply and prevented the occurrence of CWC (Dorschel et al., 2005; Kano et al., 2007; Raddatz et al., 2014). Therefore, mound growth in the Porcupine Seabight was restricted to warm-climate periods driven mostly by intermediate-depth circulation changes that increased the food supply, enhanced the current regime and led to a more favorable depositional environment (De Mol et al., 2007; Dorschel et al., 2005; Frank et al., 2009; Kano et al., 2007; Raddatz et al., 2014; Thierens et al., 2010).

Further south, along the Moroccan margin, southern Gulf of Cádiz (Fig. 6), hundreds of mounds (of up to 60 m height) covered with fossil *L. pertusa* and *M. oculata* exist at water depths between 400 and 960 m (Foubert et al., 2008; Wienberg et al., 2010, 2009). The mostly glacial CWC occurrence observed, with earliest occurrence documented at 430 ka (Frank et al., 2011; Wienberg et al., 2010, 2009), is mostly caused by increased glacial food supply driven by enhanced productivity (Foubert et al., 2008; Wienberg et al., 2010, 2009). This enhancement was most probably caused by an increased input of aeolian dust combined with the shift of the Azores Front towards the Gulf of Cádiz, which triggered an intense local upwelling (Wienberg et al., 2010).

Along the Mauritanian margin, a large field of 100 m-high mounds, dominantly covered by L. pertusa coral rubble, exists at water depths of about 450-550 m (Colman et al., 2005). The long-term coral mound development in the Mauritanian margin was investigated for the Banda Mound Province (Eisele et al., 2011; Westphal et al., 2007), where *L. pertusa* occurred during three distinct cool periods of the last glacial period (Eisele et al., 2011). CWC mound growth appears to have halted with the onset of the Holocene (C. Wienberg, personal communication). The glacial CWC mound growth off Mauritania has been linked to periods of locally increased productivity, which indicates that productivity might be the major steering factor for CWC in this area (Eisele et al., 2011).

The sum of studies regarding CWC occurrence and coral mound development in the NE Atlantic reveals a clear pattern. Over the past three glacial-interglacial cycles, enhanced coral mound aggradation in the northern NE Atlantic, from Norway to the Irish margin, occurred mostly during interglacial periods (de Haas et al., 2009; Dorschel et al., 2007; Douarin et al., 2013; Eisele et al., 2008; Frank et al., 2011, 2009, 2005; López Correa et al., 2012; Mienis et al., 2009; Raddatz et al., 2014; Roberts et al., 2005; Schröder-Ritzrau et al., 2005; Titschack et al., 2015). The CWC mound development in these areas is thought to be caused by enhanced food supply, which was associated to (i) enhanced interglacial surface ocean productivity, (ii) tidal or internal waves caused by the presence of specific water masses (as the NAC, at the Stjernsund Reef and the Mingulay Reef, Douarin et al., 2013; López Correa et al., 2012; Roberts et al., 2009; Rüggeberg et al., 2011; and the ENAW, at the Rockall Trough, Mienis et al., 2007); and/or (iii) the presence of a pycnocline between water masses, such as the ENAW and MOW in the Porcupine Seabight (De Mol et al., 2002; White, 2007). Stronger current intensities were also suggested as an additional factor favoring CWC mound growth during interglacial periods (Dorschel et al., 2005; Rüggeberg et al., 2007). On the contrary, CWC occurrence in the southern NE Atlantic mound areas is mostly restricted to glacial periods (Eisele et al., 2011; Frank et al., 2011; Wienberg et al., 2010, 2009). Both, off Morocco and off Mauritania, the increased food supply favorable for coral occurrence and pronounced coral mound development was mainly triggered by enhanced productivity (Eisele et al., 2011; Wienberg et al., 2010). The local productivity increase was either caused by an increased input of aeolian dust (in the Gulf of Cadiz, Wienberg et al., 2010) or by a sea-level driven displacement of the upwelling area towards the CWC mound province (off Mauritania, Eisele et al., 2011). Overall, the geographical distribution and sustained development of CWC mound areas within the NE Atlantic reveals a climate-dependent pattern following the glacial-interglacial changes of the sea surface conditions and intermediate-depth circulation (Frank et al., 2011).

1.4 The northwestern Atlantic cold-water coral mound areas

Framework-forming CWC have been documented for the NW Atlantic for over a century with the dominant species being *L. pertusa*, *Enallopsammia profunda*, *M. oculata, O. varicosa and Solenosmilia variabilis* (Reed, 2002). Over the last decades, also coral mounds have been observed, however (and in contrast with the NE Atlantic areas) not much is known about the real distribution and especially about the temporal development of these mounds. An investigation regarding the pattern of CWC occurrence and coral mound formation in the NW Atlantic, combined with a better understanding about their environmental controls, is essential to better comprehend the relationship between CWC mound development and the intermediate-depth circulation. The NW Atlantic coral mound areas documented so far are described below, organized in three regions: Gulf of Mexico, East Florida Strait and Florida-Hatteras Slope (Fig. 7).

1.4.1 Water mass distribution

The West Atlantic surface- and intermediate-depth circulation is dominated by strong currents, namely the Loop and Florida Currents and the Gulf Stream (Fig. 7). The southern and northern areas of the temperate North Atlantic present somewhat different water mass profiles and will, thus, be described separately, focusing on the two main working areas of this study off Campeche and off Cape Lookout.

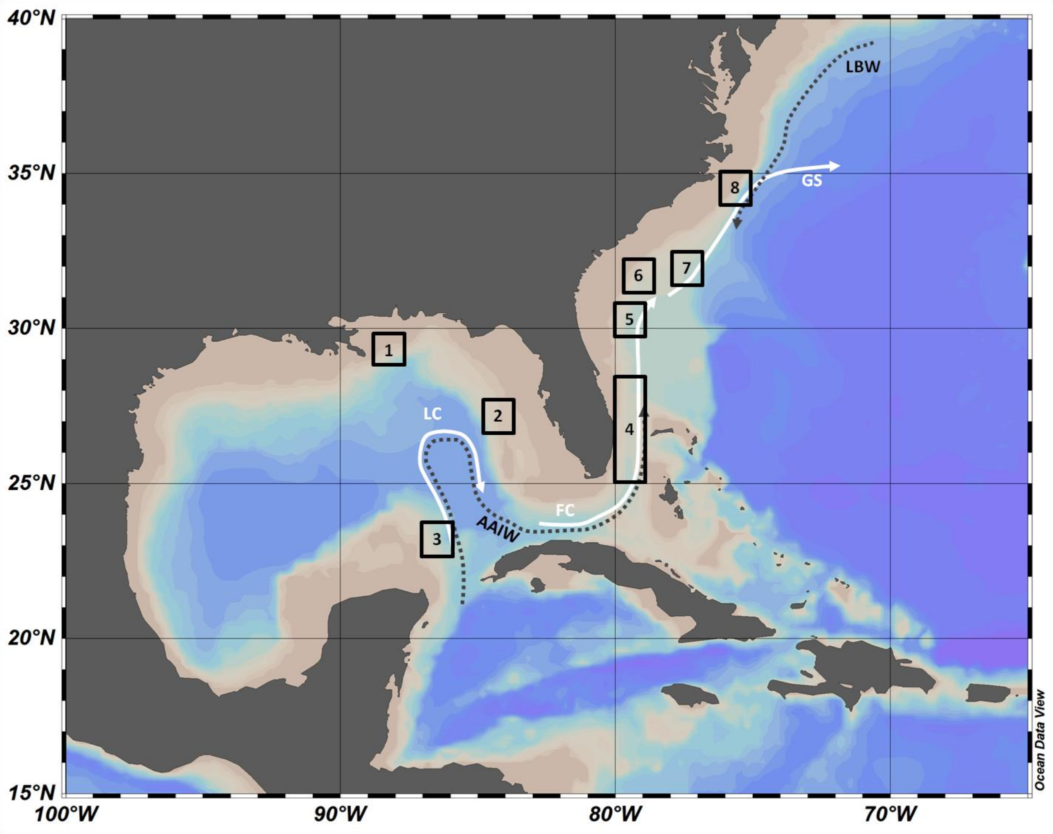

Figure 7. Approximate location of CWC mound areas in the NW Atlantic: (1) Vioska Knoll, (2) West Florida Slope and (3) Campeche Bank, in the Gulf of Mexico; (4) East Florida Strait; (5) off Georgia, (6) off Savannah, (7) Stetson Banks and (8) off Cape Lookout, at the Florida-Hatteras Slope; combined with the approximate path of the main surface currents: Loop Current (LC), Florida Current (FC) and Gulf Stream (GS); and of the intermediate water masses: Antarctic Intermediate Water (AAIW) and Labrador Basin Water (LBW).

The northward flow through the Yucatan Channel (between Mexico and Cuba), connecting the Caribbean Sea to the Gulf of Mexico, influences the coral mound areas located downstream at the Campeche margin (Fig. 7). At the Yucatan Strait, and thus at the entrance of the Gulf of Mexico, five water masses are constantly present. The two most superficial water masses (< 200 m water depth) are the Caribbean Surface Water (confined to depths shallower than 80 m) and the Subtropical Underwater (also called Subtropical Intermediate Water) (Merino, 1997; Rivas et al., 2005). At intermediate water depths two water masses are observed: the Tropical Atlantic Central Water (400–600 m water depth) and the AAIW (600–900 m water depth), which is characterized by its salinity minimum close to 34.8 (Merino, 1997; Rivas et al., 2005). The North Atlantic Deep Water is found below 1000 m water depth, as indicated by its oxygen and salinity maxima (Rivas et al., 2005).

The hydrological setting is different in the vicinity of the Cape Lookout CWC area (Fig. 7). The surface and subsurface flow is dominated by the Gulf Stream, which is a swift, warm and saline current reaching 1000 m depth. Current velocities decrease downward from 2-2.5 m s^{-1} at the surface to 0.2 m s^{-1} at depth (Richardson, 2001). Within this northward current a remaining cell of AAIW can still be detected at around 600-800 m water depth, characterized by salinities below 35 (Richardson, 1977). Inshore, between the Gulf Stream main axis and the continental shelf, the fresher and cooler Labrador Current (also called Labrador Basin Water) flows in a southward direction (Richardson, 1977) (Fig. 7). At depths greater than 1000 m, the Western Boundary Undercurrent flows south-westward beneath the mean axis of the Gulf Stream (Richardson, 2001).

Climate-induced changes in the upper intermediate water masses of the NW Atlantic are still poorly resolved (e.g. Huang et al., 2014; Pahnke et al., 2008). Studies on the temporal pattern of CWC occurrence and coral mound development at the NW Atlantic may improve the current knowledge on past changes in the intermediate water mass circulation.

1.4.2 Gulf of Mexico

Of the CWC mound areas reported from the Gulf of Mexico, the Viosca Knoll area is certainly one of the most exuberant. Located on the upper De Soto Slope, in the northeastern part of the gulf (Fig. 7), this mound is intensively colonized by *L. pertusa*, whose closely aggregated colonies attain up to 2 m in height and 3–4 m in length (Schroeder, 2002). A long-term (~1 year) monitoring of the environmental parameters at the seafloor revealed temperature (6.5–11.6 °C), salinity (34.9–35.4) and current speed (average 8 cm s^{-1}, max. 38 cm s^{-1}) conditions similar to settings in the NE Atlantic CWC areas (Mienis et al., 2012). Tidal periodicity was not observed at this site. Instead, a cyclic alternation in the flow direction imposes changes in the environmental setting, with the westward flow bringing warm turbid water influenced by the Mississippi outflow, while the eastward flow pushes colder and less turbid water upslope (Mienis et al., 2012). The nutrient-rich discharge of the Mississippi river increases the local primary productivity that may ultimately increase food availability to the CWC (Mienis et al., 2012). Not much is known regarding the past occurrence of CWC in this area; however, two *L. pertusa* ages of around 25 ka (Sulak, 2008) proof their presence also under cold, glacial conditions.

Another CWC area along the West Florida Slope (Fig. 7) has initially been described by Newton et al. (1987). The several dozens of 5-15 m high structures extending along the 500 m isobath and mostly covered by live and dead *L. pertusa* (Newton et al., 1987; Reed et al., 2006) were firstly considered to be rocky boulders overgrown by CWC (Hebbeln et al., 2012; Hübscher et al., 2010). However, a recent study has shown some of these high-relief structures (of up to 37 m high) to be coral mounds, as they are composed of unconsolidated sediments and coral rubble, topped by living and/or dead coral (Ross et al., 2016). The build-up of the coral mounds is favored by a locally enhanced primary productivity (caused by fluctuations of the Loop Current) and the occurrence of strong bottom currents (Ross et al., 2016 and references therein). The depth of occurrence of the sedimentary features reported for the West Florida Slope (mostly between depths of 450-550 m) coincide with the transition between the NACW and the AAIW (Hübscher et al., 2010; Ross et al., 2016). Although a study on the long-term coral mound development is still missing, radiocarbon dating of three dead coral samples revealed ages older than 40 ka (beyond the technique's temporal resolution) or around 31 ka old (Newton et al., 1987).

An additional coral mound area has been suggested in the southeastern Gulf of Mexico, at the eastern slope of the Campeche Bank (Fig. 7), where several mounded elongated structures were recorded between 530 and 610 m water depth (Hübscher et al., 2010). Also here, the observed sedimentary features correlate with the upper boundary of the AAIW, where higher current velocities have been suggested (Hübscher et al., 2010).

1.4.3 East Florida Strait

Several CWC mound areas have been described for the Florida Strait (Fig. 7), including the western margin of the Little Bahama Bank from where the first mounds in the region have been described (e.g. Messing et al., 1990; Neumann et al., 1977). These submersible-based studies identified elongated coral mounds occurring in 500-700 m water depth parallel to the prevailing northward bottom currents (Messing et al., 1990; Neumann et al., 1977). The mounds are hundreds of meters long and up to 50 m high and their tops contain living and dead CWC coverage (namely *L. pertusa* and *E. profunda*), which show an up-current orientation (Messing et al., 1990; Neumann et al., 1977). Bottom currents in this study area are in the order of 10-20 ± 12-14 cm s^{-1} and temperatures range from 10 to 12 °C (Leaman et al., 1987). CWC and associated fauna are preferentially attached to the carbonate cemented substrate and baffle suspended matter further facilitating its deposition (Neumann et al., 1977). Although there is yet no data to reconstruct coral mound development in this area, one CWC radiocarbon dating revealed an approximate age of 32 cal ka BP (Neumann et al., 1977).

Mullins et al. (1981) described mounds along the northern margin of the Little Bahama Bank that are located in water depths of 1,000-1,300 m. These mounds are up to 40 m high and bear a prolific community of CWC such as *E. profunda* and *M. oculata*, however without any evidence for the occurrence of *L. pertusa* (Mullins et al., 1981).

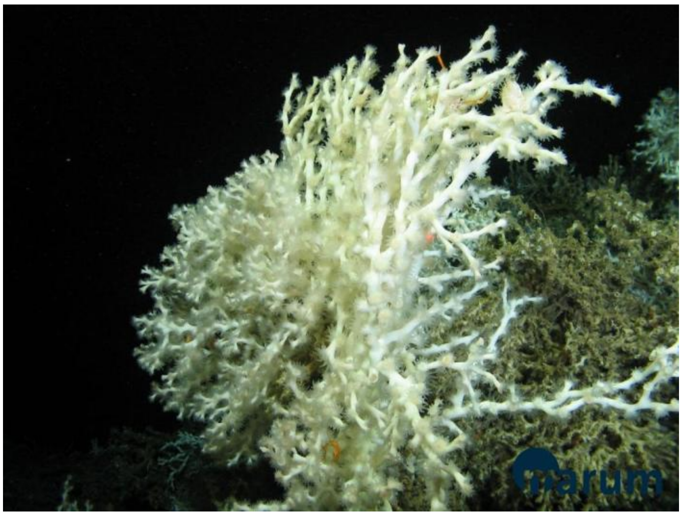

Figure 8. Thicket of living *L. pertusa* growing over dead coral framework on a CWC mound of the Great Bahama Bank, East Florida Strait. Photo credits: MARUM.

More recently, a review on the CWC mounds of the southeastern margin of the United States listed numerous mounds along the Florida Strait (Reed et al., 2006). Mounds of the northern East Florida Strait, are located in 670-870 m water depth and are covered by dense 1-m tall thickets of *L. pertusa* and *E. profunda*, with varying amounts of live coral (at the mound tops) and coral rubble (Reed et al., 2006). Mounds further south, at the base of the Miami Terrace escarpment (at around 670 m), are covered by scattered 30–60 cm-high thickets of *L. pertusa*, *E. profunda* and *M. oculata* (Reed et al., 2006). Grasmueck et al., (2006) described a mound field in the western margin of Great Bahama Bank (at about 24.5° N; and 600–800 m water depth) that consists of more than 200 coral mounds reaching up to 90 m high, with the peak of one of the tallest mounds being covered by living corals (Fig. 8). Interestingly, the north facing slope of this mound was covered with dead coral rubble (Grasmueck et al., 2006). These mounds are aligned in east-westerly direction and are subject to a tidal north-south current regime (of up to 50 cm s^{-1}) that reverses on average every 6 hours (Grasmueck et al., 2006). Such a dynamic oceanographic environment affects local mound organisms and may be the cause for the observed diversity in mound morphology (Grasmueck et al., 2006). Another detailed mapping study was performed at three sites of the toe of slope of Great Bahama Bank (between 580-840 m water depth) and revealed this area as a major coral mound region

(Correa et al., 2012). The mounds are characterized by variable heights (up to 83 m), areas, shapes and orientations. However, living CWC colonies of predominantly *L. pertusa* and *E. profunda* (up to 2 m high) were observed at the mound tops at all three sites (Correa et al., 2012). Also this study observed the north–south flowing tidal current, reversing approximately every six hours, which likely contributes to the observed mound complexity (Correa et al., 2012). Alternatively, the spatial distribution and alignment of mounds was suggested to be related to gravity mass deposits (Correa et al., 2012).

1.4.4 Florida-Hatteras Slope

Paull et al. (2000) reported about a CWC mound area off southern Georgia. Several coral mounds, often exceeding 40 m in height, were found between 440 and 914 m water depth, with the largest mounds concentrated in 500-750 m depth (Paull et al., 2000). These structures have very steep slopes (30-60°), have their crests and up-stream flanks coated by living CWC (mainly *L. pertusa*) and may reveal cemented crust exposed by erosion (Paull et al., 2000; Reed, 2002). Constantly enhanced current speeds (of up to 100 cm s^{-1}) provide an increased food supply to the CWC communities on the southern flanks and the crests. Early diagenesis involved in the formation of cemented crusts might contribute to stabilize the steep-sided mounds (Paull et al., 2000). One dated fossil coral sample from the mounds revealed a radiocarbon age of 20 cal ka BP (Paull et al., 2000), suggesting that CWC lived in this region not only during interglacial but also during glacial times.

Further to the north, the so-called Savannah coral mounds are elongated structures 10-83 m high that occur at depths of 490–550 m (Millman et al., 1967; Reed et al., 2006). Oriented NNE–SSW, these mounds are covered by variable amounts of live colonies of *E. profunda* and *L. pertusa* and coral rubble (Millman et al., 1967; Reed et al., 2006).

The Stetson Banks are located at the South Carolina margin (Reed et al., 2006; Stetson et al., 1962). There, over 200 mounds are found between about 510 and 870 m water depth. These are mostly covered by *E. profunda*, but with *L. pertusa* being concentrated at the mound tops (Stetson et al., 1962). One of the tallest peaks investigated (ca. 150 m high, with 3-4 m-high ridges) was almost completely covered by live and dead colonies and coral rubble of *L. pertusa*, in association with colonies of *E. profunda* and *S. variabilis* (Reed et al., 2006).

Further north, at the North Carolina margin lays one of the best documented CWC areas within the Florida-Hatteras Slope, the Cape Lookout CWC area (e.g. Mienis et al., 2014; Ross and Quattrini, 2007). The mounds occur between 320 and 550 m water depth and may rise 80-100 m above the seafloor with steep slopes of up to 60° (Mienis et al., 2014; Ross and Quattrini, 2007). A matrix composed of coral rubble and sediment is covered by live and dead *L. pertusa* colonies (of up to 3 m high) occurring close to the summits of the SSW side of the mounds facing the strongest currents (Mienis et al., 2014; Ross and Quattrini, 2007). The mounds are occasionally affected by events of increased temperature (up to 9 °C increase), salinity and flow speed (towards the NNE), related to the occurrence of Gulf Stream meanders (Mienis et al., 2014). These events also coincided with increased near-bed acoustic backscatter, likely related to resuspension of seabed particles, which might sand blast the corals. Such living conditions were considered extreme for the CWC and potentially limiting the mound growth in this area (Mienis et al., 2014).

1.5 Motivation and Objectives

The geographical distribution and temporal development of CWC mound areas within the NE Atlantic reveals a see-saw pattern with thriving CWC contributing to coral mound aggradation occurring during interglacial periods in the northern (> 50° N) areas and during glacial periods in the southern (< 37° N) areas. This suggests a climate-dependent pattern following glacial-interglacial changes of the surface ocean conditions and the intermediate-depth circulation (Frank et al., 2011).

Also for the NW Atlantic several CWC mound areas have been described (e.g. Reed et al., 2006). Studies regarding the current environmental conditions at some of these areas suggest that living CWC may benefit from enhanced food supply associated with the presence of (i) strong bottom currents (off the southern Georgia; Paull et al., 2000), (ii) tidal currents (at the East Florida Strait; Correa et al., 2012; Grasmueck et al., 2006) or (iii) a local increase in primary productivity caused by the nutrient-rich Mississippi river discharge (at the Viosca Knoll; Mienis et al., 2012) or by the occurrence of an upwelling cell (at the West Florida Slope; Ross et al., 2016). While the presence of living reef-like structures in the NW Atlantic advocates for favorable conditions for CWC at present, a limited number of CWC radiocarbon ages ranging between 20 cal ka BP and >40 cal ka BP (Neumann et al., 1977; Newton et al., 1987; Paull et al., 2000; Sulak, 2008) further suggests that conditions were also favorable during the last glacial. This study aims to elucidate the temporal pattern of CWC occurrence in the NW Atlantic by performing the first investigation of the long-term CWC mound development.

Therefore, the main objectives of this study are:

- To identify the environmental factors (and especially the hydrological settings) influencing CWC proliferation in the NW Atlantic coral mound areas;
- To identify periods of sustained CWC growth in coral mound areas of the NW Atlantic, especially regarding the existence of a temporal pattern of CWC occurrence and coral mound growth.

References

Aït-Ameur, N., Goyet, C., 2006. Distribution and transport of natural and anthropogenic CO2 in the Gulf of Cádiz. Deep Sea Res. Part II Top. Stud. Oceanogr. 53, 1329–1343. doi:10.1016/j.dsr2.2006.04.003

Colman, J.G., Gordon, D.M., Lane, A.P., Forde, M.J., Fitzpatrick, J.J., 2005. Carbonate mounds off Mauritania, Northwest Africa: status of deep-water corals and implications for management of fishing and oil exploration activities, in: Freiwald, A., Roberts, J.M. (Eds.), Cold-Water Corals and Ecosystems, Erlangen Earth Conference Series. Springer-Verlag, Berlin/Heidelberg, pp. 417–441.

Correa, T.B.S., Grasmueck, M., Eberli, G.P., Reed, J.K., Verwer, K., Purkis, S., 2012. Variability of cold-water coral mounds in a high sediment input and tidal current regime, Straits of Florida. Sedimentology 59, 1278–1304. doi:10.1111/j.1365-3091.2011.01306.x

Davies, A.J., Duineveld, G., Lavaleye, M., Bergman, M.J., van Haren, H., Roberts, J.M., 2009. Downwelling and deep-water bottom currents as food supply mechanisms to the cold-water coral Lophelia pertusa (Scleractinia) at the Mingulay Reef Complex. Limnol. Oceanogr. 54, 620–629. doi:10.4319/lo.2009.54.2.0620

Davies, A.J., Duineveld, G.C.A., van Weering, T.C.E., Mienis, F., Quattrini, A.M., Seim, H.E., Bane, J.M., Ross, S.W., 2010. Short-term environmental variability in cold-water coral habitat at Viosca Knoll, Gulf of Mexico. Deep. Res. Part I Oceanogr. Res. Pap. 57, 199–212. doi:10.1016/j.dsr.2009.10.012

Davies, A.J., Guinotte, J.M., 2011. Global habitat suitability for framework-forming cold-water corals. PLoS One 6, e18483. doi:10.1371/journal.pone.0018483

Davies, A.J., Wisshak, M., Orr, J.C., Murray Roberts, J., 2008. Predicting suitable habitat for the cold-water coral Lophelia pertusa (Scleractinia). Deep Sea Res. Part I Oceanogr. Res. Pap. 55, 1048–1062. doi:10.1016/j.dsr.2008.04.010

de Haas, H., Mienis, F., Frank, N., Richter, T.O., Steinacher, R., de Stigter, H., van der Land, C., van Weering, T.C.E., 2009. Morphology and sedimentology of (clustered) cold-water coral mounds at the south Rockall Trough margins, NE Atlantic Ocean. Facies 55, 1–26. doi:10.1007/s10347-008-0157-1

De Mol, B., Kozachenko, M., Wheeler, A., Alvares, H., Henriet, J.-P., Olu-Le Roy, K., 2007.

Thérèse Mound: a case study of coral bank development in the Belgica Mound Province, Porcupine Seabight. Int. J. Earth Sci. 96, 103–120. doi:10.1007/s00531-005-0496-x

De Mol, B., Van Rensbergen, P., Pillen, S., Van Herreweghe, K., Van Rooij, D., McDonnell, a, Huvenne, V., Ivanov, M., Swennen, R., Henriet, J.., 2002. Large deep-water coral banks in the Porcupine Basin, southwest of Ireland. Mar. Geol. 188, 193–231. doi:10.1016/S0025-3227(02)00281-5

Dorschel, B., Hebbeln, D., Rueggeberg, A., Dullo, W., Freiwald, A., 2005. Growth and erosion of a cold-water coral covered carbonate mound in the Northeast Atlantic during the Late Pleistocene and Holocene. Earth Planet. Sci. Lett. 233, 33–44. doi:10.1016/j.epsl.2005.01.035

Dorschel, B., Hebbeln, D., Rüggeberg, A., Dullo, C., 2007. Carbonate budget of a cold-water coral carbonate mound: Propeller Mound, Porcupine Seabight. Int. J. Earth Sci. 96, 73–83. doi:10.1007/s00531-005-0493-0

Douarin, M., Elliot, M., Noble, S.R., Sinclair, D., Henry, L.A., Long, D., Moreton, S.G., Murray Roberts, J., 2013. Growth of north-east Atlantic cold-water coral reefs and mounds during the Holocene: A high resolution U-series and 14C chronology. Earth Planet. Sci. Lett. 375, 176–187. doi:10.1016/j.epsl.2013.05.023

Duineveld, G.C.A., Lavaleye, M.S.S., Bergman, M.J.N., de Stigter, H., Mienis, F., 2007. Trophic structure of a cold-water coral mound community (Rockall Bank, NE Atlantic) in relation to the near-bottom particle supply and current regime. Bull. Mar. Sci. 81, 449–467.

Dullo, W.C., Flögel, S., Rüggeberg, A., 2008. Cold-water coral growth in relation to the hydrography of the Celtic and Nordic European continental margin. Mar. Ecol. Prog. Ser. 371, 165–176. doi:10.3354/meps07623

Eisele, M., Frank, N., Wienberg, C., Hebbeln, D., López Correa, M., Douville, E., Freiwald, A., 2011. Productivity controlled cold-water coral growth periods during the last glacial off Mauritania. Mar. Geol. 280, 143–149. doi:10.1016/j.margeo.2010.12.007

Eisele, M., Hebbeln, D., Wienberg, C., 2008. Growth history of a cold-water coral covered carbonate mound — Galway Mound, Porcupine Seabight, NE-Atlantic. Mar. Geol. 253, 160–169. doi:10.1016/j.margeo.2008.05.006

Fosså, J.H., Lindberg, B., Christensen, O., Lundälv, T., Svellingen, I., Mortensen, P.B., Alvsvåg, J., 2005. Mapping of Lophelia reefs in Norway: experiences and survey methods, in: Freiwald, P.D.A., Roberts, D.J.M. (Eds.), Cold-Water Corals and Ecosystems. Springer Berlin Heidelberg, pp. 359–391. doi:10.1007/3-540-27673-4_18

Foubert, A., Depreiter, D., Beck, T., Maignien, L., Pannemans, B., Frank, N., Blamart, D., Henriet, J.-P., 2008. Carbonate mounds in a mud volcano province off north-west Morocco: Key to processes and controls. Mar. Geol. 248, 74–96. doi:10.1016/j.margeo.2007.10.012

Foubert, a., Beck, T., Klages, M., Wheeler, A.J., Thiede, J., Party, P.A.-X.S., 2005. New view of the Belgica Mounds, Porcupine Seabight, NE Atlantic: preliminary results from the Polarstern ARK-XIX/3a ROV cruise, in: Freiwald, A., Roberts, J.M. (Eds.), Cold-Water Corals and Ecosystems. Springer-Verlag Berlin Heidelberg, pp. 403–415. doi:10.1007/3-540-

27673-4_20

Frank, N., Freiwald, a., Correa, M.L., Wienberg, C., Eisele, M., Hebbeln, D., Van Rooij, D., Henriet, J.-P., Colin, C., van Weering, T., de Haas, H., Buhl-Mortensen, P., Roberts, J.M., De Mol, B., Douville, E., Blamart, D., Hatte, C., 2011. Northeastern Atlantic cold-water coral reefs and climate. Geology 39, 743–746. doi:10.1130/G31825.1

Frank, N., Lutringer, A., Paterne, M., Blamart, D., Henriet, J., Rooij, D. Van, Weering, T.C.E. Van, Cea-cnrs, D.R., Terrasse, A. De, Cedex, Y., 2005. Deep-water corals of the northeastern Atlantic margin: carbonate mound evolution and upper intermediate water ventilation during the Holocene, in: Freiwald, A., Roberts, J.M. (Eds.), Cold-Water Corals and Ecosystems. Springer-Verlag Berlin Heidelberg, pp. 113–133. doi:10.1007/3-540-27673-4_6

Frank, N., Ricard, E., Lutringer-Paquet, A., van der Land, C., Colin, C., Blamart, D., Foubert, A., Van Rooij, D., Henriet, J.-P., de Haas, H., van Weering, T., 2009. The Holocene occurrence of cold water corals in the NE Atlantic: Implications for coral carbonate mound evolution. Mar. Geol. 266, 129–142. doi:10.1016/j.margeo.2009.08.007

Frederiksen, R., Jensen, A., Westerberg, H., 1992. The distribution of the scleractinian coral Lophelia pertusa around the Faroe Islands and the relation to internal tidal mixing. Sarsia 77, 157–171. doi:10.1080/00364827.1992.10413502

Freiwald, A., 2003. Reef-Forming Cold-Water Corals, in: Wefer, G., Billett, D., Hebbeln, D., Jørgensen, B.B., Schlüter, M., van Weering, T.C.E. (Eds.), Ocean Margin Systems. Springer Berlin Heidelberg, Berlin, Heidelberg, pp. 365–385. doi:10.1007/978-3-662-05127-6_23

Grasmueck, M., Eberli, G.P., Viggiano, D.A., Correa, T., Rathwell, G., Luo, J., 2006. Autonomous underwater vehicle (AUV) mapping reveals coral mound distribution, morphology, and oceanography in deep water of the Straits of Florida. Geophys. Res. Lett. 33, 2–7. doi:10.1029/2006GL027734

Hebbeln, D., Wienberg, C., Beuck, L., Dehning, K., Dullo, W.-C., Eberli, G., Freiwald, A., Glogowski, S., Garlichs, T., Jansen, F., Joseph, N., Klann, M., Matos, L., Nowald, N., Reyes, H., Ruhland, G., Taviani, M., Wilke, T., Wilsenack, M., Wintersteller, P., 2012. West Atlantic Cold-Water Coral Ecosystems: The west side story, R/V Maria S. Merian Cruise No. 20, Leg 4.

Hovland, M., Croker, P.F., Martin, M., 1994. Fault-associated seabed mounds (carbonate knolls?) off western Ireland and north-west Australia. Mar. Pet. Geol. 11, 232–246. doi:10.1016/0264-8172(94)90099-X

Huang, K.-F., Oppo, D.W., Curry, W.B., 2014. Decreased influence of Antarctic intermediate water in the tropical Atlantic during North Atlantic cold events. Earth Planet. Sci. Lett. 389, 200–208. doi:10.1016/j.epsl.2013.12.037

Hübscher, C., Dullo, C., Flögel, S., Titschack, J., Schönfeld, J., 2010. Contourite drift evolution and related coral growth in the eastern Gulf of Mexico and its gateways. Int. J. Earth Sci. 99, 191–206. doi:10.1007/s00531-010-0558-6

Huvenne, V.A.I., Beyer, A., de Haas, H., Dekindt, K., Henriet, J.P., Kozachenko, M., Olu-Le Roy, K., Wheeler, A.J., TOBI/Pelagia 197, CARACOLE Cruise Participants, 2005. The seabed appearance of different coral bank provinces in the Porcupine Seabight, NE Atlantic: results from sidescan sonar and ROV seabed mapping, in: Freiwald, A., Roberts, J.M. (Eds.), Cold-Water Corals and Ecosystems. Springer-Verlag Berlin Heidelberg, pp. 535–569. doi:10.1007/3-540-27673-4_27

Huvenne, V.A.I., De Mol, B., Henriet, J.P., 2003. A 3D seismic study of the morphology and spatial distribution of buried coral banks in the Porcupine Basin, SW of Ireland. Mar. Geol. 198, 5–25. doi:10.1016/S0025-3227(03)00092-6

Inall, M., Gillibrand, P., Griffiths, C., MacDougal, N., Blackwell, K., 2009. On the oceanographic variability of the North-West European Shelf to the West of Scotland. J. Mar. Syst. 77, 210–226. doi:10.1016/j.jmarsys.2007.12.012

Kano, A., Ferdelman, T.G., Williams, T., Henriet, J.-P., Ishikawa, T., Kawagoe, N., Takashima, C., Kakizaki, Y., Abe, K., Sakai, S., Browning, E.L., Li, X., 2007. Age constraints on the origin and growth history of a deep-water coral mound in the northeast Atlantic drilled during Integrated Ocean Drilling Program Expedition 307. Geology 35, 1051. doi:10.1130/G23917A.1

Kenyon, N.H., Akhmetzhanov, A.M., Wheeler, A.J., van Weering, T.C.E., de Haas, H., Ivanov, M.K., 2003. Giant carbonate mud mounds in the southern Rockall Trough. Mar. Geol. 195, 5–30. doi:10.1016/S0025-3227(02)00680-1

Leaman, K.D., Molinari, R.L., Vertes, P.S., 1987. Structure and Variability of the Florida Current at 27°N: April 1982–July 1984. J. Phys. Oceanogr. 17, 565–583.

López Correa, M., Montagna, P., Joseph, N., Rüggeberg, A., Fietzke, J., Flögel, S., Dorschel, B., Goldstein, S.L., Wheeler, A., Freiwald, A., 2012. Preboreal onset of cold-water coral growth beyond the Arctic Circle revealed by coupled radiocarbon and U-series dating and neodymium isotopes. Quat. Sci. Rev. 34, 24–43. doi:10.1016/j.quascirev.2011.12.005

Merino, M., 1997. Upwelling on the Yucatan Shelf: hydrographic evidence. J. Mar. Syst. 13, 101–121. doi:10.1016/S0924-7963(96)00123-6

Messing, C.G., Neumann, A.C., Lang, J.C., 1990. Biozonation of deep-water lithoherms and associated hardgrounds in the Northeastern straits of Florida, USA. Palaios 5, 15–33. doi:10.2307/3514994

Mienis, F., de Stigter, H.C., White, M., Duineveld, G., de Haas, H., van Weering, T.C.E., 2007. Hydrodynamic controls on cold-water coral growth and carbonate-mound development at the SW and SE Rockall Trough Margin, NE Atlantic Ocean. Deep Sea Res. I 54, 1655–1674. doi:10.1016/j.dsr.2007.05.013

Mienis, F., Duineveld, G.C.A., Davies, A.J., Lavaleye, M.M.S., Ross, S.W., Seim, H., Bane, J., van Haren, H., Bergman, M.J.N., de Haas, H., Brooke, S., van Weering, T.C.E., 2014. Cold-water coral growth under extreme environmental conditions, the Cape Lookout area, NW Atlantic. Biogeosciences 11, 2543–2560. doi:10.5194/bg-11-2543-2014

Mienis, F., Duineveld, G.C.A., Davies, A.J., Ross, S.W., Seim, H., Bane, J., van Weering, T.C.E., 2012. The influence of near-bed hydrodynamic conditions on cold-water corals in the Viosca Knoll area, Gulf of Mexico. Deep. Res. Part I Oceanogr. Res. Pap. 60, 32–45. doi:10.1016/j.dsr.2011.10.007

Mienis, F., van der Land, C., de Stigter, H.C., van de Vorstenbosch, M., de Haas, H., Richter, T., van Weering, T.C.E., 2009. Sediment accumulation on a cold-water carbonate mound at the Southwest Rockall Trough margin. Mar. Geol. 265, 40–50. doi:10.1016/j.margeo.2009.06.014

Millman, J.D., Manheim, F.T., Pratt, R.M., Zarudzki, E.F.K., 1967. ALVIN dives on the continental margin off the southeastern United States, July 2-13, 1967. doi:10.1575/1912/1521

Mittelstaedt, E., 1991. The ocean boundary along the northwest African coast: Circulation and oceanographic properties at the sea surface. Prog. Oceanogr. 26, 307–355. doi:10.1016/0079-6611(91)90011-A

Mullins, H.T., Newton, C.R., Heath, K., Van Buren, H.M., 1981. Modern deep-water coral mounds north of Little Bahama Bank; criteria for recognition of deep-water coral bioherms in the rock record. J. Sediment. Res. 51, 999 LP-1013.

Neumann, A.C., Kofoed, J.W., Keller, G.H., 1977. Lithoherms in the Straits of Florida. Geology 5, 4–10.

New, A., Smythe-Wright, D., 2001. Aspects of the circulation in the Rockall Trough. Cont. Shelf Res. 21, 777–810. doi:10.1016/S0278-4343(00)00113-8

Newton, C.R., Mullins, H.T., Gardulski, A.F., Hine, A.C., Dix, G.R., 1987. Coral Mounds on the West Florida Slope: Unanswered Questions regarding the Development of Deep-Water Banks. Palaios 2, 359–367.

Pahnke, K., Goldstein, S.L., Hemming, S.R., 2008. Abrupt changes in Antarctic Intermediate Water circulation over the past 25,000 years. Nat. Geosci. 1, 870–874. doi:10.1038/ngeo360

Paull, C.., Neumann, a. ., am Ende, B.., Ussler III, W., Rodriguez, N.., 2000. Lithoherms on the Florida–Hatteras slope. Mar. Geol. 166, 83–101. doi:10.1016/S0025-3227(00)00003-7

Raddatz, J., Rüggeberg, A., Liebetrau, V., Foubert, A., Hathorne, E.C., Fietzke, J., Eisenhauer, A., Dullo, W.-C., 2014. Environmental boundary conditions of cold-water coral mound growth over the last 3 million years in the Porcupine Seabight, Northeast Atlantic. Deep Sea Res. Part II Top. Stud. Oceanogr. 99, 227–236. doi:10.1016/j.dsr2.2013.06.009

Read, J.., 2000. CONVEX-91: water masses and circulation of the Northeast Atlantic subpolar gyre. Prog. Oceanogr. 48, 461–510. doi:10.1016/S0079-6611(01)00011-8

Reed, J.K., 2002. Comparison of deep-water coral reefs and lithoherms off southeastern USA. Hydrobiologia 471, 57–69.

Reed, J.K., Weaver, D.C., Pomponi, S. a., 2006. Habitat and fauna of Deep-Water Lophelia Pertusa Coral Reefs Off the Southeastern U.S.: Blake Plateau , Straits of Florida , and Gulf of Mexico. Bull. Mar. Sci. 78, 343–375.

Richardson, P.L., 2001. Florida Current, Gulf Stream, and Labradro Current, in: Steele, J.H., Turekian, K.K., Thorpe, S.A. (Eds.), Encyclopedia of Ocean Sciences. Elsevier, pp. 1054–1064. doi:10.1006/rwos.2001.0357

Richardson, P.L., 1977. On the crossover between the Gulf Stream and the Western Boundary Undercurrent. Deep Sea Res. 24, 139–159. doi:10.1016/0146-6291(77)90549-5

Rivas, D., Badan, A., Ochoa, J., 2005. The Ventilation of the Deep Gulf of Mexico. J. Phys. Oceanogr. 35, 1763–1781. doi:10.1175/JPO2786.1

Roberts, J.M., Brown, C.J., Long, D., Bates, C.R., 2005. Acoustic mapping using a multibeam echosounder reveals cold-water coral reefs and surrounding habitats. Coral Reefs 24, 654–669. doi:10.1007/s00338-005-0049-6

Roberts, J.M., Davies, A.J., Henry, L.A., Dodds, L.A., Duineveld, G.C.A., Lavaleye, M.S.S., Maier, C., van Soest, R.W.M., Bergman, M.J.N., Huhnerbach, V., Huvenne, V.A.I., Sinclair, D.J., Watmough, T., Long, D., Green, S.L., van Haren, H., 2009. Mingulay reef complex: an interdisciplinary study of cold-water coral habitat, hydrography and biodiversity. Mar. Ecol. Prog. Ser. 397, 139–151. doi:10.3354/meps08112

Roberts, J.M., Wheeler, A., Freiwald, A., Cairns, S., 2009. Cold-Water Corals: The Biology and Geology of Deep-Sea Coral Habitats. Cambrigde University Press.

Roberts, J.M., Wheeler, A.J., Freiwald, A., 2006. Reefs of the deep: the biology and geology of cold-water coral ecosystems. Science 312, 543–547. doi:10.1126/science.1119861

Ross, S.W., Quattrini, A.M., 2007. The fish fauna associated with deep coral banks off the southeastern United States. Deep Sea Res. Part I Oceanogr. Res. Pap. 54, 975–1007. doi:10.1016/j.dsr.2007.03.010

Ross, S.W., Rhode, M., Brooke, S., 2016. Deep-Sea Coral and Hardbottom Habitats on the West Florida Slope, Eastern Gulf of Mexico. Deep Sea Res. Part I Oceanogr. Res. Pap. 120, 14–28. doi:10.1016/j.dsr.2016.12.005

Rüggeberg, A., Dullo, C., Dorschel, B., Hebbeln, D., 2007. Environmental changes and growth history of a cold-water carbonate mound (Propeller Mound, Porcupine Seabight). Int. J. Earth Sci. 96, 57–72. doi:10.1007/s00531-005-0504-1

Rüggeberg, A., Flögel, S., Dullo, W.C., Hissmann, K., Freiwald, A., 2011. Water mass characteristics and sill dynamics in a subpolar cold-water coral reef setting at Stjernsund, northern Norway. Mar. Geol. 282, 5–12. doi:10.1016/j.margeo.2010.05.009

Schröder-Ritzrau, A., Freiwald, A., Mangini, A., 2005. U/Th-dating of deep-water corals from the eastern North Atlantic and the western Mediterranean Sea, in: Freiwald, A., Roberts, J.M. (Eds.), Cold-Water Corals and Ecosystems, Erlangen Earth Conference Series. Springer-Verlag, Berlin/Heidelberg, pp. 157–172. doi:10.1007/3-540-27673-4

Schroeder, W.W., 2002. Observations of Lophelia pertusa and the surficial geology at a deep-water site in the northeastern Gulf of Mexico. Hydrobiologia 471, 29–33. doi:10.1023/A:1016580632501

Stetson, T.R., Squires, D.F., Pratt, R.M., 1962. Coral banks occurring in deep water on the Blake Plateau. American Museum novitates ; no. 2114.

Stramma, L., Schott, F., 1999. The mean flow field of the tropical Atlantic Ocean. Deep Sea Res. Part II Top. Stud. Oceanogr. 46, 279–303. doi:10.1016/S0967-0645(98)00109-X

Sulak, K.J., 2008. Origins, composition, age and structural diversification of Viosca Knoll Lophelia coral reefs and substrate - A synopsis of preliminary results, in: OCS Reports. U. S. Minerals Management Service.

Thierens, M., Browning, E., Pirlet, H., Loutre, M.F., Dorschel, B., Huvenne, V.A.I., Titschack, J., Colin, C., Foubert, A., Wheeler, A.J., 2013. Cold-water coral carbonate mounds as unique palaeo-archives: The Plio-Pleistocene Challenger Mound record (NE Atlantic). Quat. Sci. Rev. 73, 14–30. doi:10.1016/j.quascirev.2013.05.006

Thierens, M., Titschack, J., Dorschel, B., Huvenne, V.A.I., Wheeler, A.J., Stuut, J.B., O'Donnell, R., 2010. The 2.6 Ma depositional sequence from the Challenger cold-water coral carbonate mound (IODP Exp. 307): Sediment contributors and hydrodynamic palaeo-environments. Mar. Geol. 271, 260–277. doi:10.1016/j.margeo.2010.02.021

Titschack, J., Baum, D., De Pol-Holz, R., López Correa, M., Forster, N., Flögel, S., Hebbeln, D., Freiwald, A., 2015. Aggradation and carbonate accumulation of Holocene Norwegian cold-water coral reefs. Sedimentology 62, 1873–1898. doi:10.1111/sed.12206

Titschack, J., Thierens, M., Dorschel, B., Schulbert, C., Freiwald, A., Kano, A., Takashima, C., Kawagoe, N., Li, X., 2009. Carbonate budget of a cold-water coral mound (Challenger Mound, IODP Exp. 307). Mar. Geol. 259, 36–46. doi:10.1016/j.margeo.2008.12.007

Van Weering, T.C.E., De Haas, H., De Stigter, H.C., Lykke-Andersen, H., Kouvaev, I., 2003. Structure and development of giant carbonate mounds at the SW and SE Rockall Trough margins, NE Atlantic Ocean. Mar. Geol. 198, 67–81. doi:10.1016/S0025-3227(03)00095-1

Vermeulen, N.J., 1997. Hydrography, Surface Geology and Geomorphology of the Deep Water Sedimentary Basins to the West of Ireland. Mar. Resour. Ser.

Victorero, L., Blamart, D., Pons-Branchu, E., Mavrogordato, M.N., Huvenne, V.A.I., 2016. Reconstruction of the formation history of the Darwin Mounds, N Rockall Trough: How the dynamics of a sandy contourite affected cold-water coral growth. Mar. Geol. 378, 186–195. doi:10.1016/j.margeo.2015.12.001

Westphal, H., Freiwald, A., Hanebuth, T., Eisele, M., Gürs, K., Heindel, K., Michel, J., Reumont, J. v, 2007. Report of Poseidon cruise 346—MACUMA: integrating carbonates, siliciclastics and deep-water reefs for understanding a complex environment, Las Palmas (Spain)–Las Palmas (Spain), 28.12. 2006–15.1. 2007.

White, M., 2007. Benthic dynamics at the carbonate mound regions of the Porcupine Sea Bight continental margin. Int. J. Earth Sci. 96, 1–9. doi:10.1007/s00531-006-0099-1

White, M., Mohn, C., Stigter, H., Mottram, G., 2005. Deep-water coral development as a function of hydrodynamics and surface productivity around the submarine banks of the Rockall Trough, NE Atlantic, in: Freiwald, A., Roberts, J.M. (Eds.), Cold-Water Corals and Ecosystems. Springer-Verlag Berlin Heidelberg, pp. 503–514. doi:10.1007/3-540-27673-4_25

Wienberg, C., Frank, N., Mertens, K.N., Stuut, J.-B., Marchant, M., Fietzke, J., Mienis, F., Hebbeln, D., 2010. Glacial cold-water coral growth in the Gulf of Cádiz: Implications of increased palaeo-productivity. Earth Planet. Sci. Lett. 298, 405–416. doi:10.1016/j.epsl.2010.08.017

Wienberg, C., Hebbeln, D., Fink, H.G., Mienis, F., Dorschel, B., Vertino, A., Correa, M.L., Freiwald, A., 2009. Scleractinian cold-water corals in the Gulf of Cádiz—First clues about their spatial and temporal distribution. Deep Sea Res. Part I Oceanogr. Res. Pap. 56, 1873–1893. doi:10.1016/j.dsr.2009.05.016

Wienberg, C., Titschack, J., 2017. Framework-Forming Scleractinian Cold-Water Corals Through Space and Time: A Late Quaternary North Atlantic Perspective, in: Rossi, S., Bramanti, L., Gori, A., del Valle, C. (Eds.), Marine Animal Forests: The Ecology of Benthic Biodiversity Hotspots. Springer International Publishing, pp. 1–34. doi:10.1007/978-3-319-17001-5_16-1

Zibrowius, H.W., 1980. Les scléractiniaires de la Méditerranée et de l'Atlantique nord-oriental. Mémoires de l'Institut océanographique, no 11. Institut océanographique, Monaco.

2 Material and Methods

Two study sites were selected for this first investigation of the (long-term) temporal occurrence of CWC in coral mound areas of the NW Atlantic: the Campeche CWC Province (Gulf of Mexico) and the Cape Lookout CWC area (eastern US margin) (Fig. 7). The main selection criterion was the location given that these two areas are the southern and northern most areas within the known NW Atlantic CWC mound areas. They are also located in the path of the most relevant currents of this region. The selected sites were expected to represent good examples of the actual and past environmental conditions and, thus, of the temporal occurrence of CWC in the NW Atlantic. The data produced in this study derives from material collected during expeditions MSM 20-4 (R/V *Maria S. Merian;* Hebbeln *et al.*, 2012), DISCOVRE 2009-IV (R/V *Cape Hatteras*; Ross 2009) and 64PE320 TRACOS-2010 (R/V *Pelagia*; Mienis *et al.*, 2010).

In order to achieve the main goals of this study, a methodology was defined to characterize the actual environmental conditions at the study sites, to reconstruct the past environmental conditions and to identify the periods of prolific CWC development. The collected material includes hydroacoustic data, water column data, seabed ROV video footage and sediment samples (comprising sediment cores and seabed surface samples).

2.1 Hydroacoustic Measurements

Multibeam echo sounders (MBES) are used to map the seafloor. They compute water depths based on the two-way travel time of individual sound pulses called *pings*, transmitted from the vessel-mounted MBES. Additionally to the MBES, acoustic Doppler current profilers (or ADCP), another type of sonar equipment that uses the acoustic backscatter and the Doppler effect of sound waves, may be used to measure water current velocities and its particle load.

In this study, hydroacoustic measurements were performed for seabed mapping of the Campeche CWC province using a KONGSBERG EM1002 multibeam echosounder (95 kHz frequency; 111 beams per ping), which covered a depth range of 2 to 1000 m and achieved a swath width of up to 5 times the water depth. Sound velocity profiles through the water column (to calibrate the system) were obtained from the SEABIRD CTD (see section 2.2). Positioning was given by the ship's SEAPATH 200 inertial navigation system, including differential global positioning system (DGPS) information. Data processing, editing and evaluation was performed with the MB-System v.5.3.1 (Caress and Chayes, 1996) and the Generic Mapping Tool (GMT) v.4.3.1 (Wessel and Smith, 1998). In addition, this area was surveyed using RDI Ocean Surveyor ADCP (at a 75 kHz frequency) and Vessel-Mounted Data Acquisition software (using 128 depth bins of 5 m bin size), which allowed the quantification of current velocity, current direction and backscatter. The backscatter data presented in this study considered a constant water absorption coefficient of 0.0272 dB/m (Schulkin and Marsh, 1962) and were corrected for beam spreading and water absorption (Deines, 1999). See Hebbeln et al. (2012) for further details.

2.2 Water column analyses

The water masses are characterized by specific physical parameters such as temperature, salinity and oxygen. One of the equipments commonly used to measure these parameters is a conductivity, temperature and depth profiler (CTD). CTDs have sensors that determine conductivity (allowing the calculation of salinity), temperature and hydrostatic pressure (from which depth is derived). CTDs may also integrate an array of Niskin bottles that collect water samples for further analyses.

The physical parameters of the water in the area of the Campeche CWC province were determined using the SEABIRD CTD SBE 911 plus which contains a SBE 9 plus underwater unit and a SBE 11 plus V2 deck unit. This CTD was further equipped with an auxiliary sensor to measure dissolved oxygen. The values measured by the sensor were validated by measuring the dissolved oxygen on collected water samples by iodometric Winkler titration method after Grasshoff (1983) (see Hebbeln et al. (2012) for further details). Water mass variability was investigated by a Yoyo CTD (descending and ascending vertical, sequential profiles) comprising 13 individual casts taken within 12 h just above the Campeche CWC province. In addition, one longer (and deeper) water profile reaching a maximum water depth of 1246 m was done in close vicinity.

2.3 ROV video observation and sampling

ROVs (remotely operated underwater vehicles) are highly maneuverable mobile devices operated from the vessel. The advantage of using ROVs is based on their accurate navigation systems, good imaging quality (incl. strong lighting systems and high-quality cameras), and diverse sampling devices (such as sediment push-corers, suction samplers, water sampling bottles, hydraulic manipulators and draw boxes that bring collected samples on board). ROVs also allow other sensors and devices to be added to the ROV frame, depending on the objective of the conducted research.

Video surveys at the Campeche CWC province were conducted with the ROV *Cherokee* (Sub-Atlantic, Scotland; operated by MARUM, Germany), a 450 kg ROV with a maximum depth range of 1,000 m. A positioning accuracy within 1-2% of the slant range was obtained coupling the IXSEA global acoustic positioning system of the ship with its differential global positioning system (DGPS). The ROV was equipped with four video cameras including the Tritech Typhoon PAL color zoom camera and the still imaging KONGSBERG OE-14 5-Megapixel digital camera. Further equipment included a Tritech Seaking sonar, for obstacle detection; a laser scaling, to measure size of objects on the seafloor; and a hydraulical manipulator and toolbox, for sample collection and storage (see Hebbeln et al. (2012) for further details). Navigational data, video recordings and still images were all time-referenced. The ROV video observations have allowed the characterization of the CWC mounds regarding, for example, their morphology, density and composition of the coral coverage and their associated fauna.

2.4 Sediment sampling and analyses

2.4.1 Sediment sampling

The sediments used in this study were collected using gravity, piston and box coring systems. The gravity corer used is a 6 or 12 m long metallic barrel that holds a plastic liner inside and carries a 1.6 ton core head weight on top (Hebbeln et al., 2012). The corer is pushed into the sediment simply by its weight, whereby the penetrated sediment is collected inside the plastic liner. A core catcher at the base prevents the sediment from coming out while the corer ascends to the sea surface. The piston corer is a 6 m long barrel fitted with a core head weight of 1.5 ton (Mienis et al., 2010). It differs from the gravity corer by having a trigger arm that once in contact with the seafloor releases the head weight making the core barrel freefall into the sediment. The cores collected with both gravity and piston corers were then cut into 1 m long sections, capped, labeled and stored in a cold room. Box coring was done with a 55 cm long stainless steel cylindrical box-corer with a trip valve seal (Netherlands; Mienis *et al.*, 2010). Once the box-cores were on deck, the overlying water was carefully removed and the sediment surface was photographed and described. A sub-core for sedimentological analyses was then taken with a PVC liner pushed into the sediment. These sub-cores were also capped, labeled and stored in a cold room. When the retrieved material was dominated by coral fragments, inhibiting the collection of a sub-core, the collected material was sieved and the skeletal content was stored for later analysis.

Sediment sampling was performed in two different environmental settings: on the cold-water coral mounds and on the sediment drift in close vicinity of the mound areas. The cores retrieved on the mounds, designated as on-mound cores, contain coral fragments and were used to reconstruct periods of past cold-water coral occurrence. As such on-mound cores are composed of a mixture of solid coral fragments loosely embedded in soft matrix sediments, the on-mound cores were firstly frozen (-20°C) for 24 hours before they were cut with a diamond saw, which ensured the preservation of the cores' internal structure. Cold-water coral fragments were then sampled at various core depths of the on-mound cores for Uranium-series dating. The cores retrieved from the sediment drifts, designated as off-mound cores, contain no coral fragments. To reconstruct past environmental conditions, these cores were sampled for grain size and carbonate analyses, as well as for foraminifera-based analyses such as radiocarbon dating, stable isotope analyses, Mg/Ca analysis and assemblage studies.

2.4.2 Uranium-series dating of cold-water corals

The uranium-series (or uranium-thorium) method is a radioactive dating technique based on the decay of ^{238}U into its intermediate daughter isotopes ^{234}U and ^{230}Th. It differs from other radioactive decay systems by the fact that the daughter isotope considered (^{230}Th) is not the final end-member and is also itself decaying. The age calculation depends on the degree of secular equilibrium (the state of equal decay rates between parent and daughter isotopes) reached between the ^{230}Th isotope and its radioactive parents. The technique allows determination of ages of up to 500,000 years.

Prior to the analyses, the samples need to be cleaned mechanically and leached chemically to remove any detrital phase or other remains such as ferromanganese coatings, which may contain unsupported thorium that would affect the uranium-thorium results. Any thorium incorporated during crystallization (due to increased occurrence of thorium in deeper seawater) is not separable from the radiogenic thorium and needs to be accounted for in age calculations. Corrections can be based either on local seawater thorium measurements (when available) or on a calculated constant that represents seawater thorium. Further caution needs to be taken from possible effects of diagenesis (change of the carbonate structure), which would increase the uranium in the skeletons. Possible diagenetic effects are usually checked by the initial δ^{234}U values and data are discarded when falling outside the defined seawater range. For more details on Uranium-series dating of cold-water corals see Sherwood & Risk (2007).

The isotopic measurements were performed on a ThermoFisher Neptune Plus Multicollector inductively coupled plasma mass spectrometer (ICP-MS) at the Laboratoire des Sciences du Climat et de l'Environnement (Gif-sur-Yvette, France) and on a ThermoFisher iCAP-Qs ICP-MS at the Institut für Umweltphysik (University of Heidelberg, Germany). ICP-MS equipments ionize the samples with inductively coupled plasma and use a mass spectrometer to separate and quantify the produced ions. The spectrometer identifies the ions from their mass to charge ratio based on the deflection suffered as they move. The deflection is mass dependent, as lighter elements will be affected by larger deflections.

2.4.3 Radiocarbon dating of foraminifera

Radiocarbon dating is based on the radioactive decay of ^{14}C. This cosmogenic isotope is continuously formed in the upper atmosphere and transferred homogeneously into the ocean. Living organisms exchange carbon (and are at equilibrium) with their environment until they die. Once dead, exchange between the organism and its environment stops, this way the ^{14}C present in a fossil sample will depend on the rate of radioactive decay and the time elapsed. Quantification of ^{14}C in a sample allows estimation of the elapsed time after the organism's death. Although current high-precision techniques allow the precise measurement of ^{14}C even in small samples, certain aspects of the method need to be considered when applied to marine records. Given the global ocean circulation, deep waters will present a ^{14}C offset to the ocean surface (and to the atmosphere) dependent on the distance traveled (and time spent) away from the source area, meaning that different ocean areas present different ^{14}C reservoir ages that need to be corrected. Further possible effects of sediment bioturbation and carbonate diagenesis should be checked. Radiocarbon allows the accurate dating of samples from around 50,000 years ago (after which the method sensitivity decreases) until 1950 AD (pre-bomb period). For more details see review by Hughen (2007).

The radiocarbon dating of this study was performed on samples of mixed planktic foraminifera of the size fraction >150 µm. The samples were analyzed at the Poznań Radiocarbon Laboratory (Poznań, Poland) using accelerator mass spectrometry (AMS; that directly counts ^{14}C and ^{12}C atoms of the sample). The obtained ages were corrected for the mean ocean reservoir age and calibrated using the MARINE13 calibration curve (Reimer et al., 2013) of the CALIB7.0 software (Stuiver and Reimer, 1993).

2.4.4 Stable isotope analysis of foraminifera

Stable isotopes are isotopes that differ on their atomic masses, but do not decay (are not radioactive). In the case of carbon and oxygen, the lighter ^{12}C and ^{16}O isotopes are far more abundant and preferably mobilized than their heavier relatives ^{13}C and ^{18}O, respectively. The ^{12}C is preferably taken up by autotrophic organisms to build organic matter and more steadily released once the organic matter decomposes. In relation to ^{18}O, the ^{16}O is preferably evaporated from the sea surface to ascend into the atmosphere and firstly lost through rain after water vapor condensation. This way, climate related changes such as polar ice cap size and precipitation/evaporation rates will affect the relative ratio between the stable oxygen isotopes while surface productivity will affect the relative ratio of carbon isotopes. Such isotopic variations are preserved in the foraminifera carbonate tests and can be used to reconstruct past environmental changes. The rarest isotopes are reported as a rate in relation to their lightest counterpart. To allow study comparisons, the isotopic ratios are then compared to a standard (traditionally the VPDB, i.e. Vienna Pee Dee Belemnite) and reported as $\delta^{13}C$ and $\delta^{18}O$, for carbon and oxygen respectively. See Ravelo & Hillaire-Marcel (2007) for a review.

In this study, the carbon and oxygen stable isotopes were analyzed with the Finnigan MAT 251 and 252 gas isotope ratio mass spectrometers, housed at the Isotope Laboratory at MARUM (University of Bremen, Germany). The internal standard is Solnhofen Limestone, calibrated against NBS 19 (which is calibrated against the VPDB) and with a long-term standard deviation of <0.05 ‰ for $\delta^{13}C$ and <0.07 ‰ for $\delta^{18}O$. As mentioned above (section 2.4.2), this technique identifies the elements (isotopes) through their mass to charge ratio, based on the deflection suffered by the ions as they move. The samples are analyzed in gaseous state for which they are dissolved in phosphoric acid. When necessary, the samples used in this study were split samples where one half was used for stable isotope analysis and the other half was used for Mg/Ca analysis (section 2.4.5). For the split, the samples were gently crushed in a water drop between two smear slides, mixed (for homogenization) and then separated into two similar portions. The three foraminifera species used for stable isotope analysis were: *Globigerinoides ruber* sensu stricto (white variety) (split samples of 17-78 specimens; size fraction 250-355 µm), *Cibicides pachyderma* (split samples of 14-38 specimens; size fraction 250-355 µm), and *Planulina ariminensis* (8-10 specimens; size fraction >150 µm).

2.4.5 Mg/Ca analysis of foraminifera

The reconstruction of past temperature and salinity is crucial to identify past water mass distribution most likely reflecting changes in the paleo-climate. The Mg/Ca measured on foraminifera tests is one of the proxies to reconstruct past ocean temperatures. As the organisms build their tests, small amounts of Mg are incorporated in the calcite (as impurities). This process is temperature-dependent, thus increased Mg incorporation (and higher Mg/Ca ratio) is expected to occur in warmer waters. Since vital effects may influence the Mg incorporation process, the Mg/Ca-temperature calibrations used to relate the measured ratios to ambient water temperature are usually species-specific. See review by Rosenthal (2007).

In this study, the Mg/Ca measurements were performed on split samples (where the remaining half was used for stable isotope analysis; see section 2.4.4) of *G. ruber* sensu stricto (white variety) and of *C. pachyderma* (size fraction 250-355 µm; 17-78 specimens of *G. ruber* s.s. and 14-38 specimens of *C. pachyderma*). The conversion of Mg/Ca ratios into temperatures followed the calibration proposed by Cléroux et al. (2012) for *G. ruber* and the calibration of Lear et al. (2002) for *C. pachyderma*. The elemental analysis was performed in the Agilent 700 Inductively Coupled Plasma Optical Emission Spectrometer (ICP-OES), housed at the Department of Geosciences (University of Bremen, Germany). The ICP-OES identifies the different elements present in a sample by measuring the wavelengths produced once the sample is ionized. The concentration of a specific element is given by the intensity of the emission.

The Mg/Ca further allows the computation of the seawater $\delta^{18}O$ ($\delta^{18}O_{SW}$; an indicator of salinity) when combined with the $\delta^{18}O$ measured on the same foraminifera sample (using split samples). This is done by decoupling the various factors influencing the foraminifera $\delta^{18}O$ record (i.e. temperature, salinity and sea level/ice accumulation at the poles). The effect of salinity was isolated using the Mg/Ca-temperature record to remove the effect of temperature, a sea-level reconstruction (such as the one by Waelbroeck et al. 2002) to remove the effect of ice volume-related sea level changes and by solving the Shackleton equation (Shackleton, 1974) for $\delta^{18}O_{SW}$.

2.4.6 Benthic foraminifera assemblages

Benthic foraminifera assemblages have commonly been used to investigate past environmental conditions at the sea floor. The method involves quantification and identification of a certain number of individual shells. It is based on the fact that specific taxa have a particular ecology and may, thus, be related to particular boundary conditions such as water depth, salinity, oxygenation, organic carbon flux to (and food availability at) the seafloor. Species assemblages may concern studies of presence/absence data, faunal density or biodiversity, or definition of the dominant taxa, etc. (see review by Jorissen et al. 2007).

In the present study, benthic foraminifera assemblages (considering groups of around 300 individuals) were used to evaluate benthic ecosystem stability (Shannon-Wiener diversity index), lateral (downslope) transport, bottom water oxygenation and food availability at the seafloor. Temporal changes in the faunal assemblages were further investigated performing a Q-mode Principal Component Analysis (PCA) with Varimax rotation, by using the software Systat (version 5.2.1), which allows the definition of the dominant species along a time-series record.

2.4.7 Grain size analysis

Currents at the seafloor have the ability of drag, suspend and transport seabed particles. With the exception of clays (that may form aggregates and behave as bigger/heavier particles), a direct relationship exists between particle size and current speed. Under increased seafloor currents, the larger particles are more abundant and the particle size distribution tends to be skewed towards the larger sizes. Therefore, particle sorting (standard deviation) and mean (or median) grain size of a sediment sample (or of its silt fraction) can be used as an indicator of bottom current strength (Folk and Ward, 1957).

Before any analysis, the samples were treated for removal of the organic carbon by boiling (until the reaction stopped) with hydrogen peroxide (H_2O_2) which avoided aggregation of the sediment particles. The grain size analyses were then performed both on the bulk (inorganic) fraction as well as on the terrigenous (also named decarbonated or siliciclastic) fraction of the sediment. The terrigenous fraction excludes the calcitic and opal components, which may accumulate locally and not be controlled by bottom currents. Removal of the carbonate was done either by boiling the sample (until the reaction stopped) in an acid solution of acetic acid (CH_3COOH) and ammonium acetate ($C_2H_3O_2NH_4$), or by boiling (1 min) in hydrochloric acid

(HCl). To remove the biogenic opal the samples were boiled (10 min) with sodium hydroxide (NaOH). The samples prepared at MARUM endured an additional preparation step to destroy any remaining aggregates, for which were boiled (3 min) with tetra-sodium diphosphate decahydrate ($Na_4P_2O_7 * 10H_2O$). In all cases, sample preparation and measurement was done with deionized, degassed and filtered water to reduce the influence of gas bubbles or particles within the water. The samples are also stirred before and/or along the analyses to ensure homogenization.

The particle size measurements were performed on the sample's size fraction <2 mm. Two models of the Beckman Coulter Laser Diffraction Particle Size Analyzer were used: the LS230 housed at IPMA, I.P. (Lisbon, Portugal); and the LS 13320 housed at the Particle-Size Laboratory at MARUM (University of Bremen, Germany). There was no need to calibrate the two different equipments because the results of each laboratory were used independently.

The calculation of the particle sizes is based on the changes experienced by the light while it traverses the sample, either light diffraction (following the Fraunhofer diffraction theory) or polarization (following the Polarization Intensity Differential Scattering - *PIDS*; if particles are smaller than 0.4 µm). The particle-size distribution of a sample is provided by size classes (the number of classes varies according to the Coulter model). The measurement for each size class is presented as volume percentage, for which it is assumed that particles tend to be spherical in shape. During the analyses, the possible occurrence of sample aggregation is monitored and suspected if sequential spectra of one sample show decreasing volume percentage of small (clay-sized) particles and increased volume percentage of bigger (silt/sand-sized) particles, simultaneously. In which case the results can be rejected and the samples re-treated and reanalyzed. In this study, all statistic values used (mode, median, mean, standard deviation and cumulative volume percentage) are based on geometric statistics.

2.4.8 Carbonate analysis

The accumulation of $CaCO_3$ at the seafloor (above the calcite lysocline and away from coral mound settings) and its abundance in the sediments has been used as indication of surface productivity changes (Calvert and Pedersen, 2007). In this study, the $CaCO_3$ content in the sediment was not measured directly but rather computed from the inorganic carbon weight (Baumann et al., 1993), according to the formula below:

$$CaCO_3 \text{ [weight \%]} = \text{inorganic carbon [weight \%]} \times 8.332$$

Before the analysis, the samples were dried and homogenized. Approximately 1 cc of sediment was then subject to calcination (at 400°C, during 3 hours) to remove the organic carbon fraction. The quantification of the inorganic carbon fraction of the sediment was done on a CHNS-932 LECO elemental analyzer housed at IPMA, I.P. (Lisbon, Portugal; see Abrantes et al., 2005). This equipment quantifies the inorganic carbon using individual and selective infrared (IR) detectors to measure the CO_2 produced from the sample's complete combustion. The results are given as a percentage of the sample's weight.

References

Calvert, S.E., Pedersen, T.F., 2007. Elemental Proxies for Palaeoclimatic and Palaeoceanographic Variability in Marine Sediments: Interpretation and Application, in: Hillaire-Marcel, C., de Vernal, A. (Eds.), Developments in Marine Geology - Proxies in Late Cenozoic Paleoceanography. Elsevier B.V., pp. 567–644. doi:10.1016/S1572-5480(07)01019-6

Caress, D.W., Chayes, D.N., 1996. Improved processing of Hydrosweep DS multibeam data on the R/V Maurice Ewing. Mar. Geophys. Res. 18, 631–650. doi:10.1007/BF00313878

Deines, K.L., 1999. Backscatter estimation using Broadband acoustic Doppler current profilers, in: Proceedings of the IEEE Sixth Working Conference on Current Measurement, 1999. pp. 1–5. doi:10.1109/CCM.1999.755249

Folk, R.L., Ward, W.C., 1957. Brazos River Bar: a study in the significance of grain size parameters. J. Sediment. Petrol. 27, 3–26.

Grasshoff, K., 1983. Determination of oxygen, in: Grasshoff, K., Ehrhardt., M., Kremling, K. (Eds.), Methods of Seawater Analysis. Verlag Chemie Weinheim, New York, pp. 61–72.

Hebbeln, D., Wienberg, C., Beuck, L., Dehning, K., Dullo, W.-C., Eberli, G., Freiwald, A., Glogowski, S., Garlichs, T., Jansen, F., Joseph, N., Klann, M., Matos, L., Nowald, N., Reyes, H., Ruhland, G., Taviani, M., Wilke, T., Wilsenack, M., Wintersteller, P., 2012. West Atlantic Cold-Water Coral Ecosystems: The west side story, R/V Maria S. Merian Cruise No. 20, Leg 4.

Hughen, K.A., 2007. Radiocarbon Dating of Deep-Sea Sediments, in: Hillaire-Marcel, C., de Vernal, A. (Eds.), Developments in Marine Geology - Proxies in Late Cenozoic Paleoceanography. Elsevier B.V., pp. 185–210. doi:10.1016/S1572-5480(07)01010-X

Jorissen, F.J., Fontanier, C., Thomas, E., 2007. Paleoceanographical Proxies Based on Deep-Sea Benthic Foraminiferal Assemblage Characteristics, in: Hillaire-Marcel, C., de Vernal, A. (Eds.), Developments in Marine Geology - Proxies in Late Cenozoic Paleoceanography. Elsevier B.V., pp. 263–325. doi:10.1016/S1572-5480(07)01012-3

Mienis, F., Duineveld, G., Lavaleye, M., shipboard scientific crew, 2010. Biodiversity, ecosystem functioning and mound development of cold-water coral reefs in the Cape Lookout area, W Atlantic. Cruise Report 64PE320, Bermuda-Bermuda, 27 May-10 June 2010, R.V. Pelagia. Texel, The Netherlands.

Ravelo, A.C., Hillaire-Marcel, C., 2007. The Use of Oxygen and Carbon Isotopes of Foraminifera in Paleoceanography, in: Hillaire-Marcel, C., de Vernal, A. (Eds.), Developments in Marine Geology - Proxies in Late Cenozoic Paleoceanography. Elsevier B.V., pp. 735–764. doi:10.1016/S1572-5480(07)01023-8

Reimer, P.J., Bard, E., Bayliss, A., Beck, J.W., Blackwell, P.G., Ramsey, C.B., Buck, C.E., Cheng, H., Edwards, R.L., Friedrich, M., Grootes, P.M., Guilderson, T.P., Haflidason, H., Hajdas, I., Hatté, C., Heaton, T.J., Hoffmann, D.L., Hogg, A.G., Hughen, K.A., Kaiser, K.F., Kromer, B., Manning, S.W., Niu, M., Reimer, R.W., Richards, D.A., Scott, E.M., Southon, J.R., Staff, R.A., Turney, C.S.M., van der Plicht, J., 2013. Intcal13 and marine13 radiocarbon age calibration curves 0–50,000 years cal BP. Radiocarbon 55, 1869–1887. doi:10.2458/azu_js_rc.55.16947

Rosenthal, Y., 2007. Elemental Proxies for Reconstructing Cenozoic Seawater Paleotemperatures from Calcareous Fossils, in: Hillaire-Marcel, C., de Vernal, A. (Eds.), Developments in Marine Geology - Proxies in Late Cenozoic Paleoceanography. Elsevier B.V., pp. 765–797. doi:10.1016/S1572-5480(07)01024-X

Ross, S.W., 2009. Discovre 2009 - Cruise 4. Retrieved from: https://archive.usgs.gov/archive/sites/fl.biology.usgs.gov/DISCOVRE/discovre_2009/discovre_09_cruise_4.html.

Schulkin, M., Marsh, H.W., 1962. Sound Absorption in Sea Water. J. Acoust. Soc. Am. 34, 864–865. doi:10.1121/1.1918213

Sherwood, O.A., Risk, M.J., 2007. Deep-Sea Corals: New Insights to Paleoceanography, in: Hillaire-Marcel, C., de Vernal, A. (Eds.), Developments in Marine Geology - Proxies in Late Cenozoic Paleoceanography. Elsevier B.V., pp. 491–522. doi:10.1016/S1572-5480(07)01017-2

Stuiver, M., Reimer, P.J., 1993. Extended 14C data base and revised CALIB 3.0 14C age calibration program. Radiocarbon 35, 215–230.

Wessel, P., Smith, W.H.F., 1998. New, improved version of generic mapping tools released. Eos, Trans. Am. Geophys. Union 79, 579–579. doi:10.1029/98EO00426

3 Overview of own research

The research conducted during this study has allowed a first investigation of the temporal pattern of CWC occurrence in the NW Atlantic coral mound areas combined with the characterization of the present and past environmental conditions favoring their occurrence. The results of this investigation are presented in three chapters (sections 4 to 6) in the form of manuscripts. The main outcome and description of the contribution given by the different authors is summarized below.

The first manuscript (chapter 4)

Environmental forcing of the Campeche cold-water coral province, southern Gulf of Mexico

D. Hebbeln, C. Wienberg, P. Wintersteller, A. Freiwald, M. Becker, L. Beuck, C. Dullo, G.P. Eberli, S. Glogowski, L. Matos, N. Forster, H. Reyes-Bonilla, M. Taviani & the MSM 20-4 shipboard scientific party

Published in *Biogeosciences*, vol. 11, pp. 1799–1815, 2014
www.biogeosciences.net/11/1799/2014/
doi:10.5194/bg-11-1799-2014

The recently discovered Campeche CWC province in the southern Gulf of Mexico was mapped and described, for which the province was investigated regarding its hydrographic setting and its mound morphology, coral density and assemblage, and associated fauna. The mounds, occurring in water depths of 500 to 600 m, are colonized by a vivid cold-water coral community dominated by *E. profunda* and *L. pertusa*. The environmental setting includes a local upwelling center and a dynamic bottom water regime which favors CWC growth by securing their food supply.

Contribution: The study was designed by C. Wienberg and D. Hebbeln. L. Matos participated in coral mound sample acquisition together with C. Wienberg, A. Freiwald, L. Beuck, N. Forster, H. Reyes-Bonilla, and M. Taviani. ROV-based visual characterization of the mounds was performed by C. Wienberg, L. Beuck, A. Freiwald and D. Hebbeln. The hydrographic characterization was performed by C. Dullo and S. Glogowski. Mapping was performed by P. Wintersteller and G.P. Eberli. M. Becker evaluated the ADCP data. All authors participated in the writing of the text, which was compiled by D. Hebbeln and C. Wienberg.

The second manuscript (chapter 5)

Coral mound development at the Campeche cold-water coral province, southern Gulf of Mexico: implications of Antarctic Intermediate Water increased influence during interglacials

L. Matos, C. Wienberg, J. Titschack, G. Schmiedl, N. Frank, F. Abrantes, M.R. Cunha, D. Hebbeln

Submitted to *Marine Geology*
(moderate revisions requested)

The temporal pattern of CWC occurrence in a coral mound area within the Gulf of Mexico is investigated for the first time and combined with a reconstruction of the paleo-environmental conditions. For the last 260 kyr, CWC growth at the Campeche CWC province predominantly coincided with interglacial periods. The reduced occurrence of CWC and almost complete stagnation in mound aggradation during glacial periods could be linked to a diminished influence of the AAIW, causing a reduced food supply to the CWC.

Contribution: The study was designed by L. Matos, C. Wienberg, D. Hebbeln, F. Abrantes and M.R. Cunha. L. Matos and C. Wienberg acquired and prepared the coral samples and developed the age model. L. Matos participated in coral dating with main contribution from N. Frank. J. Titschack performed grain size analysis. G. Schmiedl performed benthic foraminifera assemblage analysis and interpreted the results. L. Matos interpreted the data and wrote the manuscript with contribution from D. Hebbeln, C. Wienberg and J. Titschack. All authors participated in the manuscript revision.

The third manuscript (chapter 6)

Interglacial occurrence of cold-water corals off Cape Lookout (NW Atlantic): first evidence of the Gulf Stream influence

L. Matos, F. Mienis, C. Wienberg, N. Frank, C. Kwiatkowski, J. Groeneveld, F. Thil, F. Abrantes, M.R. Cunha, D. Hebbeln

Published in *Deep-Sea Research I*, vol. 105, pp. 158–170, 2015
http://dx.doi.org/10.1016/j.dsr.2015.09.003

The Cape Lookout CWC area was the first site of the NW Atlantic to be investigated regarding the temporal distribution of CWC in coral mound areas. The study additionally comprised the reconstruction of the paleo-environmental conditions. Results suggest that CWC occurrence in this area is restricted to interglacial periods. The favorable conditions for CWC growth found during the Mid- to Late Holocene include enhanced bottom current strength and a slightly higher bottom water temperature, which coincide with the occasional presence of the Gulf Stream over the site.

Contribution: The study was designed by F. Mienis, L. Matos, D. Hebbeln, F. Abrantes and M.R. Cunha. L. Matos acquired and prepared the coral samples and developed the age model. L. Matos participated in coral dating with main contribution from N. Frank and F. Thil. C. Kwiatkowski, L. Matos and J. Groeneveld acquired and prepared the samples and interpreted results from the Mg/Ca analysis, performed by J. Groeneveld. L. Matos interpreted the data and wrote the manuscript with contribution from F. Mienis, D. Hebbeln and C. Wienberg. All authors participated in the manuscript revision.

4 Environmental forcing of the Campeche cold-water coral province, southern Gulf of Mexico

D. Hebbeln[a], C. Wienberg[a], P. Wintersteller[a], A. Freiwald[b], M. Becker[a], L. Beuck[b], C. Dullo[c], G.P. Eberli[d], S. Glogowski[c], L. Matos[a,e,f], N. Forster[b], H. Reyes-Bonilla[g], M. Taviani[h,i] & the MSM 20-4 shipboard scientific party

[a] Center for Marine Environmental Sciences (MARUM), University of Bremen, Bremen, Germany

[b] Senckenberg am Meer, Marine Research Department, Wilhelmshaven, Germany

[c] Helmholtz Centre for Ocean Research Kiel (GEOMAR), Kiel, Germany

[d] Rosenstiel School for Marine and Atmospheric Science (RSMAS), University of Miami, Miami, USA

[e] Instituto Portugues do Mar e da Atmosfera (IPMA), Lisbon, Portugal

[f] Centro de Estudos do Ambiente e do Mar (CESAM), Aveiro, Portugal

[g] Universidad Autónoma de Baja California Sur, La Paz, Mexico

[h] Institute of Marine Sciences, National Research Council, Bologna, Italy

[i] Biology Department, Woods Hole Oceanographic Institution, Woods Hole, USA

Correspondence to: D. Hebbeln (dhebbeln@marum.de)

Abstract

With an extension of >40 km^2 the recently discovered Campeche cold-water coral province located at the northeastern rim of the Campeche Bank in the southern Gulf of Mexico belongs to the largest coherent cold-water coral areas discovered so far. The Campeche province consists of numerous 20 to 40 m high elongated coral mounds that are developed in intermediate water depths of 500 to 600 m. The mounds are colonized by a vivid cold-water coral ecosystem that covers the upper flanks and summits. The rich coral community is dominated by the framework-building scleractinia *Enallopsammia profunda* and *Lophelia pertusa* while the associated benthic megafauna shows a rather scarce occurrence. The recent environmental setting is characterized by a high surface water production caused by a local upwelling center and a dynamic bottom water regime comprising vigorous bottom currents, obvious temporal variability, and strong density contrasts, which all together provide optimal conditions for the growth of cold-water corals. This setting - potentially supported by the diel

vertical migration of zooplankton in the Campeche area - controls the delivering of food particles to the corals. The Campeche cold-water coral province is, thus, an excellent example highlighting the importance of the oceanographic setting in securing the food supply for the development of large and vivid cold-water coral ecosystems.

4.1 Introduction

The last decade has witnessed a tremendous progress in our knowledge about "framework-building cold-water corals" (CWC) as their role as ecosystem engineers creating highly diverse ecosystems in water depths far beyond the shelf edge is becoming more and more obvious (Roberts et al., 2009). The biodiversity associated with these ecosystems may be comparable to that found in tropical coral reefs (Roberts et al., 2006), and they occur almost world-wide except for the highest latitudes (Davies and Guinotte, 2011). The availability of advanced deep-sea technologies (e.g., remotely operated vehicles) greatly supported the discovery and investigation of large, thriving and (so far) unknown CWC ecosystems in remote places. Successful studies such as those performed off Mauritania (Colman et al., 2005), off Angola (Le Guilloux et al., 2009), and in various parts of the Mediterranean Sea (Freiwald et al., 2009; Orejas et al., 2009; Fink et al., 2013; Gori et al., 2013), demonstrate the potential use of these technologies for future discoveries.

With their rigid carbonate skeletons that can persist over geological time scales CWC shape the sea floor by creating large three-dimensional structures, e.g., >300-m-high coral carbonate mounds along the Irish margin (e.g., Kenyon et al., 2003; Mienis et al., 2007) reaching back to Pliocene times (~2.6 Ma; Kano et al., 2007) and >100-km^2-large reef structures off Norway (Fosså et al., 2005) formed during the Holocene (e.g., López Correa et al., 2012). These structures consist of a mixture of coral skeletons, the skeletal remains of the coral-associated megafaunal community, and pelagic or hemipelagic sediments that can serve as paleo-environmental archives allowing to reconstruct the long-term development of the CWC ecosystems (e.g., Dorschel et al., 2005; Frank et al., 2009; Titschack et al., 2009; Wienberg et al., 2009; Eisele et al., 2011; Fink et al., 2012; López Correa et al., 2012; Douarin et al., 2013; Thierens et al., 2013).

The scleractinian coral *Lophelia pertusa* is among the most common and most widespread CWC species world-wide and is particularly abundant in the NE Atlantic (Davies and Guinotte, 2011). This species withstands a rather wide range of physico-chemical conditions (see summary in Davies et al., 2008), a fact that explains its almost global distribution in depths between a few tens of meters to over 2000 m (Freiwald and Roberts, 2005). Another critical factor controlling its distribution is sufficient food supply that is commonly driven by the interplay of surface water productivity and the local nature of the bottom current regime (e.g., currents, stratification, internal waves and tides) delivering food particles to the CWC (Duineveld et al., 2004; White et al., 2005; Duineveld et al., 2007). Paleo-environmental studies revealed that food supply often is the decisive factor triggering on- or off-sets of coral growth in a given setting (e.g., Dorschel et al., 2005; Wienberg et al., 2010; Eisele et al., 2011; Fink et al., 2013).

In addition to the CWC hotspot in the NE Atlantic, *L. pertusa* also contributes to numerous coral mound structures in the NW Atlantic along the continental margin from North Carolina (Ross and Nizinski, 2007), along the Florida-Hatteras slope (Paull et al., 2010), and the Bahamas to the Florida Straits (e.g., Neumann et al., 1977; Mullins et al., 1981; Grasmueck et al., 2006; Correa et al., 2012a; Correa et al., 2012b). Further west in the Gulf of Mexico, *L. pertusa* appears to be more scattered, forming isolated mound-like structures along the West Florida slope (Newton et al., 1987; Hübscher et al., 2010) and in the northern Gulf of Mexico (Moore and Bullis, 1960; Schroeder, 2002; Reed et al., 2006; Cordes et al., 2008; Becker et al., 2009; Davies et al., 2010). Summarizing the current knowledge, Mienis et al. (2012) conclude that within the Gulf of Mexico CWC mound structures have been rarely found, except on the West Florida slope and in the Viosca Knoll area (Fig. 1). The latter area has been considered the most extensive *Lophelia* habitat found so far in this region (Brooke and Schroeder, 2007; Davies et al., 2010) probably as a consequence of enhanced productivity driven by nutrient-enriched Mississippi River outflow (Wawrik and Paul, 2004). Apart from the Campeche Bank, the southern Gulf of Mexico is generally characterized by meager planktonic biomass along the Mexican slope mirroring the low-productivity Caribbean water that enters the Gulf of Mexico through the Yucatan Strait (Wei et al., 2012).

In this paper, we document for the first time build-ups at the sea floor formed by framework-building scleractinian corals on the slope of the Mexican Campeche Bank, southern Gulf of Mexico. These build-ups are mainly formed by *Enallopsammia profunda – Lophelia pertusa* communities. This finding was unexpected as available data from a few dredge haul stations only described the occurrence of the scleractinian CWC *Madrepora oculata* along the margin of the Campeche Bank, north of the Mexican Yucatan peninsula (Cairns, 1979; Schroeder et al., 2005). Only in 2010 more detailed information was provided, when hydroacoustic surveys revealed "mound-like" structures between 500 and 600 m water depth along the margin of the bank (Hübscher et al., 2010). Without any groundtruthing being available at that time it only has been speculated that these structures might be CWC mounds (Hübscher et al., 2010).

This region was revisited in 2012 and extensive field data (bathymetry, hydrography, and video observations) revealed the existence of a large thriving CWC ecosystem, which is the focus of this paper. This hitherto unknown CWC site is here termed the "Campeche CWC province". The scope of the present study is to describe this extensive (>40 km^2) CWC province with respect to morphology, the megafaunal community, and the oceanographic setting and to put it into a larger framework analyzing the overall forcing factors controlling its development.

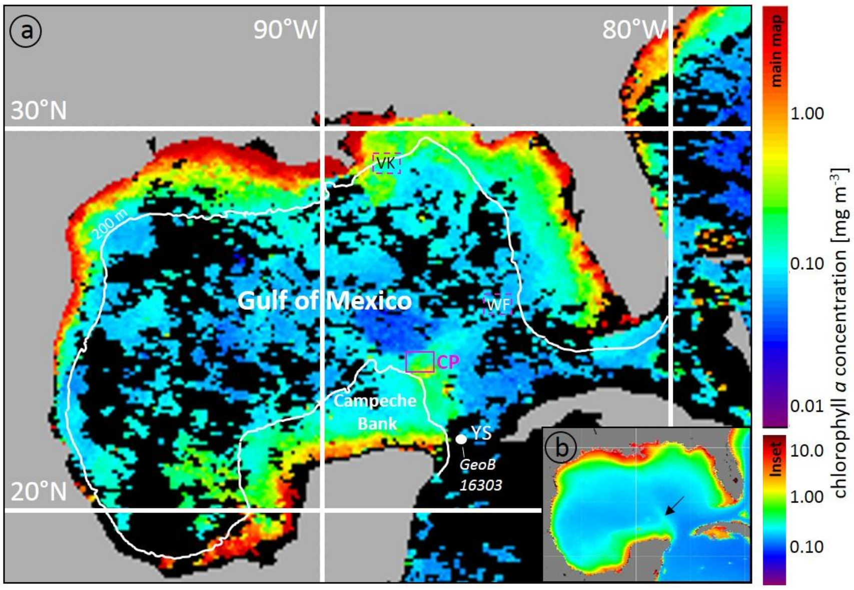

Figure 1. SEAWIFS satellite ocean color data transferred into chlorophyll *a* concentrations for the Gulf of Mexico (source: http://oceancolor.gsfc.nasa.gov). (a) The map refers to an 8 days composite representing the period 22-29 September 2010. Black indicates data gaps. The Campeche cold-water coral province (CP) is influenced by increased productivity probably forced by local upwelling at the northeastern rim of the Campeche Bank (Molinari and Morrison, 1988). The white dot in the Yucatan Strait (YS) indicates CTD station GeoB 16303-1. The white line marks the 200 m isobath within the Gulf of Mexico. VK: Viosca Knoll cold-water coral setting (e.g., Brooke and Schroeder, 2007), WF: West-Florida cold-water coral mounds (Newton et al., 1987). (b) The inset shows the same data as a composite for the entire SEAWIFS mission (Sep 4, 1997 to Nov 30, 2010). The black arrow indicates the area of the Campeche cold-water coral province that is located in a region marked by a long-term enhanced productivity.

4.2 Regional setting

The Campeche Bank is a large shelf area extending approximately 200 km northward from the Mexican Yucatan peninsula into the Gulf of Mexico (Fig. 1). The Gulf of Mexico is a largely oligotrophic basin with enhanced productivity only along the continental shelves (Müller-Karger et al., 1991), where seasonal coastal upwelling provides additional nutrients to the surface waters (Zavala-Hidalgo et al., 2006). A major source of nutrients is the Mississippi plume fertilizing the northeastern shelves of the Gulf with enhanced productivity partly extending over the continental slope (Wawrik and Paul, 2004). The enhanced productivity triggered by the Mississippi plume most likely plays an important role in sustaining CWC populations along the Louisiana and Florida continental slopes (e.g., Newton et al., 1987; Schroeder, 2002; Fig. 1).

Apart from the typical coastal upwelling, another upwelling regime has been described further offshore along the eastern margin of Campeche Bank (Merino, 1997). As the curl of the prevailing wind stress is not likely to induce upwelling along the eastern Yucatan slope, the upwelling observed there is probably caused by bottom friction or other topographical effects (Merino, 1997). Nevertheless, the advection of nutrients into the photic zone (although rarely to the sea surface; Merino, 1997), induces very high productivity reaching a peak in September (Zavala-Hidalgo et al., 2006) when sites near the Campeche CWC province appear prominently in satellite-based productivity maps (Fig. 1).

Along its eastern edge the Campeche Bank borders the Yucatan Strait that forms the main passage connecting the Caribbean Sea and the Gulf of Mexico through which the Yucatan Current transports ~24 Sv from South to North (Sheinbaum et al., 2002). According to Merino (1997) three main water masses comprise the water column there. Salinity and temperature increase together from the Antarctic Intermediate Water (AAIW, 7°C, salinity 34.9) in the deep towards the salinity maximum of the Subtropical Intermediate Water (STUW, 23°C, salinity 36.8) at ~150 m depth. Further above temperature rises and salinity declines until from 50 m to the surface both parameters remain relatively constant (26-27.5°C, salinity <36.4) representing the Caribbean Surface Water (CSW). In depths greater than ~650 m, the Yucatan and Cuban Countercurrents transport water southward while being confined to the western, Mexican side and to the eastern, Cuban side of the Yucatan Strait, respectively (Sheinbaum et al., 2002).

With respect to the strength of the bottom current regime, the best information is provided by mooring data obtained slightly further south in the Yucatan Strait (~21.5°N; e.g., Sheinbaum et al., 2002). Along a W-E transect through the area, the mean northward current velocities at the western margin decrease rapidly from almost 100 cm s^{-1} at the surface to <10 cm s^{-1} at 200 m water depth. However, at the depth of the Campeche CWC province (~550 m) the bottom current velocities in the Yucatan Strait increase again to >10 cm s^{-1} (Sheinbaum et al., 2002).

4.3 Methods

All data presented here were collected during expedition MSM 20-4 with the German R/V MARIA S. MERIAN in spring 2012 (Hebbeln et al., 2012). They include hydroacoustic measurements, water column studies, and seabed ROV video observation (see Table 1 and Fig. 2 for relevant site information). Instrument specifications and applied settings for the hydroacoustic measurements are described in detail in Hebbeln et al. (2012). For all hydroacoustic measurements introduced below, the essential sound velocity profile through the water column was obtained from two CTD casts in (GeoB 16305-1) and close (GeoB 16303-1) to the working area (Figs. 1 and 2, Table 1).

Table 1. Metadata of CTD casts and ROV CHEROKEE video surveys conducted at the Campeche cold-water coral province during R/V MARIA S. MERIAN cruise MSM20-4. Abbreviations: WD water depth.

Station [GeoB-N°]	**Gear**		**Date [2012]**	**UTC [hh:mm]**	**Latitude [N]**	**Longitude [W]**	**WD [m]**	**Remark**
16303-1	CTD		21 March	14:59	22°00.98'	86°02.95'	1246	sound velocity profile
16305-1	CTD		22 March	05:21	23°49.87'	87°12.27'	506	sound velocity profile
16316-1 to 16316-13	Yoyo CTD	Start:	24 March	00:20	23°51.51'	87°12.12'	576	hourly casts over ~12 hours; ADCP data were recorded simultaneously over ~13 hours
		End:	24 March	12:01	23°51.52'	87°12.13'	558	
16307-1	ROV	Start:	22 March	13:51	23°40.83'	87°10.03'	547	video observation
		End:	22 March	16:20	23°50.49’	87°10.71'	577	
16312-1	ROV	Start:	23 March	14:31	23°50.35'	87°11.76'	523	video observation
		End:	23 March	18:31	23°52.52'	87°12.49'	531	
16317-1	ROV	Start:	24 March	13:37	23°51.12'	87°12.53'	555	video observation
		End:	24 March	15:02	23°51.77'	87°12.16'	556	

4.3.1 Hydroacoustic measurements

4.3.1.1. Multibeam echosounder (MBES)

Seabed mapping was performed using a KONGSBERG EM1002 multibeam echosounder system (MBES) operating at a frequency of 95 kHz. The EM1002 emitted 111 beams per ping, covered a depth range of 2 to 1,000 m and achieved a high depth resolution of 2-8 cm, depending on the pulse length (0.2-2 ms). Achievable swath width on a flat bottom was up to 5 times the water depth dependent on the character of the seafloor. Spatial integrity of the mapping data was achieved by combining the ship's SEAPATH 200 Inertial Navigation System (INS) including Differential Global Positioning System (DGPS) information with motion data (roll, pitch, heave) provided by the motion reference unit (MRU) 5. The open-source software package MB-System v.5.3.1 (Caress and Chayes, 1996) and the Generic Mapping Tool (GMT) v.4.3.1 (Wessel and Smith, 1998) were used for bathymetric data processing, editing and evaluation. ESRI ArcGIS v.10 was used to create maps (grid cell size: 10 m) and a sustainable spatial data management.

4.3.1.2. Acoustic Doppler Current Profiler (ADCP)

Current velocity and direction, and backscatter data through the water column were measured with an RDI Ocean Surveyor Acoustic Doppler Current Profiler (ADCP) operating at a frequency of 75 kHz. Data were acquired using the RDI software VMDAS (Vessel-Mount Data Acquisition) using 128 depth bins of 5 m bin size. Backscatter data were corrected for beam spreading and water absorption (Deines, 1999). For the backscatter data set presented in this study, a constant water absorption coefficient of 0.0272 dB/m was used (Schulkin and Marsh, 1962). Due to the simultaneous deployment of several hydroacoustic devices, backscatter and current velocity data was affected by acoustic interference, which were removed using appropriate filters. Backscatter data close to the seafloor was biased by side-lobe interferences and not used for interpretation. ADCP data are presented as a stationary 12-hours-record collected at site GeoB 16316 (Fig. 2, Table 1).

4.3.2 ROV video observation and sampling

Three video surveys (GeoB 16307-1, GeoB 16312-1, GeoB 16317-1; Table 1, Fig. 2) were conducted with the ROV CHEROKEE (Sub-Atlantic, Aberdeen, Scotland; operated by MARUM, Bremen, Germany) crossing several CWC mounds along the Campeche margin. The ship-based IXSEA global acoustic positioning system (GAPS) coupled with the ship's differential global positioning system (DGPS) provided an absolute positioning accuracy within 1-2% of the slant range. The ROV was equipped with a hydraulic manipulator system for sampling purposes and four video cameras including a color video zoom camera for detailed seafloor observation and a digital still camera. The cameras were equipped with two lasers for object size measurements on the seabed, thereby laser scaling was adjusted to 11.5 cm in a horizontal direction. All video and still image data were digitally stored. Navigational data (ship, ROV), video recordings, and still images are all time-referenced. With the manipulator of the ROV several coral samples were collected to assess the phenotypes of the different CWC species.

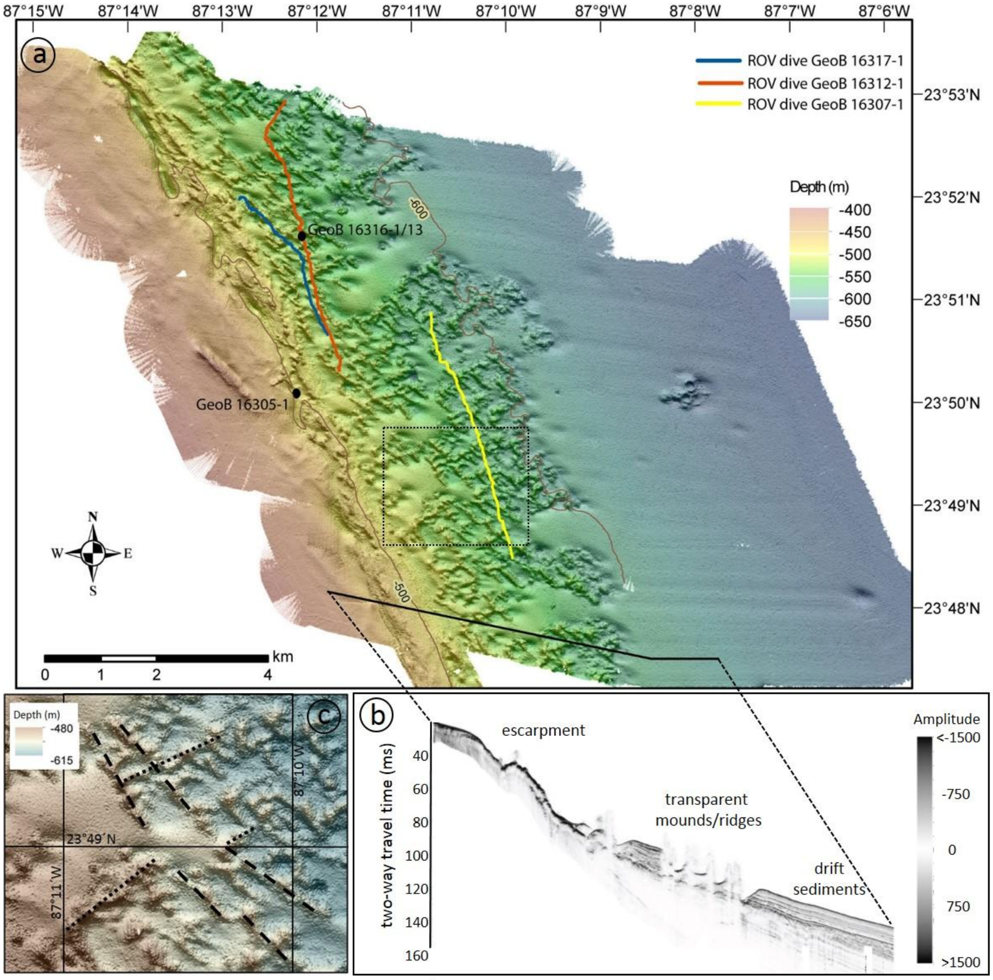

Figure 2. Overview about the Campeche cold-water coral province (for location see Fig. 1) (a) Detailed bathymetric map showing the eastern margin of the Campeche Bank comprising the Campeche cold-water coral province revealing numerous individual elongated coral mounds located mainly between 500 m and 600 m water depth. Indicated are CTD sites (black dots) and ROV dive tracks (colored lines; GeoB station numbers are indicated) conducted during R/V MARIA S. MERIAN cruise MSM20-4 (for detailed site information see Table 1). (b) PARASOUND profile crossing the slope and highlighting the main morphological units. (c) High resolution view on some of the elongated coral mounds (for position see dotted rectangle in (a)) with the dominant northwesterly directions marked by dashed lines and with the sub-dominant northeasterly directions marked by the dotted lines.

4.3.3 Water column analyses

To determine the physical parameters of the water masses in the area of the Campeche CWC province and to trace their variability, CTD measurements were performed as a Yoyo-CTD comprising 13 individual casts taken within 12 hours at station GeoB 16316 (Fig. 2, Table 1). The CTD measurements of the water column down to a maximum water depth of 1246 m were conducted using a SEABIRD 'SBE 9 plus' underwater unit and a SEABIRD 'SBE 11 plus V2' deck unit. The vertical profile over the water column provided standard data for conductivity, temperature, pressure, and dissolved oxygen. Conductivity and temperature data were used to compute salinity (with the latter being presented here unitless). The data presented here all refer to the down cast of the individual CTD deployments.

4.4 Results

4.4.1 Morphology and dimensions of the Campeche cold-water coral province

The hydroacoustic mapping encompasses an area of 180 km^2 along the northeastern slope of the Campeche Bank and displays three distinct topographical features (Fig. 2). The western part of the map shows an extensive more or less plain area at ~440 m water depth. A NNW-SSE orientated and ~40-m-high escarpment separates this rather shallow and plain area from a gently dipping slope to the east, which covers the water depths between 480 and 600 m. Further downslope below ~600 m water depth, the slope is followed by a more gently dipping area which comprises smooth sediment of a major drift sediment body (Hübscher et al., 2010). The first 3-5 km of the dipping slope east of the edge are covered by linear and steep-sided elongated mounds between 500 and 600 m water depth. This belt of parallel elongated mounds is situated between the escarpment and the continuous drift deposit with a few stratified sediment bodies also occurring between the mounds. Both, the mounds and the sediment drift overlay a regional truncation surface (Fig. 2b; Hübscher et al., 2010).

The mounds have average heights between 20 and 40 m but can even reach heights of up to 50 m. They vary in length between a few tens of meters to >1000 m, and trend in two directions. The dominant direction is NW-SE and the second one NE-SW (Fig. 2c). In many cases both directions merge thereby forming V-shaped elongated mounds pointing with the tip to the WNW. ROV-based video observations reveal that the morphology of these mounds is mostly rather steep with estimated angles of up to 30° (e.g., Fig. 3e). These elongated mounds are often aligned by a moat towards the next mound (Fig. 2). In addition, on some of the mound flanks exhumed carbonate crusts with irregular upper and lower surfaces have been observed (Fig. 3h). As the video observations clearly indicate that these mounds are covered by a vivid CWC ecosystem (Fig. 3a, b; Fig. 4a, b), the entire structure is termed here the "Campeche CWC province". The minimum extension of the Campeche CWC province is 40 km^2, however, most likely this CWC province is even larger, as it still has a significant width at the northern and southern boundaries of the mapped area (Fig. 2). Thus, the ultimate northern and southern boundaries of the Campeche CWC province still need to be verified.

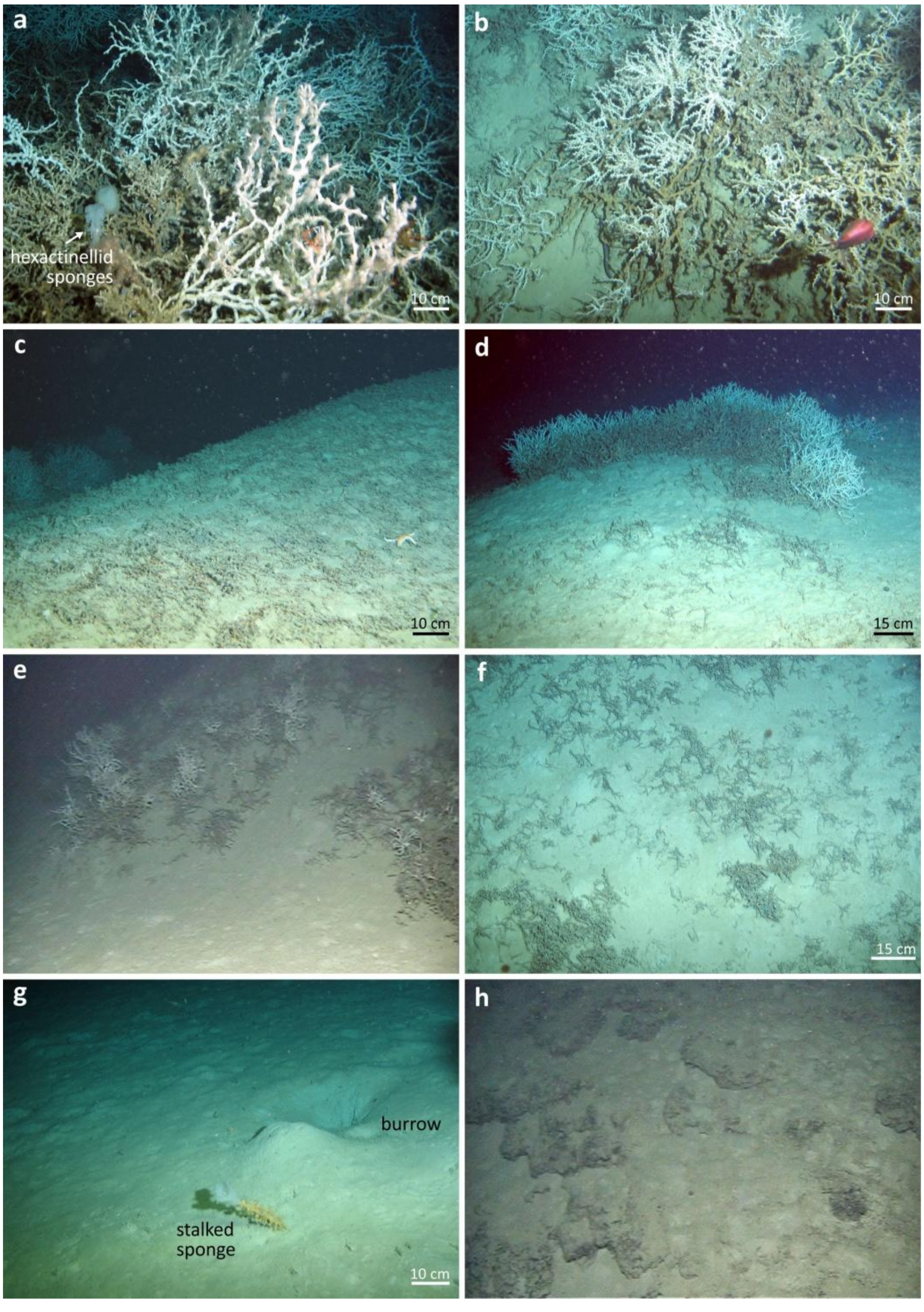

4.4.2 The Campeche cold-water coral ecosystem

Observations during three ROV dives that cross several mounds of the Campeche CWC province reveal the composition of the structure-forming CWC and their associated megafaunal community. The dive tracks of the video surveys had an NNW-SSE orientation in water depths ranging between 510-580 m (Fig. 2). All mounds studied are colonized by colonial scleractinians representing *Enallopsammia profunda – Lophelia pertusa* communities (Figs. 3 and 4), whereas the flat seabed between the mounds consists of pelagic unconsolidated mud enriched by globigerinid foraminifers and thecosomatous gastropods, locally admixed with patches of coral rubble and mollusk shell hash (see detailed description of collected sediment samples in Hebbeln et al., 2012). These intermound areas are strongly bioturbated as indicated by widespread lebensspuren and burrows (Fig. 3g).

Coral colonization, coral density and coral species distribution show a clear zonation related to current exposure and position on the mound flank. In general, living corals occur at the highest parts of the mounds, followed downslope by a zone of coral rubble and by plain soft sediments in the lower parts of the mounds and in the areas between the mounds (Fig. 3). However, on some steeply inclined mounds (up to 30°), coral colonization starts already at the base of their current-exposed side (SSE), thereby generating a sharp change of sedimentary facies from pelagic muds to a living CWC ecosystem. On less steep mounds live coral colonies start to appear halfway upslope the current-exposed flank, or the mound flanks are entirely covered by a dead and collapsed coral framework or coral rubble with only few live coral colonies in between. For both types of mounds, corals fade off halfway along the leeward flanks of the mounds. Overall, the density of coral framework and the proportion of live coral colonies become progressively higher towards the summit, where they can form very dense coral thickets up to 60 cm thick. The mound flanks are dominated by *E. profunda* whereas *L. pertusa* becomes increasingly abundant, if not dominant on the summits.

Figure 3 (previous page). ROV images showing the variety of facies types observed for the Campeche cold-water coral province (images copyright MARUM, Bremen, ROV CHEROKEE Team). (a) Coral mound summit: dense colonies of *Lophelia pertusa*, note hexactinellid sponges *(Aphrocallistes* sp.*)* and squat lobster, (b) current-exposed coral mound flank: ensemble of the fragile *Enallopsammia profunda* and the *brachycephala* morphotype of *L. pertusa*, (c) mound flank packed with dead coral framework, (d) arcuate *E. profunda* thicket on a low-relief mound, (e) sudden facies change from flat soft sediment plain to steeply inclined coral mound flank, (f) lower coral mound flank: dispersed fragments of *E. profunda*, (g) intermound area: strongly bioturbated soft sediment, note stalked sponge (*Hyalonema* sp.) colonized by actiniarians, (h) occasionally observed outcropping carbonate crusts.

The dendroid *E. profunda* colonies display an open-spaced growth habit with individual colony branches pointing to all directions (Fig. 4 a, b). This growth habit results in a loose mesh of coral framework thus facilitating framework disintegration of individual branches into stick-like fragments. Colony heights vary from 20 to 60 cm, thereby only the upper 10-15 cm of a colony yields live coral polyps and translucent tissue. *Lophelia pertusa* also constructs an open-spaced coral framework. However, secondary fusion between adjacent coral branches is a very common feature, thus increasing the structural integrity of the entire framework considerably in comparison to *E. profunda*. The branches of *L. pertusa* are strongly calcified and slender with individual corallite lengths of 2.5–3.5 cm and calicular diameters of 0.5–0.8 cm. This phenotype has been described as forma *gracilis* by Duncan (1873) and is in contrast to the stout branches with extremely wide calicular diameters of the *brachycephala* form (Fig. 4a) described by Moseley (1881) and Cairns (1979). The latter phenotype occurs in low numbers in the Campeche CWC province but the co-occurrence of the two *L. pertusa* growth forms is a well-known phenomenon in the northern Gulf of Mexico (Newton et al., 1987; Brooke et al., 2009). The *Lophelia* framework can attain heights of 50 cm and the zone of live polyps and translucent tissue coverage stretch over a range of 20-30 cm.

The live coral zone is utilized by the associated community in various ways and differs largely in terms of species composition and richness from the associated community found in the tissue-barren, exposed coral framework beneath. Common organisms observed (although not exclusively) in the live zone are the predatory decapods *Bathynectes longispina, Eumunida picta, Chaceon fenneri*, *Munidopsis* sp. and *Rochinia crassa* and the grazing echinoids *Cidaris* sp. and *Gracilechinus* sp. (Fig. 4e). The latter echinoid has been recognized as a corallivore in CWC habitats of the eastern North Atlantic (Stevenson and Rocha, 2013). Other organisms with corallivore affinities in the live coral zone are hippasterinid star fishes (Mah et al., 2010) and the muricid gastropod *Coralliophila richardi* (Taviani et al., 2009), which were commonly collected from the live coral zone. Stalkless crinoids have been occasionally observed to take advantage of the elevated and current-exposed position of live coral branches for filtering particles from the water. Indication of probably necrotic epibiosis of live scleractinians by zoanthids and actiniarians in some scleractinian colonies is a common feature and seems to cause local mortality. Polychaetes of the Genus *Eunice*, from which several species are known as symbionts of *L. pertusa* and other colonial CWC (e.g., Buhl-Mortensen and Mortensen, 2004; Mueller et al., 2013) are surprisingly rare in the Campeche CWC province.

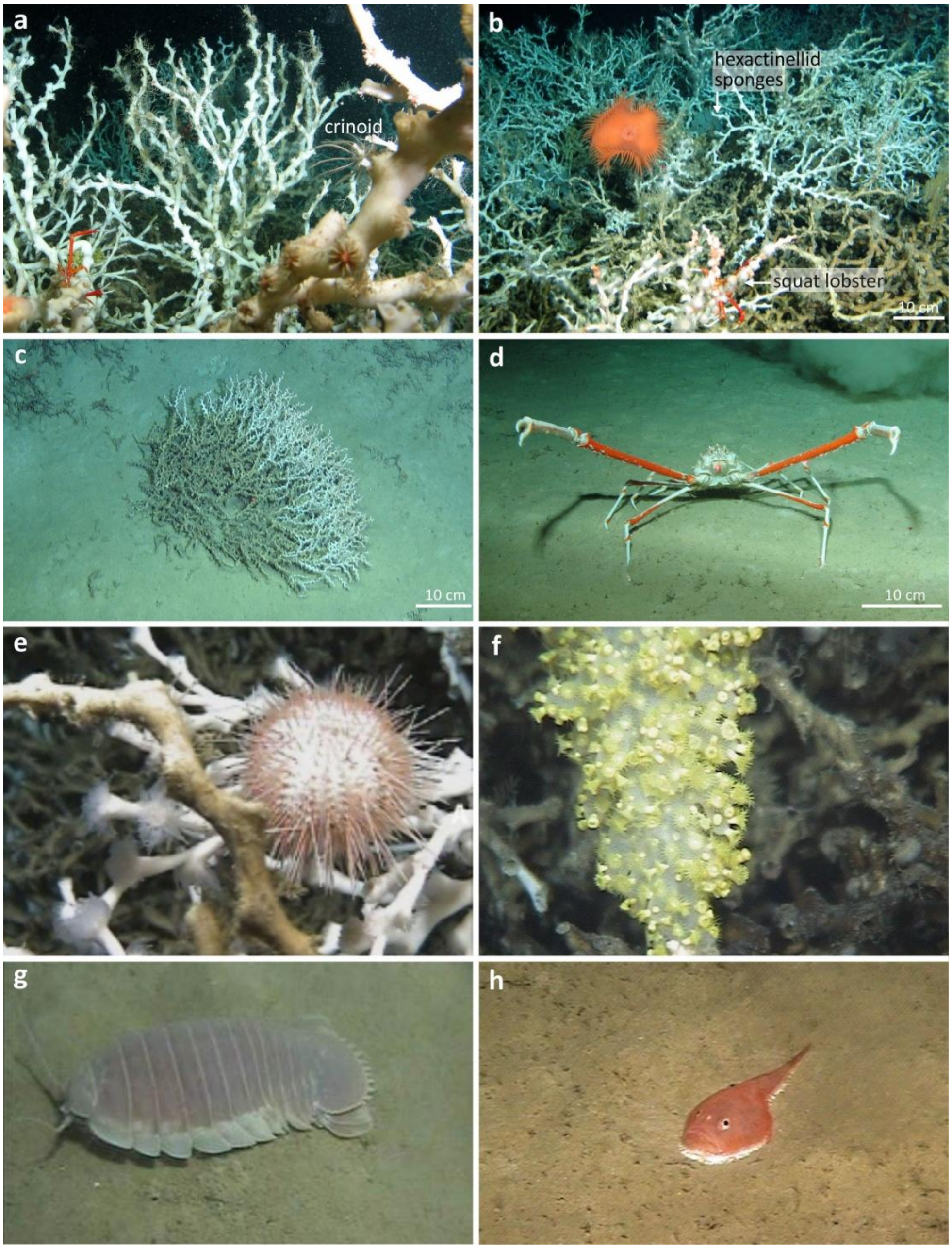

Figure 4. ROV images showing examples for the megafaunal community present in the Campeche cold-water coral province (images copyright MARUM, Bremen, ROV CHEROKEE Team). (a) Dense colonization of *Lophelia pertusa* at the coral mound top, (b) flytrap anemone (probably *Actinoscyphia* sp.) colonizing tissue-barren, exposed coral framework, (c) displaced but still alive colony of *Enallopsammia profunda*, (d) brachyuran crab *Rochinia crassa*, (e) grazing of living corals by the echinoid *Gracilechinus* sp., (f) glass sponge *Aphrocallistes* sp. living together with masses of yellow actiniarians, (g) the giant cirolanid isopod *Bathynomus giganteus*, (h) the anglerfish *Chaunax suttkusi* commonly spotted near the coral mounds resting on the seabed.

Characteristic organisms of the tissue-barren, exposed coral framework are flytrap anemones (probably *Actinoscyphia* sp.; Fig. 4b), isidid corals (*Keratoisis* sp.), and solitary scleractinians (*Desmophyllum dianthus, Javania cailetti, Stenocyathus vermiformis, Trochopsammia* *infundibulum*). The glass sponge *Aphrocallistes* sp. was found attached to the coral framework. Apparently the glass sponges are living together with masses of yellow actiniarians (Fig. 4f), thus resembling the recently described symbiotic relationship between the glass sponge *Hyalonema sieboldi* with the actiniarian *Spongiactis japonica* (Sanamyan et al., 2012). Common fishes encountered frequently in the coral framework were *Helicolenus dactylopterus* and *Nettenchelys exoria*. Gorgonians and antipatharians that are elsewhere common in CWC ecosystems are extremely rare here.

The coral rubble is strongly admixed with unconsolidated pelagic mud thereby providing small hard-substrate islands within soft sediment. Common megafaunal organisms are large astrorhizid foraminifers, cerianthids, pennatulaceans, stalked glass sponges (*Hyalonema* sp.), and the common decapods (same as in the live zone) and shrimps. Amongst the mobile organisms, the giant isopod crustacean *Bathynomus giganteus* was detected (Fig. 4g). Like in other coral rubble habitats elsewhere in the Gulf of Mexico and in the northern Atlantic, the anglerfish *Chaunax suttkusi* (Fig. 4h)*,* was commonly spotted near the coral mounds resting on the seabed (Caruso et al., 2007). Other common fishes observed in the coral rubble and pelagic mud areas are *Chlorophthalmus agassizi*, *Laemonema* sp., *Nezumia* sp., Phycidae and Rajidae.

4.4.3 Water column structure / dynamics

The CTD measurements allow the identification of the most important regional water masses, based on temperature (potential temperature) and mainly on salinity data (Fig. 5). The uppermost ~80 m of the water column are characterized by water with salinities of <36.4 which is indicative for the presence of the CSW. The salinity maximum (~36.8) between 100 and 160 m water depth is characteristic for the STUW. At 540 m water depth salinity drops below 35.0 marking the presence of AAIW. In the depth range where living CWC have been observed (520 to 580 m) temperatures range between 7.5-9.5°C and salinities between 34.9-35.1. Dissolved oxygen contents vary between 2.74 and 2.8 mL L^{-1}.

The Yoyo-CTD station (GeoB 16316) consisting of 13 individual, hourly taken casts reveal small, but significant variations also in the deepest part of the water column just above the Campeche CWC province (Fig. 6): for example, at 519 m water depth the temperature varies by almost 1°C up to three times over the 12 hours measuring period (Fig. 6c). These temperature changes are also reflected in the depth position of individual isotherms (8 to 9.5°C, Fig. 6b). They fluctuate vertically by up to 20 m thereby reflecting the same temporal forcing as the temperatures at 519 m depth. Along with these temperature changes a distinct density gradient induced by temperature and salinity changes, almost reaching 0.7°C and 0.07, respectively, over a 10 m depth interval (Fig. 6d) propagates across the site. With ~0.06 kg m^{-3} per 10 m depth interval this density gradient is strongest for the lower part of the water column at 525 m depth and significantly higher than the density gradients between 380 m and the sea floor that otherwise reach maximum values of ~0.04 kg m^{-3} per 10 m depth interval (Fig. 6a).

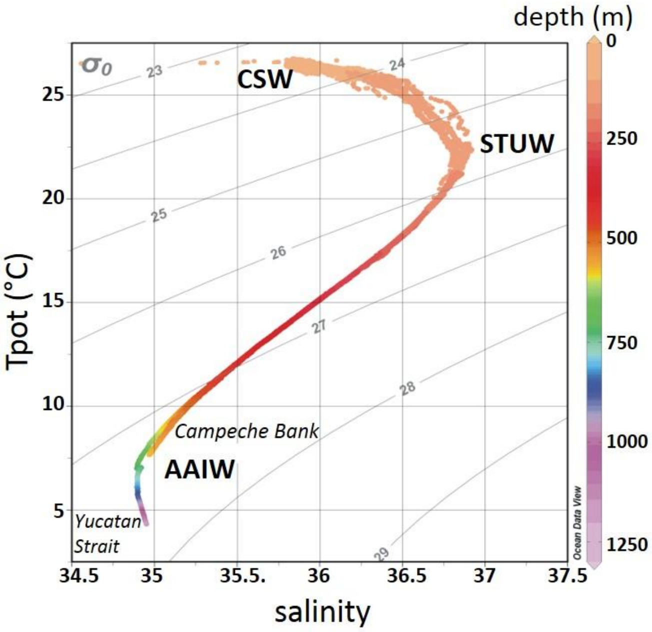

Figure 5. Water mass structure in the Yucatan Strait (GeoB 16303-1) and in the Campeche cold-water coral province (GeoB 16316-1 to -16, Yoyo-CTD station; see Table 1). Shown is a temperature-salinity plot, temperature is displayed as potential temperature (Tpot), grey lines indicate levels of isodensity (σ_Θ) in kg m^{-3} (plotted using Ocean Data View v.4.5.1; http://odv.awi.de; Schlitzer, R., 2012). Abbreviations: CSW Caribbean Surface Water, STUW Subtropical Intermediate Water, AAIW Antarctic Intermediate Water.

The ADCP data collected over a 13 hour time interval (simultaneously to the Yoyo-CTD data; see Table 1) allow to distinguish between three major layers that show some internal (although less pronounced) horizontal structuring (Fig. 7, 8). Within the upper 130 m of the water column, the highest current velocities (74-83 cm s^{-1}) occur together with a high backscatter (94-98 dB). Current directions vary between 322° and 335°. The second layer between 130 and 460 m is characterized by continuously decreasing current velocities from 63 to 42 cm s^{-1}, again by rather stable current directions similar to the uppermost layer (325° to 336°), and by low backscatter values (84-94 dB). The bottom layer (>460 m) is marked by a significant change in current direction (343° to 360°) and by the lowest but still strong currents flowing with 24 to 42 cm s^{-1}.

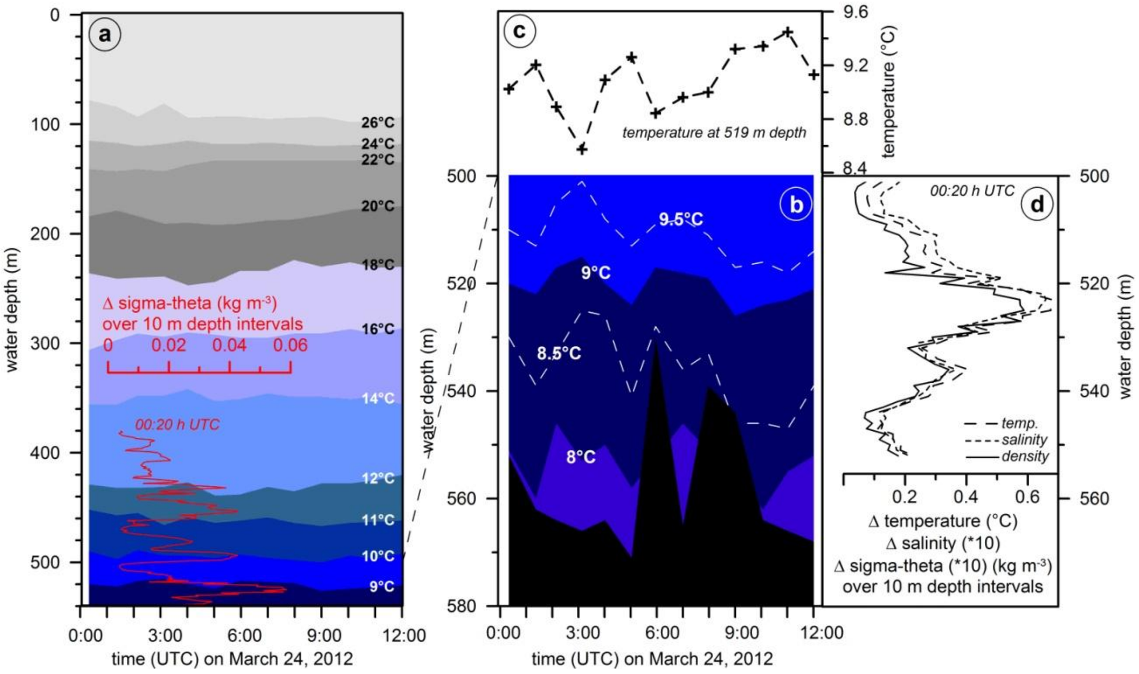

Figure 6. Hydrological variability derived from the Yoyo-CTD station GeoB 16316 (see also Table 1 and Fig. 1). (a) Variability of the temperature distribution in the entire water column over a time interval of 12 hours (comprising 13 individual CTD casts). The red inset shows the density gradient over 10 m depth intervals for the water column below 380 m taken from CTD cast GeoB 16316-1 (00:20h UTC). (b) Depth variation of the 8°C to 9.5°C isotherms in the lower part of the water column >500 m water depth over the same time period show partly vertical movements of >20 m. Variations in water depth (black denotes the sea floor) are caused by slight movements of the vessel (~600 m N-S, ~50 m E-W) during the Yoyo-CTD station (including the crossing of a CWC mound). (c) Water temperature in 519 m depth measured over the same time period indicates a variability of up to 1°C. (d) Gradients in temperature, salinity, and density over 10 m depth intervals. Data were obtained during the individual CTD cast GeoB 16316-1 (00:20h UTC) and reveal particularly strong gradients around 520 m water depth (see also (a)).

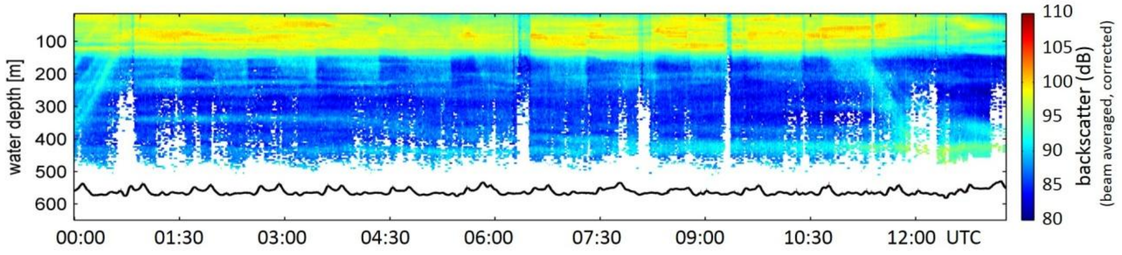

Figure 7. ADCP-derived backscatter data obtained during a 13 h stationary measurement from 0:00 h to 13:00 h UTC on March 24, 2012. ADCP data were recorded simultaneously to the Yoyo-CTD station GeoB 16316 (see Table 1). This backscatter record shows the upward (0:00-0:30 h UTC, local sunset) and downward (11:30-12:00 h UTC, local sunrise) migration of the zooplankton. Probably biased data close to the seafloor have been omitted.

At the beginning of the stationary ADCP record (ca. 00:00 h UTC, March 24 2012) enhanced backscatter signals move upward through the water column towards the sea surface. By the end (ca. 11:30 h UTC), similar signals move downward towards the seabed (Fig. 7). Similar observations were made during additional ADCP surveys in the working area during cruise MSM20-4 (Hebbeln et al., unpubl. data). In total, four upward (always at around 0:00 h UTC, corresponding to 18:15 h local "solar" time at 86°W, i.e. sunset) and two downward movements (always at around 11:30 h UTC, corresponding 5:45 h local "solar" time at 86°W, i.e. sunrise) were observed.

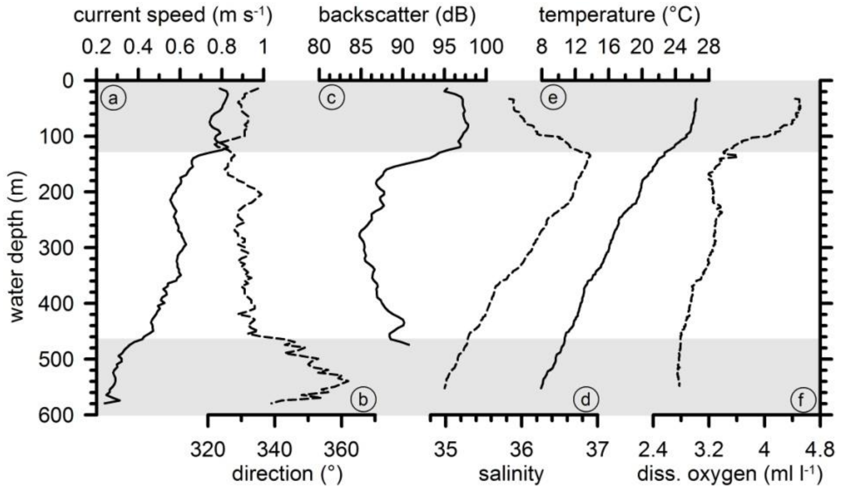

Figure 8. Water column data for the Yoyo-CTD site GeoB 16316. Mean values for (a) current speed, (b) current direction, and (c) backscatter averaged from the 13 h stationary ADCP measurement. CTD-data from cast GeoB 16316-1 for (d) salinity, (e) temperature, and (f) dissolved oxygen. The dashed lines refer to the lower x-axes. The grey shadings delineate the different layers of the water column as derived from the ADCP data.

4.5 Discussion

Large CWC-formed seafloor structures have been reported from many regions in the world's oceans (see compilation in Freiwald and Roberts, 2005). In addition to the >300 m high CWC mounds off Ireland (Kenyon et al., 2003; Mienis et al., 2007; Dorschel et al., 2010), the extensive reefs off Norway (e.g., Fosså et al., 2005) are the most impressive features. Extending over tens of kilometers (e.g., the Sula Reef, ~14x0.5 km, Freiwald et al., 2002; the Røst Reef, ~40x3 km, Fosså et al., 2005) and reaching up to ~40 m in height these reefs generally comprise clusters of individual frameworks rather than a single coalescent structure (Freiwald et al., 2002). The Campeche CWC province shows a similar appearance as it comprises a cluster of individual elongated coral mounds rather than a single clearly confined reef structure. The term "province" is used for the present study to describe the CWC mounds along the Campeche Bank following the nomenclature developed for the Irish margin where numerous individual CWC mounds occur clustered in provinces (e.g., White and Dorschel, 2010). With its mapped area of 10x4 km, and most likely further northwest- and southeastward extensions, the Campeche CWC province is comparable with the large Norwegian reefs and, thus, belongs to the largest mapped CWC provinces in the world. In addition, the Campeche CWC province represents the most important and extensive flourishing azooxanthellate coral area in the entire Gulf of Mexico discovered so far. The geographically closest CWC province is situated along the Miami Terrace in the Straits of Florida, where 27 km^2 of elongated coral mounds are mapped in detail by an autonomous under water vehicle (Correa et al., 2012a) in an area where earlier studies have reported occurrences of "muddy mounds" and "sand ridges" (Neumann and Ball, 1970).

Whereas the large Irish coral mounds have been accumulated over >2 million years (Kano et al., 2007), the Norwegian reefs have been formed only during the last ~10,000 years of the Holocene (e.g., López Correa et al., 2012), when during the last deglaciation the Fennoscandian Ice Sheet retreated beyond the present-day coastline. Large seafloor structures formed by CWC cannot easily be transferred into age, as, for example, the Irish mounds at some point in time changed from a distinct accumulation stage into an almost stagnation stage marked by CWC growth and sediment deposition alternating with extensive periods dominated by erosion (Dorschel et al., 2005; Kano et al., 2007; Eisele et al., 2008). Thus, the average height of the Campeche coral mounds of 20 to 40 m does not allow for estimating the onset of coral growth in the region. Nevertheless, their size and the collection of a >10 m long sediment core containing abundant coral fragments embedded in a matrix of hemipelagic sediments (Hebbeln et al., 2012) reveal that also the Campeche CWC ecosystem has a relevant, although yet not constrained history.

This sedimentary record adds to the PARASOUND evidence for a “CWC-origin” of these mounds. The coral mounds show little to no internal layering and are often transparent (Fig. 2b), which is a common feature for coral carbonate mounds (e.g., Van Rooij et al., 2003; Savini et al., 2014). The PARASOUND profile crossing the Campeche CWC province from west to east displays a strong reflection underneath the drift sediment bodies and the CWC mounds developed along the Campeche Bank slope (Hübscher et al., 2010). It is assumed that this continuous strong reflector forms the base of the coral mounds (Hübscher et al. 2010) that might have provided the hardground allowing for the initial coral settlement similar to the erosional unconformity forming the base of the Irish CWC mounds (Van Rooij et al., 2003; Kano et al., 2007).

CWC are often forming coral mounds that can have a variety of shapes from circular to elongate (Roberts et al., 2009). Elongated mounds often have been related to the presence of an unidirectional bottom current regime, however, with elongated coral mounds sometimes occurring perpendicular (Correa et al., 2012a) and sometimes parallel (Messing et al., 1990) to the main current direction. The elongated coral mounds within the Campeche CWC province appear to be generally aligned parallel to the main current direction possibly following an upstream growth pattern as outlined by Messing et al. (1990). They mostly stretch towards 330° with some heading towards 300° (with a second order direction NE-SW; see above). These directions are close to the two main current directions of 330° (above ~470 m) and 360° (below ~470 m) derived from the ADCP data (Fig. 8) which, however, only represent a snapshot in time. Temporal variations (e.g., lunar, seasonal) below 470 m might result in the different directions of the coral mounds observed. Then, the 30° offset between both current directions and both mound directions observed could speculatively related to an inherent 30° relationship between coral mound extension and prevailing current direction.

4.5.1 The Campeche cold-water corals and associated community

The Campeche CWC province is constructed by *Enallopsammia profunda* and to a lesser degree by *Lophelia pertusa*. Neither of the scleractinians have been reported in previous publications from the Campeche slope (e.g., Cairns, 1979; Cairns et al., 1993) but are known from several locations in the Caribbean Sea and northern Gulf of Mexico (see compilations of published and unpublished information by Brooke and Schroeder, 2007; Lutz and Ginsburg, 2007; Messing et al., 2008). While *L. pertusa* has a nearly cosmopolitan distribution, *E. profunda* is endemic to the western Atlantic from the Antilles in the south to off Massachusetts in the north at water depths of 146-1748 m (Cairns, 1979). Structure-forming *Enallopsammia-Lophelia* frameworks are known from the base of the Florida-Hatteras slope in 500-800 m water depth and from Miami to South Carolina (Reed, 2002). Correa et al. (2012a) describe an approximately 20 km^2 field of *Enallopsammia-Lophelia* coral mounds at the base of the Miami Terrace, Straits of Florida, at 630–870 m depth, with more dense coral framework on current-facing flanks and summits. The same coral association is present in the CWC mound province at the toe of the Great Bahama Bank (Correa et al., 2012b). Interestingly, on the ROV tracks studied only a low abundance of associated megafauna in the Campeche CWC province was documented. This is in contrast to other scleractinian coral framework habitats at the northern Gulf of Mexico (Lessard-Pilon et al., 2010) or in the NE Atlantic (e.g., Henry & Roberts, 2007; Roberts et al., 2006). For instance, with the exception of *Aphrocallistes* sp. and few *Keratoisis* sp., no other large suspension-feeding megabenthos was observed during the three ROV dives. It should be kept in mind that the visually inspected portion of the Campeche coral province is far too small for a solid conclusion at present and further inspections may change this first impression considerably.

Regarding the structure-forming CWC from the Campeche Bank on a wider perspective, this newly found CWC province is located at a key position, namely at the beginning of the Loop Current that passes over the well-known CWC occurrences of Louisiana and West Florida before it becomes the Florida Current flowing through the Straits of Florida. North of the Straits of Florida the Florida Current forms 90% of the Gulf Stream, passing north along the margins of South Carolina and Georgia, from where also large CWC provinces have been reported (Ross, 2007; Ross and Quattrini, 2007; Messing et al., 2008). South of the Campeche CWC province, *Lophelia* is known from off Brazil, Venezuela and Colombia and was recently mapped off Roatan, Honduras (Reyes et al., 2005; Lutz and Ginsburg, 2007; Arantes et al., 2009; Mangini et al., 2010; Etnoyer et al., 2011), thus, following the path of the northward flowing AAIW that bypasses the Campeche Bank (Merino, 1997). Such an oceanic intermediate water gateway (sensu Henry, 2011) may exert strong control on coral larval dispersal routes as has been documented for *Desmophyllum dianthus* populations in the South Pacific (Miller et al., 2011).

4.5.2 Environmental control on the Campeche cold-water coral ecosystem

The known ranges of temperature (4-13.9°C; Roberts et al., 2006; Freiwald et al., 2009), salinity (31.7-38.8; Freiwald et al., 2004; Davies et al., 2008), dissolved oxygen (2.7-7.2 mL L^{-1}; Dodds et al., 2007; Davies et al., 2008; Davies et al., 2010) and other physico-chemical parameters defining the ecological niche of *L. pertusa* in the NE Atlantic (see summary in Davies et al., 2008) are found in many parts of the world's oceans (Davies and Guinotte, 2011). Water mass properties obtained for the Campeche margin, such as temperature (9.5-7.5°C) and salinity (35.1-34.9), fit well into these defined thresholds (Fig. 7). The observed content of dissolved oxygen of ~2.7 mL L^{-1} matches observations from the Viosca Knoll area in the northern Gulf of Mexico, where *Lophelia* colonies currently thrive at the lowest reported oxygen levels of 2.7–2.8 mL L^{-1} (Davies et al., 2010). It is assumed that these extreme oxygen conditions cause decreased growth rates or even inhibits reproductive processes (Brooke and Young, 2003).

However, despite a suited physico-chemical setting, the presence of suitable hardgrounds for the corals to settle on, and even more important, the availability of sufficient food is crucial for the establishment and long-lasting development of a vivid CWC ecosystem. In general CWC feed on fresh phytodetritus (Duineveld et al., 2004; Kiriakoulakis et al., 2005; Duineveld et al., 2007), on zooplankton (Carlier et al., 2009; Dodds et al., 2009) or on a combination of both (Becker et al., 2009; van Oevelen et al., 2009). Recent laboratory studies also revealed the importance of dissolved organic matter which might be actively absorbed by CWC especially during periods when particulate food is scarce (Gori et al., in press). However, independent of the food source, the sessile CWC rely on sufficient food supply, which is based on primary production in the surface waters and the delivery of food particles to the CWC living at intermediate depths. For the latter, various mechanisms were identified to enhance and transport food particles to the CWC including strong bottom currents, downwelling and cascading, internal tides and waves, and nepheloid layers which act as a pathway for lateral transport (White et al., 2005; Dorschel et al., 2007; Duineveld et al., 2007; Mienis et al., 2007; Davies et al., 2009; Orejas et al., 2009). On the local to regional scale, topography also influences hydrodynamic processes, as e.g., internal waves, down- or upwelling. Thus, for any given location it is the interplay of all these factors allowing for or prohibiting the presence of CWC.

For the Campeche CWC province, the provision of food to the CWC appears to be almost optimal, and therefore, the observed paucity of the coral-associated megafauna remains to be explained. Primary productivity in the surface waters is high (up to ~1 mg Chl *a* m-^{3}; Fig. 1) due to the local upwelling center that is located just above the Campeche CWC province (Merino, 1997). Current meter data from the Yucatan Strait (Sheinbaum et al., 2002) as well as the ADCP data collected during cruise MSM 20-4 reveal reasonably strong bottom currents with average velocities of ~30 cm s^{-1} between 500 and 600 m water depth (Fig. 8). These numbers are in line with *in situ* current measurements at other CWC sites indicating maximum velocities of >50 cm s^{-1} (Dorschel et al., 2007; Mienis et al., 2007) whereas average current velocities can be as low as 8 cm s^{-1} (Mienis et al., 2007).

Furthermore, the strong density gradient undulating around 520 m (Fig. 6d) might act as a decelerator for sinking (food) particles, thereby prolonging their residence time within the reach of the CWC and, thus, enhancing the probability of these particles to be caught by the corals. With salinities varying around 35 this density gradient possibly marks the upper limit of the core of the AAIW. A similar mechanism has been suggested to support the CWC off Ireland, there benefitting from the density gradient developed at the upper limit of the Mediterranean

Outflow Water (White and Dorschel, 2010). For the northern NE Atlantic, Dullo et al. (2008) described a narrow potential density envelope of sigma-theta (σ_Θ) = 27.35-27.65 kg m^{-3} preferred by the CWC. Along the Campeche Bank the density of the water masses surrounding the CWC is slightly lower with 27.18-27.29 kg m^{-3} and, thus, close to data reported from the Viosca Knoll area (27.1-27.2 kg m^{-3}) (Davies et al., 2010). In contrast, living CWC settings in the Mediterranean Sea are associated with much higher densities of >29 kg m^{-3}. Thus, if applicable, the concept of a narrow density envelope defining the overall habitat range of the CWC as suggested by Dullo et al. (2008) needs to be regionalized (see also Flögel et al., in press). However, the obvious steep gradient in density (Fig. 6d) seems to be a sensitive indicator for living CWC reef communities.

As indicated by the undulating isotherms (Fig. 6), the temporal variability of the local hydrographic setting, that might reflect the presence of internal waves, literally might pump the food particles through the CWC ecosystem, especially those particles temporarily accumulating along the strong density gradient, as suggested by Mienis et al. (2012). Over the observed 13 hours, the depth range covered by the fluctuating maximum near-bottom density gradient aligns with the upper range of observed living CWC in ~515-530 m water depth. Assuming a larger variability associated with monthly (i.e. lunar) to seasonal forcing, one may speculate that the entire depth range of living CWC off the Campeche Bank might intermittently be affected by such a pumping process. Due to the limited length of the 13 hours of observation no tidal signal providing additional energy to the bottom current regime could have been clearly detected. However, along the mooring transect across the Yucatan Strait mentioned before (Sheinbaum et al., 2002), a comparably high amplitude of the major axis of the dominant diurnal O_1 tide was observed exactly in the depth range of the Campeche CWC province (Carrillo González et al., 2007).

The ADCP data also point to another possible food source for the corals. The strong upward rising backscatter signal at dusk and the down going signal at dawn (Fig. 7) are indicative for the diel vertical migration of zooplankton (Heywood, 1996). According to the backscatter data shown in Fig. 7 the migrating zooplankton spends the day in depths of >300 m with any deeper reaching migration being obscured by bottom interferences of the backscatter signal. In case the zooplankton would actively descend to the depths of the CWC, it might serve as an additional process enhancing the delivery of food to the CWC. The depth range of the Campeche CWC is often reached by migrating zooplankton. For instance, off the California coast, a depth of ~560 m, has been shown to be a preferred depth of the zooplankton to spend the daytime (Plüddemann and Pinkel, 1989). The potential of daily migrating zooplankton as an additional food source for the CWC has also been put forward by Mienis et al. (2012) based on ADCP observations in the Viosca Knoll area in the northern Gulf of Mexico.

4.6 Conclusions

The Campeche CWC province is one of the largest coherent CWC areas discovered so far, and the most relevant in the western Atlantic Ocean. A healthy and highly diverse CWC ecosystem is developed on top of a complex system of 20 to 40 m high, partly interconnected elongated mounds, which probably can serve as a paleo-environmental archive enabling the reconstruction of the long-term development of the Campeche CWC province over the Late Quaternary climatic cycles.

The location of the Campeche CWC province appears to be almost perfect for the establishment of such a large CWC ecosystem. It is (a) located underneath a local upwelling center providing high primary production, (b) influenced by a very dynamic bottom current regime delivering food particles to the corals, and (c) characterized by a physico-chemical setting that fits the recognized ecological needs of *L. pertusa*. The observed diel vertical migration of zooplankton possibly reaching the intermediate depth of the CWC ecosystem may even serve as a supplemental food source as already indicated by Mienis et al. (2012). These observations fits several paleo-environmental studies, highlighting the controlling role of the food supply on the long-term development of such ecosystems (Dorschel et al., 2005; Wienberg et al., 2010; Eisele et al., 2011; Fink et al., 2013).

In many places in the world oceans the physico-chemical setting comply with the niche requirements of *L. pertusa* and other CWC (Davies and Guinotte, 2011), however, only in some of these places CWC ecosystems have developed. Thus, the Campeche CWC province appears to be an excellent example showing that food supply - controlled by a variety of mechanisms - plays a major role in the development of CWC ecosystems.

Acknowledgements

The research leading to these results has received support from the Deutsche Forschungsgemeinschaft (DFG) through funding of the WACOM - West Atlantic Cold-water Coral Ecosystems projects, grants HE 3412/17-1 and DU 129/47-1, and through providing ship time. We thank the officers and crew of the R/V MARIA S. MERIAN, the MARUM ROV

CHEROKEE team, and the scientific crew for on-board assistance during cruise MSM20-4 (2012). The cruise was further supported through the DFG-Research Center/Cluster of Excellence „MARUM - The Ocean in the Earth System“. We are grateful to the Mexican Government for providing access to conduct scientific work in Mexican waters. A. Freiwald received funds from the Hessian LOEWE BiK-F Project A3.10 and G.P. Eberli acknowledges the donors of the American Chemical Society Petroleum Research Fund (Grant# 49017-ND8) for partial support of this research and the industrial associates of the CSL – Center for Carbonate Research at the University of Miami for additional funding. L. Matos has been supported by the FCT scholarship SFRH/BD/72149/2010. This is ISMAR-CNR Bologna scientific contribution n. 1801. This study contributes to the international research program TRACES –Trans-Atlantic Coral Ecosystem Study.

References

Arantes, R. C. M., Castro, C. B., Pires, D. O., and Seoane, J. C. S.: Depth and water mass zonation and species associations of cold-water octocoral and stony coral communities in the southwestern Atlantic, Mar. Ecol.-Prog. Ser., 397, 71-79, 2009.

Becker, E. L., Cordes, E. E., Macko, S. A., and Fisher, C. R.: Importance of seep primary production to *Lophelia pertusa* and associated fauna in the Gulf of Mexico, Deep-Sea Res. Pt. I, 56, 786-800, 2009.

Brooke, S., and Young, C. M.: Reproductive ecology of a deep-water scleractinian coral, Oculina varicosa, from the southeast Florida shelf, Cont. Shelf Res., 23, 847-858, 2003.

Brooke, S., and Schroeder, W. W.: State of the U.S. deep coral ecosystems in the northern Gulf of Mexico region: Florida Straits to Texas, in: The State of Deep Coral Ecosystems of the United States, edited by: Lumsden, S. E., Hourigan, T. F., and Bruckner, A. W., NOAA Technical Memorandum CRCP-3, Silver Spring MD, 271-306, 2007.

Brooke, S. D., Holmes, M. W., and Young, C. M.: Sediment tolerance of two different morphotypes of the deep-sea coral *Lophelia pertusa* from the Gulf of Mexico, Mar. Ecol.-Prog. Ser., 390, 137-144, 2009.

Buhl-Mortensen, L., and Mortensen, P. B.: Symbiosis in deep-water corals, Symbiosis, 37, 33-61, 2004.

Cairns, S. D.: The Deep-Water Scleractinia of the Caribbean Sea and Adjacent Waters, Studies on the Fauna of Curaçao and Other Caribbean Islands, Vol. 57 (180), 341 pp., 1979.

Cairns, S. D., Opresko, D. M., Hopkins, T. S., and Schroeder, W. W.: New records of deep-water Cnidaria (Scleractinia and Antipatharia) from the Gulf of Mexico, Northeast Gulf Science, 13, 1-11, 1993.

Caress, D. W., and Chayes, D. N.: Improved processing of Hydrosweep DS Multibeam Data on the R/V MAURICE EWING, Geophys. Res., 18, 631-650, 1996.

Carlier, A., Le Guilloux, E., Olu-Le Roy, K., Sarrazin, J., Mastrototaro, F., Taviani, M., and Clavier, J.: Trophic relationships in a deep Mediterranean cold-water coral bank (Santa Maria di Leuca, Ionian Sea), Mar. Ecol.-Prog. Ser., 397, 125-137, 2009.

Carrillo González, F., Ochoa, J., Candela, J., Badan, A., Sheinbaum, J., and González Navarro, J. I.: Tidal currents in the Yucatan Channel, Geof. Int., 46, 199-209, 2007.

Caruso, J. H., Ross, S. W., Sulak, K. J., and Sedberry, G. R.: Deep-water chaunacid and lophiid anglerfishes (Pisces: Lophiiformes) off the south-eastern United States, J. Fish Biol., 70, 1015-1026, 2007.

Colman, J. G., Gordaon, D. M., Lane, A. P., Forde, M. J., and Fitzpatrick, J.: Carbonate mounds off Mauretania, Northwest Africa: status of deep-water corals and implications for management of fishing and oil exploration activities, in: Cold-water Corals and Ecosystems, edited by: Freiwald, A., and Roberts, J. M., Springer, Berlin-Heidelberg, 417-441, 2005.

Cordes, E. E., McGinley, M. P., Podowski, E. L., Becker, E. L., Lessard-Pilon, S., Viada, S. T., and Fisher, C. R.: Coral communities of the deep Gulf of Mexico, Deep-Sea Res. Pt. I, 55, 777-787, 2008.

Correa, T. B. S., Eberli, G. P., Grasmueck, M., Reed, J. K., and Correa, A. M. S.: Genesis and morphology of cold-water coral ridges in a unidirectional current regime, Mar. Geol., 326–328, 14-27, 2012a.

Correa, T. B. S., Grasmueck, M., Eberli, G. P., Reed, J. K., Verwer, K., and Purkis, S. A. M.: Variability of cold-water coral mounds in a high sediment input and tidal current regime, Straits of Florida, Sedimentology, 59, 1278-1304, 2012b.

Davies, A. J., Wisshak, M., Orr, J. C., and Roberts, J. M.: Predicting suitable habitat for the cold-water coral *Lophelia pertusa* (Scleractinia), Deep-Sea Res. Pt. I, 55, 1048-1062, 2008.

Davies, A. J., Duineveld, G., Lavaleye, M., Bergman, M. J., van Haren, H., and Roberts, J. M.: Downwelling and deep-water bottom currents as food supply mechanisms to the cold-water coral *Lophelia pertusa* (Scleractinia) at the Mingulay Reef Complex, Limnol. Oceanogr., 54, 620-629, 10.4319/lo.2009.54.2.0620, 2009.

Davies, A. J., Duineveld, G. C. A., van Weering, T. C. E., Mienis, F., Quattrini, A. M., Seim, H. E., Bane, J. M., and Ross, S. W.: Short-term environmental variability in cold-water coral habitat at Viosca Knoll, Gulf of Mexico, Deep-Sea Res. Pt. I, 57, 199-212, 2010.

Davies, A. J., and Guinotte, J. M.: Global habitat suitability for framework-forming cold-water corals, Plos One, 6, e18483, 10.1371/journal.pone.0018483, 2011.

Deines, K. L.: Backscatter estimation using broadband acoustic Doppler current profilers, Proceedings of the Sixth Working Conference on Current Measurement, San Diego, CA, IEEE, 249-253, 1999.

Dodds, L. A., Roberts, J. M., Taylor, A. C., and Marubini, F.: Metabolic tolerance of the cold-water coral *Lophelia pertusa* (Scleractinia) to temperature and dissolved oxgen change, J. Experim. Mar. Biol. Ecol., 349, 205-214, 2007.

Dodds, L. A., Black, K. D., Orr, H., and Roberts, J. M.: Lipid biomarkers reveal geographical differences in food supply to the cold-water coral *Lophelia pertusa* (Scleractinia), Mar. Ecol.-Prog. Ser., 397, 113-124, 2009.

Dorschel, B., Hebbeln, D., Rüggeberg, A., and Dullo, W.-C.: Growth and erosion of a cold-water coral covered carbonate mound in the Northeast Atlantic during the Late Pleistocene and Holocene, Earth Planet. Sci. Lett., 233, 33-44, 2005.

Dorschel, B., Hebbeln, D., Foubert, A., White, M., and Wheeler, A. J.: Hydrodynamics and cold-water coral facies distribution related to recent sedimentary processes at Galway Mound west of Ireland, Mar. Geol., 244, 184-195, 2007.

Dorschel, B., Wheeler, A., Monteys, X., and Verbruggen, K.: Atlas of the Deep-Water Seabed: Ireland, Springer, 164 pp., 2010.

Douarin, M., Elliot, M., Noble, S. R., Sinclair, D., Henry, L.-A., Long, D., Moreton, S. G., and Murray Roberts, J.: Growth of north-east Atlantic cold-water coral reefs and mounds during the Holocene: A high resolution U-series and 14C chronology, Earth Planet. Sci. Lett., 375, 176-187, 2013.

Duineveld, G. C. A., Lavleye, M. S. S., and Berghuis, E. M.: Particle flux and food supply to a seamount cold-water coral community (Galicia Bank, NW Spain), Mar. Ecol.-Prog. Ser., 277, 13-23, 2004.

Duineveld, G. C. A., Lavaleye, M. S. S., Bergman, M. J. N., De Stigter, H., and Mienis, F.: Trophic structure of a cold-water coral mound community (Rockall Bank, NE Atlantic) in relation to the near-bottom particle supply and current regime, B. Mar. Sci., 81, 449-467, 2007.

Dullo, W.-C., Flögel, S., and Rüggeberg, A.: Cold-water coral growth in relation to the hydrography of the Celtic and Nordic European continental margin, Mar. Ecol.-Prog. Ser., 371, 165-176, 2008.

Duncan, P. M.: A description of the Madreporaria dredged up during the expeditions of HMS Porcupine in 1869 and 1870. Part I, Trans. Zool. Soc. London, 8, 303-344, 1873.

Eisele, M., Hebbeln, D., and Wienberg, C.: Growth history of a cold-water coral covered carbonate mound - Galway Mound, Porcupine Seabight, NE-Atlantic, Mar. Geol., 253, 160-169, 2008.

Eisele, M., Frank, N., Wienberg, C., Hebbeln, D., López Correa, M., Douville, E., and Freiwald, A.: Productivity controlled cold-water coral growth periods during the last glacial off Mauritania, Mar. Geol., 280, 143-149, 2011.

Etnoyer, P., Shirley, T., and Lavelle, K. A.: Deep coral and associated species taxonomy and ecology (DeepCAST) II expedition report, NOAA Technical Memorandum. NOAA/NOS Center for Coastal Environmental Health and Biomolecular Research, Charleston, 1-42, 2011.

Fink, H. G., Wienberg, C., Hebbeln, D., McGregor, H. V., Schmiedl, G., Taviani, M., and Freiwald, A.: Oxygen control on Holocene cold-water coral development in the eastern Mediterranean Sea, Deep-Sea Res. Pt. I, 62, 89-96, 2012.

Fink, H. G., Wienberg, C., De Pol-Holz, R., Wintersteller, P., and Hebbeln, D.: Cold-water coral growth in the Alboran Sea related to high productivity during the Late Pleistocene and Holocene, Mar. Geol., 339, 71-82, 2013.

Flögel, S., Dullo, W. C., Pfannkuche, O., Kiriakoulakis, K., and Rüggeberg, A.: Geochemical and physical constraints for the occurrence of living cold-water corals, Deep-Sea Res. Pt. II, in press.

Fosså, J. H., Lindberg, B., Christensen, O., Lundälv, T., Svellingen, I., Mortensen, P. B., and Alsvag, J.: Mapping of *Lophelia* reefs in Norway: experiences and survey methods, in: Cold-water Corals and Ecosystems, edited by: Freiwald, A., and Roberts, J. M., Springer, Berlin-Heidelberg, 359-391, 2005.

Frank, N., Ricard, E., Lutringer-Paquet, A., van der Land, C., Colin, C., Blamart, D., Foubert, A., Van Rooij, D., Henriet, J.-P., de Haas, H., and van Weering, T.: The Holocene occurrence of cold water corals in the NE Atlantic: Implications for coral carbonate mound evolution, Mar. Geol., 266, 129-142, 2009.

Freiwald, A., Hühnerbach, V., Lindberg, B., Wilson, J. B., and Campbell, J.: The Sula Reef Complex, Norwegian Shelf, Facies, 47, 179-200, 2002.

Freiwald, A., Fosså, J. H., Grehan, A., Koslow, T., and Roberts, J. M.: Cold-water Coral Reefs, UNEP-WCMC, Cambridge, UK, Biodiversity Series 22, 84 pp., 2004.

Freiwald, A., and Roberts, J. M.: Cold-water Corals and Ecosystems, Springer, Berlin-Heidelberg, 1243 pp., 2005.

Freiwald, A., Beuck, L., Rüggeberg, A., Taviani, M., Hebbeln, D., and R/V Meteor Cruise M70-1 participants: The white coral community in the central Mediterranean Sea revealed by ROV surveys, Oceanography, 22, 58-74, 2009.

Gori, A., Orejas, C., Madurell, T., Bramanti, L., Martins, M., Quintanilla, E., Marti-Puig, P., Lo Iacono, C., Puig, P., Requena, S., Greenacre, M., and Gili, J. M.: Bathymetrical distribution and size structure of cold-water coral populations in the Cap de Creus and Lacaze-Duthiers canyons (northwestern Mediterranean), Biogeosciences, 10, 2049-2060, 2013.

Gori, A., Grover, R., Orejas, C., Sikorski, S., and Ferrier-Pagès, C.: Uptake of dissolved free amino acids by four cold-water coral species from the Mediterranean Sea, Deep-Sea Res. Pt. II, in press.

Grasmueck, M., Eberli, G. P., Viggiano, D. A., Correa, T., Rathwell, G., and Luo, J.: Autonomous underwater vehicle (AUV) mapping reveals coral mound distribution, morphology, and oceanography in deep water of the Straits of Florida, Geophys. Res. Lett., 33, L23616, 2006.

Hebbeln, D., Wienberg, C., and cruise participants: Report and preliminary results of R/V MARIA S. MERIAN cruise MSM20-4. WACOM - West-Atlantic Cold-water Coral Ecosystems: The West Side Story. Bridgetown – Freeport, 14 March – 7 April 2012, University of Bremen,, 120, 2012.

Henry, L. A. & Roberts, J.M.: Biodiversity and ecological composition of macrobenthos on cold-water coral mounds and adjacent off-mound habitat in the bathyal Porcupine Seabight, NE Atlantic. Deep Sea Res. Part I, 54, 654-672, 2007.

Henry, L. A.: A deep-sea coral 'gateway' in the Northwestern Carribbean, in: Too precious to drill: The marine biodiversity of Belize, edited by: Palomares, M. L. D., and Pauly, D., Fisheries Centre Research Reports, 120-124, 2011.

Heywood, V. H.: The Global Biodiversity Assessment, The Globe, 30, 2-4, 1996.

Hübscher, C., Dullo, W. C., Flögel, S., Titschack, J., and Schönfeld, J.: Contourite drift evolution and related coral growth in the eastern Gulf of Mexico and its gateways, Int. J. Earth Sci., 99, S191-S206, 2010.

Kano, A., Ferdelman, T. G., Williams, T., Henriet, J.-P., Ishikawa, T., Kawagoe, N., Takashima, C., Kakizaki, Y., Abe, K., Sakai, S., Browning, E. L., Li, X., and Integrated Ocean Drilling Program Expedition 307 Scientists: Age constraints on the origin and growth history of a deep-water coral mound in the northeast Atlantic drilled during Integrated Ocean Drilling Program Expedition 307, Geology, 35, 1051-1054, 2007.

Kenyon, N. H., Akhmetzhanov, A. M., Wheeler, A. J., van Weering, T. C. E., de Haas, H., and Ivanov, M. K.: Giant carbonate mud mounds in the southern Rockall Trough, Mar. Geol., 195, 5-30, 2003.

Kiriakoulakis, K., Harper, E., and Wolff, G. A.: Lipids and nitrogeen isotopes of two deep-water corals from the North-East Atlantic: initial results and implications for their nutrition, in: Cold-water Corals and Ecosystems, edited by: Freiwald, A., and Roberts, J. M., Springer, Berlin-Heidelberg, 715-729, 2005.

Le Guilloux, E., Olu-Le Roy, K., Bourillet, J. F., Savoye, B., Iglésias, S. P., and Sibuet, M.: First observations of deep-sea coral reefs along the Angola margin, Deep-Sea Res. Part II, 56, 2394-2403, 2009.

Lessard-Pilon, S., Podowski, E. L., Cordes, E. E., and Fisher, C. R.: Megafauna community composition associated with *Lophelia pertusa* colonies in the Gulf of Mexico. Deep-Sea Res. Part II, 57, 1882-1890, 2010.

López Correa, M., Montagna, P., Joseph, N., Rüggeberg, A., Fietzke, J., Flögel, S., Dorschel, B., Goldstein, S. L., Wheeler, A., and Freiwald, A.: Preboreal onset of cold-water coral growth beyond the Arctic Circle revealed by coupled radiocarbon and U-series dating and neodymium isotopes, Quat. Sci. Rev., 34, 24-43, 2012.

Lutz, S. J., and Ginsburg, R. N.: State of the U.S. deep coral ecosystems in the United States Caribbean region: Puerto Rico and U.S. Virgin Islands, in: The State of Deep Coral Ecosystems of the United States, edited by: Lumsden, S. E., Hourigan, T. F., and Bruckner, A. W., NOAA Technical Memorandum CRCP-3, Silver Spring MD, 307-365, 2007.

Mah, C., Nizinski, M., and Lundsten, L.: Phylogenetic revision of the Hippasterinae (Goniasteridae; Asteroidea): systematics of deep sea corallivores, including one new genus and three new species, Zool. J. Linnean Soc., 160, 266-301, 2010.

Mangini, A., Godoy, J. M., Godoy, M. L., Kowsmann, R., Santos, G. M., Ruckelshausen, M., Schroeder-Ritzrau, A., and Wacker, L.: Deep sea corals off Brazil verify a poorly ventilated Southern Pacific Ocean during H2, H1 and the Younger Dryas, Earth Planet. Sci. Lett., 293, 269-276, 2010.

Merino, M.: Upwelling on the Yucatan Shelf: hydrographic evidence, J. Marine Syst., 13, 101-121, 1997.

Messing, C. G., Neumann, A. C., and Lang, J. C.: Biozonation of deep-water lithoherms and associated hardgrounds in the northeastern Straits of Florida, Palaois, 5, 15-33, 1990.

Messing, C. G., Reed, J. K., Brooke, S. D., and Ross, S. W.: Deep-Water Coral Reefs of the United States, in: Coral Reefs of the USA, edited by: Riegl, B., and Dodge, R. E., Springer, 763-787, 2008.

Mienis, F., de Stigter, H. C., White, M., Duineveld, G., de Haas, H., and van Weering, T. C. E.: Hydrodynamic controls on cold-water coral growth and carbonate-mound development at the SW and SE Rockall Trough Margin, NE Atlantic Ocean, Deep-Sea Res. Pt. I, 54, 1655-1674, 2007.

Mienis, F., Duineveld, G. C. A., Davies, A. J., Ross, S. W., Seim, H., Bane, J., and Van Weering, T. C. E.: The influence of near-bed hydrodynamic conditions on cold-water corals in the Viosca Knoll area, Gulf of Mexico, Deep-Sea Res. Pt. I, 60, 32-45, 2012.

Miller, K. J., Rowden, A. A., Williams, A., and Häussermann, V.: Out of their depth? Isolated deep populations of the cosmopolitan coral *Desmophyllum dianthus* may be highly vulnerable to environmental change, Plos One, 6, e19004, 2011.

Molinari, R. L., and Morrison, J.: The separation of the Yucatan Current from the Campeche Bank and the intrusion of the Loop Current into the Gulf of Mexico, J. Geophysic. Res., 93, 10645-10654, 1988.

Moore, D. R., and Bullis, H. R.: A deep-water coral reef in the Gulf of Mexico, Bull. Mar. Sci. Gulf Caribbean, 10, 125-128, 1960.

Moseley, H. N.: Report on certain hydroid, alcyonarian, and madreporarian corals procured during the voyage of H.M.S. Challenger, in the years 1873-1876. Report of Scientific Research of H.M.S. Challenger, Zoology, 2, 1-248, 1881.

Mueller, C. E., Lundälv, T., Middelburg, J. J., and Van Oevelen, D.: The symbiosis between *Lophelia pertusa* and *Eunice norvegica* stimulates coral calcification and worm assimilation, Plos One, 8, e58660, 2013.

Müller-Karger, F. E., Walsh, J. J., Evans, R. H., and Meyers, M. B.: On the seasonal phytoplankton concentration and sea surface temperature cycles of the Gulf of Mexico as determined by satellites, J. Geophysic. Res., 96, 12645-12665, 1991.

Mullins, H. T., Newton, C. R., Heath, K., and Vanburen, H. M.: Modern deep-water coral mounds north of Little Bahama Bank: criteria for recognition of deep-water coral bioherms in the rock record, J. Sed. Petrol., 51, 999-1013, 1981.

Neumann, A. C., and Ball, M. M.: Submersible observations in Straits of Florida - geology and bottom currents, Geol. Soc. Americ. Bull., 81, 2861-2873, 1970.

Neumann, A. C., Kofoed, J. W., and Keller, G. H.: Lithoherms in the Straits of Florida, Geology, 5, 4-10, 1977.

Newton, C. R., Mullins, H. T., and Gardulski, A. F.: Coral mounds on the West Florida Slope: unanswered questions regarding the development of deepwater banks, Palaois, 2, 359-367, 1987.

Orejas, C., Gori, A., Lo Iacono, C., Puig, P., Gili, J. M., and Dale, M. R.: Cold-water corals in the Cap de Creus canyon (north-western Mediterranean): spatial distribution, density and anthropogenic impact, Mar. Ecol.-Prog. Ser., 397, 37-51, 2009.

Paull, C. K., Neumann, A. C., am Ende, B. A., Ussler III, W., and Rodriguez, N. M.: Lithoherms on the Florida–Hatteras slope, Mar. Geol., 166, 83–101, 2010.

Plüddemann, A. J., and Pinkel, R.: Characterization of the patterns of diel migration using a doppler sonar, Deep-Sea Res., 36, 509-530, 1989.

Reed, J. K.: Comparison of deep-water coral reefs and lithoherms off southeastern USA, Hydrobiol., 471, 57-60, 2002.

Reed, J. K., Weaver, D., and Pomponi, S. A.: Habitat and fauna of deep-water *Lophelia pertusa* coral reefs off the Southeastern USA: Blake Plateau, Straits of Florida, and Gulf of Mexico, B. Mar. Sci., 78, 343-375, 2006.

Reyes, J., Santodomingo, N., Gracia, A., Borrero-Pérez, G., Navas, G., Mejía-Ladino, L. M., Bermudéz, A., and Benavidos, M.: Southern Caribbean azooxanthellate coral communities off Colombia, in: Cold-water Corals and Ecosystems, edited by: Freiwald, A., and Roberts, J. M., Springer, Berlin-Heidelberg, 309-330, 2005.

Roberts, J. M., Wheeler, A. J., and Freiwald, A.: Reefs of the deep: The biology and geology of cold-water coral ecosystems, Science, 312, 543-547 2006.

Roberts, J. M., Wheeler, A. J., Freiwald, A., and Cairns, S. D.: Cold-water corals. The biology and geology of deep-sea coral habitats, Cambridge University Press, 336 pp., 2009.

Ross, S. W.: Unique deep-water ecosystems off the southeastern United States, Oceanography, 20, 130-139, 2007.

Ross, S. W., and Nizinski, M. S.: State of the U.S. deep coral ecosystems in the southeastern United States region: Cape Hatteras to the Florida Straits, in: The State of Deep Coral Ecosystems of the United States, edited by: Lumsden, S. E., Hourigan, T. F., and Bruckner, A. W., NOAA Technical Memorandum CRCP-3, Silver Spring MD, 233-270, 2007.

Ross, S. W., and Quattrini, A. M.: The fish fauna associated with deep coral banks off the southeastern United States, Deep-Sea Res. Pt. I, 54, 975-1007, 2007.

Sanamyan, N. P., Sanamyan, K. E., and Tabachnick, K. R.: The first species of Actiniaria, Spongiactis japonica gen.n., sp.n. (Cnidaria: Anthozoa), an obligate symbiont of a glass sponge, Invert. Zool., 9, 127-141, 2012.

Savini, A., Vertino, A., Marchese, F., Beuck, L., and Freiwald, A.: Mapping Cold-Water Coral Habitats at Different Scales within the Northern Ionian Sea (Central Mediterranean): An Assessment of Coral Coverage and Associated Vulnerability. PLoS ONE 9(1): e87108. doi:10.1371/journal.pone.0087108, 2014.

Schroeder, W. W.: Observations of *Lophelia pertusa* and the surficial geology at a deep-water site in the northeastern Gulf of Mexico, Hydrobiol., 471, 29-33, 2002.

Schroeder, W. W., Brooke, S. D., Olson, J. B., Phaneuf, B., McDonough, J. J., and Etnoyer, P.: Occurrence of deep-water *Lophelia pertusa* and *Madrepora oculata* in the Gulf of Mexico, in: Cold-water Corals and Ecosystems, edited by: Freiwald, A., and Roberts, J. M., Springer, Berlin-Heidelberg, 297-307, 2005.

Schulkin, M., and Marsh, H. W.: Sound absorption in seawater, J. Acoust. Soc. Am., 34, 864-865, 1962.

Sheinbaum, J., Candela, J., Badan, A., and Ochoa, J.: Flow structure and transport in the Yucatan Channel, Geophys. Res. Lett., 29, 1040, 10.1029/2001GL013990, 2002.

Stevenson, A., and Rocha, C.: Evidence for the bioerosion of deep-water corals by echinoids in the Northeast Atlantic, Deep-Sea Res. Pt. I, 71, 73-78, 2013.

Taviani, M., Angeletti, L., Dimech, M., Mifsud, C., Freiwald, A., Harasewych, M. G., and Oliverio, M.: Coralliophilinae (Gastropoda: Muricidae) associated with deep-water coral banks in the Mediterranean, The Nautilus, 123, 106-112, 2009.

Thierens, M., Browning, E., Pirlet, H., Loutre, M. F., Dorschel, B., Huvenne, V. A. I., Titschack, J., Colin, C., Foubert, A., and Wheeler, A. J.: Cold-water coral carbonate mounds as unique palaeo-archives: the Plio-Pleistocene Challenger Mound record (NE Atlantic), Quat. Sci. Rev., 73, 14-30, 2013.

Titschack, J., Thierens, M., Dorschel, B., Schulbert, C., Freiwald, A., Kano, A., Takashima, C., Kawagoe, N., and Li, X.: Carbonate budget of a cold-water coral mound (Challenger Mound, IODP Exp. 307), Mar. Geol., 259, 36-46, 2009.

van Oevelen, D., Duineveld, G., Lavaleye, M., Mienis, F., Soetaert, K., and Heip, C. H. R.: The cold-water coral community as a hot spot for carbon cycling on continental margins: A food-web analysis from Rockall Bank (northeast Atlantic), Limnol. Oceanogr., 54, 1829-1844, 2009.

Van Rooij, D., De Mol, B., Huvenne, V., Ivanov, M., and Henriet, J. P.: Seismic evidence of current-controlled sedimentation in the Belgica mound province, upper Porcupine slope, southwest of Ireland, Mar. Geol., 195, 31-53, 2003.

Wawrik, B., and Paul, J. H.: Phytoplankton community structure and productivity along the axis of the Mississippi River Plume in oligotrophic Gulf of Mexico waters, Aqua. Microb. Ecol., 35, 185-196, 2004.

Wei, C. L., Rowe, G. T., Escobar-Briones, E., Nunnally, C., Soliman, Y., and Ellis, N.: Standing stocks and body size of deep-sea macrofauna: Predicting the baseline of 2010 Deepwater Horizon oil spill in the northern Gulf of Mexico, Deep-Sea Res. Pt. I, 69, 82-99, 2012.

Wessel, P., and Smith, W. H. F.: New, improved version of Generic Mapping Tools released, EOS, 79, 579, 1998.

White, M., Mohn, C., de Stigter, H., and Mottram, G.: Deep-water coral development as a function of hydrodynamics and surface productivity around the submarine banks of the

Rockall Trough, NE Atlantic, in: Cold-Water Corals and Ecosystems, edited by: Freiwald, A., and Roberts, J. M., Springer, Berlin-Heidelberg, 503-514, 2005.

White, M., and Dorschel, B.: The importance of the permanent thermocline to the cold water coral carbonate mound distribution in the NE Atlantic, Earth Planet. Sci. Lett., 296, 395-402, 2010.

Wienberg, C., Hebbeln, D., Fink, H. G., Mienis, F., Dorschel, B., Vertino, A., López Correa, M., and Freiwald, A.: Scleractinian cold-water corals in the Gulf of Cádiz - first clues about their spatial and temporal distribution, Deep-Sea Res. Pt. I, 56, 1873-1893, 2009.

Wienberg, C., Frank, N., Mertens, K. N., Stuut, J.-B., Marchant, M., Fietzke, J., Mienis, F., and Hebbeln, D.: Glacial cold-water coral growth in the Gulf of Cádiz: Implications of increased palaeo-productivity, Earth Planet. Sci. Lett., 298, 405-416, 2010.

Zavala-Hidalgo, J., Gallegos-García, A., Martínez-López, B., Morey, S. L., and O'Brien, J. J.: Seasonal upwelling on the Western and Southern Shelves of the Gulf of Mexico, Ocean Dynam., 56, 333-338, 2006.

5 Coral mound development at the Campeche cold-water coral province, southern Gulf of Mexico: implications of Antarctic Intermediate Water increased influence during interglacials

Lélia Matos[a,b,c], Claudia Wienberg[a], Jürgen Titschack[a], Gerhard Schmiedl[d], Norbert Frank[e], Fatima Abrantes[b,f], Marina R. Cunha[c,g], Dierk Hebbeln[a]

[a] Center for Marine Environmental Sciences (MARUM), University of Bremen, Germany
[b] Portuguese Institute for Sea and Atmosphere (IPMA), Portugal
[c] Center for Environmental and Marine Studies (CESAM), University of Aveiro, Portugal
[d] Center for Earth System Research and Sustainability, Inst. Geology, University of Hamburg, Germany
[e] Institut für Umweltphysik, Ruprecht-Karls Universität Heidelberg, Germany
[f] Center of Marine Sciences (CCMAR), University of Algarve, Portugal
[g] Departament of Biology, University of Aveiro, Portugal

Correspondence to: Lélia Matos (lmatos@marum.de)

Abstract

Coral mounds formed by framework-forming scleractinian cold-water corals (CWC; mainly *Lophelia pertusa*) are a common seabed feature along the Atlantic continental margins. While coral mound areas in the NE Atlantic reveal a climate-dependent temporal pattern of CWC occurrence and mound aggradation that is related to distinct environmental conditions (e.g., productivity, water mass properties, hydrodynamics), the long-term development of CWC and coral mounds at the western side of the Atlantic is less well documented and understood. Here, we present a 260-kyr coral record from the recently described Campeche CWC province in the southern Gulf of Mexico, combined with a reconstruction of the paleo-environmental conditions for the last 140 kyr. Uranium-series dating of 26 coral samples reveals that CWC growth predominantly coincided with interglacial periods. Highest vertical mound aggradation rates of 34 to 40 cm kyr^{-1} occurred during the Holocene. The reduced occurrence of CWC and the concurrent almost complete stagnation in mound aggradation during glacial periods could be linked to a diminished presence of Antarctic Intermediate Water at those intermediate depths in which the coral mounds occur. Such setting would have caused a less dynamic

bottom current regime resulting in a reduced food supply to the CWC along the Campeche Bank.

5.1 Introduction

The framework-forming scleractinian cold-water corals (CWC) *Lophelia pertusa* and *Madrepora oculata* are known to have the capability of forming large three-dimensional seabed structures, called coral mounds (Freiwald and Roberts, 2005; Hebbeln and Samankassou, 2015; Roberts et al., 2009; Wienberg and Titschack, *in press*). Coral mounds form when the environmental conditions, such as food availability, distinct physico-chemical water mass properties and a vigorous bottom current regime (see Davies and Guinotte, 2011) allow steady CWC growth and sufficient sediment is supplied and deposited to secure the stabilization of the biogenic framework (e.g., de Haas et al., 2009; Hebbeln and Samankassou, 2015; Huvenne et al., 2009; Wienberg and Titschack, *in press*). Such coral mounds can form impressive paleo-archives preserving the history of CWC development for more than 2 million years (e.g., Kano et al. 2007).

So far, numerous coral mounds have been described mainly from the North Atlantic Ocean, where they are often arranged in clusters or provinces covering extended areas along the shelf and continental margins of NW Europe, NW Africa and the eastern US margin (e.g. Colman et al. 2005; Correa et al. 2012; De Mol et al. 2002; Fosså et al. 2005; Glogowski et al. 2015; Paull et al. 2000). Several studies from the extensively studied NE Atlantic have reconstructed the temporal occurrence of *Lophelia pertusa* and *Madrepora oculata* as well as the past development of coral mounds formed by these species during the past thousands to millions of years (e.g. Kano et al. 2007), thereby revealing a climate-dependent pattern (e.g. Frank et al. 2011). In the northern NE Atlantic (>50°N; mainly comprising the Norwegian shelf and the Irish slope), CWC occurrence and coral mound aggradation are documented mainly for interglacial periods (Dorschel et al., 2005; Eisele et al., 2008; Frank et al., 2009; López Correa et al., 2012; Raddatz et al., 2014; Van der Land et al., 2014). Contrarily, the formation of coral mounds in the southern NE Atlantic (<37°N), namely along the Moroccan and Mauritanian margins, was largely restricted to glacial periods (Eisele et al., 2011; Taviani et al., 1991; Wienberg et al., 2010, 2009).

Previous studies dealing with the temporal occurrence of CWC in the NW Atlantic and using them for palaeo-oceanographic and ecological studies mainly focused on solitary corals such as *Desmophyllum dianthus* collected from various seamounts (New England seamounts; Robinson et al. 2007; Thiagarajan et al. 2013). However, the long-term development of NW Atlantic coral mounds formed by *L. pertusa*, comprising CWC areas along the eastern US slope, the Florida Straits, and the Gulf of Mexico (GoM), are less well documented. Besides the three *L. pertusa* datings obtained from the northern and eastern GoM (Viosca Knoll and West Florida Slope), presenting ages from the last glacial period (~25-31 calibrated (cal) ka BP; Newton et al., 1987; Sulak, 2008), only one stratigraphic study based on sediment cores is available. The single long-term record regarding coral mound development along the NW Atlantic margin comes from the Cape Lookout CWC area (off North Carolina, USA; Matos et al., 2015). Here, coral mounds are mainly formed by *L. pertusa* and the sustained occurrence of this species and concurrent mound aggradation seem to have been restricted to interglacial periods, displayed by coral ages spanning from 123-128 ka and the last 6.8 kyr (Matos et al., 2015).

The recent discovery of the large Campeche CWC province in the southern GoM, comprising numerous coral mounds presently covered by extensive living CWC (Hübscher et al. 2010; Hebbeln et al. 2014) advocates for favorable conditions (at least) under the present-day setting. Nonetheless, nothing is known so far about the temporal occurrence of CWC and the development of the Campeche coral mounds in the past. Newly obtained sediment cores, collected from the Campeche CWC province, provide unique palaeo-records which allow to unravel periods of sustained CWC occurrence and mound formation in this area and to relate these to a distinct environmental setting. Regarding the still limited knowledge about the past occurrence of CWC and development of coral mounds in the NW Atlantic, this study provides an important contribution to (a) increase our understanding on the likely climate-dependent development of CWC sites at this side of the Atlantic and to (b) identify any potential linkage between CWC sites in the NW and NE Atlantic in relation to intermediate water mass circulation.

5.2 Regional setting

The Campeche CWC province is a coral mound area (>40 km^2) at the northeastern rim of the Campeche Bank (Hebbeln et al., 2014), an extensive carbonate platform situated in the north of the Yucatán Peninsula in the southern GoM (Fig. 1). It is limited to the west by a 40-m-high escarpment that separates the coral mounds from the shallower Campeche Bank and to the east by a major sediment drift in water depths of >600 m (Hebbeln et al., 2014; Hübscher et al., 2010). The Campeche coral mounds occur along a gently dipping slope between 480 m and 600 m water depth. They have an elongated shape with lengths varying from a few tens of meters to >1000 m and heights between 20-40 m. Their surface is covered by a live coral framework composed of *L. pertusa* and *Enallopsammia profunda* (Hebbeln et al., 2014).

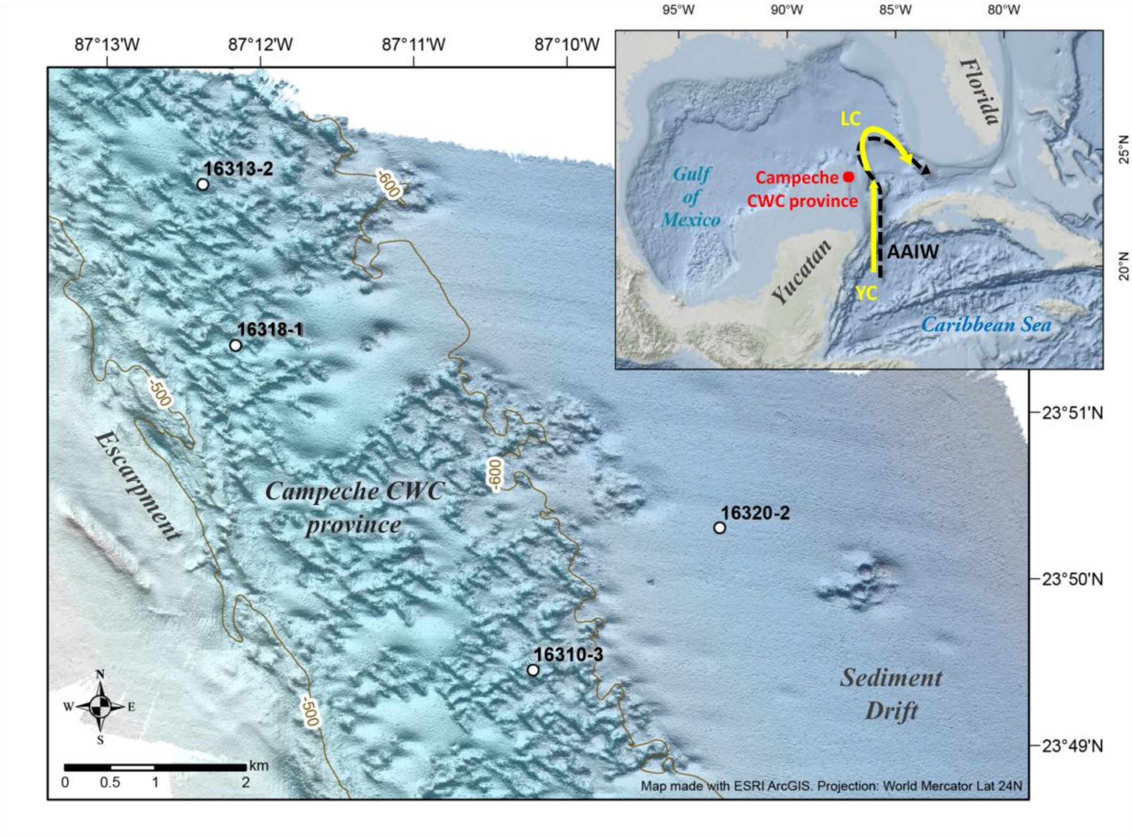

Figure 1. Map of the Campeche cold-water coral mounds between the escarpment of the Campeche Bank to the west and the drift sediments downslope (>600 m water depth) to the east. Locations of the four gravity cores analyzed for this study are marked with white dots and are labeled by their GeoB core-ID (see Table 1 for metadata). The 500 and 600 m isobaths are marked by grey lines. The inset puts the study area along the northeastern Campeche Bank (red dot) in the context of the Gulf of Mexico. Surface currents are indicated by the yellow lines (LC, Loop current; YC, Yucatan current), whereas the dashed black line indicates the Antarctic Intermediate Water (AAIW).

The local oceanography is mainly characterized by five water masses. The Caribbean Surface Water is confined to depths shallower than 80 m (salinity <36.4; 26–27.5 °C; Hebbeln et al., 2014; Merino, 1997). Below, we find the Subtropical Intermediate Water, whose core is characterized by a salinity maximum at 100-160 m water depth (salinity 36.8; 23 °C; Hebbeln et al., 2014; Merino, 1997); followed by the Tropical Atlantic Central Water (TACW) presenting an oxygen minimum at depths ~500 m and thermohaline characteristics (salinity 35–36.1; 8–16 °C; Rivas et al., 2005) and the Antarctic Intermediate Water (AAIW). The upper boundary of the AAIW is identified by the salinity minimum found at ~540 m water depth (salinity <35; 7 °C; Hebbeln et al., 2014; Rivas et al., 2005). The North Atlantic Deep Water can be found at depths deeper than 1000 m, characterized by a salinity maximum (salinity 35; 4°C; Rivas et al., 2005). A strong density gradient is found at around 520–540 m (the upper range of observed living CWC; Hebbeln et al., 2014) that is likely related to the boundary (pycnocline) between the TACW and the AAIW. The presence of internal waves is suggested by the presence of undulating isotherms (Hebbeln et al., 2014).

The Campeche CWC province is dominated by SE-NW currents, influenced by the Yucatán and Loop currents (Fig. 1), which are strongest at the surface (<130 m water depth; 74–83 cm s^{-1}) (Hebbeln et al., 2014). Between 500 and 600 m water depth (the depth interval in which the Campeche coral mounds occur), lower but still strong bottom currents with average velocities of ca. 30 cm s^{-1} are observed (Hebbeln et al., 2014).

5.3 Material and methods

All the sediment cores used in this study were acquired during the WACOM MSM 20-4 expedition (German R/V *Maria S. Merian*) in Spring 2012 (Hebbeln et al., 2012). Coral-bearing gravity cores collected from the coral mounds (on-mound cores) have been studied in order to investigate the pattern of temporal CWC occurrence in the Campeche CWC province. Three on-mound cores were collected at water depths ranging between 553 and 573 m having recoveries between 2.5 and 10.5 m (Table 1). The usage of three on-mound cores from three coral mounds (Fig. 1) allows the detection of potential spatial variability in coral mound development and increases the representativeness of the data. Prior to sampling in the lab, the cores were cut frozen with a diamond saw, in order to keep the internal sedimentary structure intact.

Additionally, a paleoceanographic record has been developed from a core barren of CWC fragments collected from the nearby sediment drift (off-mound core) in order to define the environmental factors controlling CWC mound development. The off-mound core was collected at 626 m water depth, slightly downslope of the Campeche CWC province, and had a total recovery of 4.4 m (Fig. 1, Table 1).

Table 1. Metadata of the sediment cores (on- and off-mound cores) collected with gravity corers at the Campeche cold-water coral province during the WACOM MSM 20-4 expedition (German R/V *Maria S. Merian*; Hebbeln et al. 2012). WD: water depth.

Core ID	**Latitude** º [N]	**Longitude** º [W]	**WD** (m)	**Location**	**Coral-bearing**	**Recovery** (m)
GeoB16310-3	23.820	87.170	573	on-mound	yes	10.56
GeoB16313-2	23.867	87.200	553	on-mound	yes	2.51
GeoB16318-1	23.850	87.200	556	on-mound	yes	4.73
GeoB16320-2	23.838	87.150	626	off-mound	no	4.39

5.3.1 Uranium-series dating on cold-water corals

In order to identify periods of sustained CWC occurrence, 26 well-preserved fragments of *L. pertusa* (24x) and *E. profunda* (2x) were sampled from various depths of the three on-mound gravity cores and used for Uranium-series dating. Prior to the analyses, the coral samples were cleaned mechanically to remove small borings by organisms and remains of organic tissue and non-coral contaminants from the skeleton surfaces (e.g. epibionts, iron–manganese crusts, coatings). They were then prepared chemically using weak acid leaching and water rinsing procedures as described by Frank et al. (2004). The aragonite fragments were then weighed, dissolved and spiked as described in Matos et al. (2015). Thorium (Th) and Uranium (U) were extracted and purified from the sample solutions using the ion exchange resin U-TEVA according to Douville et al. (2010). Finally, the Th and U fractions were prepared and the isotopic measurements were performed either on a ThermoFisher Neptune Plus MC-ICPMS at the Laboratoire des Sciences du Climat et de l'Environnement (Gif-sur-Yvette, France) or on a ThermoFisher iCAP-Qs ICP-MS at the Institute for Environmental Physics (Heidelberg University, Germany) using the methods and yielding reproducibility previously published by Douville et al. (2010). Isotopic ratios were normalized to the isotopic compositions of the secular equilibrium standard (Harwell Uraninite) HU-1 (Cheng et al., 2000). Full procedural chemical blanks were considered for data adjustment; and age calculation based on isotopic ratios was performed through iterative age estimation (Ludwig and Titterington, 1994), propagating all analytical errors into the Monte-Carlo age and uncertainty simulation. Finally, ages were corrected for ^{230}Th contribution from seawater and/or residual non-carbonate contamination using an estimated (^{230}Th/^{232}Th) activity ratio of 10±6 for sub-surface seawater. This correction is however negligible within uncertainty of the initial age estimates. One sample presenting a low initial δ^{234}U value of 131 ‰, quite below the 146.8 ‰ value of open ocean seawater (Andersen et al., 2010), was found to be likely influenced by diagenetic alteration that may lead to an unreliable age and was, thus, discarded.

For each of the three studied cores, mound aggradation rates (reported in cm kyr^{-1}) were calculated between consecutive coral datings, except for ages that were similar within the error and for core units presenting age reversals or large age gaps of several tens of thousands of years.

5.3.2 Analyses on the off-mound core GeoB16320-2

5.3.2.1 Accelerator mass spectrometry (AMS) radiocarbon (^{14}C) dating

To obtain a stratigraphy for the off-mound core GeoB16320-2, five samples consisting of ~8 mg calcium carbonate of mixed planktic foraminifera of the size fraction >150 µm were collected along the core. AMS ^{14}C dating was performed at the Poznań Radiocarbon Laboratory (Poznań, Poland). The obtained ages were corrected for ^{13}C and a mean ocean reservoir age of 405 years, and converted to calendar years (cal yr BP, present is AD 1950) using the MARINE13 calibration curve (Reimer et al., 2013) of the CALIB7.0 software (Stuiver and Reimer, 1993).

5.3.2.2 Benthic foraminifera stable isotopes

Stable oxygen ($\delta^{18}O$) and carbon ($\delta^{13}C$) isotopes were analyzed from shells of the benthic foraminifera *Planulina ariminensis.* Well-preserved and clean specimens (size fraction >150 µm; 8-10 specimens) were picked from 86 sediment samples collected at 5-cm-interval along the core. Stable isotopes were analyzed with a Finnigan MAT 252 gas isotope ratio mass spectrometer connected to an automated carbonate preparation device, housed at the Isotope Laboratory at MARUM (University of Bremen, Germany). Solnhofen Limestone calibrated against NBS 19 (in its turn calibrated against the Vienna Pee Dee Belemnite) was used as an internal standard, with a long-term standard deviation of <0.07‰ for oxygen and 0.05‰ for carbon.

5.3.2.3 Sediment particle size

The siliciclastic particle size spectrum of the terrigenous fraction of the sediment was determined in 5-cm-intervals. Particle-size measurements were performed in the Particle-Size Laboratory at MARUM, University of Bremen with a Beckman Coulter Laser Diffraction Particle Size Analyzer LS 13320. Prior to the measurements, the terrigenous sediment fractions were isolated by removing organic carbon, calcium carbonate, and biogenic opal by boiling the samples (in about 200 ml water) with 10 ml of H_2O_2 (35%; until the reaction stopped), 10 ml of HCl (10%; 1 min) and 6 g NaOH pellets (10 min), respectively. After each preparation step the samples were diluted (dilution factor: >25). Finally, remaining aggregates were destroyed prior to the measurements by boiling the samples with ~0.3 g tetra-sodium diphosphate decahydrate ($Na_4P_2O_7 * 10H_2O$, 3 min) (see also McGregor et al., 2009). Sample preparation and measurements were carried out with deionized, degassed and filtered water (filter mesh size: 0.2 µm) to reduce the potential influence of gas bubbles or particles within the water. The obtained results provide the particle-size distribution of a sample from 0.04 to 2000 µm divided in 116 size classes. The calculation of the particle sizes relies on the Fraunhofer diffraction theory and the Polarization Intensity Differential Scattering (PIDS) for particles from 0.4 to 2000 µm and from 0.04 to 0.4 µm, respectively. The reproducibility was checked regularly by replicate analyses of three internal glass-bead standards and is found to be better than ±0.7 µm for the mean and ±0.6 µm for the median particle size (1σ). The average standard deviation integrated overall size classes is better than ±4 vol% (note that the standard deviation of the individual size classes is not distributed uniformly). All provided statistic values are based on a geometric statistic.

5.3.2.4 Benthic foraminifera species assemblages

A set of 20 samples was selected to study benthic foraminifera species composition in order to investigate the environmental changes related to the CWC occurrence pattern. Sampling concentrated on the last ~20 kyr to gain a higher data resolution during this time interval. On average, census counts of ca. 300 individual shells were performed on representative splits of the size fraction >150 µm. For the evaluation of the benthic ecosystem stability, the Shannon-Wiener diversity index H(*S*) was calculated following Buzas & Gibson (1969). Bottom water oxygenation was assessed by the percentage of species typical of high (HO) and low (LO) oxygen environments according to Schmiedl et al. (2003). The selected HO species included assorted miliolids, *Cibicidoides* spp. and *P. ariminensis*; while LO species considered were *Chilostomella oolina*, *Globobulimina pacifica*, *Fursenkoina* spp. and *Stainforthia concava*. The percentage of shallow water species (shallower than the study site) was considered as an indicator of lateral/downslope transport. The species considered as shallow water indicators include *Amphistegina lessonii*, *Cancris auriculus*, *Cymbaloporetta atlantica*, *Discorbis* spp., *Elphidium* spp., *Neoconorbina terquemi*, *Nonion* spp., *Patellina corrugata*, *Peneroplis bradyi* and *Rosalina* spp. based on their common association with shelf or near-shore environments (e.g. Murray 2006; Milker & Schmiedl 2012). Furthermore, a Q-mode Principal Component Analysis (PCA) with Varimax rotation was performed using the software Systat (version 5.2.1) in order to investigate temporal changes in the faunal assemblages. PC loadings >0.4 were considered significant (Malmgren and Haq, 1982), PC scores >3 were assigned to dominant taxa and PC scores between 2 and 3 to associated taxa.

5.4 Results

5.4.1 Coral ages and mound aggradation rates

On core GeoB16310-3, a total of 16 CWC fragments revealed U-series ages ranging from 257 ka to 1.6 ka, hence spanning from the late MIS 8 to the Late Holocene (Fig. 2A, Table 2). The ages cluster in three units, which suggest the occurrence of three distinct coral mound aggradation periods with all of them being related to interglacial periods. The first unit is found at a core depth between 1055 and 516 cm and presents ages between 257 ka and 215 ka, corresponding to the late MIS 8 and to the MIS 7. This unit presents some age reversals between 935 and 831 cm and at 516 cm core depth (Fig. 2.1). Although possibly reworked, the CWC fragments from this unit still document the presence of living corals at the yielded age. However, they have not been considered when calculating mound aggradation rates. The average mound aggradation rate for the core interval with consecutive ages (and without age reversals) within the unit (core depth: 804-637 cm; corresponding to the MIS 7 ages) is 13.8 cm kyr^{-1} (Fig. 2.1). A second unit occurring between 390 and 319 cm core depth presents ages of 114 ka and 95 ka (corresponding to the MIS 5) and has an aggradation rate of 3.8 cm kyr^{-1} (Fig. 2.1). Lastly, a third unit occurs between 286 and 11 cm core depth and presents ages between 10.1 ka and 1.6 ka that correspond to the Holocene period. The average aggradation rate estimated for this unit is 34.2 cm kyr^{-1} (Fig. 2.1).

The six U-series ages obtained for core GeoB16318-1 span from 99.1 ka to 4.4 ka (Fig. 2B, Table 2) and cluster in two units that also suggest the occurrence of two distinct coral mound aggradation periods. The first unit corresponds to the core depth interval between 437 and 133 cm and includes the four oldest coral ages, which correspond to the MIS 5 and the early MIS 4. The average mound aggradation rate for this unit is 10.7 cm kyr^{-1} (Fig. 2B). The second unit includes two samples of the same age (within the dating error) from the Mid-Holocene (Fig. 2B, Table 2).

Table 2 (next page). U-series ages, isotope concentrations and ratios. U-series datings were performed on fragments of the two cold-water coral species *Lophelia pertusa* (Lp) and *Enallopsammia profunda* (Ep). ^{1}Th corrected ages; *discarded (see text). CD: core depth.

Core	CD (cm)	Species	Lab ID	[^{238}U] (ng/g)	[^{232}Th] (ng/g)	$\delta^{234}U_m$ (‰)	(^{230}Th/^{232}Th)	^{230}Th/^{238}U	age (kyr)	$\delta^{234}U_{initial}$ (‰)	corrected age (kyr)[1]
GeoB16310-3	11	Lp	LSCE-3370	3.717 ±0.006	0.8371 ±0.0007	146.8 ±1.1	208 ±1	0.0163 ±0.0001	1.562 ±0.011	147.4 ±1.1	1.465 ±0.063
GeoB16310-3	66	Ep	LSCE-3371	4.390 ±0.010	0.3709 ±0.0005	144.7 ±1.2	1159 ±4	0.0362 ±0.0001	3.505 ±0.017	146.2 ±1.3	3.466 ±0.038
GeoB16310-3	66	Ep	LSCE-3371-rep	4.389 ±0.010	0.3709 ±0.0005	144.3 ±1.2	1157 ±4	0.0360 ±0.0001	3.492 ±0.017	145.7 ±1.3	3.452 ±0.038
GeoB16310-3	140	Lp	LSCE-3416	3.773 ±0.010	0.1912 ±0.0003	145.3 ±2.2	2916 ±7	0.0499 ±0.0001	4.861 ±0.021	147.3 ±2.2	4.840 ±0.032
GeoB16310-3	214	Ep	LSCE-3417	4.444 ±0.005	0.4516 ±0.0003	141.7 ±1.4	2180 ±3	0.0749 ±0.0001	7.400 ±0.021	144.7 ±1.5	7.358 ±0.044
GeoB16310-3	286	Lp	LSCE-3418	3.385 ±0.005	0.3296 ±0.0005	145.2 ±1.3	2955 ±6	0.1015 ±0.0002	10.119 ±0.034	149.4 ±1.3	10.077 ±0.057
GeoB16310-3	319	Lp	LSCE-3420	3.019 ±0.004	1.4276 ±0.0008	110.4 ±1.7	3922 ±5	0.6548 ±0.0009	95.367 ±0.460	144.6 ±2.3	95.160 ±0.570
GeoB16310-3	390	Lp	LSCE-3421	3.992 ±0.008	0.3230 ±0.0007	104.2 ±1.6	25234 ±25	0.7244 ±0.0007	113.724 ±0.516	143.6 ±2.2	113.688 ±0.534
GeoB16310-3	430	Lp	LSCE-3422	3.829 ±0.006	0.6894 ±0.0005	93.6 ±1.3	13774 ±10	0.8801 ±0.0007	170.772 ±0.846	151.7 ±2.1	170.693 ±0.888
GeoB16310-3	516	Lp	LSCE-3423	4.128 ±0.007	0.2267 ±0.0003	80.8 ±0.9	49268 ±24	0.9599 ±0.0005	223.887 ±1.074	152.2 ±1.8	223.862 ±1.087
GeoB16310-3	637	Lp	LSCE-3424	3.615 ±0.006	0.2512 ±0.0002	77.3 ±1.1	38218 ±23	0.9433 ±0.0006	214.877 ±1.192	141.9 ±2.1	214.845 ±1.208
GeoB16310-3	712	Lp	LSCE-3426	3.430 ±0.005	0.2122 ±0.0004	79.4 ±1.1	43313 ±38	0.9519 ±0.0008	219.206 ±1.452	147.6 ±2.1	219.178 ±1.466
GeoB16310-3	804	Lp	LSCE-3427	3.535 ±0.005	0.2979 ±0.0003	78.3 ±1.6	32144 ±25	0.9628 ±0.0008	228.187 ±1.978	149.2 ±3.3	228.149 ±1.997
GeoB16310-3	831	Lp	LSCE-3398	3.374 ±0.005	0.6443 ±0.0010	78.4 ±2.0	13997 ±17	0.9849 ±0.0012	246.482 ±3.105	157.4 ±4.2	246.396 ±3.149
GeoB16310-3	831	Lp	LSCE-3398-rep	3.385 ±0.008	0.6433 ±0.0009	76.1 ±1.4	14042 ±16	0.9856 ±0.0012	249.544 ±2.611	154.0 ±3.1	248.709 ±3.043
GeoB16310-3	883	Lp	LSCE-3399	3.191 ±0.004	0.6326 ±0.0007	78.4 ±2.1	13298 ±13	0.9715 ±0.0010	235.050 ±2.685	152.3 ±4.2	234.960 ±2.731
GeoB16310-3	935	Lp	LSCE-3400	3.387 ±0.006	0.1690 ±0.0006	77.0 ±1.8	52038 ±49	0.9559 ±0.0009	224.126 ±2.177	145.0 ±3.6	224.102 ±2.189
GeoB16310-3	935	Lp	LSCE-3400-rep	3.385 ±0.006	0.1688 ±0.0006	77.8 ±1.6	52129 ±44	0.9571 ±0.0008	224.275 ±1.940	146.7 ±3.2	224.098 ±2.031
GeoB16310-3	1055	Lp	LSCE-3401	3.340 ±0.006	0.3731 ±0.0006	75.5 ±1.8	24144 ±26	0.9928 ±0.0011	257.183 ±3.190	156.1 ±4.1	257.132 ±3.215
GeoB16313-2	33	Lp	IUPH-6795	3.528 ±0.005	0.1060 ±0.0100	149.4 ±3.9	4198 ±491	0.0411 ±0.0030	3.980 ±0.290	151.1 ±4.0	3.970 ±0.290
GeoB16313-2	85	Lp	IUPH-6796	4.086 ±0.010	0.1360 ±0.0100	148.1 ±4.3	5541 ±454	0.0597 ±0.0021	5.820 ±0.210	150.5 ±4.4	5.830 ±0.210
GeoB16313-2	108	Lp	IUPH-6797	3.953 ±0.012	0.4470 ±0.0150	145.7 ±3.7	1611 ±83	0.0593 ±0.0024	5.800 ±0.240	148.1 ±3.7	5.770 ±0.240
GeoB16313-2	208	Lp	IUPH-6798	4.069 ±0.010	0.4030 ±0.0160	144.3 ±3.5	2435 ±123	0.0785 ±0.0024	7.750 ±0.240	147.5 ±3.6	7.720 ±0.240
GeoB16318-1	44	Lp	IUPH-6788	3.675 ±0.010	0.5570 ±0.0070	147.6 ±3.0	942 ±60	0.0462 ±0.0029	4.490 ±0.280	149.4 ±3.0	4.450 ±0.290
GeoB16318-1	76	Lp	IUPH-6789	3.788 ±0.012	0.1210 ±0.0030	147.7 ±3.8	4506 ±321	0.0467 ±0.0031	4.540 ±0.310	149.6 ±3.9	4.530 ±0.320
GeoB16318-1	133	Lp	IUPH-6790	3.279 ±0.009	0.5030 ±0.0100	128.4 ±4.7	10708 ±288	0.5319 ±0.0100	68.600 ±1.820	155.9 ±5.8	68.560 ±1.850
GeoB16318-1	168	Lp	IUPH-6791	3.756 ±0.009	0.3320 ±0.0080	116.4 ±3.3	20566 ±534	0.5894 ±0.0077	80.630 ±1.630	146.2 ±4.2	80.610 ±1.510
GeoB16318-1	217	Lp	IUPH-6792	4.319 ±0.011	0.2070 ±0.0140	111.0 ±3.4	30285 ±2183	0.4711 ±0.0085	59.610 ±1.440	131.3 ±4.1	59.600 ±1.480 *
GeoB16318-1	332	Lp	IUPH-6793	4.326 ±0.009	1.8070 ±0.0270	111.8 ±2.9	4738 ±114	0.6415 ±0.0123	92.170 ±2.610	145.0 ±3.9	92.070 ±2.880
GeoB16318-1	437	Lp	IUPH-6794	3.261 ±0.008	0.2550 ±0.0120	111.5 ±3.9	26452 ±1330	0.6718 ±0.0120	99.140 ±2.950	147.5 ±5.3	99.120 ±3.000

Four U-series ages were obtained for core GeoB16313-2, spanning from 7.7 ka to 3.9 ka (corresponding to a core depth interval between 208 and 33 cm; Fig. 2C, Table 2), hence coinciding with the Mid- to Late Holocene period. The two samples collected at 108 cm and 85 cm core depth (being just 23 cm apart) show a similar age of around 5.8 ka (within the dating error; Table 2). The average mound aggradation rate found for this core is 39.9 cm kyr^{-1} during the Holocene (Fig. 2C), and thus, is in the same range as Holocene rates found for core GeoB16310-3.

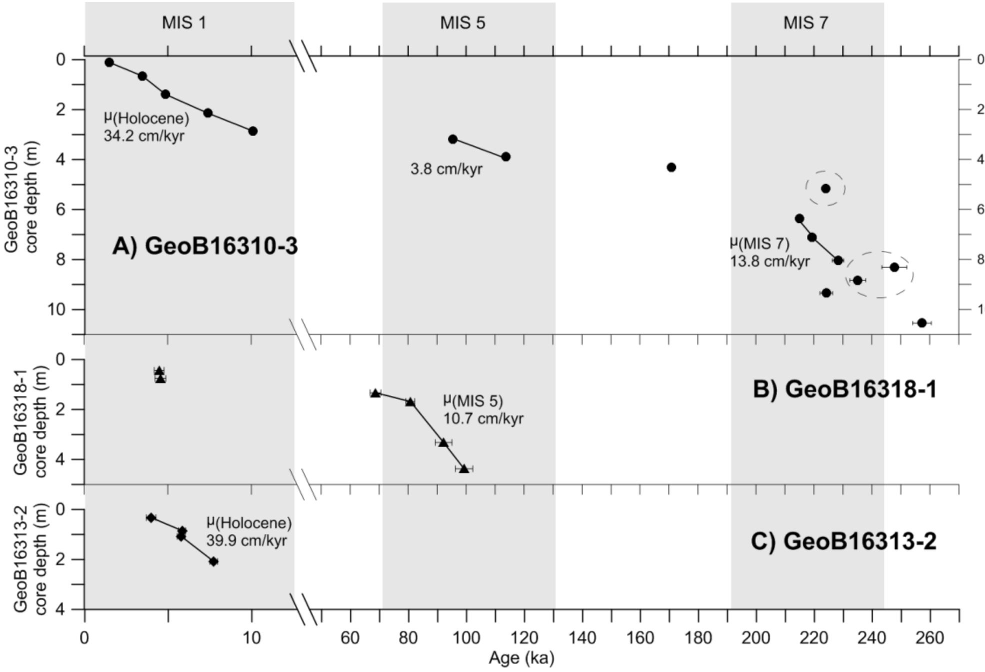

Figure 2. U-series CWC ages (plotted against core depth) obtained from the three cores collected from coral mounds of the Campeche cold-water coral province in relation to the Marine Isotope Stage (MIS) boundaries (grey bars) according to Lisiecki & Raymo (2005): (A) GeoB16310-3; (B) GeoB16318-1; (C) GeoB16313-2. The lines between the age-points and text represent the average (μ) aggradation rates for the Holocene, MIS 5 and 7. Dashed grey circles mark possibly dislocated/re-deposited sections. Note the horizontal axis break and scale change.

5.4.2 Analyses of the off-mound core GeoB16320-2

5.4.2.1 Age model based on radiocarbon dates and stable oxygen isotope stratigraphy

The age model of the off-mound core GeoB16320-2 is based on five AMS ^{14}C ages, ranging from 37.4 to 1.5 cal ka BP, and six visual correlation-points of the benthic foraminifera δ^{18}O measurements with the δ^{18}O record (LR04 stack) published by Lisiecki & Raymo (2005) (Table 3). The benthic δ^{18}O data of core GeoB16320-2 vary between 3.05‰ and 1.48‰ (Fig.3b), with light values (<1.8‰) coinciding with peak interglacial periods (MIS 5e and the Holocene). The age model was established by performing linear interpolation between the consecutive dated/correlated age levels and extrapolating the sedimentation rate between the two oldest correlated-points towards the base of the core. The estimated age of the core base is 138 cal ka BP, thus the age model spans from late MIS 6 to the Late Holocene. Sedimentation rates vary between 1.25 and 7.73 cm kyr^{-1}, being lower (<4 cm kyr^{-1}) before 40 cal ka BP and higher (>4 cm kyr^{-1}) afterwards (Fig. 3a).

Table 3. AMS ^{14}C ages determined on multi-species samples of planktic foraminifera from the sediment core Geob16320-2. The AMS ^{14}C ages were corrected for ^{13}C and a mean reservoir age of 400 yrs; and were converted into calibrated years before present (cal yr BP) using the Marine13 calibration curve (Reimer et al., 2013) of the CALIB 7.0 software (Stuiver and Reimer, 1993). Estimated sedimentation rates for core Geob16320-2 are supplemented. CD: core depth, σ: standard deviation, MPA: median probability age, SR: sedimentation rate**.**

Core ID	CD (cm)	Lab code	14C-age (year)	1σ error (±year)	2σ calibrated age range (year BP, P= AD 1950)	MPA (year BP)	SR (cm/kyr)
GeoB16320-2	3	Poz-60996	2375	30	1418 - 1618	1534	
GeoB16320-2	48	Poz-60997	9110	40	9278 - 9471	9389	5.73
GeoB16320-2	83	Poz-60998	15500	60	17682 - 18060	17886	4.12
GeoB16320-2	118	Poz-60999	19520	90	22386 - 22834	22572	7.47
GeoB16320-2	178	Poz-72321	33610	510	36184 - 38621	37412	4.04
GeoB16320-2	198	Correlation points to the benthic foraminifera δ^{18}O Stack (Lisiecki and Raymo, 2005)				40000	7.73
GeoB16320-2	233					55000	2.33
GeoB16320-2	253					71000	1.25
GeoB16320-2	313					88000	3.53
GeoB16320-2	353					116000	1.43
GeoB16320-2	408					131000	3.67

5.4.2.2 Environmental proxy data

The benthic foraminiferal δ^{13}C record shows values between 0.86‰ and 1.63‰ and follows a pattern similar to the δ^{18}O record (Fig. 3d). Heavy values (>1.5‰) are found mostly during the last glacial maximum (LGM), whereas light values (<1.3‰) occur predominantly during the interglacial periods (and the last deglaciation) (Fig. 3d).

The cumulative volume percentage of the coarse silt fraction (20-63 µm) in the sediment varies between 8.6 and 38.4 vol% (Fig. 3e). Low percentages (<20%) are common during colder periods, approximately before 129 cal ka BP and between 41 and 11 cal ka BP, whereas high percentages (>20%) mark the remaining, mostly warmer periods (Fig. 3e).

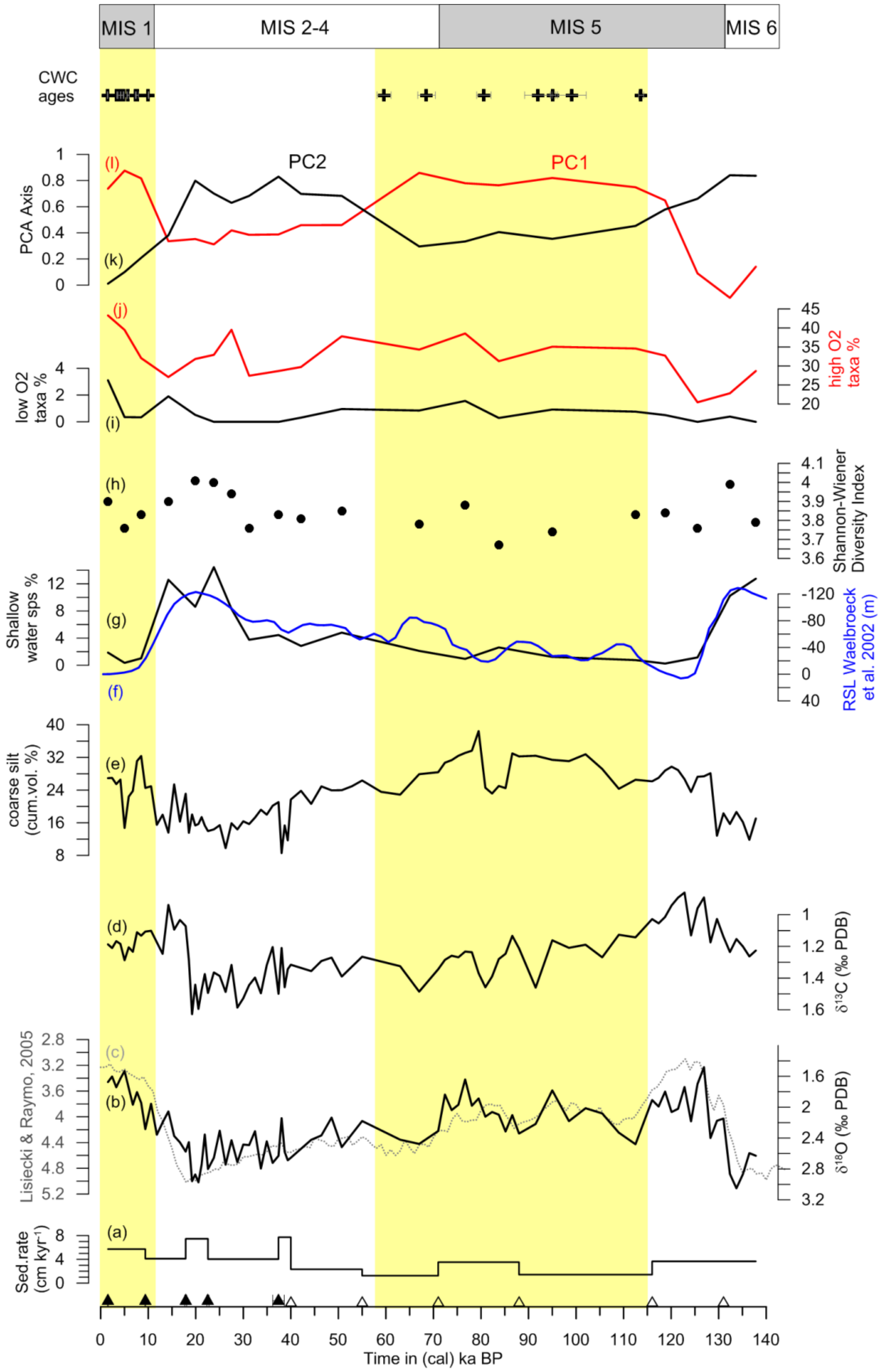

Figure 3. Multi-proxy data of the off-mound core GeoB16320-2. From bottom to top: (a) estimated sedimentation rate; (b) *Planiulina ariminensis* (benthic) $\delta^{18}O$ record superimposed on (c) the Lisiecki & Raymo (2005) record (grey curve); (d) *P. ariminensis* $\delta^{13}C$ record; (e) cumulative weight percentage of the coarse silt (20-63 µm) fraction; and benthic foraminifera assemblage results: (g) percentage of displaced shallow water species superimposed on (f) the relative sea level curve (RSL; note inverted scale) of Waelbroeck et al. (2002); (h) Shannon-Wiener diversity index H(S); (i) percentage of species typical of low- (black curve) and (j) high-oxygen (red curve) environments; and principal component (PC) loadings of Q-mode benthic foraminiferal assemblages PC1 (l) and PC2 (k).

Figure 3 (cont.). The age model was developed using AMS ^{14}C ages (black triangles) presented in calibrated kilo-years before present (cal ka BP) and correlation points (open triangles) to the benthic $\delta^{18}O$ record of Lisiecki & Raymo (2005), all displayed at the bottom of the graph. Based on the U-Th CWC ages of the last 140 ka (top black crosses), periods marked by sustained CWC occurrence are highlighted in yellow. Marine Isotope Stage (MIS) boundaries (top white/grey bars) are displayed according to Lisiecki & Raymo (2005).

The benthic foraminifera census data revealed very high diversity throughout the record, with H(*S*) values always above 3.6 (Fig. 3h). Relative abundance of shallow-water taxa was higher before 133 cal ka BP (MIS 6) and between 27 and 14 cal ka BP (LGM to deglaciation) (Fig. 3g). Both LO and HO taxa percentage records show small oscillations, especially the LO taxa varying between 0.3 and 3.1% throughout the record (Fig. 3i). The HO taxa record varies between 20 and 43%, presenting higher (>31%) values between 114 and 57, 28 and 20, and after 9 cal ka BP (Fig. 3j). The two main faunal assemblages obtained from the Q-mode PCA explained 67.7% of the total variance (Table 4). The first assemblage (PC1) explained 34.2% of the total variance and was dominated (PC score >3) by the species *Epistominella rugosa* and *Gavelinopsis translucens*, followed by *Globocassidulina subglobosa* and *Sphaeroidina bulloides* (PC score >2). The second assemblage (PC2) explained 33.5% of the total variance and was dominated (PC score >3) by *Cassidulina optusa*, *Uvigerina proboscidea* and *Globocassidulina subglobosa*, followed by *Bulimina aculeata* and *Miliolinella* spp. (PC score >2). The proportion of PC1 and PC2 varies along the record (Fig. 3). Assemblage PC1 is dominant in the record (PC loading >0.5) between 114-58 cal ka BP and after 14 cal ka BP (Fig. 3l), while assemblage PC2 is dominant before 108 cal ka BP and between 58-19 cal ka BP (Fig. 3k).

5.5 Discussion

5.5.1 Coral occurrence and mound aggradation at the Campeche CWC province

For the past ~260 kyr, a sustained occurrence of CWC, and hence, periods of pronounced mound aggradation at the Campeche CWC province predominantly coincides with interglacial periods, namely the MIS 7, the MIS 5 and the Holocene (Fig. 2). The few glacial CWC ages (15% of all obtained ages) indicate that also during glacial times CWC were still present at the Campeche mounds, possibly as scattered isolated colonies. However, coral mound aggradation largely stagnated during those cold climate periods (Fig. 2).

Table 4. Results of the Q-mode Principal Component Analysis (PCA) for the benthic foraminifera population of core GeoB16320-2. Displayed are the dominant (score≥3) and important associated (3>score≥1) species for the first two principal components (PC), including their explained variation percentage.

Axis no.	Dominant Species	Score	Important associated species	Score	Explained variance (%)
PC1	*Epistominella rugosa*	5	*Globocassidulina subglobosa*	2.9	34.2
	Gavelinopsis translucens	3.4	*Sphaeroidina bulloides*	2.5	
			Cassidulina laevigata	1.5	
			Cornuloculina inconstans	1.3	
			Siphonina tubulosa	1.3	
			Bulimina aculeata	1.2	
			Pullenia bulloides	1.1	
PC2	*Cassidulina optusa*	3.7	*Bulimina aculeata*	2.3	33.5
	Uvigerina proboscidea	3.1	*Miliolinella* spp.	2.1	
	Globocassidulina subglobosa	3	*Textularia* sp.	2	
			Rosalina spp.	1.5	
			Discorbis spp.	1.4	
			Uvigerina peregrina	1.3	
			Ehrenbergina trigona	1.1	
			Planulina ariminensis	1.1	
			Textularia agglutinans	1.1	

The average coral mound aggradation rates differ for each of the interglacial periods covered by our coral records. Holocene mound aggradation rates of 34-40 cm kyr^{-1} are one order of magnitude higher than those estimated for the MIS 5 and 7 (Fig. 2). This implies that the factors favorable for mound formation, comprising advantageous environmental conditions for the development of dense widespread CWC frameworks (e.g., sufficient food availability, distinctive physicochemical water mass properties, vigorous current dynamics) and sufficient sediment supply that covers, infills and stabilizes the coral remnants (Hebbeln et al., 2016; Huvenne et al., 2009; Titschack et al., 2015; Wienberg and Titschack, *in press*) varied from one interglacial to another and were less favorable during MIS 5 and 7. In comparison to other coral mound areas in the Atlantic Ocean, the average mound aggradation rates at the Campeche CWC province are in the lower range of aggradation rates described so far, which can reach values up to 3 magnitudes higher, as is exemplified by the Norwegian coral mounds (218-1500 cm kyr^{-1}; López Correa et al. 2012; Titschack et al. 2015). Similar aggradation rates to the Campeche CWC province are known from the Brazilian margin during the last deglaciation and Early Holocene (14-34 cm kyr^{-1}; Mangini et al. 2010) and from the Moroccan margin during the last glacial (11-15 cm kyr^{-1}; Wienberg & Titschack *in press*). Given the Campeche CWC province large area (>40km2) and its current numerous coral mounds covered by extensive living CWC, environmental conditions for CWC growth are surely suitable. Therefore, we could speculate if the relatively lower aggradation rates are due to low sediment input, negatively affecting the stabilization of the coral framework. Clarification requires a further study of the mound aggradation process at the Campeche CWC province.

5.5.2 The local paleoceanographic setting at the Campeche area since MIS 5

The benthic foraminifera record of the last ~140 kyr clearly shows that the environmental conditions at the core site were always favorable for the foraminifera population, as indicated by the consistently high diversity levels (above 3.6; see Fig. 3). Furthermore, the persistently very low percentage of LO species throughout the record (Fig. 3) indicates that the benthic foraminiferal fauna was never significantly affected by low dissolved oxygen concentrations. However, the alternating dominance of the two defined foraminiferal assemblages, PC1 and PC2, reveal changes in the environmental conditions since the MIS 5.

PC1 is characterized by a dominance of the epifaunal taxa *E. rugosa* and *G. translucens* (Table 4), which indicate well-oxygenated water masses (Licari et al., 2003; Schmiedl et al., 1997). This relatively enhanced oxygenation is corroborated by the small increase in the percentage of foraminifera species typical for HO environments. The association of the dominant species with some shallow infaunal taxa (such as *C. laevigata*, *B. aculeata*, and *P. bulloides*) indicates mesotrophic conditions (Fontanier et al., 2002; Licari et al., 2003; Mackensen et al., 1995; Schmiedl et al., 1997). The periods of PC1 dominance generally coincide with higher percentages of coarse silt (Fig. 3) that, at first glance, point to enhanced bottom current strength during this interval.

PC2 is marked by the dominance of shallow infaunal species (*U. proboscidea* and *C. optusa*) that, in combination with the presence of the infaunal taxa *B. aculeata* and *Uvigerina peregrina* (Table 4), indicate an adaptation to enhanced food availability compared to the intervals of PC1 dominance (Koho et al., 2008; Schmiedl et al., 1997). This enhanced food availability could be caused by an increased primary production; an improved export of organic matter to the seafloor, potentially positively affected by the lowered sea level during glacial times; and/or a reduced organic matter re-mineralization within the water column due to a less-oxygenated bottom water mass. An improved export of organic matter to the seafloor might have been additionally benefited from lateral organic matter import from various shelf environments. Just as the reduced shelf width during the last glacial facilitated the export of shallow-water foraminifera to the slope, as seen by their relatively increased abundance during this period, it could have also affected the export of organic matter. The increased abundance of *U. peregrina* and *B. aculeata* in the PC2 assemblage (Table 4) is usually interpreted as reduced bottom current strength. Those species are commonly associated with fine-grained organic-rich sediments that provide suitable infaunal microhabitats (Lutze and

Coulbourn, 1984; Schmiedl et al., 1997). This is also supported by the grain size data that exhibit a reduced coarse silt fraction during periods of PC2 dominance (Fig. 3). Besides the decrease in bottom current strength, an alternative explanation for the increase of fine particles in the sediment may be suggested. Fine particles could have accumulated at the seafloor due to a decreased in their accumulation in the water column if the currently seen pycnocline between the TACW and the AAIW was absent.

The reconstructed environmental changes observed for the last ~140 kyr follow a glacial-interglacial pattern, which given the observed change in bottom water oxygenation and current strength (or presence/absence of the pycnocline), could relate to a change in the prevalent water mass. Such a change is corroborated by the benthic $\delta^{13}C$ record, which shows its most prominent change concurrent with the deglacial change from PC2 to PC1 dominance. At this time the $\delta^{13}C$ values significantly decreased by ~0.7‰ to stay on a rather low level throughout the Holocene. This shift might indicate a greater contribution of AAIW waters to the site, similarly to what is observed under present-day conditions (Hebbeln et al., 2014) and in the intermediate depths of the western Atlantic Ocean, where the AAIW is characterized by the lowest $\delta^{13}C$ values (approx. 0.7‰ at 20°N; Kroopnick 1985). A shift in the intermediate (500-750 m) water mass source in the West Atlantic was previously suggested to occur, from a higher $\delta^{13}C$ (~1.8 ‰) northern source water during the last glacial to a lower $\delta^{13}C$ (~1.0 ‰) southern source water at present (Curry and Oppo, 2005).

5.5.3 Environmental control of CWC growth at the Campeche province – recent and past conditions

The modern conditions at the Campeche CWC province are obviously suitable for sustained CWC growth as indicated by the widespread occurrence of living *Lophelia* colonies (Hebbeln et al., 2014). Bottom water dissolved oxygen concentrations and temperatures (~2.8 ml L^{-1} and 7.5–9.5 °C, respectively) currently observed at the CWC depth of occurrence (Hebbeln et al., 2014) are both within the known range for *Lophelia* (see Davies & Guinotte 2011). A local upwelling cell causing enhanced primary production exists just above the Campeche CWC province (Merino, 1997), and a diel vertical migration of zooplankton that possibly reaches the intermediate depths of living CWC has been observed (Hebbeln et al., 2014). Both processes are potentially important factors regarding the food availability for the CWC (Hebbeln et al., 2014). In addition, the pycnocline, provided by the TACW – AAIW boundary, may decelerate the sinking velocity of food particles and cause a prolonged residence time of food particles within the depths of living CWC occurrence (~520 m). Contemporaneously, the most likely presence of internal waves prograding on this pycnocline, as indicated by cyclic (12-hour-period) undulating isotherms (Hebbeln et al., 2014), repeatedly flushes food particles through the CWC framework, thereby enhancing the chance for the coral polyps to catch them. Overall, such conditions suggest a highly dynamic bottom current regime that might present a crucial factor in the food supply for the suspension feeding CWC (Dorschel et al., 2007; Frederiksen et al., 1992; Hebbeln et al., 2016; Mienis et al., 2007).

Regarding the past occurrence of CWC, the temporal pattern of CWC absence and presence during the last 260 kyr predominantly follows the glacial-interglacial cycle, which points to distinct changes of the environmental setting controlling the CWC occurrence. Comparing the timing of CWC occurrence with the paleoceanographic multi-proxy data, it becomes most striking that the presence-absence pattern of CWC is in phase with the dominance change in the benthic foraminifera assemblages (PC1 and PC2; Fig. 3). Apparently, the environmental changes that affected the benthic foraminifera population have also affected the benthic CWC community, in which case the according proxy records can therefore be used to unravel the potential environmental controls of the past CWC occurrence at the Campeche site.

The interglacial occurrence of CWC coincides with phases of benthic foraminifera assemblages PC1 dominance that suggests a dynamic bottom current regime, relatively well oxygenated bottom waters and mesotrophic primary production in the surface ocean. These environmental conditions are also reflected in the modern oceanographic situation for which the occurrence of the TACW – AAIW boundary at the water depth of the Campeche coral province might be crucial.

The glacial periods of CWC absence coincide with phases of benthic foraminifera assemblage PC2 dominance that were characterized by an enhanced organic carbon availability, slightly less-oxygenated bottom water and a less dynamic bottom current regime. These conditions might be caused by the likely absence of the TACW – AAIW boundary within the water depth interval of the Campeche coral mound area, which might result from (a) a reduced northward flow of the AAIW resulting from a weaker thermohaline circulation during glacial periods (e.g., Curry & Oppo 2005) and/or (b) a lowered glacial sea level (Waelbroeck et al., 2002) probably deepening the TACW - AAIW boundary pycnocline (Fig. 4). The glacial demise of CWC within the Campeche coral mound area was most probably not caused by the slightly decreased bottom water oxygenation as the highest (although still very low, <4%) relative amount of LO foraminifera species was retrieved from the uppermost (most recent) off-mound core sample that obviously reflects the modern period of thriving CWC (Fig. 3).

Therefore, the most probable controlling factor for the observed reduced CWC occurrence during the glacial periods might be a less dynamic bottom current regime caused by the absence of the TACW – AAIW pycnocline. This absence is interpreted to have negatively affected the food supply mechanism, even though enhanced organic carbon availability at the seafloor is indicated by the proxy dataset. Consequently, the enhanced vertical flux of food particles during glacials would have been outcompeted by an effective food enrichment and delivery process to the CWCs (*sensu* Hebbeln et al. 2016) . The benefits of a strong bottom current regime for the nutrition of CWC has already been highlighted in previous studies (e.g., Frederiksen et al., 1992; Mienis et al., 2007; White and Dorschel, 2010).

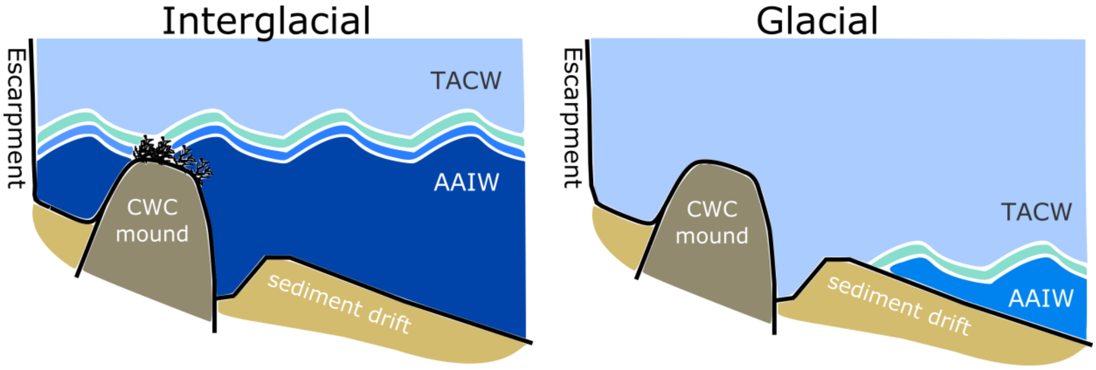

Figure 4. Schematic illustration of changes in the hydrographic conditions at the Campeche CWC province. The lower glacial sea level (right panel) deepens the boundary between the Antarctic Intermediate Water (AAIW) and the Tropical Atlantic Central Water (TACW), as well as the internal waves propagating along the water mass boundary (white lines), to depths below the CWC occurrence. Vertical displacement of the internal waves reduces CWC food delivery rates causing diminished/absent CWC growth and coral mound aggradation.

It is worth noting that the seemingly delayed re-occurrence of the CWC and the increased dominance of PC1 during MIS 5 lagged the changes in water mass provenance and increased bottom current strength (by around 15 kyr). Certainly, the absence of CWC ages between 130 cal ka BP to 115 cal ka BP does not completely rule out their occurrence in the Campeche area during that period. Nonetheless, the accordance between the CWC occurrence pattern with the shift from PC2 to PC1 dominance, point to some differences in the paleo-environmental setting between the last two peak interglacials (MIS 5e and the Holocene), which needs further investigation.

5.5.4 The Campeche CWC province in the Atlantic context – the role of intermediate-depth circulation

The study of the Campeche CWC province greatly improves the very limited knowledge of the long-term development of CWC and coral mounds along the NW Atlantic margin. The only available CWC mound-based record of the NW Atlantic originates from the Cape Lookout CWC area (off North Carolina, eastern US margin), which similarly to the Campeche CWC province reveals an interglacial occurrence of CWC, namely during the Holocene and the MIS 5 (Matos et al., 2015). There, the temporal occurrence of CWC was attributed to slightly increased bottom water temperature and enhanced bottom currents due to a locally increased influence of the Gulf Stream during times of relatively high sea level (Matos et al., 2015). Overall, CWC vitality and coral mound aggradation in both regions – off Campeche Bank and off Cape Lookout – seems to be mainly restricted to times of a dynamic bottom current regime, and thus, a likely enhancement of food supply to the corals – a pattern also described for the coral mounds off Ireland (e.g., Dorschel et al. 2007; Mienis et al. 2007). In the NW Atlantic, such enhanced hydrodynamics have been caused by changes in the water column structure. Off Cape Lookout, the coastward moving Gulf Stream started to influence the CWC mounds, while along the Campeche margin in the southern GoM, a stronger presence of the AAIW (and/or a shoaling of the TACW – AAIW boundary pycnocline) occurred.

Another example for the occurrence of CWC and coral mounds in the GoM comprises the Viosca Knoll in the northern part of the gulf. Here, *Lophelia* currently lives under environmental conditions similar to the Campeche CWC province (temperature: 6.5–11.6 °C, salinity: 34.95–35.4 and dissolved oxygen: 2.7–2.8 ml l^{-1}; Davies et al. 2010; Mienis et al. 2012). The Viosca Knoll is likewise located below an increased surface productivity area, in this case triggered by the Mississippi River outflow, which provides food for the CWC (Mienis et al., 2012). Further similarity is found on the location of both CWC areas near the upper boundary of the AAIW (Hebbeln et al., 2014; Mienis et al., 2012). However, the initially suggested presence of internal waves/tidal motion at Viosca Knoll (Davies et al., 2010) could not be confirmed by long-term lander studies at this site (Mienis et al., 2012). Regarding the past occurrence of CWC in the northern GoM, not much is known so far. The two *Lophelia* ages obtained from Viosca Knoll are both ~25 ka (Sulak 2008); the same way a published *Lophelia* dating from the West Florida Slope also provides a last glacial age of ~31 cal ka BP (Newton et al., 1987). Nevertheless, while ages from coral fragments randomly collected from the seabed surface can be used to deduce a temporal pattern of CWC past occurrence, they cannot provide any information about the aggradation history of coral mounds.

Further to the south, the CWC settings found off Brazil appear to have hosted living *Lophelia* for the last 29.3 kyr (Henry et al., 2014; Mangini et al., 2010). Although these coral mound areas are currently located at the upper boundary of the AAIW (Viana et al., 1998), the local water mass distribution as well as the past paleo-environmental setting is not well known. Therefore, it remains unclear whether coral vitality along the Brazilian margin in the past was related to the presence of the AAIW (Henry et al., 2014), as it is presently the case there (Viana et al., 1998) and also at Campeche CWC province.

In summary, although the availability of coral ages from the various coral mound areas in the western Atlantic is limited, there seems to be a potential link between the pattern of CWC occurrence and coral mound aggradation and the changes in the intermediate-depth circulation. South of 25 °N (the northern limit of the AAIW; Lambelet et al., 2016), the presence of the AAIW might be triggering CWC occurrence today. Also for the NE Atlantic, a strong relationship between the influence of intermediate water masses, namely the Eastern North Atlantic Water (ENAW) and the Mediterranean Outflow water (MOW), and the (present and past) occurrence of CWC and coral mounds in the Irish margin has been hypothesized (e.g., De Mol et al., 2005; White et al., 2007; White and Dorschel, 2010). In which case, a permanent thermocline between both water masses was associated with strong bottom current regimes promoting across-slope organic matter fluxes and, thus, supply food for the corals (White and Dorschel, 2010). Although the specific intermediate water masses and related hydrographic effects differ, in all these cases changes in the water mass distribution produced changes in the mechanisms that generate or supply food for the corals. This way, several of the long-term studied coral mound areas of the North Atlantic present this link between the presence/absence pattern of CWC occurrence and coral mound aggradation and changes in the intermediate water mass distribution.

5.6 Conclusions

This work contributes to the study of the long-term occurrence of CWC and the development of coral mounds in the NW Atlantic. Our results show that for the last ~260 kyr, CWC growth and coral mound aggradation at the Campeche CWC province in the southern Gulf of Mexico was mainly restricted to interglacial periods. These are concurrent with periods of AAIW strengthening (and/or rise of its upper boundary) that cause a local development of a density gradient between the AAIW and the overlying. Such conditions allow the accumulation and remobilization of food particles that can increase food availability for the sessile CWC. The AAIW is an important intermediate water mass within the West Atlantic and similar hydrological conditions may affect other coral mound areas existing within the AAIW area of influence, such as along the Brazilian margin. Consequently, changes in the AAIW distribution along the climatic cycles might present a considerable influence in the long-term occurrence pattern of CWC in the West Atlantic. Thus, to further unravel the long-term development of

CWC vitality and coral mound aggradation in the western Atlantic region further studies combining coral datings and paleoenvironmental reconstructions are in need.

Acknowledgements

We thank the officers and crew of the R/V Maria S. Merian and the scientific crew for on-board assistance during cruise MSM 20-4 (2012). We kindly acknowledge François Thil, René Eichstädter and Anne-Marie Wefing for support during the U-series dating; and H. Kuhnert and B. Meyer-Schack for support during isotope sample preparation and analysis. We further thank Paul Wintersteller for providing the map of the Campeche CWC province and the GeoB Core Repository at the MARUM for the assistance in providing sediment cores and sample material. The research leading to these results has received support from the Deutsche Forschungsgemeinschaft (DFG) through funding of the WACOM – West Atlantic Cold-water Coral Ecosystems project [grant HE 3412/17-1] and through providing ship time. The cruise was further supported through the DFG Research Center/Cluster of Excellence "MARUM – The Ocean in the Earth System". L. Matos was supported by a Fundação para a Ciência e Tecnologia (FCT) [SFRH/BD/72149/2010] and GLOMAR - the Bremen International Graduate School for Marine Sciences. Further support came from FCT through CESAM [PEst-C/MAR/LA0017/2013 and UID/AMB/50017/2013] and CCMAR [UID/Multi/04326/2013]. The data reported in this paper are archived in Pangaea (www.pangaea.de).

References

Andersen, M.B., Stirling, C.H., Zimmermann, B., Halliday, A.N., 2010. Precise determination of the open ocean 234 U/ 238 U composition. Geochemistry, Geophys. Geosystems 11, n/a-n/a. doi:10.1029/2010GC003318

Buzas, M.A., Gibson, T.G., 1969. Species Diversity: Benthonic Foraminifera in Western North Atlantic. Science (80-.). 163, 72–75. doi:10.1126/science.163.3862.72

Cheng, H., Adkins, J., Edwards, R.L., Boyle, E.A., 2000. U-Th dating of deep-sea corals. Geochim. Cosmochim. Acta 64, 2401–2416. doi:10.1016/S0016-7037(99)00422-6

Colman, J.G., Gordon, D.M., Lane, A.P., Forde, M.J., Fitzpatrick, J.J., 2005. Carbonate mounds off Mauritania, Northwest Africa: status of deep-water corals and implications for management of fishing and oil exploration activities, in: Freiwald, A., Roberts, J.M. (Eds.), Cold-Water Corals and Ecosystems, Erlangen Earth Conference Series. Springer-Verlag, Berlin/Heidelberg, pp. 417–441.

Correa, T.B.S., Grasmueck, M., Eberli, G.P., Reed, J.K., Verwer, K., Purkis, S., 2012. Variability of cold-water coral mounds in a high sediment input and tidal current regime, Straits of Florida. Sedimentology 59, 1278–1304. doi:10.1111/j.1365-3091.2011.01306.x

Curry, W.B., Oppo, D.W., 2005. Glacial water mass geometry and the distribution of (delta)13C of (Sigma)CO2 in the western Atlantic Ocean. Paleoceanography 20, 1–12. doi:10.1029/2004PA001021

Davies, A.J., Duineveld, G.C.A., van Weering, T.C.E., Mienis, F., Quattrini, A.M., Seim, H.E., Bane, J.M., Ross, S.W., 2010. Short-term environmental variability in cold-water coral habitat at Viosca Knoll, Gulf of Mexico. Deep. Res. Part I Oceanogr. Res. Pap. 57, 199–212. doi:10.1016/j.dsr.2009.10.012

Davies, A.J., Guinotte, J.M., 2011. Global habitat suitability for framework-forming cold-water corals. PLoS One 6, e18483. doi:10.1371/journal.pone.0018483

de Haas, H., Mienis, F., Frank, N., Richter, T.O., Steinacher, R., de Stigter, H., van der Land, C., van Weering, T.C.E., 2009. Morphology and sedimentology of (clustered) cold-water coral mounds at the south Rockall Trough margins, NE Atlantic Ocean. Facies 55, 1–26. doi:10.1007/s10347-008-0157-1

De Mol, B., Henriet, J.P., Canals, M., 2005. Development of coral banks in Porcupine Seabight : do they have Mediterranean ancestors ?, in: Freiwald, A., Roberts, J.M. (Eds.), Cold-Water Corals and Ecosystems. Springer-Verlag, pp. 515–533. doi:10.1007/3-540-27673-4_26

De Mol, B., Van Rensbergen, P., Pillen, S., Van Herreweghe, K., Van Rooij, D., McDonnell, a, Huvenne, V., Ivanov, M., Swennen, R., Henriet, J.., 2002. Large deep-water coral banks in the Porcupine Basin, southwest of Ireland. Mar. Geol. 188, 193–231. doi:10.1016/S0025-3227(02)00281-5

Dorschel, B., Hebbeln, D., Foubert, A., White, M., Wheeler, A.J., 2007. Hydrodynamics and cold-water coral facies distribution related to recent sedimentary processes at Galway Mound west of Ireland. Mar. Geol. 244, 184–195. doi:10.1016/j.margeo.2007.06.010

Dorschel, B., Hebbeln, D., Rueggeberg, A., Dullo, W., Freiwald, A., 2005. Growth and erosion of a cold-water coral covered carbonate mound in the Northeast Atlantic during the Late Pleistocene and Holocene. Earth Planet. Sci. Lett. 233, 33–44. doi:10.1016/j.epsl.2005.01.035

Douville, E., Sallé, E., Frank, N., Eisele, M., Pons-Branchu, E., Ayrault, S., 2010. Rapid and accurate U–Th dating of ancient carbonates using inductively coupled plasma-quadrupole mass spectrometry. Chem. Geol. 272, 1–11. doi:10.1016/j.chemgeo.2010.01.007

Eisele, M., Frank, N., Wienberg, C., Hebbeln, D., López Correa, M., Douville, E., Freiwald, A., 2011. Productivity controlled cold-water coral growth periods during the last glacial off Mauritania. Mar. Geol. 280, 143–149. doi:10.1016/j.margeo.2010.12.007

Eisele, M., Hebbeln, D., Wienberg, C., 2008. Growth history of a cold-water coral covered carbonate mound — Galway Mound, Porcupine Seabight, NE-Atlantic. Mar. Geol. 253, 160–169. doi:10.1016/j.margeo.2008.05.006

Fontanier, C., Jorissen, F.., Licari, L., Alexandre, A., Anschutz, P., Carbonel, P., 2002. Live benthic foraminiferal faunas from the Bay of Biscay: faunal density, composition, and microhabitats. Deep Sea Res. Part I Oceanogr. Res. Pap. 49, 751–785. doi:10.1016/S0967-0637(01)00078-4

Fosså, J.H., Lindberg, B., Christensen, O., Lundälv, T., Svellingen, I., Mortensen, P.B., Alvsvåg, J., 2005. Mapping of Lophelia reefs in Norway: experiences and survey methods, in: Freiwald, P.D.A., Roberts, D.J.M. (Eds.), Cold-Water Corals and Ecosystems. Springer Berlin Heidelberg, pp. 359–391. doi:10.1007/3-540-27673-4_18

Frank, N., Freiwald, a., Correa, M.L., Wienberg, C., Eisele, M., Hebbeln, D., Van Rooij, D., Henriet, J.-P., Colin, C., van Weering, T., de Haas, H., Buhl-Mortensen, P., Roberts, J.M., De Mol, B., Douville, E., Blamart, D., Hatte, C., 2011. Northeastern Atlantic cold-water coral reefs and climate. Geology 39, 743–746. doi:10.1130/G31825.1

Frank, N., Paterne, M., Ayliffe, L., van Weering, T., Henriet, J.-P., Blamart, D., 2004. Eastern North Atlantic deep-sea corals: tracing upper intermediate water Δ14C during the Holocene. Earth Planet. Sci. Lett. 219, 297–309. doi:10.1016/S0012-821X(03)00721-0

Frank, N., Ricard, E., Lutringer-Paquet, A., van der Land, C., Colin, C., Blamart, D., Foubert, A., Van Rooij, D., Henriet, J.-P., de Haas, H., van Weering, T., 2009. The Holocene occurrence of cold water corals in the NE Atlantic: Implications for coral carbonate mound evolution. Mar. Geol. 266, 129–142. doi:10.1016/j.margeo.2009.08.007

Frederiksen, R., Jensen, A., Westerberg, H., 1992. The distribution of the scleractinian coral Lophelia pertusa around the Faroe Islands and the relation to internal tidal mixing. Sarsia 77, 157–171. doi:10.1080/00364827.1992.10413502

Freiwald, A., Roberts, J.M., 2005. Cold-Water Corals and Ecosystems. Springer Berlin Heidelberg. doi:10.1007/3-540-27673-4

Glogowski, S., Dullo, W.-C., Feldens, P., Liebetrau, V., von Reumont, J., Hühnerbach, V., Krastel, S., Wynn, R.B., Flögel, S., 2015. The Eugen Seibold coral mounds offshore western Morocco: oceanographic and bathymetric boundary conditions of a newly discovered cold-water coral province. Geo-Marine Lett. 35, 257–269. doi:10.1007/s00367-015-0405-7

Hebbeln, D., Samankassou, E., 2015. Where did ancient carbonate mounds grow - In bathyal depths or in shallow shelf waters? Earth-Science Rev. 145, 56–65. doi:10.1016/j.earscirev.2015.03.001

Hebbeln, D., Van Rooij, D., Wienberg, C., 2016. Good neighbours shaped by vigorous currents: Cold-water coral mounds and contourites in the North Atlantic. Mar. Geol. 378, 171–185. doi:10.1016/j.margeo.2016.01.014

Hebbeln, D., Wienberg, C., Beuck, L., Dehning, K., Dullo, W.-C., Eberli, G., Freiwald, A., Glogowski, S., Garlichs, T., Jansen, F., Joseph, N., Klann, M., Matos, L., Nowald, N., Reyes, H., Ruhland, G., Taviani, M., Wilke, T., Wilsenack, M., Wintersteller, P., 2012. West Atlantic Cold-Water Coral Ecosystems: The west side story, R/V Maria S. Merian Cruise No. 20, Leg 4.

Hebbeln, D., Wienberg, C., Wintersteller, P., Freiwald, a., Becker, M., Beuck, L., Dullo, C., Eberli, G.P., Glogowski, S., Matos, L., Forster, N., Reyes-Bonilla, H., Taviani, M., 2014. Environmental forcing of the Campeche cold-water coral province, southern Gulf of Mexico. Biogeosciences 11, 1799–1815. doi:10.5194/bg-11-1799-2014

Henry, L.-A., Frank, N., Hebbeln, D., Wienberg, C., Robinson, L., de Flierdt, T. Van, Dahl, M., Douarin, M., Morrison, C.L., Correa, M.L., Rogers, A.D., Ruckelshausen, M., Roberts, J.M., 2014. Global ocean conveyor lowers extinction risk in the deep sea. Deep Sea Res. Part I Oceanogr. Res. Pap. 88, 8–16. doi:10.1016/j.dsr.2014.03.004

Hübscher, C., Dullo, C., Flögel, S., Titschack, J., Schönfeld, J., 2010. Contourite drift evolution and related coral growth in the eastern Gulf of Mexico and its gateways. Int. J. Earth Sci. 99, 191–206. doi:10.1007/s00531-010-0558-6

Huvenne, V.A.I., Van Rooij, D., De Mol, B., Thierens, M., O'Donnell, R., Foubert, A., 2009. Sediment dynamics and palaeo-environmental context at key stages in the Challenger cold-water coral mound formation: Clues from sediment deposits at the mound base. Deep. Res. Part I Oceanogr. Res. Pap. 56, 2263–2280. doi:10.1016/j.dsr.2009.08.003

Kano, A., Ferdelman, T.G., Williams, T., Henriet, J.-P., Ishikawa, T., Kawagoe, N., Takashima, C., Kakizaki, Y., Abe, K., Sakai, S., Browning, E.L., Li, X., 2007. Age constraints on the origin and growth history of a deep-water coral mound in the northeast Atlantic drilled during Integrated Ocean Drilling Program Expedition 307. Geology 35, 1051. doi:10.1130/G23917A.1

Koho, K.A., García, R., de Stigter, H.C., Epping, E., Koning, E., Kouwenhoven, T.J., van der Zwaan, G.J., 2008. Sedimentary labile organic carbon and pore water redox control on species distribution of benthic foraminifera: A case study from Lisbon–Setúbal Canyon (southern Portugal). Prog. Oceanogr. 79, 55–82. doi:10.1016/j.pocean.2008.07.004

Kroopnick, P.M., 1985. The distribution of 13C of ΣCO2 in the world oceans. Deep Sea Res. Part A, Oceanogr. Res. Pap. 32, 57–84. doi:10.1016/0198-0149(85)90017-2

Lambelet, M., van de Flierdt, T., Crocket, K., Rehkämper, M., Kreissig, K., Coles, B., Rijkenberg, M.J.A., Gerringa, L.J.A., de Baar, H.J.W., Steinfeldt, R., 2016. Neodymium isotopic composition and concentration in the western North Atlantic Ocean: Results from the GEOTRACES GA02 section. Geochim. Cosmochim. Acta 177, 1–29. doi:10.1016/j.gca.2015.12.019

Licari, L.N., Schumacher, S., Wenzhöfer, F., Zabel, M., Mackensen, A., 2003. Communities and microhabitats of living benthic Foraminifera from the tropical East Atlantic: impact of different productivity regimes. J. Foraminifer. Res. 33, 10–31. doi:10.2113/0330010

Lisiecki, L.E., Raymo, M.E., 2005. A Pliocene-Pleistocene stack of 57 globally distributed benthic δ 18 O records. Paleoceanography 20, 1–17. doi:10.1029/2004PA001071

López Correa, M., Montagna, P., Joseph, N., Rüggeberg, A., Fietzke, J., Flögel, S., Dorschel, B., Goldstein, S.L., Wheeler, A., Freiwald, A., 2012. Preboreal onset of cold-water coral growth beyond the Arctic Circle revealed by coupled radiocarbon and U-series dating and neodymium isotopes. Quat. Sci. Rev. 34, 24–43. doi:10.1016/j.quascirev.2011.12.005

Ludwig, K.R., Titterington, D.M., 1994. Calculation of 230Th U isochrons, ages, and errors. Geochim. Cosmochim. Acta 58, 5031–5042.

Lutze, G.F., Coulbourn, W.T., 1984. Recent benthic foraminifera from the continental margin of northwest Africa: Community structure and distribution. Mar. Micropaleontol. 8, 361–401. doi:10.1016/0377-8398(84)90002-1

Mackensen, A., Schmiedl, G., Harloff, J., Giese, M., 1995. Deep-Sea Foraminifera in the South Atlantic Ocean: Ecology and Assemblage Generation. Micropaleontology 41, 342–358. doi:10.2307/1485808

Malmgren, B.A., Haq, B.U., 1982. Assessment of quantitative techniques in paleobiogeography. Mar. Micropaleontol. 7, 213–236. doi:10.1016/0377-8398(82)90003-2

Mangini, A., Godoy, J.M., Godoy, M.L., Kowsmann, R., Santos, G.M., Ruckelshausen, M., Schroeder-Ritzrau, A., Wacker, L., 2010. Deep sea corals off Brazil verify a poorly ventilated Southern Pacific Ocean during H2, H1 and the Younger Dryas. Earth Planet. Sci. Lett. 293, 269–276. doi:10.1016/j.epsl.2010.02.041

Matos, L., Mienis, F., Wienberg, C., Frank, N., Kwiatkowski, C., Groeneveld, J., Thil, F., Abrantes, F., Cunha, M.R., Hebbeln, D., 2015. Interglacial occurrence of cold-water corals off Cape Lookout (NW Atlantic): First evidence of the Gulf Stream influence. Deep Sea Res. Part I Oceanogr. Res. Pap. 105, 158–170. doi:10.1016/j.dsr.2015.09.003

Merino, M., 1997. Upwelling on the Yucatan Shelf: hydrographic evidence. J. Mar. Syst. 13, 101–121. doi:10.1016/S0924-7963(96)00123-6

Mienis, F., de Stigter, H.C., White, M., Duineveld, G., de Haas, H., van Weering, T.C.E., 2007. Hydrodynamic controls on cold-water coral growth and carbonate-mound development at the SW and SE Rockall Trough Margin, NE Atlantic Ocean. Deep Sea Res. I 54, 1655–1674. doi:10.1016/j.dsr.2007.05.013

Mienis, F., Duineveld, G.C.A., Davies, A.J., Ross, S.W., Seim, H., Bane, J., van Weering, T.C.E., 2012. The influence of near-bed hydrodynamic conditions on cold-water corals in the Viosca Knoll area, Gulf of Mexico. Deep. Res. Part I Oceanogr. Res. Pap. 60, 32–45. doi:10.1016/j.dsr.2011.10.007

Milker, Y., Schmiedl, G., 2012. A taxonomic guide to modern benthic shelf foraminifera of the western Mediterranean Sea. Palaeontol. Electron. 15, 1–134.

Murray, J.W., 2006. Ecology and Applications of Benthic Foraminifera. Cambridge University Press, Cambridge. doi:10.1017/CBO9780511535529

Newton, C.R., Mullins, H.T., Gardulski, A.F., Hine, A.C., Dix, G.R., 1987. Coral Mounds on the West Florida Slope: Unanswered Questions regarding the Development of Deep-Water Banks. Palaios 2, 359–367.

Paull, C.., Neumann, a. ., am Ende, B.., Ussler III, W., Rodriguez, N.., 2000. Lithoherms on the Florida–Hatteras slope. Mar. Geol. 166, 83–101. doi:10.1016/S0025-3227(00)00003-7

Raddatz, J., Rüggeberg, A., Liebetrau, V., Foubert, A., Hathorne, E.C., Fietzke, J., Eisenhauer, A., Dullo, W.-C., 2014. Environmental boundary conditions of cold-water coral mound growth over the last 3 million years in the Porcupine Seabight, Northeast Atlantic. Deep Sea Res. Part II Top. Stud. Oceanogr. 99, 227–236. doi:10.1016/j.dsr2.2013.06.009

Reimer, P.J., Bard, E., Bayliss, A., Beck, J.W., Blackwell, P.G., Ramsey, C.B., Buck, C.E., Cheng, H., Edwards, R.L., Friedrich, M., Grootes, P.M., Guilderson, T.P., Haflidason, H., Hajdas, I., Hatté, C., Heaton, T.J., Hoffmann, D.L., Hogg, A.G., Hughen, K.A., Kaiser, K.F., Kromer, B., Manning, S.W., Niu, M., Reimer, R.W., Richards, D.A., Scott, E.M., Southon, J.R., Staff, R.A., Turney, C.S.M., van der Plicht, J., 2013. Intcal13 and marine13 radiocarbon age calibration curves 0–50,000 years cal BP. Radiocarbon 55, 1869–1887. doi:10.2458/azu_js_rc.55.16947

Rivas, D., Badan, A., Ochoa, J., 2005. The Ventilation of the Deep Gulf of Mexico. J. Phys. Oceanogr. 35, 1763–1781. doi:10.1175/JPO2786.1

Roberts, J.M., Wheeler, A., Freiwald, A., Cairns, S., 2009. Cold-Water Corals: The Biology and Geology of Deep-Sea Coral Habitats. Cambrigde University Press.

Robinson, L.F., Adkins, J., Scheirer, D., Fernandez, D.P., Gagnon, a C., Waller, R., 2007. Deep-sea scleractinian coral age and depth distributions in the NW Atlantic for the last 225 thousand years. Bull. Mar. Sci. 81, 371–391.

Schmiedl, G., Mackensen, A., Müller, P.J., 1997. Recent benthic foraminifera from the eastern South Atlantic Ocean: Dependence on food supply and water masses. Mar. Micropaleontol. 32, 249–287. doi:10.1016/S0377-8398(97)00023-6

Schmiedl, G., Mitschele, A., Beck, S., Emeis, K.-C., Hemleben, C., Schulz, H., Sperling, M., Weldeab, S., 2003. Benthic foraminiferal record of ecosystem variability in the eastern Mediterranean Sea during times of sapropel S5 and S6 deposition. Palaeogeogr. Palaeoclimatol. Palaeoecol. 190, 139–164. doi:10.1016/S0031-0182(02)00603-X

Stuiver, M., Reimer, P.J., 1993. Extended 14C data base and revised CALIB 3.0 14C age calibration program. Radiocarbon 35, 215–230.

Sulak, K.J., 2008. Origins, composition, age and structural diversification of Viosca Knoll Lophelia coral reefs and substrate - A synopsis of preliminary results, in: OCS Reports. U. S. Minerals Management Service.

Taviani, M., Bouchet, P., Metivier, B., Fontugne, M., Delibrias, G., 1991. Intermediate steps of southwards faunal shifts testified by last glacial submerged thanatocoenoses in the Atlantic ocean. Palaeogeogr. Palaeoclimatol. Palaeoecol. 86, 331–338. doi:10.1016/0031-0182(91)90089-A

Thiagarajan, N., Gerlach, D., Roberts, M.L., Burke, A., McNichol, A., Jenkins, W.J., Subhas, A. V., Thresher, R.E., Adkins, J.F., 2013. Movement of deep-sea coral populations on climatic timescales. Paleoceanography 28, 227–236. doi:10.1002/palo.20023

Titschack, J., Baum, D., De Pol-Holz, R., López Correa, M., Forster, N., Flögel, S., Hebbeln, D., Freiwald, A., 2015. Aggradation and carbonate accumulation of Holocene Norwegian cold-water coral reefs. Sedimentology 62, 1873–1898. doi:10.1111/sed.12206

Van der Land, C., Eisele, M., Mienis, F., de Haas, H., Hebbeln, D., Reijmer, J.J.G., van Weering, T.C.E., 2014. Carbonate mound development in contrasting settings on the Irish margin. Deep. Res. Part II Top. Stud. Oceanogr. 99, 297–306. doi:10.1016/j.dsr2.2013.10.004

Viana, A.R., Faugeres, J.C., Kowsmann, R.O., Lima, J.A.M., Caddah, L.F.G., Rizzo, J.G., 1998. Hydrology, morphology and sedimentology of the Campos continental margin, offshore Brazil. Sediment. Geol. 115, 133–157. doi:10.1016/S0037-0738(97)00090-0

Waelbroeck, C., Labeyrie, L., Michel, E., Duplessy, J.C., McManus, J.F., Lambeck, K., Balbon, E., Labracherie, M., 2002. Sea-level and deep water temperature changes derived from benthic foraminifera isotopic records. Quat. Sci. Rev. 21, 295–305. doi:10.1016/S0277-3791(01)00101-9

White, M., Dorschel, B., 2010. The importance of the permanent thermocline to the cold water coral carbonate mound distribution in the NE Atlantic. Earth Planet. Sci. Lett. 296, 395–402. doi:10.1016/j.epsl.2010.05.025

White, M., Roberts, J.M., van Weering, T., 2007. Do bottom-intensified diurnal tidal currents shape the alignment of carbonate mounds in the NE Atlantic? Geo-Marine Lett. 27, 391–397. doi:10.1007/s00367-007-0060-8

Wienberg, C., Frank, N., Mertens, K.N., Stuut, J.-B., Marchant, M., Fietzke, J., Mienis, F., Hebbeln, D., 2010. Glacial cold-water coral growth in the Gulf of Cádiz: Implications of increased palaeo-productivity. Earth Planet. Sci. Lett. 298, 405–416. doi:10.1016/j.epsl.2010.08.017

Wienberg, C., Hebbeln, D., Fink, H.G., Mienis, F., Dorschel, B., Vertino, A., Correa, M.L., Freiwald, A., 2009. Scleractinian cold-water corals in the Gulf of Cádiz—First clues about their spatial and temporal distribution. Deep Sea Res. Part I Oceanogr. Res. Pap. 56, 1873–1893. doi:10.1016/j.dsr.2009.05.016

Wienberg, C., Titschack, J., *in press*. Framework-Forming Scleractinian Cold-Water Corals Through Space and Time: A Late Quaternary North Atlantic Perspective, in: Rossi, S., Bramanti, L., Gori, A., del Valle, C. (Eds.), Marine Animal Forests: The Ecology of Benthic Biodiversity Hotspots. Springer International Publishing, pp. 1–34. doi:10.1007/978-3-319-17001-5_16-1

6 Interglacial occurrence of cold-water corals off Cape Lookout (NW Atlantic): first evidence of the Gulf Stream influence

Lélia Matos[a,b,c], Furu Mienis[a,1], Claudia Wienberg[a], Norbert Frank[d,2], Cornelia Kwiatkowski[a], Jeroen Groeneveld[a], François Thil[d], Fatima Abrantes[b], Marina R. Cunha[c], and Dierk Hebbeln[a]

[a] Center for Marine Environmental Sciences (MARUM), University of Bremen, Germany

[b] Instituto Português do Mar e da Atmosfera (IPMA), Portugal

[c] Departamento de Biologia & CESAM, Universidade de Aveiro, Portugal

[d] Laboratoire des Sciences du Climat et de L´Environnement (LSCE), CEA - CNRS - University Versailles - St. Quentin, France

[1] present address: Royal Netherlands Institute for Sea Research (NIOZ), Netherlands

[2] present address: Institut für Umweltphysik, Ruprecht-Karls Universität Heidelberg, Germany

Correspondence to: Lélia Matos (lmatos@marum.de)

Abstract

Climatic and oceanographic changes, as occurring at a glacial-interglacial scale, may alter the environmental conditions needed for the development of prolific cold-water coral reefs and mounds. Studies constraining the temporal distribution of cold-water corals in the NE Atlantic suggested the cyclic changes of the Atlantic Meridional Overturning Circulation as the main driver for the development and dispersal of cold-water coral ecosystems. However, conclusions were hindered by lack of data from the NW Atlantic. Aiming to overcome this lack of data, the temporal occurrence of cold-water corals in the Cape Lookout area along the southeastern US margin was explored by U-series dating. Furthermore, the local influence of the regional water masses, namely the Gulf Stream, on cold-water coral proliferation and occurrence since the Last Glacial Maximum was examined. Results suggest that the occurrence of cold-water corals in the Cape Lookout area is restricted to interglacial periods, with corals being present during the last ~7 kyr and also during the Eemian (~125 ka). The reconstructed local environmental conditions suggest an offshore displacement of the Gulf Stream and increased influence from the Mid-Atlantic Bight shelf waters during the last glacial period. During the deglacial sea level rise, the Gulf Stream moved coastward providing present-day-

like conditions to the surface waters. Nevertheless, present-day conditions at the ocean sea floor were not established before 7.5 cal ka BP once the ultimate demise of the Laurentide ice-sheet caused the final sea level rise and the displacement of the Gulf Stream to its present location. Occasional presence of the Gulf Stream over the site during the Mid- to Late Holocene coincides with enhanced bottom current strength and a slightly higher bottom water temperature, which are environmental conditions that are favorable for cold-water coral growth.

6.1 Introduction

Cold-water corals (CWC), also known as deep-water corals, are azooxanthellate, ahermatypic corals commonly living in subphotic intermediate depths between 200-1000 m (Roberts et al., 2009). An important group of CWC are framework-forming scleractinian CWC (with *Lophelia pertusa* being the most common species), which are capable of forming reefs that may develop into coral mounds (Freiwald et al., 2004; Dorschel et al., 2005). Framework-forming scleractinian CWC are geographically widespread (Cairns, 2007) and numerous studies have documented their occurrence within the North Atlantic, in particular along the continental margins at both sides of the Atlantic basin (e.g., Colman et al., 2005; Cordes et al., 2008; Fosså et al., 2005; Messing et al., 2008; Reed, 2002; Wheeler et al., 2007; Wienberg et al., 2009). The proliferation of CWC has been related to specific environmental conditions, such as enhanced bottom currents and availability of sufficient food (e.g., Davies et al., 2009; Dorschel et al., 2007a; Duineveld et al., 2007; Frederiksen et al., 1992; White et al., 2005).

Absolute dating of CWC allows the definition of periods with favorable conditions that triggered pronounced CWC reef and mound development, thus enabling the establishment of a temporal framework for CWC occurrence during the Late Quaternary (Frank et al., 2011). On the northern margins of the NE Atlantic (>50°N), CWC flourished mainly during interglacial periods over the last 500 kyr and formed partly large and extended reef and mound structures (Dorschel et al., 2007b; Eisele et al., 2008; Frank et al., 2009; López-Correa et al., 2012; Raddatz et al., 2014; van der Land et al., 2014). In contrast, in the southern areas of the NE Atlantic (<37°N), CWC mounds developed predominantly during glacial periods (Eisele et al., 2011; Frank et al., 2011; Taviani et al., 1991; Wienberg et al., 2009; Wienberg et al., 2010). Overall, it appears that the distribution of NE Atlantic CWC shifted from the southern margins (<37°N) during glacial periods to more northern locations (>50°N) during interglacial periods (Frank et al., 2011). Changing environmental conditions triggered by glacial and interglacial variability have thus affected CWC distribution through time. During glacial periods, differences in wind patterns and sea level led to changes of regional upwelling with increased surface productivity in the Gulf of Cádiz (Wienberg et al., 2010) and along the Mauritanian margin (Eisele et al., 2011), respectively. Increased productivity in the surface ocean, in turn, allowed for a higher downward food export to intermediate depths, supporting CWC growth. Contrarily, ice-sheet coverage on the Norwegian shelf (López-Correa et al., 2012) and a decrease of bottom current strength and food supply (Dorschel et al., 2005; Frank et al., 2011) have been suggested to have erased or at least negatively affected the proliferation of CWC during glacial periods. Frank et al. (2011) mentioned some of the environmental changes affecting CWC to occur synchronously to hydrographic changes resulting from the glacial southward displacement of the polar front. A recent study using *L. pertusa* as a model has shown how the Atlantic Meridional Overturning Circulation (AMOC) as part of the global ocean conveyor possibly influences CWC development and larvae dispersal through cyclic climatic changes (Henry et al., 2014). Unfortunately, conclusions were somehow limited by lack of data from the NW Atlantic. It is therefore crucial to overcome this data shortage in order to better constrain how basin-wide circulation patterns might affect CWC distribution in the North Atlantic.

In the NW Atlantic, CWC dominated by *L. pertusa* occur from the Gulf of Mexico, through the Straits of Florida and off North Carolina (Brooke and Schroeder, 2007; Messing et al., 2008; Ross and Nizinski, 2007). During recent years, extensive mapping and numerous ecological and environmental studies were performed on these CWC sites (e.g., Brooke and Ross, 2014; Cordes et al., 2008; Correa et al., 2007; Davies et al., 2010; Grasmueck et al., 2006; Hebbeln et al., 2014; Mienis et al., 2014). However, the stratigraphic range of the NW Atlantic CWC occurrences during the recent past remains poorly constrained. So far, a very limited number of eight framework-forming CWC samples (all randomly collected from the seabed surface by dredge or ROV) has been dated. Three datings were obtained for *L. pertusa* collected in the Gulf of Mexico showing glacial ages (24.6 ka, 24.9 ka, and 31.3 calibrated (cal) ka BP; Newton et al., 1987; Sulak, 2008) and five datings were derived from CWC samples collected along the Florida-Hatteras slope (~30-32°N) revealing very young ages of <0.6 ka, with two exceptions providing older ages of 9.5 ka and 23.9 cal ka BP (Paull et al., 2010; van de Flierdt et al., 2010). As these coral ages are all obtained from individual fragments, of colonial, framework-building corals the resulting ages most likely do not fully represent the occurrence pattern of the NW Atlantic CWC areas.

Here we present the first study on sediment cores taken from the Cape Lookout coral area (North Carolina margin, ~34°N; Fig. 1) that is the northernmost location of CWC mounds along the NW Atlantic margin (Partyka et al., 2007). The mounds are teardrop-shaped structures with a SSW-NNE orientation at depths between 320 and 550 m (Mienis et al., 2014) and are composed of a sediment and coral rubble matrix topped mostly with live and dead *L. pertusa* reefs (up to 5 m high) (Ross and Quattrini, 2007; Ross and Quattrini, 2009). The most abundant living CWC thickets were found on the mound slopes facing the strongest currents (Mienis et al., 2014).

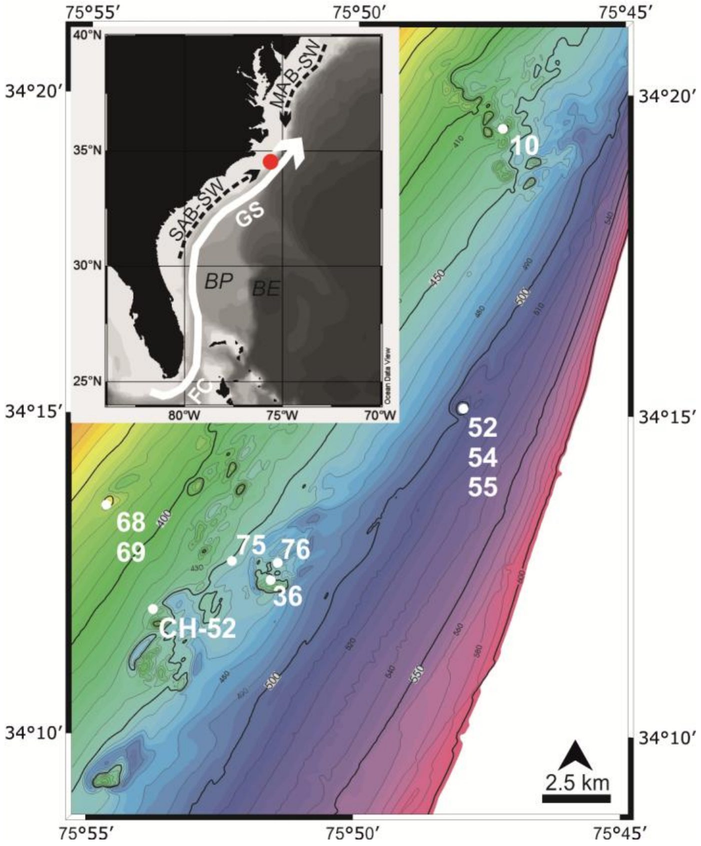

Figure 1. Study site location and position of sampled cores (white numbers; metadata of cores are given in Table 1), including local bathymetry (isobaths of 10 m). Inserted map (top left) places the study site (red circle) within the regional continental margin, including location of the Blake Plateau (BP), Blake Escarpment (BE), South (SAB-SW) and Mid (MAB-SW) Atlantic Bight shelf waters, Florida current (FC) and the present-day Gulf Stream main axis (GS).

The Cape Lookout CWC area is located on the northern end of the Blake Plateau where the continental slope meets the deeper Blake Escarpment. The Blake Plateau, with a depth of 600-1200 m, is considered to be the northern continuation of the Bahamas Bank carbonate province (Pratt and Heezen, 1964). Surface sediments are mostly medium-sized carbonate sands (mean grain sizes of 250 to 500 µm) dominated by planktic foraminifera derived from the Gulf Stream (GS) system flowing above (Gorsline, 1963). The GS has been mentioned as the main regional regulator of local sedimentation for the past 10 Myr (Pinet and Popenoe, 1985). Sea floor photographs have indicated sediment rippling at depths <1000 m showing the presence of currents strong enough to produce rapid accumulations of foraminifera tests and subsequent re-working of sediments by re-suspension and transport (Gorsline, 1963; Rowe and Menzies, 1968).

On the continental shelf (<200 m), the hydrological setting is defined by the warm and salty South Atlantic Bight shelf water (SAB-SW) flowing mostly northward between Florida and North Carolina, and the colder, fresher Middle Atlantic Bight shelf water (MAB-SW) running southward along the northern coastline to Cape Hatteras (Savidge, 2002). The SAB-SW is mostly influenced by the Florida current (FC) and to a lesser extent by regional river runoff. Current direction is related to the prevailing winds presenting a predominant northward direction, although entrainments of FC eddies and seasonal northerly winds can trigger a change to a southward current direction (Bumpus, 1973 and references therein). The MAB-SW is formed in the Gulf of Maine where the cold, low-salinity water from the Scotian Shelf joins the warmer, more saline Slope waters, which originated seaward of the shelf (Mountain, 2003). Manning (1991) defined the MAB-SW within water depths of 0-100 m as having a characteristic salinity of 32.5-33.5 staying fairly constant during the year, and a seasonally changing temperature of 4-15 °C. The SAB-SW and the MAB-SW converge near Cape Hatteras, in what is known as the Hatteras Front (Savidge, 2002). The front migrates seasonally and the MAB-SW can leak into the northern SAB area, which will reverse the local northward currents to a southward direction, mainly during late summer and early autumn (Bumpus, 1973).

Further offshore, the GS is the dominant current in this region. It flows from the Strait of Florida to Cape Hatteras (here GS is called the FC) and turns eastward near 40°N to cross the North Atlantic towards the NE Atlantic margin. It is a warm, saline swift current that may reach down to 1000 m depth along the Blake Plateau (Richardson, 2001). The average surface (0-10 m) water temperatures fluctuate year round between 24-29 °C, respectively, while average salinity ranges between 36 and 36.2 (Fig. 2) (Locarnini et al., 2013; Zweng et al., 2013). The GS speed may reach 2-2.5 m s^{-1} at the surface and up to 0.2 m s^{-1} around 1000 m depth (Richardson, 2001). In the Cape Lookout study area, the GS flows from SSW-NNE and its presence is occasionally observed at the sea floor during events of increasing temperature and salinity (Mienis et al., 2014). This entire hydrographical setting is very dynamic in space and time, mainly driven by the meandering component of the GS (Bane and Brooks, 1979) and eddy shedding occurring north and south of the jet (Joyce, 1985; The Ring Group, 1981). The GS and the SAB-SW interact at frontal eddies that, together with the upwelling of waters from the nitrogen bearing strata below the GS (~1000 m), influence local primary production in the Cape Lookout area (Lee at al., 1991). Near Cape Hatteras, the inshore area of the GS is underlain by the fresher and cooler Labrador Current flowing in a southward direction (Richardson, 1977). The Western Boundary Undercurrent (WBUC) is only found deeper, at depths of >1000 m (Fig. 2), flowing south-westward beneath the mean axis of the GS (Richardson, 2001).

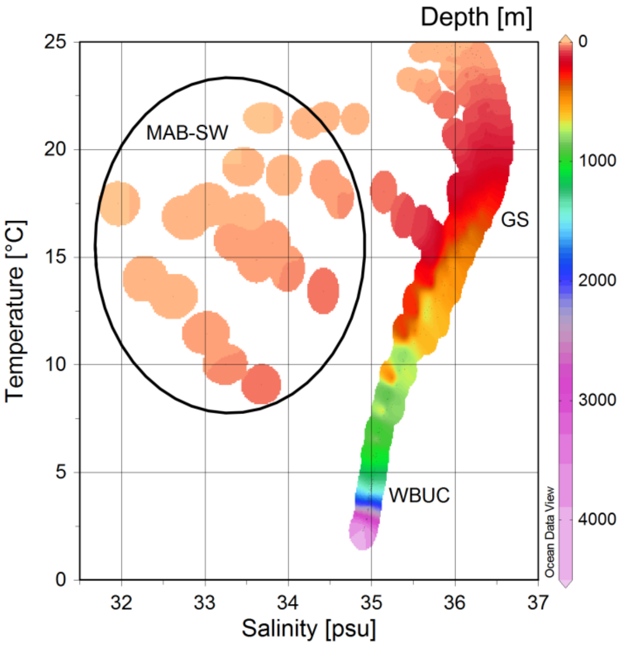

Figure 2. Water mass structure in the East American Shelf around Cape Hatteras. A Temperature-Salinity (T-S) plot is displayed using Ocean Data View v.4.5.1 (Schlitzer, 2012). Data were compiled from the World Ocean Atlas (Locarnini et al., 2013; Zweng et al., 2013). Abbreviations: MAB-SW – Mid-Atlantic Bight Shelf Water, GS – Gulf Stream, WBUC – Western Boundary Undercurrent.

The main aim of this study is to constrain the local climatic periods favorable for CWC growth and mound development along the North Carolina margin and to investigate how the regional water masses (and especially the Gulf Stream, as the regional dominant current and part of the AMOC) are locally influencing CWC proliferation and therefore mound aggradation. Furthermore, newly obtained coral ages of *L. pertusa* provide an important contribution to the limited stratigraphic data available so far on CWC occurrences in the NW Atlantic, and thus will help to unravel their temporal development at this side of the Atlantic.

6.2 Material and methods

The samples used in this study were collected during the DISCOVRE 2009 Cruise IV (R/V *Cape Hatteras*) and the TRACOS-2010 64PE320 Cruise (R/V *Pelagia*). The sampled mounds are distributed along the Cape Lookout CWC area, differing slightly in location, distance to shore and depth (Table 1), and lying within an area of ~120 km^2 (Fig. 1). Eight box cores and a 3.5-m-long piston core were collected from the mound structures (on-mound cores) between 330-470 m water depth (Table 1), all containing coral-bearing sediments. With the exception of the TRACOS2010-36 box core, of which samples were sieved, sub cores were taken from the box cores by inserting wet PVC liners into the sediment. The coral-bearing piston core and sub cores of the box cores were cut frozen with a diamond saw, in order to keep the internal sedimentary structure undisturbed. For paleo-environmental reconstruction, a box core barren of any CWC fragments was retrieved off-mound (TRACOS2010-75, 450 m water depth; Table 1) and sub-sampled with a wet PVC liner pushed into the sediment. The off-mound box core was collected in close vicinity of the CWC mounds (Fig. 1) to ensure that reconstructed environmental conditions can be related to the stratigraphic data obtained from the on-mound cores.

Table 1. Metadata of piston and box cores collected off Cape Lookout (North Carolina margin) during the DISCOVRE 2009 Cruise IV (R/V *Cape Hatteras*) and the TRACOS-2010 64PE320 Cruise (R/V *Pelagia*). PC: piston core; BC: box core, WD: water depth.

Sample-ID	**Gear**	**Latitude** [N]	**Longitude** [W]	**WD** [m]	**Location**	**Coral-bearing**	**Recovery** [cm]
CH-2009-52	BC	34° 11' 56.280''	75° 53' 46.440''	427	on-mound	yes	19
TRACOS2010-10	BC	34° 19' 28.153''	75° 47' 17.179''	393	on-mound	yes	30
TRACOS2010-52	BC	34° 15' 06.145''	75° 47' 59.417''	435	on-mound	yes	8
TRACOS2010-54	BC	34° 15' 05.767''	75° 47' 59.759''	435	on-mound	yes	11
TRACOS2010-55	BC	34° 15' 05.911''	75° 47' 59.172''	436	on-mound	yes	15
TRACOS2010-68	BC	34° 13' 33.481''	75° 54' 39.636''	337	on-mound	yes	20
TRACOS2010-69	BC	34° 13' 33.535''	75° 54' 39.971''	335	on-mound	yes	18
TRACOS2010-36	BC	34° 12' 40.392''	75° 51' 26.683''	470	on-mound	yes	22
TRACOS2010-76	PC	34° 12' 24.293''	75° 51' 34.661''	443	on-mound	yes	360
TRACOS2010-75	BC	34° 12' 42.055''	75° 52' 18.390''	450	off-mound	no	49

6.2.1 U-series dating on cold-water corals

To identify periods of sustained CWC occurrence, nineteen well-preserved fossil *L. pertusa* fragments were selected from different depths in box and piston cores and used for Uranium-series dating (Table 2). Prior to the analyses, the coral samples were cleaned mechanically to remove remains of organic tissue and non-carbonate contaminants from the skeleton surfaces (borings by organisms, iron–manganese crusts, coatings) and prepared chemically using weak acid leaching and water rinsing procedures as described by Frank et al. (2004). The aragonite fragments were then weighed and dissolved in 6N HNO_3 acid in clean Teflon vials containing a known quantity of a ^{229}Th, ^{233}U and ^{236}U triple spike. The dissolved sample-spike mixture was dried on a hot plate overnight and re-dissolved in 3N HNO_3. Thorium (Th) and Uranium (U) were extracted and purified from the sample solutions using the ion exchange resin U-TEVA according to Douville et al. (2010). Finally, the Th and U fractions were reduced to less than 10 µl solution on a hot plate and re-dissolved in a mixture of 0.1N HNO_3 and 0.01N HF. In order to simultaneously measure both Th and U isotopes, the Th fractions (100%) were doped with a small amount (typically 5-10%) of the sample U fractions. Isotopic measurements of ^{229}Th ^{230}Th, ^{232}Th, ^{233}U, ^{234}U, ^{235}U, ^{236}U and ^{238}U were subsequently carried out on a ThermoFisher Neptune Plus MC-ICPMS instrument at the Laboratoire des Sciences du Climat et de l'Environnement (Gif-sur-Yvette, France) using a standard sample bracketing technique. Here samples and appropriate instrumental and chemical blank solutions were interspaced. Using a peak-jump routine ^{234}U and ^{230}Th were measured on the central electron multiplier. Initially, uranium isotopes were measured for 4 seconds simultaneously on Faraday cups (^{233}U, ^{235}U ^{236}U and ^{238}U) and on the central ion counter (^{234}U). Secondly, after a peak-jump, all thorium isotopes are measured for 8 seconds on Faraday cups (^{229}Th and ^{232}Th) and on the central ion counter (^{230}Th). This peak jump routine is repeated 24 times to get a precision around 2‰ (depending on the age of the sample) for thorium ratios and 1‰ for uranium ratios. Sample standard measurements were interspaced with measurements of Ion counter to Faraday Cup Yield as well as with measurements of hydrate interferences and peak tailing to accurately correct for isobaric interferences. Data reprocessing was performed to remove instrumental blanks and to correct for mass fractionation using the natural ^{235}U/^{238}U atomic ratio (137.88). Hydrate and peak tailing interferences were removed based on the mass ratio 239/238 and half mass measurements. Finally, isotopic ratios were normalized to the isotopic compositions of the secular equilibrium standard (Harwell Uraninite) HU-1 (Cheng et al., 2000). Full procedural chemical blanks were considered for data adjustment, and age calculation based on isotopic ratios was performed through iterative age estimation (Ludwig and Titterington, 1994) propagating all analytical errors into the Monte-Carlo age and uncertainty simulation. Ultimately, ages need to be corrected for the possible ^{230}Th contribution from seawater and/or residual non-carbonate contamination. This was done using an estimated activity ratio of (^{230}Th/^{232}Th) of 10±6 for sub-surface seawater. However, this correction is negligible within uncertainty of the initial age estimates.

Table 2. U-series ages, isotope concentrations and ratios. U-series datings were performed on *Lophelia pertusa* cold-water coral fragments. *Th corrected ages, see text. CD: core depth, ppm: parts per million, ppb: parts per billion.

Sample name	CD (cm)	[^{238}U] ppm	[^{232}Th] ppb	d^{234}U$_m$	(^{230}Th/^{232}Th)	(^{230}Th/^{238}U)	d^{234}U$_{(0)}$ (‰)	Age (years)	Age* (years)
CH-09-52	4-5	2.24 ±0.003	2.1420 ±0.0052	146.2 ±2.2	34.71 ±0.40	0.01120 ±0.00013	146.6 ±2.2	1,073 ± 15	766 ± 137
CH-09-52	16.5-18	3.38 ±0.005	0.1696 ±0.0006	148.4 ±1.1	437.2 ±3.7	0.00737 ±0.00006	148.7 ±1.1	703.5 ± 6.5	688 ± 13
Tracos2010-10	0-1.5	8.954 ±0.054	0.4162 ±0.0033	148.5 ±1.4	142.2 ±4.5	0.00223 ±0.00007	148.6 ±1.4	212.0 ± 7.0	198 ± 13
Tracos2010-10	26.5-27.5	3.094 ±0.007	0.7019 ±0.0007	145.2 ±1.7	105.3 ±1.1	0.00805 ±0.00008	145.5 ±1.7	770.0 ± 9.0	698 ± 38
Tracos2010-52	2-4	3.69 ±0.011	0.8265 ±0.0016	146.6 ±1.2	56.54 ±0.79	0.00426 ±0.00006	146.7 ±1.2	407.5 ± 6.5	336 ± 35
Tracos2010-54	0-2	3.578 ±0.007	0.5770 ±0.0016	148.3 ±1.1	140.2 ±1.4	0.00763 ±0.00008	148.6 ±1.2	728.0 ± 8.0	676 ± 29
Tracos2010-54	7-10	3.621 ±0.012	0.2458 ±0.0008	144.7 ±2.0	330.0 ±3.1	0.00752 ±0.00007	145.0 ±2.0	720.5 ± 8.5	699 ± 17
Tracos2010-55	0-2	3.793 ±0.009	0.3932 ±0.0006	147.6 ±1.4	55.6 ±1.1	0.00194 ±0.00004	147.7 ±1.4	185.0 ± 4.0	153 ± 18
Tracos2010-55	10-14	4.152 ±0.013	0.2977 ±0.0035	145.7 ±1.3	387.0 ±7.7	0.00935 ±0.00019	146.1 ±1.3	895 ± 19	873 ± 29
Tracos2010-68	2-4	3.275 ±0.007	0.6403 ±0.0010	147.5 ±1.2	84.6 ±1.1	0.01116 ±0.00007	147.9 ±1.2	1,067.0 ± 8.0	942 ± 58
Tracos2010-68	18.5-19.5	3.346 ±0.006	0.2387 ±0.0005	146.2 ±1.3	102.5 ±1.2	0.00246 ±0.00003	146.3 ±1.3	235.0 ± 3.0	212 ± 12
Tracos2010-69	1-2	3.858 ±0.013	0.4922 ±0.0007	147.2 ±1.9	68.97 ±0.81	0.00298 ±0.00004	147.3 ±1.9	284.5 ± 3.5	244 ± 21
Tracos2010-69	16-17.5	3.589 ±0.008	0.4038 ±0.0006	144.8 ±1.2	206.3 ±1.4	0.00781 ±0.00005	145.1 ±1.2	748.5 ± 5.5	712 ± 20
Tracos2010-76	18-20	4.138 ±0.009	6.1886 ±0.1355	141.2 ±4.7	151 ±16	0.07391 ±0.00764	144.2 ±4.7	7,309 ± 811	6,836 ± 983
Tracos2010-76	60-61	3.147 ±0.007	1.2519 ±0.0130	143.8 ±3.1	510 ±31	0.06637 ±0.00399	146.5 ±3.1	6,522 ± 422	6,396 ± 468
Tracos2010-76	160	3.802 ±0.005	1.0917 ±0.0141	140.9 ±4.2	641 ±74	0.00632 ±0.00096	143.3 ±4.2	5,925 ± 720	5,598 ± 937
Tracos2010-76	240	3.744 ±0.005	1.0613 ±0.0160	148.3 ±3.9	679 ±49	0.00806 ±0.00078	150.9 ±3.9	6,152 ± 465	5,868 ± 649
Tracos2010-36	0-22	4.434 ±0.013	1.3700 ±0.0064	105.0 ±1.1	7,308 ±39	0.76081 ±0.00408	149.0 ±1.6	123,840 ± 1449	123,741 ± 1,487
Tracos2010-36	0-22	2.903 ±0.008	0.4837 ±0.0005	103.8 ±1.5	13,829 ±23	0.77500 ±0.00128	149.2 ±2.2	128,415 ± 772	128,361 ± 792

6.2.2 Analyses on the off-mound core TRACOS2010-75

The stratigraphy for the 49-cm-long off-mound box core was established by three AMS ^{14}C dates determined on ~10 mg calcium carbonate of mixed planktic foraminifera of the size fraction >150 µm. The samples were analyzed at the Poznań Radiocarbon Laboratory (Poznań, Poland). All ages were corrected for ^{13}C and a mean ocean reservoir age of 400 years was used. AMS ^{14}C ages were converted to calendar years (cal yr BP, present is AD 1950) using the MARINE13 calibration curve (Reimer et al., 2013) of the CALIB7.0 software (Stuiver and Reimer, 1993).

Stable oxygen isotope ($\delta^{18}O$) composition and Mg/Ca ratios were analyzed from shells of the planktic foraminifera *Globigerinoides ruber* sensu stricto (s.s.) (white variety) and of the benthic foraminifera *Cibicides pachyderma*. *G. ruber* is commonly used to reconstruct sea surface conditions and is assumed to record annual average surface water temperatures of the present-day mixed layer (Deuser et al., 1981). During the Last Glacial Maximum (LGM), this species is believed to record summer temperatures at the studied location (Fraile et al., 2009). *C. pachyderma* (Murray, 2008; Rosenthal et al., 1997) is an epifaunal species that primarily inhabits intermediate water depths (200-600 m water depth) (van Morkhoven et al., 1986). The species is abundant in both Holocene and glacial sediments which makes it a prime candidate for paleoceanographic studies (Rosenthal et al., 1997). Well-preserved and clean specimens (size fraction 250-355 µm; 17-78 specimens of *G. ruber* s.s. and 14-38 specimens of *C. pachyderma*) were picked from 20 sediment samples at different core depths. For homogeneity, the selected specimens were gently crushed, mixed and split to be used in both Mg/Ca and stable oxygen isotopes analyses.

Stable oxygen isotopes were analyzed with a Finnigan MAT 251 mass spectrometer at the Isotope Laboratory at MARUM (University of Bremen, Germany). Solnhofen Limestone calibrated against NBS 19 (in its turn calibrated against the Pee Dee Belemnite) was used as an internal standard, with a long-term deviation of <0.07‰.

For the Mg/Ca measurements, the crushed foraminiferal calcite was cleaned according to the protocol developed by Barker et al. (2003). Mg/Ca ratios (reported in mmol mol^{-1}, see Table 1 of Supplementary Material) were measured using the Agilent 700 Inductively Coupled Plasma Optical Emission Spectrometer with a Cetac ASX-520 autosampler, housed at the Department of Geosciences (University of Bremen, Germany). Analytical precision of an in-house standard (Mg/Ca = 2.93 mmol mol^{-1}), *G. ruber*, and *C. pachyderma* was 0.049, 0.041, and 0.075 mmol mol^{-1}, respectively, for Mg/Ca. Two samples were considered as contaminated by clays and excluded from further discussion (outliers) as their Al/Ca and Fe/Ca values were more than 2 standard deviations away from the average. The same procedure was applied to Mn/Ca values, which indicated no contamination by Mn-oxyhydroxides and/or Mn-carbonates. Mg/Ca ratios from *G. ruber* s.s. were converted into sea surface temperature (SST) following the calibration equation proposed by Cléroux et al. (2012), with a calibration associated error of 1.3°C (Cléroux et al., 2008). Mg/Ca ratios from *C. pachyderma* were converted into bottom water temperature (BWT) following the calibration equation of Lear et al. (2002), with a standard error of 1.7°C. Both SST and BWT reconstructions were found reliable after comparison between the youngest measured sample and present-day observations. SST is in agreement with the Stéfansson et al. (1971) description of the area and with the World Ocean Atlas (WOA) database (Locarnini et al., 2013). The reconstructed BWT are lower than values provided by the WOA, however resemble previous *in situ* measurements (Brooke et al., 2013; Mienis et al., 2014; Stefánsson et al., 1971) and are, therefore, considered reliable.

As an indicator of changes in salinity, the seawater $\delta^{18}O$ ($\delta^{18}O_{SW}$) was computed solving the Shackleton equation (Shackleton, 1974) for $\delta^{18}O_{SW}$. This was performed for changes in sea surface salinity (SSS) by using the *G. ruber* s.s. $\delta^{18}O$ data and the Mg/Ca-derived SST, as well as for changes in bottom salinity by using the *C. pachyderma* $\delta^{18}O$ data and the Mg/Ca-derived BWT. The $\delta^{18}O_{SW}$ values were corrected to account for the difference between PDB and Standard Mean Ocean Water (adding 0.27‰) and for ice volume-related sea level changes, as reconstructed by Waelbroeck et al. (2002). The propagated uncertainty of $\delta^{18}O_{SW}$ calculated following Cléroux et al. (2012) is 0.31 for *G. ruber* s.s. and 0.41 for *C. pachyderma*.

Grain size analyses were performed on 3–7 g of eleven sediment samples (size fraction <2 mm) using a Coulter LS230 laser particle analyzer housed at IPMA, I.P. (Lisbon, Portugal). The laser determines particle grain sizes from 0.4 to 2000 µm grouped into 92 size classes. A pre-treatment of the samples was done to remove the organic carbon using hydrogen peroxide (H_2O_2). Before measurement, the samples were homogenized by stirring. Samples were later treated with an acid solution (acetic acid and ammonium acetate) and the remaining decarbonated (terrigenous) fraction was reanalyzed. The particle size spectra are presented as volume % in logarithmic size classes, assuming spherical particle diameter, whereas for the down core record the mean grain size is displayed, as well as the standard deviation as a measure for particle sorting (Folk and Ward, 1957).

The $CaCO_3$ content was determined using a CHNS-932 LECO elemental analyzer at IPMA, I.P. (Lisbon, Portugal; see Abrantes et al., 2005). Eleven samples were analyzed collected from the same core depths as those used for grain size analyses. The samples were dried and ~1 cc of homogenized sediment was subject to combustion (3 h, up to 400°C) to remove organic carbon and then analyzed for inorganic carbon. The $CaCO_3$ content was then computed from the inorganic carbon weight (Baumann et al., 1993).

6.3 Results

6.3.1 Range of cold-water coral ages obtained for the Cape Lookout area

All CWC samples from the piston core (TRACOS2010-76; n=4) reveal a narrow age range of 5.6-6.8 ka, whereas samples from most of the box cores (n=13) are significantly younger with <1 ka (Table 2). Only two samples of a box core collected just north of the piston core (Fig. 1) reveal much older ages of 123.7 ka and 128.4 ka (Table 2). The coral datings indicate three age clusters with most of the *L. pertusa* ages coinciding with the Holocene, either the Mid-Holocene or the Late Holocene, while two datings are from the peak of the last interglacial, the Eemian (MIS 5e). No distinctive age pattern was found between the sampled CWC mounds regarding their spatial distribution (Fig. 1; Table 2).

6.3.2 Stratigraphy and proxy data of the off-mound core TRACOS2010-75

The stratigraphy of the off-mound core is based on three AMS ^{14}C ages ranging from 35 to 6.9 cal ka BP (Table 3) and linear interpolation between these levels. The age model obtained spans from MIS 3 to the Holocene (Fig. 3). The model was constructed assuming a present-day age at the top and extrapolating the sedimentation rate between the two oldest datings towards the bottom of the core. The estimated bottom age of the core is 39.5 cal ka BP (Table 1 of Supplementary Material).

Table 3. AMS ^{14}C ages determined on multi-species samples of planktic foraminifera from the TRACOS2010-75 sediment core. The AMS ^{14}C ages were corrected for ^{13}C and a mean reservoir age of 400 yrs, and were converted into calibrated years before present (cal yr BP) using the Marine13 calibration curve (Reimer et al., 2013) of the CALIB 7.0 software (Stuiver and Reimer, 1993). Estimated sedimentation rates for core TRACOS2010-75 are supplemented. CD: core depth, σ: standard deviation, MPA: median probability age, SR: sedimentation rate.

Sample-ID	**CD** [cm]	**Lab code**	**^{14}C-age** [year]	**1σ error** [±year]	**2σ calibrated age range** [year BP, P= AD 1950]	**MPA** [year BP]	**SR** [cm/kyr]
TRACOS2010-75	5	Poz-48032	6,405	35	6,986 - 6,774	6,880	0.727
TRACOS2010-75	25	Poz-48033	11,290	60	12,906 - 12,636	12,771	3.395
TRACOS2010-75	45	Poz-48034	31,500	360	35,765 - 34,303	35,034	0.898

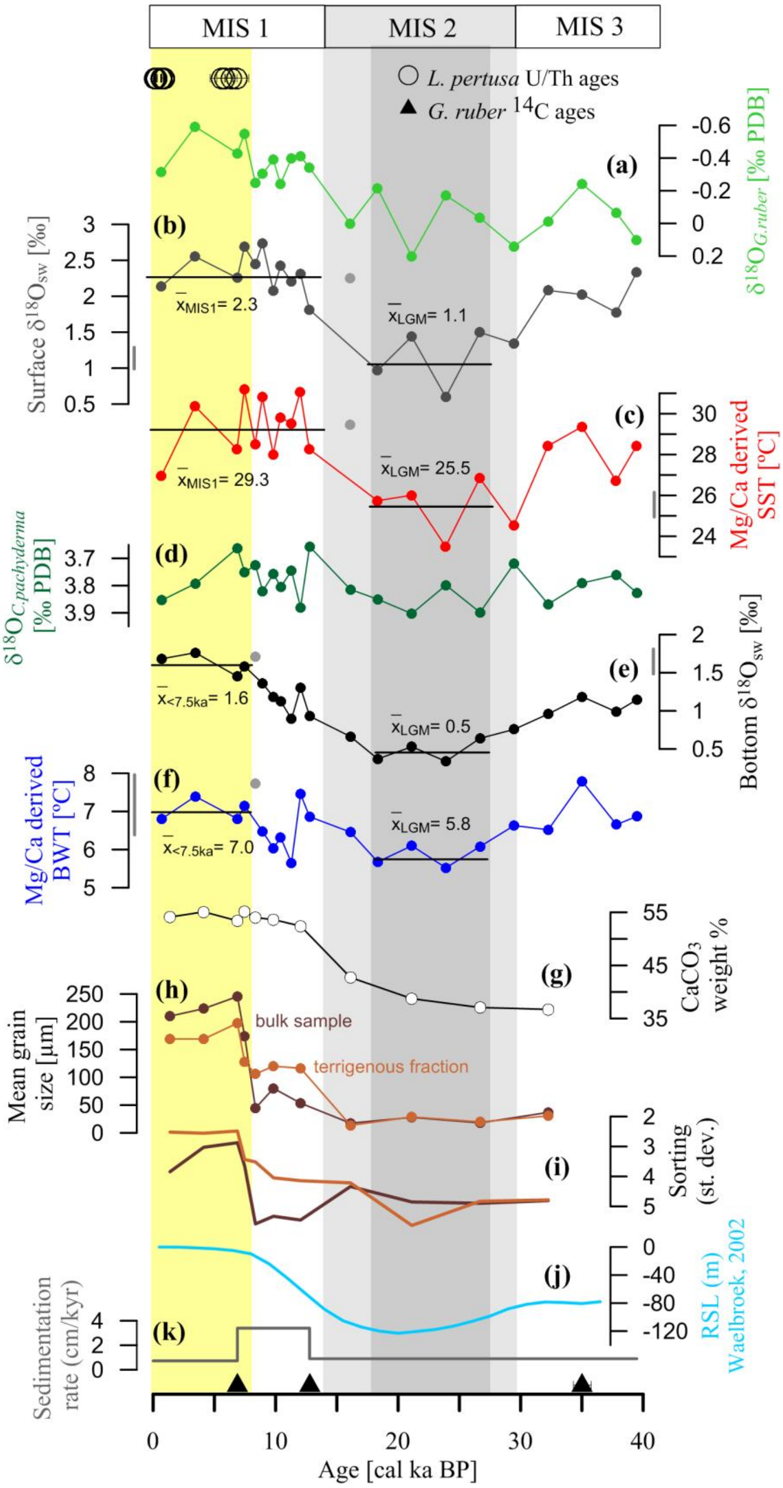

Figure 3. Multi-proxy data of the off-mound core TRACOS2010-75. From top to bottom: (**a**) *G. ruber* s.s. $\delta^{18}O$, (**b**) surface ice-volume-corrected seawater $\delta^{18}O$ ($\delta^{18}O_{SW}$), (**c**) Mg/Ca derived sea surface temperature (SST), (**d**) *C. pachyderma* $\delta^{18}O$, (**e**) bottom $\delta^{18}O_{SW}$**, (f)** Mg/Ca derived bottom water temperature (BWT), **(g)** carbonate ($CaCO_3$) fraction of the sediment, (**h**) mean grain size of the bulk sample (dark brown) and terrigenous fraction (light brown), (**i**) sorting (grain size standard deviation) of the bulk sample (dark brown) and terrigenous fraction (light brown), (**j**) relative sea level curve (RSL) according to Waelbroeck et al. (2002), included for comparison, (**k**) estimated sedimentation rate. Average $\delta^{18}O_{SW}$, SST and BWT are given for the LGM ($\bar{x}_{LGM}$) as well as the average surface $\delta^{18}O_{SW}$ and SST for MIS 1 ($\bar{x}_{MIS1}$) and the average bottom $\delta^{18}O_{SW}$ and BWT for the last 7.5 kyr ($\bar{x}_{<7.5ka}$).

Figure 3 (cont.). Grey vertical bars correspond to temperature calibration errors and $\delta^{18}O_{SW}$ propagated errors. Grey dots correspond to excluded outliers (see Material and Methods chapter for details). The AMS ^{14}C ages of the TRACOS2010-75 core are marked with black triangles and presented as calibrated kilo-years before present (cal ka BP). Holocene U-Th ages obtained for *Lophelia pertusa* (top open circles) are included in the graph. The period marked by sustained CWC occurrence is highlighted in yellow. The LGM period considered (26.7-18.3 cal ka BP) is marked in darker grey. Marine Isotope Stage (MIS) boundaries are displayed according to Lisiecki and Raymo (2005).

The *G. ruber* s.s. $\delta^{18}O$ fluctuated between 0.2 and -0.2‰ PDB during MIS 3 and 2, decreased after 21 cal ka BP towards MIS 1 and reached a minimum of -0.6‰ PDB at around 3.4 cal ka BP (Fig. 3). The ice volume-corrected surface seawater $\delta^{18}O$ ($\delta^{18}O_{SW}$) decreased from MIS 3 to MIS 2, reaching a minimum value of 0.6‰ PDB at 23.9 cal ka BP and increased gradually, reaching a maximum of 2.74‰ PDB during the Holocene (Fig. 3). During the MIS 1, the surface $\delta^{18}O_{SW}$ oscillated around an average of 2.3‰ PDB, a value 1.2‰ higher than the average found for the LGM (Clark et al., 2009; considered in our record as the 26.7-18.3 cal ka BP period) that corresponds to a salinity increase of 2.87 (Cléroux et al., 2012; calculations not shown) (Table 1 of Supplementary Material). The SST reveals variations similar to the $\delta^{18}O_{SW}$ record (Fig. 3). After decreasing from MIS 3 to MIS 2, SST reached a minimum estimated temperature of 23.5 °C at 23.9 cal ka BP. SST increased thereafter until the onset of MIS 1, when it fluctuated between 26.9 and 31.2 °C. The average SST during the MIS 1 was 3.8 °C higher than during the LGM.

The *C. pachyderma* $\delta^{18}O$ fluctuated between 3.6 and 3.9‰ PDB throughout the record (Fig. 3). The bottom $\delta^{18}O_{SW}$ decreased from MIS 3 to MIS 2, reaching a minimum value of 0.34‰ PDB at 23.9 cal ka BP and increased gradually, reaching a maximum of 1.76‰ PDB in the Late Holocene (Fig. 3). Since 7.5 cal ka BP to the present, the $\delta^{18}O_{SW}$ oscillated around an average of 1.6‰ PDB, a value 1.1‰ higher than the average found for the LGM, which corresponds to a salinity increase of 2.74 (Cléroux et al., 2012; calculations not shown) (Table 1 of Supplementary Material). BWT varied by 2.3 °C throughout the record (5.5-7.8 °C) with cooler temperatures (<6.1 °C) found during the LGM and at 11.3 and 9.8 cal ka BP (Fig. 3). Since 7.5 cal ka BP to the present, the BWT increased, stabilizing at an average of 7 °C, 1.2 °C warmer than the average found for the LGM (Table 1 of Supplementary Material). Although the difference in temperature indicated for the LGM and the Late Holocene falls within the calibration standard error, a further Student t-test showed the two averages to be significantly different (P=0.001).

The carbonate content of the core is comparably low (<40%) for most of the MIS 2 sediments (Fig. 3). Increasing values characterize sediments deposited between 21.1 and 12 cal ka BP and highest values >50% mark the sediments younger than 12 cal ka BP (Table 2 of Supplementary Material).

The mean grain size values found are overall high, ranging from medium silt to fine sands (Fig. 3). The mean grain size of the terrigenous fraction is comparably small (≤31 µm) for MIS 3 and 2 sediments and larger (≥106 µm) after 12 cal ka BP. The highest value (197 µm) is found at 6.9 cal ka BP (Fig. 3). The change between MIS 2 and MIS 1 is observed in the mean as well as in the sorting, where a lower value (indicating better sorting) is found for MIS1 (Fig. 3). The mean grain size of bulk sediment is also small (≤37 µm) for MIS 3 and 2 and slightly higher for the 12-8 cal ka BP period (44-80 µm). Highest values (≥174 µm) are found in the sediments younger than 7.5 cal ka BP (Fig. 3). The sorting of the bulk sediment shows an evident difference before and after 7.5 cal ka BP (Fig. 3). This difference is further observed in the comparison of the bulk sediment grain size spectra of the individual samples, that shows (according to Folk and Ward, 1957) a clear change from very-poorly-sorted, finer sediment deposited during MIS 3 and 2, to poorly-sorted, coarser grained sediment characteristic for the sediments of the last 7.5 kyr (Fig. 4; Table 3 of Supplementary Material).

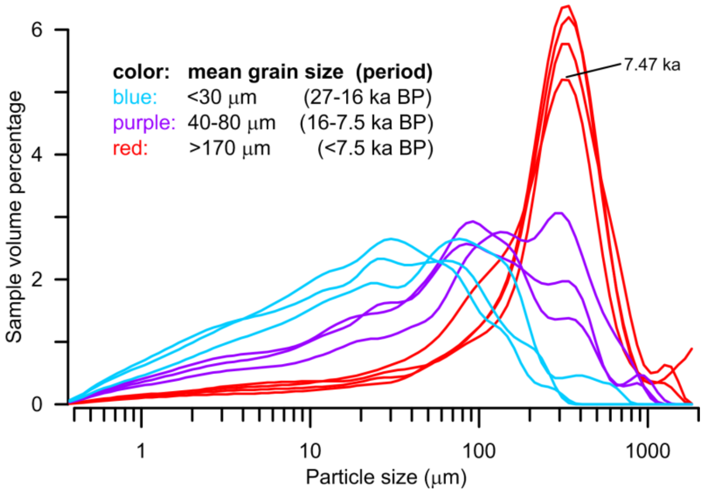

Figure 4. Grain size spectra for the TRACOS2010-75 samples along the core. The bulk sediment grain size spectra (in volume percentage) are categorized in 3 groups: last glacial samples (27-16 cal ka BP) with small mean grain size (<30 µm; blue curves), deglacial to Early Holocene samples (16-7.5 cal ka BP) with slightly higher mean (40-80 µm; purple curves), and Mid- to Late Holocene samples (<7.5 cal ka BP) with highest mean (>170 µm; red curves).

6.4 Discussion

The record of coral ages from the Cape Lookout area reveals a distinct clustering of the ages in interglacial periods, the Eemian and the Holocene. And although the lack of dated corals of a glacial age does not preclude the existence of CWC under glacial conditions, the observed pattern clearly points to better living conditions for the CWC under interglacial conditions. Age reversals in the coral datings found in some of the cores (see Table 2) are either related to collapsed *in situ* coral framework or to the local CWC growth pattern in the direction of the strongest currents, similar to descriptions made for CWC sites off Norway (López-Correa et al., 2012). Nonetheless, this study is focused on the collection of individual CWC ages, regardless of their stratigraphic sequence, in order to identify periods of sustained CWC occurrence.

To put the record of coral ages in perspective, a set of paleoceanographic proxies has been investigated for this study. These revealed relevant environmental changes that affected the Cape Lookout CWC area over the last ~40 kyr, and that culminated in the (re-)occurrence or at least the stronger growth of CWC, namely *L. pertusa*, at ~7 ka (Table 2, Fig. 3).

In this region, with predominantly northward directed currents, the supply of CWC larvae needed to (re-)establish sites of distinct CWC proliferation most likely has a southward origin. On a larger scale, two possible source areas located upstream from the Cape Lookout site are the Gulf of Mexico (Newton et al., 1987; Schroeder, 2002) and the western South Atlantic area off Brazil (Mangini et al., 2010; Viana et al., 1998). Both regions have been reported to host CWC also under glacial conditions (Mangini et al., 2010; Newton et al., 1987). CWC settings in the Gulf of Mexico are linked to the Gulf Stream region by the Loop Current and some degree of genetic connectivity has been shown between these areas (Morrison et al., 2011); while sites further south might be connected to the Cape Lookout area by the Antarctic Intermediate Waters (AAIW). Henry et al. (2014) recently suggested a southern origin of the subtropical NW Atlantic CWC driven by an increased influence of AAIW supporting a northward transport of larvae from CWC sites off Brazil (see also Mangini et al., 2010). This northward transport might have followed a series of “stepping stones” along the pathway through areas along the Guyana coasts and the Caribbean islands from where CWC have been described (Roberts et al., 2006). Glacial-interglacial changes in the circulation patterns are believed to have affected the extent of AAIW in the North Atlantic. According to Henry et al. (2014), the return of the AAIW to the Straits of Florida at the onset of the Holocene, after its weakening (or even absence) during the last glacial (Came et al., 2008; Xie et al., 2012), led to a regional (re-)colonization by CWC, although this assumption was based on one single *Lophelia* age of 9.5 ka obtained from the Florida-Hatteras slope (van de Flierdt et al., 2010). Whether being a result of re-colonization (from either the southern Atlantic or the Gulf of Mexico) or the re-initiation of mound aggradation, the time difference found between (the first known) CWC occurrences at the Cape Lookout area and at the Florida Strait might have been caused by the local environmental conditions at the Cape Lookout site. To better constrain the environmental drivers behind this apparent re-establishment or re-enforcement of CWC growth at this site at ~7 ka, the local environmental history of the Cape Lookout area from the LGM until the present is discussed.

6.4.1 The Last Glacial Maximum

During the LGM, summer SST and SSS values (the latter indicated as surface $\delta^{18}O_{SW}$ in Figure 3) in the Cape Lookout area were lower than today. When comparing the locally reconstructed temperatures and salinities with the expected LGM summer conditions for the two closest water masses, i.e. the FC and the MAB-SW, it becomes clear that MAB-SW influence over the study site was larger during the LGM than today (Fig. 5). Consequently, the FC (and thus the GS) influence was most likely weakened in the Cape Lookout area during the LGM, which is likely related to a lower sea level. Assuming a sea level drop of ~120 m during the LGM (Waelbroeck et al., 2002), the coastline near Cape Lookout was shifted approximately 60 km offshore of its current location (Fig. 6), which likely resulted in an offshore displacement of the GS. While the studied CWC area is currently located at approximately 75 km from the shore (and under the GS), its distance to the LGM coastline was only ca. 15 km (Fig. 6), hence the site was bathed in local shelf waters. An offshore position of the GS main axis is expected during sea level lowstands caused by a prominent bathymetric high at the Blake Plateau, called the Charleston Bump (Pinet et al., 1981; Pinet and Popenoe, 1985). In a model-based study, Hewitt et al. (2003) also suggested a displacement of the GS position (although to the south) during the last glacial period leading to cooler conditions over the areas where the GS was replaced by a stronger glacial Labrador Current. The cooling is due to the temperature difference found between the GS and MAB-SW, since the GS waters are currently ~10 °C warmer than MAB-SW when compared at the same depth. The average glacial SST observed in this study is too high to consider a complete replacement of the GS by waters with a Labrador-origin (such as the MAB-SW), but a partial or seasonal substitution is corroborated by the lower SST and SSS (Fig. 3). De Vernal et al. (2000) suggested on a dinocyst-based study that the area was subject to a strong seasonal change resulting from a varying influence of the MAB-SW during the year. On one hand, average SST is still warm (at least during summer), as is demonstrated by the local presence of *G. ruber* s.s. itself being a subtropical species (Kucera, 2007). On the other hand, there are reports of iceberg scours in areas south of the study location (Hill et al., 2008) suggesting that icebergs might have been occasionally present at the study site, even though ice-rafted debris was not found in our samples. Nevertheless, an overall greater regional seasonality might have prevailed during the LGM with cooler, fresher waters from the MAB dominating and allowing some influence of the GS during summer.

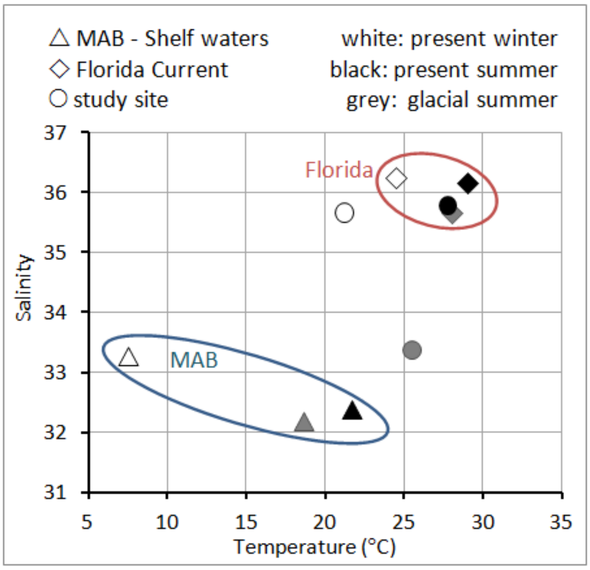

Figure 5. Sea surface Temperature-Salinity (T-S) plot for the Mid-Atlantic Bight shelf waters (MAB-SW) (triangles), the Gulf Stream/Florida current (diamonds), and for the TRACOS2010-75 core location (circles). Included are present-day winter (white) and summer (black) conditions compiled from the World Ocean Atlas (Locarnini et al., 2013; Zweng et al., 2013) and reconstructed LGM summer conditions (grey). The reconstruction presumes decreases in sea surface temperature (SST) and sea surface salinity (SSS) of (i) 3.05°C and 0.2 in the MAB-SW (de Vernal et al., 2000), (ii) 1°C and 0.5 in the Gulf Stream/Florida Current (Shin et al., 2003; Waelbroeck et al., 2009), and (iii) 2.3°C and 2.41 at the TRACOS2010-75 core location (present study).

A change in the location of the GS due to a lowered sea level would imply a similar displacement of the organic carbon production areas presently located over the Cape Lookout CWC area (Bé, 1959; Lee et al., 1991). Although CWC might feed on different food sources, such as fresh phytodetritus (e.g., Duineveld et al., 2007), zooplankton (e.g., Carlier et al., 2009), a combination of both (van Oevelen et al., 2009) or dissolved organic matter (Gori et al., 2014), a reduced/low surface productivity could have prevented the proliferation of CWC in the area. Carbonate content has been suggested by Rühlemann et al. (1999) as a paleoproductivity estimator in low productive areas (such as the western Atlantic margins) and might be related to a decrease in the foraminiferal population and flux. The lower carbonate values observed during the LGM (Fig. 3) corroborate the occurrence of reduced surface productivity, as it was previously suggested by Mix (1989) for the glacial North Atlantic margin.

The comparatively low BWT and lower bottom salinity during the LGM could, similarly, be due to a larger influence of cooler, fresher waters flowing from the north and a seaward displacement of the GS. Although a recent laboratory study by Naumann et al. (2014) showed a 58% reduction in *L. pertusa* calcification rate at 6 °C, the reconstructed glacial BWT values of on average 5.8 °C (Fig. 3) remain within the known temperature range for *L. pertusa* in the North Atlantic (4-12 °C; Roberts et al., 2006). Therefore, the lowered LGM BWT are most likely not the (main) cause hampering coral growth off Cape Lookout during the LGM.

Alternatively, the relatively small grain sizes and very poorly sorted grain size distributions (Figs. 3, 4) suggests the occurrence of weaker and irregular bottom currents during the LGM. A local weakening of the bottom current strength could either be related to a weakening of the GS (as suggested by Lynch-Stieglitz et al., 1999), or could be the result of a smaller influence of the GS at the study site due to its offshore displacement (and local increase of the MAB-SW influence). Weaker bottom currents have been identified as being a major cause for periods of limited CWC proliferation or even the absence of CWC in the Porcupine Seabight area (off Ireland; Dorschel et al., 2005; Eisele et al., 2008; Frank et al., 2009). However, since modal grain size values reported for the western slope of the Porcupine Bank (Øvrebø et al., 2006) were smaller than the ones found for the Cape Lookout CWC area (Table 3 of Supplementary Material), it is not obvious how much these reduced currents would have jeopardized coral growth (or coral mound aggradation) at Cape Lookout.

An additional factor affecting the proliferation of CWC is the concentration of oxygen in the water. Based on a global data set, Davies et al. (2008) and Davies and Guinotte (2011) state that *L. pertusa* can persist with oxygen concentrations as low as 3 ml l^{-1}. Even lower oxygen concentrations of 2.6-3.2 ml l^{-1} in the Gulf of Mexico appear to sustain a thriving CWC community (Schroeder, 2002). And indeed, past variations in oxygen probably reaching below these levels have been identified as the cause for the temporary extinction of CWC in the Ionian Sea (Fink et al., 2012). However, according to the WOA (Garcia et al., 2014), the lowest oxygen concentrations in the water column off Cape Lookout are still above 3.5 ml l^{-1} with the most pronounced minimum in ~750 m water depth, thus, well below the coral mounds. With an assumed lower productivity during the LGM (see above and Mix, 1989), the LGM oxygen concentrations around the coral mounds were most likely not lower then at present and, thus, are probably not hampering coral growth at that time.

Overall, environmental conditions during the LGM point towards an offshore displacement of the GS (at least partially) forced by the lowered sea level effect on the water masses' distribution (Fig. 6). Such a displacement might have affected CWC proliferation (and coral mound aggradation) by lowering BWT, as well as food availability by reducing the surface productivity and weakening the bottom currents. It is likely that one (or most likely a combination) of these factors hampered CWC growth and mound development off Cape Lookout during the LGM.

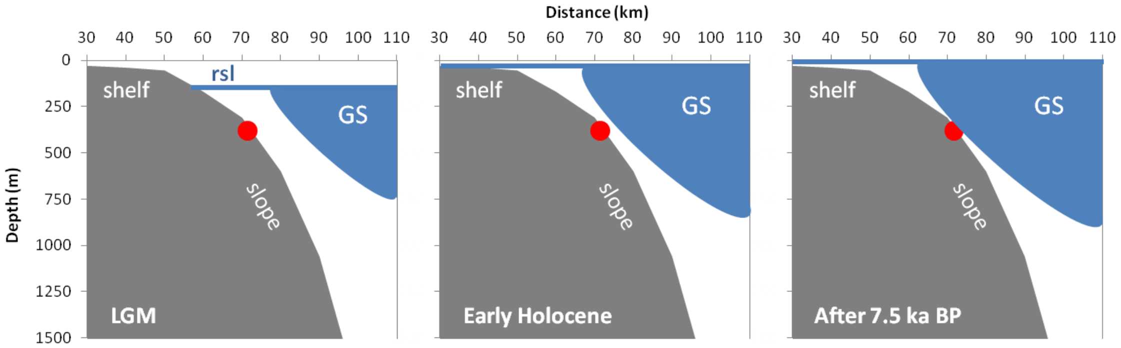

Figure 6. Schematic representation of the North Carolina shelf and slope profile and of the position of the V-shaped Gulf Stream (GS) under different scenarios: (i) last glacial maximum (LGM), (ii) Early Holocene and (iii) the last 7.5 kyr. The red circle represents the Cape Lookout CWC site, rsl is relative sea level. Drawing not to scale.

6.4.2 Deglaciation and Early Holocene

A transitional period between 18.3 and 8.4 cal ka BP is apparent in the data. During this period, while sea level was rising by around 110 m (Waelbroeck et al., 2002), a clear increase in SSS and SST to levels similar to present-day values (Fig. 3) occurred at Cape Lookout CWC area. The increase in SSS and SST was probably due to an increasing influence of GS waters as the current moved coastward and occupied the areas previously influenced by the shelf waters (Fig. 6). This scenario is further corroborated by the concurrent increase in carbonate content, probably reflecting the rather high abundance of foraminifera in GS waters (Bé, 1959). At the onset of the Holocene, the carbonate content was fairly constant (Fig. 3) and within the range of present-day values (Pratt and Heezen, 1964). With reconstructed surface conditions close to present-day observations it seems that during the Early Holocene the coastward-moving GS had already reached the study site. Subsequently, local GS meanders and fronts were likely at play as currently seen, resulting in increased local upwelling (Yoder et al., 1983) and organic carbon production (Lee et al., 1991). As a consequence, the availability of food for the CWC might have been similar to the present.

While the sea surface was already reaching present-day conditions, some differences were still found near the sea floor. During this transitional period the bottom salinity slowly increased while the BWT fluctuated, increasing during the deglacial and returning to glacial-like values in the Early Holocene. Although the overall change in BWT was small and within the known temperature range for *L. pertusa* in the North Atlantic (4-12 °C; Roberts et al., 2006), the values oscillated around the values that may affect *L. pertusa*'s calcification rate (Naumann et al., 2014). This way, it remains uncertain how the lowered BWT have affected CWC growth during the Early Holocene. At the same time an increase in mean grain size (Fig. 3) suggests that bottom currents were enhanced although moderately. Such changes could also be related to an increasing influence of the coastward-moving GS over the region, although the impact felt near the sea floor was limited compared to surface waters.

The environmental conditions off Cape Lookout found for the deglacial period and the Early Holocene suggest a gradual coastward displacement of the GS that provided present-day-like surface conditions, while conditions at the sea floor still differed considerably. This lag might result from the typical V-shape of the GS cross-section (Fig. 6), presently responsible for a ~50 km off-set between the maximum current velocities registered at the ocean surface and at the sea floor (Richardson and Knauss, 1971).

Our data (which did not include deglacial and Early Holocene coral ages) indicate that CWC growth seems to have been largely hampered during this time interval, thus, inhibiting the aggradation of mounds in the Cape Lookout area. Although present-day-like conditions (likely leading to higher food availability) were already present at the surface, the conditions at the sea floor (with moderate bottom currents and/or low BTW) might have been still far from being optimal for pronounced CWC growth.

6.4.3 The Mid- to Late Holocene (<7.5 cal ka BP)

For the last 7.5 cal kyr, surface conditions maintained the trend observed since the beginning of the Holocene and to the present, with high SSS and SST values and constant carbonate content (Fig. 3) indicating a more permanent presence of GS waters. However, conditions at the sea floor changed at 7.5 cal ka BP, with the greatest change being observed in the grain size distributions. The mean grain size increase (reaching over 250 µm on the bulk sediment record; Fig. 3; Table 3 of Supplementary Material) and the shift to better sorted sediments (peaking around modal values of 350 µm; Fig. 4) suggest a considerable enhancement of bottom current strength and sediment winnowing. Enhanced bottom currents, which were previously mentioned to occur during periods of strong coral proliferation (Davies et al., 2009;

Dorschel et al., 2005; Mienis et al., 2007), were recently reported to also occur at the Cape Lookout CWC site (Mienis et al., 2014). The stronger currents (0.3 m s^{-1}) were measured with NNE flow direction and especially in specific episodes (of up to 0.4 m s^{-1}) related to the direct influence of the GS as measured 2 m above the sea floor (Mienis et al., 2014).

After 7.5 cal ka BP, bottom salinity reached maximum values while the BWT recovered from the small decrease observed during the Early Holocene. BWT stabilized around 7 °C (Fig. 3) which is in accordance with current observations at the site (Mienis et al., 2014) and above the temperature values that may affect *L. pertusa*'s calcification rate (Naumann et al., 2014). The Mid-Holocene changes in bottom current strength; bottom salinity and BWT are likely related to an increased influence of the GS at the site. This increase could have resulted from a coastward displacement of the GS triggered by the final ~5 m rise in sea level (Fig. 6), caused by the ultimate demise of the Laurentide ice-sheet between 7.6 and 6.8 cal ka BP (Carlson et al., 2007). The GS influence might have also been intensified as the result of an enhancement of the sub-polar and sub-tropical gyres that occurred during the Mid-Holocene (between 8 and 6.5 cal ka BP) (Cléroux et al., 2012). Similar gyre strengthening has been mentioned for positive North Atlantic Oscillation (NAO+) periods (Curry and McCartney, 2001). Conditions similar to NAO+ periods could cause GS strengthening and/or dislocation of its path more to the north (Taylor and Stephens, 1998; Curry and McCartney, 2001) that would likely increase the GS influence at the study site.

The lag observed between changing surface waters and sea floor conditions is likely related to the previously mentioned V-shape of the GS cross-section (Richardson and Knauss, 1971) that implies that during the coastward displacement of the GS, for a given position (e.g., the Cape Lookout CWC area) the impact of the GS is first felt at the sea surface before it reaches the sea floor (Fig. 6). Cape Lookout CWC appear in the geologic record at ~7 ka, at the end of sea level rise and once the GS influence was maximal, with present-day-like conditions being established both in the surface and at the sea floor. Besides enhanced productivity enabling food availability to CWC, enhanced bottom currents ensured a proper particle (food) delivery, while higher BWT allowed a sustainable calcification rate, for CWC to colonize the area and enable mound growth.

6.5 Conclusions

Cold-water coral colonization and mound development in the Cape Lookout area started during the Mid-Holocene, which appears to be related to the coastward displacement of the

GS. During the last glacial period, the GS was dislocated (approximately 60 km) offshore, and likely more to the south (Hewitt et al., 2003), which was due to ice accumulation at the poles and related to lower sea level stand. While located closer to the glacial coastline, the Cape Lookout CWC area was not under the GS main axis, leading to an increase in MAB-SW influence. During glacial summers, a weakened GS led to a decrease in BWT, organic carbon production and bottom current strength that reduced the corals' calcification rate and the food availability, overall likely hampering CWC proliferation. During the deglacial and Early Holocene sea level rose and water masses gradually transgressed coastward beyond glacial shore limits. The GS coastward displacement brought present-day-like conditions to the surface waters, where increased organic carbon production (and thus food availability) was likely to prevail. However, conditions near the sea floor remained mostly unchanged, since the V-shape of the GS cross-section causes a temporal offset between the occurrence of changes at the surface waters and at the sea floor. Therefore, bottom currents were still too weak and/or BWT too cold to ensure proper conditions for CWC colonization and mound aggradation. After 7.5 cal ka BP (following the last step of sea level rise), the GS finally reached its present location establishing present-day-like conditions at the sea floor (higher BWT and enhanced bottom currents), enabling CWC colonization and the development of sustained populations. Hence, the productivity increase occurring in the area since the onset of the Holocene only had a positive impact on the corals once bottom currents prompted better food supply and the BWT rose above the 6°C. Overall, movements of the GS have been the driver for overcoming the crucial limiting factors for CWC development in the Cape Lookout area.

Apart from being prolific during the Mid- and Late Holocene, CWC were also present off Cape Lookout during the Eemian (MIS 5e). The occurrence of CWC during this period suggests that (at least regionally) Eemian conditions should have been similar to today. Expanding the coral age dataset in this area would be important to further extend our knowledge on their temporal distribution. Moreover, a longer and higher resolution off-mound record would be necessary to better constrain the environmental changes taking place at the study site, especially during MIS5 and the late Holocene.

Acknowledgements

We gratefully acknowledge the assistance of captain, crew and technicians on board the R/V *Cape Hatteras*, whose ship time was provided by the Duke-UNC Oceanographic Consortium (to S.W. Ross), as well as to the captain, crew and technicians on board the R/V *Pelagia*. We further acknowledge C. Monteiro, D. Ferreira, G. Martínez Méndez, J. Titschack, M. Segl, R. Szarek and W. Soares for support during sample preparation and analysis, and A. Völker for helping during data analysis. We thank the CEA, the CNRS and the region SESAME for supporting the MC-ICPMS infrastructure used here for U-series dating. The development of U-series protocol was part of the EU project HERMIONE (grant agreement no. 226354). We acknowledge the help of E. Douville, L. Bordier, and E. Sallé regarding the U-series preparations and MC-ICPMS-measurements. We would like to thank D. van Rooij and two anonymous reviewers for helping improving the manuscript. This paper is a contribution towards the Deutsche Forschungsgemeinschaft DFG-project "Palaeo-WACOM" (HE3412-17). During her time at MARUM, F. Mienis was funded through the DFG-Research Center/Excellence Cluster “The Ocean in the Earth System”. At present F. Mienis is supported financially by the Innovational Research Incentives Scheme of the Netherlands Organisation for Scientific Research (NWO-VENI). L. Matos is supported by Fundação para a Ciência e Tecnologia scholarship SFRH/BD/72149/2010, GLOMAR - the Bremen International Graduate School for Marine Sciences, and CESAM (European Funds through COMPETE and National Funds through PEst-C/MAR/LA0017/2013 - Fundação para a Ciência e Tecnologia). All data presented in this study are available on PANGAEA® (Data Publisher for Earth & Environmental Science doi:10.1594/PANGAEA).

References

Abrantes, F., Lebreiro, S., Rodrigues, T., Gil, I., Bartels-Jónsdóttir, H., Oliveira, P., Kissel, C., Grimalt, J.O., 2005. Shallow-marine sediment cores record climate variability and earthquake activity off Lisbon (Portugal) for the last 2000 years. Quaternary Science Reviews 24, 2477-2494.

Bane, J., Brooks, D., 1979. Gulf Stream meanders along the Continental Margin from the Florida Straits to Cape Hatteras. Geophysical Research Letters 6, 280-282.

Barker, S., Greaves, M., Elderfield, H., 2003. A study of cleaning procedures used for foraminiferal Mg/Ca paleothermometry. Geochemistry, Geophysics, Geosystems 4, 8407.

Baumann, K.-H., Lackschewitz, K.S., Erlenkeuser, H., Henrich, R., Jünger, B., 1993. Late Quaternary calcium carbonate sedimentation and terrigenous input along the east Greenland continental margin. Marine Geology 114, 13-36.

Bé, A.W.H., 1959. Ecology of Recent Planktonic Foraminifera: Part I: Areal Distribution in the Western North Atlantic. Micropaleontology 5, 77-100.

Brooke, S., Ross, S.W., 2014. First observations of the cold-water coral *Lophelia pertusa* in mid-Atlantic canyons of the USA. Deep Sea Research Part II 104, 245-251.

Brooke, S., Ross, S.W., Bane, J.M., Seim, H.E., Young, C.M., 2013. Temperature tolerance of the deep-sea coral Lophelia pertusa from the southeastern United States. Deep Sea Res. Part II Top. Stud. Oceanogr. 92, 240–248.

Brooke, S., Schroeder, W.W., 2007. State of the U.S. deep coral ecosystems in the northern Gulf of Mexico region: Florida Straits to Texas, in: Lumsden, S.E., Hourigan, T.F., Bruckner, A.W. (Eds.), The State of Deep Coral Ecosystems of the United States. NOAA Technical Memorandum CRCP-3, Silver Spring MD, pp. 271-306.

Bumpus, D., 1973. A description of the circulation on the continental shelf of the east coast of the United States. Progress in Oceanography 6, 111-157.

Cairns, S.D., 2007. Deep-water corals: an overview with special reference to diversity and distribution of deep-water scleractinian corals. Bulletin of Marine Science 81, 311-322.

Came, R.E., Oppo, D.W., Curry, W.B., Lynch-Stieglitz, J., 2008. Deglacial variability in the surface return flow of the Atlantic meridional overturning circulation. Paleoceanography 23, PA1217.

Carlier, A., Le Guilloux, E., Olu-Le Roy, K., Sarrazin, J., Mastrototaro, F., Taviani, M., Clavier, J., 2009. Trophic relationships in a deep Mediterranean cold-water coral bank (Santa Maria di Leuca, Ionian Sea). Marine Ecology Progress Series 397, 125-137.

Carlson, A.E., Clark, P.U., Raisbeck, G.M., Brook, E.J., 2007. Rapid Holocene Deglaciation of the Labrador Sector of the Laurentide Ice Sheet. J. Clim. 20, 5126–5133.

Cheng, H., Adkins, J., Edwards, R.L., Boyle, E.A., 2000. U-Th dating of deep-sea corals. Geochimica et Cosmochimica Acta 64, 2401-2416.

Clark, P., Dyke, A., Shakun, J., Carlson, A.E., Clark, J., Wohlfarth, B., Mitrovica, J.X., Hostetler, S.W., McCabe, A.M., 2009. The Last Glacial Maximum. Science 325, 710-714.

Cléroux, C., Cortijo, E., Anand, P., Labeyrie, L., Bassinot, F., Caillon, N., Duplessy, J.-C., 2008. Mg/Ca and Sr/Ca ratios in planktonic foraminifera: Proxies for upper water column temperature reconstruction. Paleoceanography 23, PA3214.

Cléroux, C., Debret, M., Cortijo, E., Duplessy, J.-C., Dewilde, F., Reijmer, J., Massei, N., 2012. High-resolution sea surface reconstructions off Cape Hatteras over the last 10 ka. Paleoceanography 27, PA1205.

Colman, J.G., Gordaon, D.M., Lane, A.P., Forde, M.J., Fitzpatrick, J., 2005. Carbonate mounds off Mauretania, Northwest Africa: status of deep-water corals and implications for management of fishing and oil exploration activities, in: Freiwald, A., Roberts, J.M. (Eds.), Cold-water Corals and Ecosystems. Springer, Heidelberg, pp. 417-441.

Cordes, E.E., McGinley, M.P., Podowski, E.L., Becker, E.L., Lessard-Pilon, S., Viada, S.T., Fisher, C.R., 2008. Coral communities of the deep Gulf of Mexico. Deep Sea Research Part I 55, 777-787.

Correa, T.B.S., Eberli, G.P., HGrasmueck, M., Viggiano, D.A., Reed, J.K., 2007. Coral ridges and buried deep-water coral mounds in the Straits of Florida, Comparative Sedimentology Laboratory Annual Review Meeting. RSMAS, University of Miami, Miami, pp. 39-44.

Curry, R.G., McCartney, M.S., 2001. Ocean Gyre Circulation Changes Associated with the North Atlantic Oscillation. J. Phys. Oceanogr. 31, 3374–3400.

Davies, A.J., Duineveld, G., Lavaleye, M., Bergman, M.J., van Haren, H., Roberts, J.M., 2009. Downwelling and deep-water bottom currents as food supply mechanisms to the cold-water coral *Lophelia pertusa* (Scleractinia) at the Mingulay Reef Complex. Limnology & Oceanography 54, 620-629.

Davies, A.J., Duineveld, G.C.A., van Weering, T.C.E., Mienis, F., Quattrini, A.M., Seim, H.E., Bane, J.M., Ross, S.W., 2010. Short-term environmental variability in cold-water coral habitat at Viosca Knoll, Gulf of Mexico. Deep Sea Research Part I 57, 199-212.

Davies, A.J., Guinotte, J.M., 2011. Global habitat suitability for framework-forming cold-water corals. PLoS One 6, e18483.

Davies, A.J., Wisshak, M., Orr, J.C., Murray Roberts, J., 2008. Predicting suitable habitat for the cold-water coral Lophelia pertusa (Scleractinia). Deep Sea Res. Part I Oceanogr. Res. Pap. 55, 1048–1062

Deuser, W.G., Ross, E.H., Hemleben, C., Spindler, M., 1981. Seasonal changes in species composition, numbers, mass, size, and isotopic composition of planktonic foraminifera settling into the deep Sargasso Sea. Palaeogeogr. Palaeoclimatol. Palaeoecol. 33, 103–127.

de Vernal, A., Hillaire-Marcel, C., Turon, J.-L., Matthiessen, J., 2000. Reconstruction of sea-surface temperature, salinity, and sea-ice cover in the northern North Atlantic during the last glacial maximum based on dinocyst assemblages. Canadian Journal of Earth Sciences 37, 725-750.

Dorschel, B., Hebbeln, D., Foubert, A., White, M., Wheeler, A.J., 2007a. Hydrodynamics and cold-water coral facies distribution related to recent sedimentary processes at Galway Mound west of Ireland. Marine Geology 244, 184-195.

Dorschel, B., Hebbeln, D., Rüggeberg, A., Dullo, W.-C., 2007b. Carbonate budget of a cold-water coral carbonate mound: Propeller Mound, Porcupine Seabight. International Journal of Earth Sciences 96, 73-83.

Dorschel, B., Hebbeln, D., Rüggeberg, A., Dullo, W.-C., 2005. Growth and erosion of a cold-water coral covered carbonate mound in the Northeast Atlantic during the Late Pleistocene and Holocene. Earth and Planetary Science Letters 233, 33-44.

Douville, E., Sallé, E., Frank, N., Eisele, M., Pons-branchu, E., Ayrault, S., 2010. Rapid and accurate Th-U dating on ancient carbonates using Inductivity Coupled Plasma-Quadrupole Mass Spectrometry. Chemical Geology 272, 1-11.

Duineveld, G.C.A., Lavaleye, M.S.S., Bergman, M.J.N., De Stigter, H., Mienis, F., 2007. Trophic structure of a cold-water coral mound community (Rockall Bank, NE Atlantic) in relation to the near-bottom particle supply and current regime. Bulletin of Marine Science 81, 449-467.

Eisele, M., Frank, N., Wienberg, C., Hebbeln, D., López Correa, M., Douville, E., Freiwald, A., 2011. Productivity controlled cold-water coral growth periods during the last glacial off Mauritania. Marine Geology 280, 143-149.

Eisele, M., Hebbeln, D., Wienberg, C., 2008. Growth history of a cold-water coral covered carbonate mound - Galway Mound, Porcupine Seabight, NE-Atlantic. Marine Geology 253, 160-169.

Fink, H.G., Wienberg, C., Hebbeln, D., McGregor, H. V., Schmiedl, G., Taviani, M., Freiwald, A., 2012. Oxygen control on Holocene cold-water coral development in the eastern Mediterranean Sea. Deep Sea Res. Part I Oceanogr. Res. Pap. 62, 89–96.

Folk, R.L., Ward, W.C., 1957. Brazos River Bar: a study in the significance of grain size parameters. J. Sediment. Petrol. 27, 3–26.

Fosså, J.H., Lindberg, B., Christensen, O., Lundälv, T., Svellingen, I., Mortensen, P.B., Alsvag, J., 2005. Mapping of *Lophelia* reefs in Norway: experiences and survey methods, in: Freiwald, A., Roberts, J.M. (Eds.), Cold-water Corals and Ecosystems. Springer, Heidelberg, pp. 359-391.

Fraile, I., Schulz, M., Mulitza, S., Merkel, U., Prange, M., Paul, A., 2009. Modeling the seasonal distribution of planktonic foraminifera during the Last Glacial Maximum. Paleoceanography 24, PA2216.

Frank, N., Freiwald, A., López Correa, M., Wienberg, C., Eisele, M., Hebbeln, D., Van Rooij, D., Henriet, J.P., Colin, C., van Weering, T., de Haas, H., Buhl-Mortensen, P., Roberts, J.M., De Mol, B., Douville, E., Blamart, D., Hatte, C., 2011. Northeastern Atlantic cold-water coral reefs and climate. Geology 39, 743-746.

Frank, N., Paterne, M., Ayliffe, L., van Weering, T.C.E., Henriet, J.-P., Blamart, D., 2004. Eastern North Atlantic deep-sea corals: tracing upper intermediate water $D^{14}C$ during the Holocene. Earth and Planetary Science Letters 219, 297-309.

Frank, N., Ricard, E., Lutringer-Paquet, A., van der Land, C., Colin, C., Blamart, D., Foubert, A., Van Rooij, D., Henriet, J.-P., de Haas, H., van Weering, T., 2009. The Holocene occurrence of cold water corals in the NE Atlantic: Implications for coral carbonate mound evolution. Marine Geology 266, 129-142.

Frederiksen, R., Jensen, A., Westerberg, H., 1992. The distribution of scleratinian coral *Lophelia pertusa* around the Faroe Islands and the relation to intertidal mixing. Sarsia 77, 157-171.

Freiwald, A., Fosså, J.H., Grehan, A., Koslow, T., Roberts, J.M., 2004. Cold-water Coral Reefs. UNEP-WCMC, Cambridge, UK, Biodiversity Series 22.

Garcia, H.E., Locarnini, R.A., Boyer, T.P., Antonov, J.I., Mishonov, A. V., Baranova, O.K., Zweng, M.M., Reagan, J.R., Johnson, D.R., 2013. Volume 3: Dissolved Oxygen, Apparent Oxygen Utilization, and Oxygen Saturation, in: World Ocean Atlas 2013. p. 27.

Gori, A., Grover, R., Orejas, C., Sikorski, S., Ferrier-Pagès, C., 2014. Uptake of dissolved free amino acids by four cold-water coral species from the Mediterranean Sea. Deep Sea Research Part II 99, 42-50.

Gorsline, D., 1963. Bottom Sediments of the Atlantic Shelf and Slope off the Southern United States. The Journal of Geology 71, 422-440.

Grasmueck, M., Eberli, G.P., Viggiano, D.A., Correa, T., Rathwell, G., Luo, J., 2006. Autonomous underwater vehicle (AUV) mapping reveals coral mound distribution, morphology, and oceanography in deep water of the Straits of Florida. Geophysical Research Letters 33, L23616, doi, 10.1029/2006GL027734.

Hebbeln, D., Wienberg, C., Wintersteller, P., Freiwald, A., Becker, M., Beuck, L., Dullo, C., Eberli, G.P., Glogowski, S., Matos, L., Forster, N., Reyes-Bonilla, H., Taviani, M., 2014. Environmental forcing of the Campeche cold-water coral province, southern Gulf of Mexico. Biogeosciences 11, 1799-1815.

Henry, L.-A., Frank, N., Hebbeln, D., Wienberg, C., Robinson, L., de Flierdt, T.v., Dahl, M., Douarin, M., Morrison, C.L., Correa, M.L., Rogers, A.D., Ruckelshausen, M., Roberts, J.M., 2014. Global ocean conveyor lowers extinction risk in the deep sea. Deep Sea Research Part I 88, 8-16.

Hewitt, C.D., Stouffer, R.J., Broccoli, A.J., Mitchell, J.F.B., Valdes, P.J., 2003. The effect of ocean dynamics in a coupled GCM simulation of the Last Glacial Maximum. Climate Dynamics 20, 203-218.

Hill, J.C., Gayes, P.T., Driscoll, N.W., Johnstone, E.A., Sedberry, G.R., 2008. Iceberg scours along the southern U.S. Atlantic margin. Geology 36, 447-450.

Joyce, T., 1985. Gulf Stream warm-core ring collection: An introduction. Journal of Geophysical Research 90, 8801-8802.

Kucera, M., 2007. Proxies in Late Cenozoic Paleoceanography, in: Hillaire-Marcel, C., de Vernal, A. (Eds.), Methods in Late Cenozoic Paleoceanography, Developments in Marine Geology. Elsevier, pp. 213–262.

Lear, C.H., Rosenthal, Y., Slowey, N., 2002. Benthic foraminiferal Mg/Ca-paleothermometry: a revised core-top calibration. Geochimica et Cosmochimica Acta 66, 3375-3387.

Lee, T.N., Yoder, J.A., Atkinson, L.P., 1991. Gulf Stream frontal eddy influence on productivity of the southeast U.S. continental shelf. Journal of Geophysical Research 96, 22191-22205.

Lisiecki, L., Raymo, M., 2005. A Pliocene-Pleistocene stack of 57 globally distributed benthic δ18O records. Paleoceanography 20, PA1003, doi:1010.1029/2004PA001071.

Locarnini, R., Mishonov, A., Antonov, J., Boyer, T., Garcia, H., Baranova, O., Zweng, M., Paver, C., Reagan, J., Johnson, D., Hamilton, M., Seidov, D., 2013. Volume 1: Temperature, in: Levitus, S., Mishonov, A. (Eds.), World Ocean Atlas. NOAA Atlas NESDIS 73, p. 40.

López-Correa, M., Montagna, P., Joseph, N., Rüggeberg, A., Fietzke, J., Flögel, S., Dorschel, B., Goldstein, S.L., Wheeler, A., Freiwald, A., 2012. Preboreal onset of cold-water coral growth beyond the Arctic Circle revealed by coupled radiocarbon and U-series dating and neodymium isotopes. Quaternary Science Reviews 34, 24-43.

Ludwig, K.R., Titterington, D.M., 1994. Calculation of 230Th U isochrons, ages, and errors. Geochimica et Cosmochimica Acta 58, 5031-5042.

Lynch-Stieglitz, J., Curry, W.B., Slowey, N., 1999. Weaker Gulf Stream in the Florida Straits during the Last Glacial Maximum. Nature 402, 644-648.

Mangini, A., Godoy, J.M., Godoy, M.L., Kowsmann, R., Santos, G.M., Ruckelshausen, M., Schroeder-Ritzrau, A., Wacker, L., 2010. Deep sea corals off Brazil verify a poorly ventilated

Southern Pacific Ocean during H2, H1 and the Younger Dryas. Earth and Planetary Science Letters 293, 269-276.

Manning, J., 1991. Middle Atlantic Bight salinity: interannual variability. Continental Shelf Research 11, 123-137.

Messing, C.G., Reed, J.K., Brooke, S.D., Ross, S.W., 2008. Deep-Water Coral Reefs of the United States, in: Riegl, B., Dodge, R.E. (Eds.), Coral Reefs of the USA. Springer, pp. 763-787.

Mienis, F., de Stigter, H.C., White, M., Duineveld, G., de Haas, H., van Weering, T.C.E., 2007. Hydrodynamic controls on cold-water coral growth and carbonate-mound development at the SW and SE Rockall Trough Margin, NE Atlantic Ocean. Deep Sea Research Part I 54, 1655-1674.

Mienis, F., Duineveld, G.C.A., Davies, A.J., Lavaleye, M.M.S., Ross, S.W., Seim, H., Bane, J., van Haren, H., Bergman, M.J.N., de Haas, H., Brooke, S., van Weering, T.C.E., 2014. Cold-water coral growth under extreme environmental conditions, the Cape Lookout area, NW Atlantic. Biogeosciences 11, 2543-2560.

Mix, A.C., 1989. Influence of productivity variations on long-term atmospheric CO2. Nature 337, 541–544.

Morrison, C.L., Ross, S.W., Nizinski, M.S., Brooke, S., Järnegren, J., Waller, R.G., Johnson, R.L., King, T.L., 2011. Genetic discontinuity among regional populations of *Lophelia pertusa* in the North Atlantic Ocean. Conservation Genetics 12: 713-729.

Mountain, D., 2003. Variability in the properties of Shelf Water in the Middle Atlantic Bight, 1977–1999. Journal of Geophysical Research 108, 3014.

Murray, J.W., 2008. Ecology and applications of benthic foraminifera. Cambridge University Press.

Naumann, M.S., Orejas, C., Ferrier-Pagès, C., 2014. Species-specific physiological response by the cold-water corals *Lophelia pertusa* and *Madrepora oculata* to variations within their natural temperature range. Deep Sea Research Part II 99, 36-41.

Newton, C.R., Mullins, H.T., Gardulski, A.F., 1987. Coral mounds on the West Florida Slope: unanswered questions regarding the development of deepwater banks. Palaois 2, 359-367.

Øvrebø, L.K., Haughton, P.D.W., Shannon, P.M., 2006. A record of fluctuating bottom currents on the slopes west of the Porcupine Bank, offshore Ireland — implications for Late Quaternary climate forcing. Marine Geology 225, 279-309.

Partyka, M.L., Ross, S.W., Quattrini, A.M., Sedberry, G.R., Birdsong, T.W., Potter, J., Gottfried, S., 2007. Southeastern United States Deep-Sea Corals (SEADESC) Initiative: A Collaborative Effort to Characterize Areas of Habitat-Forming Deep-Sea Corals, NOAA Technical Memorandum OAR OER 1. Silver Spring, MD, p. 176.

Paull, C.K., Neumann, A.C., am Ende, B.A., Ussler III, W., Rodriguez, N.M., 2000. Lithoherms on the Florida–Hatteras slope. Marine Geology 166, 83–101.

Pinet, P.R., Popenoe, P., Nelligan, D.F., 1981. Gulf Stream: Reconstruction of Cenozoic flow patterns over the Blake Plateau. Geology 9, 266–270.

Pinet, P.R., Popenoe, P., 1985. Shallow seismic stratigraphy and post-Albian geologic history of the northern and central Blake Plateau. Geological Society of America Bulletin 96, 627-638.

Pratt, R., Heezen, B., 1964. Topography of the Blake Plateau. Deep Sea Research 11, 721-728.

Raddatz, J., Rüggeberg, A., Liebetrau, V., Foubert, A., Hathorne, E.C., Fietzke, J., Eisenhauer, A., Dullo, W.-C., 2014. Environmental boundary conditions of cold-water coral mound growth over the last 3 million years in the Porcupine Seabight, Northeast Atlantic. Deep Sea Research Part II 99, 227-236.

Reed, J.K., 2002. Comparison of deep-water coral reefs and lithoherms off southeastern USA. Hydrobiologica 471, 57-60.

Reimer, P.J., Bard, E., Bayliss, A., Beck, J.W., Blackwell, P.G., Bronk Ramsey, C., Buck, C.E., Cheng, H., Edwards, R.L., Friedrich, M., Grootes, P.M., Guilderson, T.P., Haflidason, H., Hajdas, I., Hatté, C., Heaton, T.J., Hoffmann, D.L., Hogg, A.G., Hughen, K.A., Kaiser, K.F., Kromer, B., Manning, S.W., Niu, M., Reimer, R.W., Richards, D.A., Scott, E.M., Southon, J.R., Staff, R.A., Turney, C.S.M., van der Plicht, J., 2013. IntCal13 and Marine13 Radiocarbon Age Calibration Curves 0–50,000 Years cal BP. Radiocarbon 55, 1869-1887.

Richardson, P., 1977. On the crossover between the Gulf Stream and the Western Boundary Undercurrent. Deep Sea Research 24, 139-159.

Richardson, P., 2001. Florida Current, Gulf Stream, and Labradro Current, in: Steele, J., Turekian, K., Thorpe, S. (Eds.), Encyclopedia of Ocean Sciences. Elsevier, pp. 1054-1064.

Richardson, P., Knauss, J., 1971. Gulf Stream and Western Boundary Undercurrent observations at Cape Hatteras. Deep Sea Research 18, 1089-1109.

Roberts, J.M., Wheeler, A.J., Freiwald, A., 2006. Reefs of the Deep: The Biology and Geology of Cold-Water Coral Ecosystems. Science 312, 543-547.

Roberts, J.M., Wheeler, A.J., Freiwald, A., Cairns, S.D., 2009. Cold-water corals. The biology and geology of deep-sea coral habitats. Cambridge University Press.

Rosenthal, Y., Boyle, E.A., Slowey, N., 1997. Temperature control on the incorporation of magnesium, strontium, fluorine, and cadmium into benthic foraminiferal shells from Little Bahama Bank: Prospects for thermocline paleoceanography. Geochimica et Cosmochimica Acta 61, 3633-3643.

Ross, S.W., Nizinski, M.S., 2007. State of the U.S. deep coral ecosystems in the southeastern United States region: Cape Hatteras to the Florida Straits, in: Lumsden, S.E., Hourigan, T.F., Bruckner, A.W. (Eds.), The State of Deep Coral Ecosystems of the United States. NOAA Technical Memorandum CRCP-3, Silver Spring MD, pp. 233-270.

Ross, S.W., Quattrini, A.M., 2007. The fish fauna associated with deep coral banks off the southeastern United States. Deep-Sea Research Part I 54, 975-1007.

Ross, S.W., Quattrini, A.M., 2009. Deep-sea reef fish assemblage patterns on the Blake Plateau (Western North Atlantic Ocean). Marine Ecology 30, 74-92.

Rowe, G., Menzies, R., 1968. Deep bottom currents off the coast of North Carolina. Deep Sea Research 15, 711-719.

Ruhlemann, C., Muller, P.J., Schneider, R.R., 1999. Organic Carbon and Carbonate as Paleoproductivity Proxies: Examples from High and Low Productivity Areas of the Tropical Atlantic, in: Fischer, G., Wefer, G. (Eds.), Use of Proxies in Paleoceanography: Examples from the South Atlantic. pp. 315–344.

Savidge, D., 2002. Wintertime shoreward near-surface currents south of Cape Hatteras. Journal of Geophysical Research 107, 3205.

Schlitzer, R., 2012. Ocean Data View, http://odv.awi.de.

Schroeder, W.W., 2002. Observations of Lophelia pertusa and the surficial geology at a deep-water site in the northeastern Gulf of Mexico. Hydrobiologia 471, 29–33.

Shackleton, N.J., 1974. Attainment of isotopic equilibrium between ocean water and the benthonic foraminifera Genus Uvigerina: Isotopic changes in the ocean during the last glacial. Colloques Internationaux du C.N.R.S - Variation du climat au cours du Pléistocène 219, 203-209.

Shin, S.-I., Liu, Z., Otto-Bliesner, B., Brady, E., Kutzbach, J., Harrison, S., 2003. A Simulation of the Last Glacial Maximum climate using the NCAR-CCSM. Climate Dynamics 20, 127-151.

Stefánsson, U., Atkinson, L.P., Bumpus, D.F., 1971. Hydrographic properties and circulation of the North Carolina shelf and slope waters. Deep Sea Research and Oceanographic Abstracts 18, 383-420.

Stuiver, M., Reimer, P.J., 1993. Extended 14C database and revised CALIB radiocarbon calibration program. Radiocarbon 35, 215-230.

Sulak, K.J., 2008. Origins, age, and structure of reefs and biotopes, in: Sulak, K.J., Randall, M.T., Luke, K.E., Norem, A.D., Miller, J.M. (Eds.), Characterization of Northern Gulf of Mexico Deepwater Hard Bottom Communities with Emphasis on *Lophelia* Coral - *Lophelia* Reef Megafaunal Community Structure, Biotopes, Genetics, Microbial Ecology, and Geology. USGS Open-File Report 2008-1148; OCS Study MMS 2008-015, 15 April 2008.

Taviani, M., Bouchet, P., Metivier, B., Fontugne, M., Delibris, G., 1991. Intermediate steps of southwards faunal shifts testified by last glacial submerged thanatocoenoses in the Atlantic Ocean. Paleoceanography, Palaeoclimatology, Palaeoecology 86, 331-338.

Taylor, A.H., Stephens, J.A., 1998. The North Atlantic Oscillation and the latitude of the Gulf Stream. Tellus 50A, 134–142.

The Ring Group, 1981. Gulf Stream Cold-Core Rings: Their Physics, Chemistry, and Biology. Science 212, 1091-1100.

van de Flierdt, T., Robinson, L.F., Adkins, J.F., 2010. Deep-sea coral aragonite as a recorder for the neodymium isotopic composition of seawater. Geochimica et Cosmochimica Acta 74, 6014-6023.

van der Land, C., Eisele, M., Mienis, F., de Haas, H., Hebbeln, D., Reijmer, J.J.G., van Weering, T.C.E., 2014. Carbonate mound development in contrasting settings on the Irish margin. Deep Sea Research Part II 99, 297-306.

van Morkhoven, F.P.C.M., Berggren, W.A., Edwards, A.S., 1986. Cenozoic cosmopolitan deep-water benthic foraminifera. Bulletin des centres de recherches Exploration-production Elf-Aquitaine Mem. 11, 68-70.

van Oevelen, D., Duineveld, G., Lavaleye, M., Mienis, F., Soetaert, K., Heip, C.H.R., 2009. The cold-water coral community as a hot spot for carbon cycling on continental margins: A food-web analysis from Rockall Bank (northeast Atlantic). Limnology & Oceanography 54, 1829-1844.

Viana, A.R., Faugères, J.C., Kowsmann, R.O., Lima, J.A.M., Caddah, L.F.G., Rizzo, J.G., 1998. Hydrology, morphology and sedimentology of the Campos continental margin, offshore Brazil. Sedimentary Geology 115, 133-157.

Waelbroeck, C., Labeyrie, L., Michel, E., Duplessy, J.C., McManus, J.F., Lambeck, K., Balbon, E., Labracherie, M., 2002. Sea-level and deep water temperature changes derived from benthic foraminifera isotopic records. Quaternary Science Reviews 21, 295-305.

Waelbroeck, C., Paul, A., Kucera, M., Rosell-Melé, A., Weinelt, M., Schneider, R., Mix, a.C., Abelmann, A., Armand, L., Bard, E., Barker, S., Barrows, T.T., Benway, H., Cacho, I., Chen, M.-T., Cortijo, E., Crosta, X., de Vernal, A., Dokken, T., Duprat, J., Elderfield, H., Eynaud, F., Gersonde, R., Hayes, A., Henry, M., Hillaire-Marcel, C., Huang, C.-C., Jansen, E., Juggins, S., Kallel, N., Kiefer, T., Kienast, M., Labeyrie, L., Leclaire, H., Londeix, L., Mangin, S., Matthiessen, J., Marret, F., Meland, M., Morey, a.E., Mulitza, S., Pflaumann, U., Pisias, N.G., Radi, T., Rochon, A., Rohling, E.J., Sbaffi, L., Schäfer-Neth, C., Solignac, S., Spero, H., Tachikawa, K., Turon, J.-L., 2009. Constraints on the magnitude and patterns of ocean cooling at the Last Glacial Maximum. Nature Geocience 2, 127-132.

Wheeler, A.J., Beyer, A., Freiwald, A., de Haas, H., Huvenne, V.A.I., Kozachenko, M., Olu-Le Roy, K., Opderbecke, J., 2007. Morphology and environment of cold-water coral carbonate mounds on the NW European margin. International Journal of Earth Sciences 96, 37-56.

White, M., Mohn, C., de Stigter, H., Mottram, G., 2005. Deep-water coral development as a function of hydrodynamics and surface productivity around the submarine banks of the Rockall Trough, NE Atlantic, in: Freiwald, A., Roberts, J.M. (Eds.), Cold-water Corals and Ecosystems. Springer, Heidelberg, pp. 503-514.

Wienberg, C., Frank, N., Mertens, K.N., Stuut, J.-B., Marchant, M., Fietzke, J., Mienis, F., Hebbeln, D., 2010. Glacial cold-water coral growth in the Gulf of Cádiz: Implications of increased palaeo-productivity. Earth and Planetary Science Letters 298, 405-416.

Wienberg, C., Hebbeln, D., Fink, H.G., Mienis, F., Dorschel, B., Vertino, A., Lopez Correa, M., Freiwald, A., 2009. Scleractinian cold-water corals in the Gulf of Cadiz-First clues about their spatial and temporal distribution. Deep-Sea Research Part I 56, 1873-1893.

Xie, R.C., Marcantonio, F., Schmidt, M.W., 2012. Deglacial variability of Antarctic Intermediate Water penetration into the North Atlantic from authigenic neodymium isotope ratios. Paleoceanography 27, PA3221.

Yoder, J.A., Atkinson, L.P., Stephen Bishop, S., Hofmann, E.E., Lee, T.N., 1983. Effect of upwelling on phytoplankton productivity of the outer southeastern United States continental shelf. Continental Shelf Research 1, 385-404.

Zweng, M., Reagan, J., Antonov, J., Locarnini, R., Mishonov, A., Boyer, T., Garcia, H., Baranova, O., Johnson, D., Seidov, D., Biddle, M., 2013. Volume 2: Salinity, in: Levitus, S., Mishonov, A. (Eds.), World Ocean Atlas. NOAA Atlas NESDIS 73, p. 39.

Supplementary Material

Supplementary Table 1. TRACOS2010-75 off-mound core age model and isotope and Mg/Ca results for the benthic species *Cibicides pachyderma* and the planktic species *Globigerinoides ruber* sensu stricto (white variety).

			Benthic				**Planktic**			
Core	**Depth cm**	**Age cal ka BP**	**δ18O ‰ PDB**	**Mg/Ca mmol/mol**	**Temp. (°C) (Lear et al. 2002)**	**seawater ice-corr. δ18O**	**δ18O ‰ PDB**	**Mg/Ca mmol/mol**	**Temp. (°C) (Cléroux et al. 2008)**	**seawater ice-corr. δ18O**
TRACOS-75	0.5-1	0.688	3.854	1.820	6.80	1.682	-0.315	5.011	26.94	2.139
TRACOS-75	2.5-3	3.440	3.793	1.941	7.39	1.763	-0.593	6.368	30.37	2.552
TRACOS-75	5-6	**6.880**[a]	3.662	1.821	6.81	1.451	-0.429	5.495	28.26	2.256
TRACOS-75	7-8	7.469	3.751	1.889	7.14	1.585	-0.549	6.743	31.18	2.688
TRACOS-75	10-11	8.353	3.725	2.014	**7.73**[b]	**1.708**[b]	-0.249	5.591	28.51	2.445
TRACOS-75	12-13	8.942	3.820	1.756	6.47	1.357	-0.303	6.573	30.82	2.737
TRACOS-75	15-16	9.826	3.757	1.674	6.04	1.182	-0.390	5.398	28.01	2.078
TRACOS-75	17-18	10.415	3.805	1.726	6.32	1.128	-0.241	6.129	29.82	2.422
TRACOS-75	20-21	11.298	3.745	1.604	5.65	0.893	-0.398	6.003	29.52	2.205
TRACOS-75	22.5-23.5	12.035	3.880	1.955	7.46	1.306	-0.412	6.687	31.07	2.313
TRACOS-75	25-26	**12.771**[a]	3.657	1.832	6.86	0.931	-0.342	5.498	28.27	1.815
TRACOS-75	28-29	16.110	3.814	1.753	6.46	0.663	0.002	5.979	**29.47**[b]	**2.083**[b]
TRACOS-75	30-31	18.337	3.850	1.610	5.68	0.370	-0.215	4.606	25.74	0.971
TRACOS-75	32.5-33.5	21.120	3.903	1.686	6.10	0.529	0.202	4.693	26.01	1.439
TRACOS-75	35-36	23.903	3.798	1.583	5.52	0.338	-0.172	3.936	23.49	0.597
TRACOS-75	37.5-38.5	26.685	3.898	1.682	6.08	0.640	-0.035	4.975	26.84	1.498
TRACOS-75	40-41	29.468	3.719	1.786	6.63	0.757	0.140	4.235	24.54	1.344
TRACOS-75	42.5-43.5	32.251	3.868	1.765	6.52	0.959	-0.013	5.557	28.42	2.081
TRACOS-75	45-46	**35.034**[a]	3.790	2.025	7.78	1.185	-0.242	5.935	29.36	2.025
TRACOS-75	47.5-48.5	37.817	3.762	1.791	6.65	0.987	-0.066	4.932	26.72	1.775
TRACOS-75	49-50	39.487	3.827	1.833	6.87	1.146	0.101	5.561	28.43	2.335

a) ^{14}C dating of mixed planktic forminifera species. b) Outliers; excluded values.

Supplementary Table 2. TRACOS2010-75 off-mound core LECO analyses results, including carbonate ($CaCO_3$) content.

Core	Depth (cm)	Age (cal ka BP)	C total (LECO) weight%	H total (LECO) weight%	N total (LECO) weight%	C inorg. (400º/3h) weight%	N inorg. (400º/3h) weight%	%$CaCO_3$ (Cinorgx8.332) weight%
TRACOS-75	1-1.5	1.376	7.346	3.996	0.066	6.495	0.010	54.11
TRACOS-75	3-4	4.128	7.515	3.996	0.072	6.612	0.011	55.09
TRACOS-75	5-6	6.880	7.275	3.826	0.058	6.410	0.008	53.41
TRACOS-75	7-8	7.469	7.619	3.992	0.069	6.618	0.011	55.14
TRACOS-75	10-11	8.353	7.753	4.078	0.094	6.482	0.012	54.01
TRACOS-75	15-16	9.826	7.672	4.034	0.093	6.437	0.009	53.63
TRACOS-75	22.5-23.5	12.035	7.835	4.175	0.106	6.292	0.011	52.42
TRACOS-75	28-29	16.110	7.665	4.159	0.164	5.129	0.017	42.73
TRACOS-75	32.5-33.5	21.120	6.590	3.549	0.121	4.650	0.019	38.74
TRACOS-75	37.5-38.5	26.685	6.257	3.387	0.123	4.450	0.017	37.07
TRACOS-75	42.5-43.5	32.251	5.933	3.146	0.089	4.408	0.014	36.73

Supplementary Table 3. TRACOS2010-75 off-mound core grain size results for the bulk sample and terrigenous fraction.

Core	Depth (cm)	Sediment	Age (cal ka BP)	Mean (µm)	Median (µm)	Sorting (st.dev.)	Mode (µm)
TRACOS-75	1-1.5	Bulk	1.376	210	296	3.84	356
TRACOS-75	3-4	Bulk	4.128	224	283	3.03	356
TRACOS-75	5-6	Bulk	6.880	245	299	2.87	356
TRACOS-75	7-8	Bulk	7.469	174	234	3.65	324
TRACOS-75	10-11	Bulk	8.353	44	63	5.58	96
TRACOS-75	15-16	Bulk	9.826	80	117	5.33	324
TRACOS-75	22.5-23.5	Bulk	12.035	54	69	5.46	88
TRACOS-75	28-29	Bulk	16.110	17	20	4.34	32
TRACOS-75	32.5-33.5	Bulk	21.120	28	35	4.85	80
TRACOS-75	37.5-38.5	Bulk	26.685	18	22	4.90	29
TRACOS-75	42.5-43.5	Bulk	32.251	37	52	4.81	106
TRACOS-75	1-1.5	Terrigenous	1.376	169	199	2.52	245
TRACOS-75	3-4	Terrigenous	4.128	169	201	2.56	245
TRACOS-75	5-6	Terrigenous	6.880	197	231	2.48	269
TRACOS-75	7-8	Terrigenous	7.469	128	162	3.43	245
TRACOS-75	10-11	Terrigenous	8.353	106	119	3.52	128
TRACOS-75	15-16	Terrigenous	9.826	120	148	4.05	269
TRACOS-75	22.5-23.5	Terrigenous	12.035	116	151	4.14	296
TRACOS-75	28-29	Terrigenous	16.110	14	16	4.22	46
TRACOS-75	32.5-33.5	Terrigenous	21.120	29	38	5.64	96
TRACOS-75	37.5-38.5	Terrigenous	26.685	20	23	4.83	50
TRACOS-75	42.5-43.5	Terrigenous	32.251	31	47	4.78	106

7 Conclusion and Outlook

7.1 Final Remarks

This study, presenting the first results concerning the long-term development of CWC and coral mounds in the NW Atlantic, was performed in two areas: the Campeche CWC Province, in the southern Gulf of Mexico, and the Cape Lookout CWC area, off North Carolina. It concerned both the identification of the periods of CWC occurrence and sustained coral mound growth, as well as the definition of the environmental factors influencing their development. Based on the CWC record obtained for the last 260 kyr, it is evident that pronounced coral mound growth at both areas appears to be restricted to interglacial periods. At the Campeche CWC area, coral mound growth is currently favored by the increased food availability caused by the local density gradient between the AAIW and the overlying TACW, occurring at the depth level of the coral mounds. The occurrence of CWC at this site is concurrent with the presence of this density gradient that is linked to a comparably strong northward advection of AAIW. On the other hand, coral mound growth at the Cape Lookout CWC area, is steered by the Gulf Stream presence, which not only causes a local productivity increase, but most importantly, enhances bottom currents prompting food supply to the CWC. Despite the slight difference found in the environmental conditions triggering CWC mound development at each of the study sites, the final impact on the CWC populations is similar. In both cases, changes in the vertical water mass distribution led to enhanced hydrodynamics that increased the food supply for CWC. Comparable settings have been suggested for CWC mound areas in the northern NE Atlantic, such as off Norway (Rüggeberg et al., 2011) and off Ireland (De Mol et al., 2002; Mienis et al., 2009; Raddatz et al., 2014; White, 2007), where the oceanographic conditions (like the presence of pycnoclines or tidal and internal waves) enhance food supply for CWC. From the available studies it appears that (i) when physico-chemical constrains (such as temperature, oxygen, pH, density and aragonite saturation) are met and food availability and supply is sufficiently high, CWC can grow and (ii) when at the same time a proper sediment input is provided (enabling CWC framework stabilization) coral mounds develop. In high productivity settings, such as the actual conditions at the Viosca Knoll (Mienis et al., 2012) or the glacial conditions off Mauritania (Eisele et al., 2011) and in the southern Gulf of Cadiz (Wienberg et al., 2010), the high food availability might sustain coral mound development without the need for additional mechanisms. Otherwise, in settings of lower food availability, CWC seem to further depend on the occurrence of hydrodynamic mechanisms amplifying the food supply (nepheloid layers, tidal or internal waves, enhanced currents, etc).

The temporal occurrence of CWC in the studied areas in the NW Atlantic presents a climate-dependent pattern, related to glacial-interglacial changes of the intermediate-depth circulation. On one hand, changes on the AAIW distribution are believed to occur on a glacial-interglacial scale, with increased advection of southern sourced intermediate waters during interglacial periods (Curry and Oppo, 2005). On the other hand, the Gulf Stream strength and path has been suggested to be affected by the glacial-interglacial cycles, with a glacial reduction on the current strength of up to one third (Lynch-Stieglitz et al., 1999), associated with a southward displacement of the current path (Hewitt et al., 2003). However, these two areas may not fully represent the temporal occurrence pattern of the NW Atlantic CWC. The few glacial ages obtained from CWC mound areas of the NE Gulf of Mexico (Newton et al., 1987; Sulak, 2008) and of the East Florida Strait (Neumann et al., 1977; Paull et al., 2000) suggest that the occurrence pattern of CWC in the NW Atlantic does not follow a *purely* glacial-interglacial pattern. Unpublished CWC data (ages and neodymium isotopic signatures) from the East Florida Strait (off Bimini Islands) corroborate this idea by showing that CWC have been intermittently present in this area for the last 65 kyr. This data set additionally suggests that, for the last 48 kyr, CWC occurrence is also concurrent with changes in the AAIW entrainment (as seen off Campeche), which in the area off Bimini exhibits millennial-scale variability during the last glacial period. The East Florida Strait is located downstream from the Campeche CWC province and has a similar water mass distribution, thus it remains unclear why the two areas show different temporal patterns of CWC occurrence. Nevertheless, it is suggested that the occurrence pattern of NW Atlantic CWC appears to follow the climate-induced changes of the intermediate-depth circulation, which might also be occurring at timescales shorter than glacial-interglacial cycles.

7.2 Outlook

While allowing for an initial assessment of the long-term development of CWC in coral mounds areas of the NW Atlantic, this study has additionally raised further questions, presented below:

a) *Is there a general temporal pattern of CWC occurrence in the NW Atlantic when including the remaining (unstudied) coral mound areas? Why are there differences in the CWC occurrence pattern of the various mound areas?*

CWC mound areas are subject to not only regional (basin wide) conditions but also to more local conditions (i.e. within the mound area or province) which may differ between the various NW Atlantic mound areas. Therefore, the existence of similar regional conditions (such as similar hydrographic settings and namely the presence of the AAIW) does not guarantee that the CWC occurrence pattern of such areas will resemble. The apparent existence of different occurrence patterns between the Campeche and Cape Lookout CWC areas (investigated in this study) and the CWC areas of the NE Gulf of Mexico and East Florida Strait might be an example of the effect of different local conditions. A broader investigation, including (at least some of) the remaining coral mound areas (e.g. Viosca Knoll, West Florida Slope, East Florida Strait) will elucidate the possible differences in the CWC occurrence pattern of the various NW Atlantic mound areas, as well as the environmental conditions affecting each specific area. Only with this wider knowledge, we will be able to evaluate the existence of a general pattern of CWC occurrence in mound areas of the NW Atlantic.

b) *Do other CWC areas located in the pathway of the AAIW respond to the climate-related variability of this water mass?*

The AAIW was found to be the main driver behind CWC occurrence at the Campeche CWC province, as it also seems to be the case in the coral mound area off Bimini (unpublished data). The AAIW is an important intermediate water mass in the West Atlantic, which is traceable as far north as 35 °N within the Gulf Stream and south of 25 °N within the subtropical gyre; (Lambelet et al., 2016; Richardson, 1977) and, thus, hydrological conditions similar to the ones found at the Campeche CWC province may also affect other coral mound areas. For example, the CWC mound areas off Brazil (where *L. pertusa* has occurred for the last 29.3 kyr; Mangini et al. 2010; Henry et al. 2014) are currently located at the upper boundary of the AAIW (Viana et al., 1998). However, the past environmental conditions are not well understood (e.g. Ruckelshausen, 2013) and the relationship between coral vitality and the presence of the AAIW along the Brazilian margin remains unclear. It would be interesting to investigate if the temporal occurrence pattern of CWC at other coral mound areas located within the AAIW area of influence is also being steered by the AAIW variability as hypothesized by Henry et al.

(2014). Furthermore, the past variability of the AAIW is poorly constrained both in terms of its latitudinal extent as in its depth of occurrence (e.g. Huang et al., 2014; Pahnke et al., 2008; Xie et al., 2012). A better understanding of the glacial-interglacial and millennial-scale variability of the AAIW is crucial to improve our understanding of the long-term CWC development in the NW Atlantic, especially in areas where CWC occur in association with this water mass.

To overcome these newly raised questions future investigations of the unstudied NW Atlantic CWC mound areas should follow a multidisciplinary approach to determine the periods favorable for CWC growth and coral mound development paired with the reconstruction of past environmental conditions. These should include dating techniques that cover several glacial-interglacial cycles (such as the U-series dating). Such studies will allow a comparison between the several NW Atlantic CWC mound areas not only concerning the temporal pattern of CWC occurrence but also regarding the identification of their main environmental drivers. Factors such as food availability, dissolved oxygen, bottom current strength or temperature, which have been revealed as of utmost importance in previous studies, should be addressed together with the investigation of the intermediate circulation variability (using for example $\delta^{13}C$ or εNd as water mass tracers). Only with a better geographical representation we will be able to understand the regional pattern of coral mound development within the NW Atlantic and its possible connection to the intermediate-depth circulation.

References

Curry, W.B., Oppo, D.W., 2005. Glacial water mass geometry and the distribution of (delta)13C of (Sigma)CO2 in the western Atlantic Ocean. Paleoceanography 20, 1–12. doi:10.1029/2004PA001021

De Mol, B., Van Rensbergen, P., Pillen, S., Van Herreweghe, K., Van Rooij, D., McDonnell, a, Huvenne, V., Ivanov, M., Swennen, R., Henriet, J.., 2002. Large deep-water coral banks in the Porcupine Basin, southwest of Ireland. Mar. Geol. 188, 193–231. doi:10.1016/S0025-3227(02)00281-5

Eisele, M., Frank, N., Wienberg, C., Hebbeln, D., López Correa, M., Douville, E., Freiwald, A., 2011. Productivity controlled cold-water coral growth periods during the last glacial off Mauritania. Mar. Geol. 280, 143–149. doi:10.1016/j.margeo.2010.12.007

Henry, L.-A., Frank, N., Hebbeln, D., Wienberg, C., Robinson, L., de Flierdt, T. Van, Dahl, M., Douarin, M., Morrison, C.L., Correa, M.L., Rogers, A.D., Ruckelshausen, M., Roberts, J.M., 2014. Global ocean conveyor lowers extinction risk in the deep sea. Deep Sea Res. Part I Oceanogr. Res. Pap. 88, 8–16. doi:10.1016/j.dsr.2014.03.004

Hewitt, C.D., Stouffer, R.J., Broccoli, A.J., Mitchell, J.F.B., Valdes, P.J., 2003. The effect of ocean dynamics in a coupled GCM simulation of the Last Glacial Maximum. Clim. Dyn. 20, 203–218. doi:10.1007/s00382-002-0272-6

Huang, K.-F., Oppo, D.W., Curry, W.B., 2014. Decreased influence of Antarctic intermediate water in the tropical Atlantic during North Atlantic cold events. Earth Planet. Sci. Lett. 389, 200–208. doi:10.1016/j.epsl.2013.12.037

Lambelet, M., van de Flierdt, T., Crocket, K., Rehkämper, M., Kreissig, K., Coles, B., Rijkenberg, M.J.A., Gerringa, L.J.A., de Baar, H.J.W., Steinfeldt, R., 2016. Neodymium isotopic composition and concentration in the western North Atlantic Ocean: Results from the GEOTRACES GA02 section. Geochim. Cosmochim. Acta 177, 1–29. doi:10.1016/j.gca.2015.12.019

Lynch-Stieglitz, J., Curry, W.B., Slowey, N., 1999. Weaker Gulf Stream in the Florida Straits during the Last Glacial Maximum 402, 644–648. doi:10.1038/45204

Mangini, A., Godoy, J.M., Godoy, M.L., Kowsmann, R., Santos, G.M., Ruckelshausen, M., Schroeder-Ritzrau, A., Wacker, L., 2010. Deep sea corals off Brazil verify a poorly ventilated Southern Pacific Ocean during H2, H1 and the Younger Dryas. Earth Planet. Sci. Lett. 293, 269–276. doi:10.1016/j.epsl.2010.02.041

Mienis, F., Duineveld, G.C.A., Davies, A.J., Ross, S.W., Seim, H., Bane, J., van Weering, T.C.E., 2012. The influence of near-bed hydrodynamic conditions on cold-water corals in the Viosca Knoll area, Gulf of Mexico. Deep. Res. Part I Oceanogr. Res. Pap. 60, 32–45. doi:10.1016/j.dsr.2011.10.007

Mienis, F., van der Land, C., de Stigter, H.C., van de Vorstenbosch, M., de Haas, H., Richter, T., van Weering, T.C.E., 2009. Sediment accumulation on a cold-water carbonate mound at the Southwest Rockall Trough margin. Mar. Geol. 265, 40–50. doi:10.1016/j.margeo.2009.06.014

Neumann, A.C., Kofoed, J.W., Keller, G.H., 1977. Lithoherms in the Straits of Florida. Geology 5, 4–10.

Newton, C.R., Mullins, H.T., Gardulski, A.F., Hine, A.C., Dix, G.R., 1987. Coral Mounds on the West Florida Slope: Unanswered Questions regarding the Development of Deep-Water Banks. Palaios 2, 359–367.

Pahnke, K., Goldstein, S.L., Hemming, S.R., 2008. Abrupt changes in Antarctic Intermediate Water circulation over the past 25,000 years. Nat. Geosci. 1, 870–874. doi:10.1038/ngeo360

Paull, C.., Neumann, a. ., am Ende, B.., Ussler III, W., Rodriguez, N.., 2000. Lithoherms on the Florida–Hatteras slope. Mar. Geol. 166, 83–101. doi:10.1016/S0025-3227(00)00003-7

Raddatz, J., Rüggeberg, A., Liebetrau, V., Foubert, A., Hathorne, E.C., Fietzke, J., Eisenhauer, A., Dullo, W.-C., 2014. Environmental boundary conditions of cold-water coral mound growth over the last 3 million years in the Porcupine Seabight, Northeast Atlantic. Deep Sea Res. Part II Top. Stud. Oceanogr. 99, 227–236. doi:10.1016/j.dsr2.2013.06.009

Richardson, P.L., 1977. On the crossover between the Gulf Stream and the Western Boundary Undercurrent. Deep Sea Res. 24, 139–159. doi:10.1016/0146-6291(77)90549-5

Ruckelshausen, M., 2013. Cold-water corals: A paleoceanographic archive - Tracing past ocean circulation changes in the mid-depth subtropical western South Atlantic off Brazil for the last 40 ka BP. University of Heidelberg, Germany.

Rüggeberg, A., Flögel, S., Dullo, W.C., Hissmann, K., Freiwald, A., 2011. Water mass characteristics and sill dynamics in a subpolar cold-water coral reef setting at Stjernsund, northern Norway. Mar. Geol. 282, 5–12. doi:10.1016/j.margeo.2010.05.009

Sulak, K.J., 2008. Origins, composition, age and structural diversification of Viosca Knoll Lophelia coral reefs and substrate - A synopsis of preliminary results, in: OCS Reports. U. S. Minerals Management Service.

Viana, A.R., Faugeres, J.C., Kowsmann, R.O., Lima, J.A.M., Caddah, L.F.G., Rizzo, J.G., 1998. Hydrology, morphology and sedimentology of the Campos continental margin, offshore Brazil. Sediment. Geol. 115, 133–157. doi:10.1016/S0037-0738(97)00090-0

White, M., 2007. Benthic dynamics at the carbonate mound regions of the Porcupine Sea Bight continental margin. Int. J. Earth Sci. 96, 1–9. doi:10.1007/s00531-006-0099-1

Wienberg, C., Frank, N., Mertens, K.N., Stuut, J.-B., Marchant, M., Fietzke, J., Mienis, F., Hebbeln, D., 2010. Glacial cold-water coral growth in the Gulf of Cádiz: Implications of increased palaeo-productivity. Earth Planet. Sci. Lett. 298, 405–416. doi:10.1016/j.epsl.2010.08.017

Xie, R.C., Marcantonio, F., Schmidt, M.W., 2012. Deglacial variability of Antarctic Intermediate Water penetration into the North Atlantic from authigenic neodymium isotope ratios. Paleoceanography 27, PA3221. doi:10.1029/2012PA002337

Acknowledgements / *Agradecimentos*

During this journey I was helped by many people, both professionally and personally, whose support guided me to the ‘finish line’. Many of them have, one way or another, become models I can look up for. I am dearly thankful to all of them.

To Prof. Dr. Dierk Hebbeln, for accepting and supporting me as a PhD student, for always allowing me to choose my way but also guiding me when needed and, thus, for allowing me to grow as a scientist.

To Prof. Dr. Fátima Abrantes, for her co-supervision and unquestionable support, for taking me into the ‘paleoceanography world’ and leading me to the doctoral studies, and for her constant care of her ‘scientific children’.

To Dr. Marina R. Cunha, for her co-supervision and availability that has not only facilitated the development of my PhD project but also welcomed me into her working group.

To the Thesis Committee members, Prof. Dr. Dierk Hebbeln, Prof. Dr. Fátima Abrantes, Dr. Marina R. Cunha, Dr. Claudia Wienberg, Dr. Furu Mienis and Dr. Lydia Beuck, for all the support and help that guided me during the PhD project.

To the MARUM and GLOMAR personnel, especially to Dr. Christina Klose, Jutta Bülten, Carmen Murken and Dr. Nicolas Dittert, for so often making my life easier.

To Dr. Claudia Wienberg, for all the support and help, for always welcome me, for all the nice conversations, for always be there for me, for being an inspiration...

To Dr. Furu Mienis, for allowing me to participate in her research, for all the friendship and support, for giving me a home, for being able to always motivate me.

To Dr. Jürgen Titschack, for all the support and help, for teaching me patiently, for often remind me of the importance of details.

To Prof. Dr. Norbert Frank, for receiving me at his lab and teaching me about the dating techniques, for all the friendship and all the support.

To Prof. Dr. Christophe Colin, for his availability to work with me and teach me about the secrets of neodymium, for all the help and support.

To Prof. Dr. Gerhard Schmiedl, for his availability to participate in the project and travel to Bremen to meet and discuss.

To Dr. Jeroen Groeneveld, for teaching and helping me with the Mg/Ca analysis, for the constant availability, for the friendship and all the nice moments.

To Dr. Antje Völker, for caring so much, for always being available to help and teach.

To my working group members at LNEG/IPMA, for all the support and help, and for always be interested in my coral conversation and doubts.

Ao pessoal do laboratório de Sedimentologia, em especial à Apolonia Inês, Cremilde Monteiro, Daniel Ferreira e Warley Soares, pelo muito que me ajudaram e ensinaram, mas sobretudo pelo companheirismo e o carinho.

Ao gang da Sala das Lupas, Ana, Andreia, Catarina, Célia, Cristina, Dulce, Isabel e Sandra, e suas famílias, pelo apoio, o carinho, a força, o companheirismo... A vossa doce loucura atenua a loucura do mundo real!

A Gema Martínez Méndez, por todo y todo y todo, por las merendas, por me acojer a mi y a mi familia tantas veces, por ser mi casa y familia. Eres una hermana, lo sabes!

To the Bremer-gang, Mieke, Maria and Vince, Katja, Franzisca, Sarah, Claudia, Dharma, ..., for being my family away from home and keeping me company on my crazy weekend programs.

To Paul Wintersteller, for all the help and for all the friendship that always welcomes me.

To Amalia and her beautiful family, for receiving me in their house and welcome me as family.

To the present and former AG Hebbeln working group members, and especially the 'lunch-time-group', for always receiving me so warmly and making my stays in Bremen a pleasure.

À Filipa Nené, pela amizade e preocupação constante que me encorajaram tantas vezes.

À minha família que sempre me apoiou e encorajou, que foi o meu porto seguro, as minhas mãos ...e tudo o mais. Quem vos tem, tem tudo!

Ao Daniel, Elisa e bebé, por serem os meus pilares, a minha força, o meu apoio, o meu mais-que-tudo e por me compreenderem e apoiarem incondicionalmente nestes dias atarefados.

Thank you! *Obrigada!*

“Deus quer, o homem sonha, a obra nasce.
Deus quis que a terra fosse toda uma,
Que o mar unisse, já não separasse.
Sagrou-te, e foste desvendando a espuma,

E a orla branca foi de ilha em continente,
Clareou, correndo, até ao fim do mundo,
E viu-se a terra inteira, de repente,
Surgir, redonda, do azul profundo.”

Fernando Pessoa, *Mensagem*